GDAŃSK UNIVERSITY OF TECHNOLOGY

Imię i nazwisko autora rozprawy: mgr inż. Adrianna Banach-Kopeć
Dyscyplina naukowa: Nauki chemiczne

ROZPRAWA DOKTORSKA

Tytuł rozprawy w języku polskim: „Opracowanie i charakterystyka biotuszu na bazie chitozanu i agarozy wraz z oceną jego potencjału aplikacyjnego w inżynierii tkankowej"

Tytuł rozprawy w języku angielskim: „Development and characterization of a bioink based on chitosan and agarose with an assessment of its application potential in tissue engineering”

Promotor *podpis*	Promotor pomocniczy *podpis*
dr hab. inż. Robert Tylingo, profesor uczelni	dr inż. Szymon Mania

Gdańsk, rok 2024

Załącznik nr 2/1
do Zarządzenia Rektora PG nr 30/2022 z 14 kwietnia 2022 r.

GDAŃSK UNIVERSITY OF TECHNOLOGY

OŚWIADCZENIE

Autor rozprawy doktorskiej: mgr inż. Adrianna Banach-Kopeć

Ja, niżej podpisana, oświadczam, iż jestem świadoma, że zgodnie z przepisem art. 27 ust. 1 i 2 ustawy z dnia 4 lutego 1994 r. o prawie autorskim i prawach pokrewnych (t.j. Dz.U. z 2021 poz. 1062), uczelnia może korzystać z mojej rozprawy doktorskiej zatytułowanej: „Opracowanie i charakterystyka biotuszu na bazie chitozanu i agarozy wraz z oceną jego potencjału aplikacyjnego w inżynierii tkankowej"
do prowadzenia badań naukowych lub w celach dydaktycznych.[1]

Świadoma odpowiedzialności karnej z tytułu naruszenia przepisów ustawy z dnia 4 lutego 1994 r. o prawie autorskim i prawach pokrewnych i konsekwencji dyscyplinarnych określonych w ustawie Prawo o szkolnictwie wyższym i nauce (Dz.U.2021.478 t.j.), a także odpowiedzialności cywilnoprawnej oświadczam, że przedkładana rozprawa doktorska została napisana przeze mnie samodzielnie.

Oświadczam, że treść rozprawy opracowana została na podstawie wyników badań prowadzonych pod kierunkiem i w ścisłej współpracy z promotorem dr hab. inż. Robertem Tylingo, profesorem PG, promotorem pomocniczym dr inż. Szymonem Manią.

Niniejsza rozprawa doktorska nie była wcześniej podstawą żadnej innej urzędowej procedury związanej z nadaniem stopnia doktora.

Wszystkie informacje umieszczone w ww. rozprawie uzyskane ze źródeł pisanych i elektronicznych, zostały udokumentowane w wykazie literatury odpowiednimi odnośnikami, zgodnie z przepisem art. 34 ustawy o prawie autorskim i prawach pokrewnych.

Potwierdzam zgodność niniejszej wersji pracy doktorskiej z załączoną wersją elektroniczną.

Gdańsk, dnia ....
podpis doktoranta

Ja, niżej podpisana, wyrażam zgodę na umieszczenie ww. rozprawy doktorskiej w wersji elektronicznej w otwartym, cyfrowym repozytorium instytucjonalnym Politechniki Gdańskiej.

Gdańsk, dnia ....
podpis doktoranta

---

1 Art. 27. 1. Instytucje oświatowe oraz podmioty, o których mowa w art. 7 ust. 1 pkt 1, 2 i 4–8 ustawy z dnia 20 lipca 2018 r. – Prawo o szkolnictwie wyższym i nauce, mogą na potrzeby zilustrowania treści przekazywanych w celach dydaktycznych lub w celu prowadzenia działalności naukowej korzystać z rozpowszechnionych utworów w oryginale i w tłumaczeniu oraz zwielokrotniać w tym celu rozpowszechnione drobne utwory lub fragmenty większych utworów. 2. W przypadku publicznego udostępniania utworów w taki sposób, aby każdy mógł mieć do nich dostęp w miejscu i czasie przez siebie wybranym korzystanie, o którym mowa w ust. 1, jest dozwolone wyłącznie dla ograniczonego kręgu osób uczą

GDAŃSK UNIVERSITY OF TECHNOLOGY

OPIS ROZPRAWY DOKTORSKIEJ

Autor rozprawy doktorskiej: mgr inż. Adrianna Banach-Kopeć

Tytuł rozprawy doktorskiej w języku polskim: „Opracowanie i charakterystyka biotuszu na bazie chitozanu i agarozy wraz z oceną jego potencjału aplikacyjnego w inżynierii tkankowej".

Tytuł rozprawy w języku angielskim: „Development and characterization of a bioink based on chitosan and agarose with an assessment of its application potential in tissue engineering".

Język rozprawy doktorskiej: polski

Promotor rozprawy doktorskiej: dr hab. inż. Robert Tylingo, profesor uczelni

Promotor pomocniczy rozprawy doktorskiej: dr inż. Szymon Mania

Data obrony:

Słowa kluczowe rozprawy doktorskiej w języku polskim: biodruk, biotusz, polimery naturalne, inżynieria tkankowa

Słowa kluczowe rozprawy doktorskiej w języku angielskim: bioprinitng, bioink, natural polymers, tissue engineering

Streszczenie rozprawy w języku polskim:

Współczesna inżynieria tkankowa stawia na rozwój biotuszy spełniających wymagania biokompatybilności i drukowalności. Celem rozprawy doktorskiej było opracowanie optymalnej kompozycji biotuszu komórkowego na bazie chitozanu i agarozy, o prostym mechanizmie żelowania i potencjalnym zastosowaniu w inżynierii tkankowej. Jednym z aspektów pracy była redukcja zawartości endotoksyn w hydrożelach chitozanowych przy jednoczesnym zachowaniu ich stabilnych właściwości fizykochemicznych, takich jak masa cząsteczkowa i lepkość, co ma kluczowe znaczenie dla bezpieczeństwa biologicznego. Przeprowadzono analizę właściwości fizykochemicznych i biologicznych chitozanu o różnych masach cząsteczkowych i stopniach deacetylacji, oceniając jego aktywność przeciwdrobnoustrojową i cytotoksyczność. Wyniki wykazały że zmienne te mają niewielki wpływ na właściwości biologiczne, co pozwoliło zawęzić dalsze badania do różnych mas cząsteczkowych. Oceniono także wpływ agarozy jako środka

żelującego, co doprowadziło do opracowania stabilnego hydrożelu, żelującego w temperaturze zbliżonej do fizjologicznej, bez potrzeby dodatkowych czynników sieciujących. Wykazano wysoką drukowalność i stabilność biotuszu podczas wytłaczania, a także pozytywny wpływ kompozycji na cytotoksyczność, proliferację, migrację oraz przeżywalność fibroblastów i keratynocytów. Testy in vivo na modelu CAM potwierdziły brak negatywnego wpływu na angiogenezę, a badania na myszach wykazały zdolność kompozycji polimerowych do stymulowania regeneracji tkanek. Ostateczne wyniki potwierdziły, że opracowany biotusz ma duży potencjał w biodruku oraz medycynie regeneracyjnej.

Streszczenie rozprawy w języku angielskim:

Contemporary tissue engineering focuses on the development of bioinks that meet the requirements of biocompatibility and printability. The aim of the doctoral thesis was to develop an optimal composition of cellular bioink based on chitosan and agarose, with a simple gelation mechanism and potential application in tissue engineering. A key aspect of the work involved reducing endotoxin levels in chitosan hydrogels while maintaining stable physicochemical properties, such as molecular weight and viscosity, which are crucial for biological safety. A detailed analysis of the physicochemical and biological properties of chitosan with varying molecular weights and degrees of deacetylation was conducted, with an assessment of its antimicrobial activity and cytotoxicity. The results demonstrated that these variables had a minimal effect on the biological properties, allowing further studies to focus on different molecular weights. The impact of agarose as a gelling agent was also evaluated, leading to the development of a stable hydrogel that gels at a temperature close to physiological conditions without the need for additional crosslinking agents. High printability and stability of the bioink during extrusion were demonstrated, along with a positive impact of the composition on cytotoxicity, proliferation, migration, and survival of fibroblasts and keratinocytes. In vivo tests using the CAM model confirmed no adverse effects on angiogenesis, and studies in mice showed the potential of the polymer compositions to stimulate tissue regeneration. These final results confirmed the bioink's significant potential for applications in bioprinting and regenerative medicine.

ROZPRAWA DOKTORSKA

Opracowanie i charakterystyka biotuszu na bazie chitozanu i agarozy wraz z oceną jego potencjału aplikacyjnego w inżynierii tkankowej

mgr inż. Adrianna Banach-Kopeć

Promotor: dr hab. inż. Robert Tylingo, profesor uczelni

Promotor pomocniczy: dr inż. Szymon Mania

Pragnę złożyć wyrazy wdzięczności wyjątkowym osobom, które wspierały mnie swoją wiedzą, doświadczeniem oraz inspirowały na każdym etapie mojej ścieżki naukowej. Pragnę więc serdecznie podziękować:

Mojemu Promotorowi, Profesorowi Robertowi Tylingo, za nieocenioną pomoc i bezcenne wsparcie na każdym etapie mojego rozwoju naukowego. Pańska wnikliwość, merytoryczne wskazówki oraz otwartość na dialog były i pozostają dla mnie niewyczerpanym źródłem inspiracji. Dziękuję za poświęcony czas, dzielenie się przemyśleniami i cennymi radami, które nie tylko wzbogaciły moją wiedzę, ale również nauczyły patrzeć na naukę jako niekończący się proces odkrywania i zadawania pytań.

Doktorowi Szymonowi Mani za to, że zawsze mogłam liczyć na Jego koleżeńskie wsparcie, pomoc oraz cierpliwość. Dziękuję za motywację, wartościowe rozmowy i dzielenie się swoją wiedzą, które uczyniły ten początek drogi naukowej pełnym inspiracji i otuchy.

Wszystkim Pracownikom oraz Doktorantom Katedry Chemii, Technologii i Biotechnologii Żywności za tworzenie wyjątkowej atmosfery, codzienne rozmowy, cenne rady i możliwość uczenia się od nich. Jestem wdzięczna za życzliwość, wsparcie i otwartość, które sprawiły, że każdy dzień spędzony w Katedrze był nie tylko czasem intensywnej pracy, ale również przestrzenią koleżeńskich rozmów i chwil pełnych dobrego humoru.

Moim cudownym Rodzicom za miłość, mądrość i wsparcie, które towarzyszą mi przez całe życie. To Wasza niezłomna wiara we mnie, przykład codziennej wytrwałości i nieustająca inspiracja sprawiły, że miałam odwagę stawiać czoła wyzwaniom i podążać za swoimi marzeniami. Wasze wsparcie jest fundamentem, na którym zbudowałam wszystkie swoje sukcesy. Bez Was nie byłoby mnie tu, gdzie jestem dzisiaj.

Mojemu najukochańszemu mężowi, Tomaszowi, za to, że nie tylko wspiera mnie na każdym kroku, ale też dodaje odwagi, gdy jej brakuje, i wierzy we mnie nawet wtedy, gdy ja sama mam wątpliwości. Dziękuję za bycie moim największym wsparciem i najlepszym towarzyszem na każdej drodze, którą wspólnie pokonujemy.

Przygotowana rozprawa doktorska stanowi
przewodnik po artykułach naukowych
w ramach jednotematycznego cyklu publikacji.

Spis treści

WYKAZ NAJWAŻNIEJSZYCH OZNACZEŃ I SKRÓTÓW

AG – agaroza

CAM – test błony kosmówkowo-omoczniowej (z ang. chorioallantoic membrane assay)

CS – chitozan

CS/AG – kompozycja chitozanowo-agarozowa

DD – stopień deacetylacji (z ang. deacetylation degree)

HA – kwas hydroksyoctowy (z ang. hydroxyacetic acid)

HMW – wysoka masa cząsteczkowa (ang. high molecular weight)

LA – kwas mlekowy (z ang. lactic acid)

LMW – niska masa cząsteczkowa (z ang. low molecular weight)

MMW – średnia masa cząsteczkowa (z ang. medium molecular weight)

WYKAZ PUBLIKACJI BĘDĄCYCH PODSTAWĄ ROZPRAWY DOKTORSKIEJ

Oryginalne prace badawcze:

[A1] **Banach-Kopeć A.**, Mania S*., Pilch J., Augustin E., Gabriel I., & Tylingo R. (2022). A Novel Method of Endotoxins Removal from Chitosan Hydrogel as a Potential Bioink Component Obtained by CO_2 Saturation. International Journal of Molecular Sciences, 23, 5505.
Doi.org/10.3390/ijms23105505 (IF: 5,6; MNiSW: 140)

[A2] Mania S*., **Banach-Kopeć A.**, Staszczyk K., Kulesza J., Augustin E., & Tylingo R. (2023). An influence of molecular weight, deacetylation degree of chitosan xerogels on their antimicrobial activity and cytotoxicity. Comparison of chitosan materials obtained using lactic acid and CO_2 saturation. Carbohydrate Research, 534, 108973.
Doi.org/10.1016/j.carres.2023.108973 (IF: 2,4; MNiSW: 100)

[A3] **Banach-Kopeć A.** †, Mania S.*†, Tylingo R., Wawrzynowicz A., Pawłowska M., Czerwiec K., Deptuła M., Pikuła M. (2024). Thermosensitive composite based on agarose and chitosan saturated with carbon dioxide. Preliminary study of requirements for production of new CSAG bioink. Carbohydrate Polymers, 336, 122120.
Doi.org/10.1016/j.carbpol.2024.122120 (IF: 10,7; MNiSW: 140)

[A4] Mania S. †, **Banach-Kopeć A.*†**, Maciejewska N., Deptuła K., Słonimska P., Deptuła M., Baczyński-Keller J., Pikuła M., Sachadyn P., Tylingo R. (2024). From Bioink to Tissue: Exploring Chitosan-Agarose Composite in the Context of Printability and Cellular Behaviour. Molecules, *29*(19), 4648.
Doi.org/10.3390/molecules29194648 (IF: 4,2; MNiSW: 140)

Prace przeglądowe:

[A5] **Banach-Kopeć A*.**, Mania S., & Tylingo R. (2024). Marine polymers in tissue bioprinting: Current achievements and challenges. Reviews on Advanced Materials Science, 63(1), 20230180.
Doi.org/10.1515/rams-2023-0180 (IF: 3,6; MNiSW: 100)

*autor korespondencyjny; † autorzy w równym stopniu przyczynili się do tej pracy

1 WPROWADZENIE

Rozwój medycyny regeneracyjnej oraz inżynierii tkankowej to jeden z najbardziej obiecujących kierunków w poszukiwaniu rozwiązań w zakresie odbudowy uszkodzonych tkanek i organów. Jednym z czynników, który znacząco wpłynął na postęp w tej dziedzinie, było zaadaptowanie do wytwarzania materiałów sprzyjających regeneracji tkankowej technologii druku 3D. Dopiero po połączeniu możliwości i wiedzy z zakresu wytwarzania addytywnego, materiałoznawstwa i hodowli komórkowej, inżynieria tkankowa jest w stanie zrewolucjonizować współczesną medycynę [Ng i wsp., 2019; Murphy i Atala, 2014]. Pomimo zdolności ludzkiego organizmu do regeneracji, w wielu przypadkach np. oparzeń skórnych, ze względu na zbyt wolne tempo tego procesu lub zbyt duży poziom uszkodzeń tkanki, jest to niemożliwe. Obecnie, głównym rozwiązaniem stosowanym w takich przypadkach są przeszczepy. Jednakże ze względu na znaczne ograniczenie liczby dawców, są one rzadko stosowane. Co więcej, nawet w przypadku znalezienia dawcy, ryzyko odrzucenia przeszczepu wciąż pozostaje jednym z najczęstszych problemów. W związku z powyższym, tworzenie złożonych rusztowań przestrzennych, zdolnych do naśladowania właściwości biologicznych uszkodzonych tkanek oraz zgodnych z systemem immunologicznym pacjenta wydaje się być obiecującym rozwiązaniem [Wang i wsp., 2024; He i wsp., 2018]. Możliwość szybkiego prototypowania, personalizacji rusztowania oraz precyzyjnego osadzania komórek w materiale sprawia, że kluczową technologią inżynierii tkankowej jest biodruk 3D. Potencjał wykorzystania tej technologii oraz jej możliwości są znacznie szersze i nie koncentrują się tylko na drukowaniu rusztowań zawierających komórki w celu ich przeszczepiania. Drukowanie sztucznych tkanek, organów lub narządów, organoidów jako modeli w badaniach farmaceutycznych umożliwiłoby testowanie skuteczności i bezpieczeństwa nowo opracowywanych i zsyntetyzowanych leków. Modele te umożliwiłyby prowadzenie badań w celu zrozumienia mechanizmów i procesów chorobotwórczych, testowania terapii na miarę indywidualnych potrzeb pacjenta, a przede wszystkim stałby się alternatywą dla modeli zwierzęcych [Huang i wsp., 2024; Gao i wsp., 2021; Kačarević i wsp., 2018].

Pomimo dużego potencjału biodruku 3D w inżynierii tkankowej, istnieje szereg wyzwań technologicznych jak i naukowych, uniemożliwiających jego praktyczne zastosowanie. Dostępne na dzień dzisiejszy rozwiązania na rynku gotowych zestawów do biodruku, w tym biodrukarek oraz dedykowanych do nich biotuszów, nie zawsze umożliwiają ich bezpośrednie zastosowanie w prowadzonych badaniach naukowych, a tym bardziej w komercyjnym zastosowaniu medycznym. Problem ten wynika częściowo z ograniczeń technologicznych wielu biodrukarek, w tym wahań temperatury w module grzewczym oraz ciśnienia gazu tłoczącego podczas procesu druku, a także z braku możliwości współtłoczenia składników biotuszu. Konsekwencją tych ograniczeń jest opracowywanie przez wielu badaczy własnych urządzeń drukujących lub modyfikacja tych dostępnych komercyjnie, w celu dostosowania ich do indywidualnych potrzeb.

W przypadku biodruku znacznie łatwiejsze jest dostosowanie urządzenia drukującego do istniejącego biotuszu, niż modyfikacja biotuszu do pracy urządzenia. W związku z tym, kluczowe znaczenie na etapie planowania badań w zakresie biodruku, ma dokonanie świadomego wyboru dotyczącego technologii druku, urządzenia, biotuszu jak i określenie docelowego zastosowania. Te elementy stanowią nierozerwalny zestaw, w którym zmiana chociażby jednego z nich ma znaczący wpływ na pozostałe. Co więcej, rozważenie powyższych zmiennych na początkowym etapie prac decyduje o potencjalnym sukcesie projektu badawczego, podkreślając zarazem konieczność holistycznego podejścia do projektowania i realizacji badań w inżynierii tkankowej [A5].

Mimo znaczących na przestrzeni ostatnich lat postępów w zakresie biodruku i inżynierii tkankowej, istotnym wyzwaniem nadal pozostaje opracowanie metod umożliwiających produkcję rusztowań o stabilnych właściwościach mechanicznych, które jednocześnie zapewnią komórkom wysoką przeżywalność w warunkach drukowania oraz odpowiednie do ich proliferacji i różnicowania warunki w gotowych wydrukach. W biodruku spełnienie obu tych kryteriów nazywane jest „oknem biofabrykacji". Jest to kompromis pomiędzy uzyskaniem wysokiej przeżywalności a zapewnieniem drukowalności. W pracach badawczych okno biofabrykacji ma wydźwięk negatywny, ponieważ na ten moment brak jest jakichkolwiek doniesień literaturowych opisujących jednoczesne uzyskanie wysokiej precyzji wydruków przy zachowaniu jak najwyższej przeżywalności komórek [Ouyang i wsp., 2022; Gao i wsp., 2021; Levato i wps., 2020]. Problem wynika z tego, że wzrost lepkości biotuszu, choć zwiększa jego drukowalność, jednocześnie negatywnie wpływa na przeżywalność komórek w nim zawartych, co jest spowodowane koniecznością stosowania wyższego ciśnienia wytłaczania [Habib i Khoda, 2022]. W wielu pracach naukowych, przezwyciężenie „okna biofabrykacji" to główny cel, na którym skupiają się badacze. Z drugiej strony, istnieje szereg tkanek, między innymi miękkich, takich jak skóra, dla których uzyskanie parametru drukowalność na najwyższym poziomie nie jest najważniejszym kryterium. W kontekście funkcjonalności rusztowań, to zdolność komórek do migracji w rusztowaniu, zdolność proliferacji i różnicowania mają kluczowe znaczenie dla finalnej geometrii konstruktu. Bez wątpienia, geometryczna struktura rusztowania stanowi fundament dla samoorganizacji komórkowej. Jednakże, z upływem czasu, od momentu wydrukowania, jej pierwszorzędna rola zmniejsza się w miarę postępującej biodegradacji materiału, co umożliwia stopniowe zastępowanie wydrukowanej struktury przez naturalną tkankę. Pomimo że poprawa drukowalności często wiąże się z obniżeniem przeżywalności komórek po wytłoczeniu biotuszu, ważne jest, aby pamiętać, że komórki zdolne są do proliferacji po wydruku, co prowadzi do zwiększenia ich liczby z czasem. Wytwarzanie addytywne może indukować stres komórkowy, wynikający z sił ścinających występujących podczas wytłaczania biotuszu przez dyszę biodrukarki, jak podają Xu i współpracownicy (2022). Inne kluczowe czynniki wpływające na przeżywalność komórek obejmują temperaturę dyszy, czas druku, średnicę igły oraz natężenie przepływu biotuszu [Deptuła i wsp., 2023; Malekpour i Chen, 2022]. Z wielu prac naukowych wynika, że poprawa drukowalności

nawet kosztem początkowo niższej żywotności komórek może być uzasadniona, ponieważ po kilkudniowej inkubacji wydruku w medium hodowlanym obserwuje się stopniową proliferację i zwiększoną żywotność komórek. Najważniejsze jest zapewnienie komórkom biozgodnych warunków co obejmuje biologicznie bezpieczne, niecytotoksyczne i bioaktywne rusztowania, które są jednocześnie przepuszczalne. Ponadto, odpowiednie medium hodowlane oraz czynniki wspierające wzrost i proliferację komórek są niezbędne, aby umożliwić im adaptację do nowych warunków hodowlanych [A5]. Aby zapewnić dalszy rozwój komórek w funkcjonalną tkankę, badania powinny koncentrować się na szukaniu kompromisu pomiędzy fazą rozwoju komórek, a degradacją rusztowania. Punktem wyjścia powinno być ustalenie składu kompozycji stanowiącej bazę biotuszu, z uwzględnieniem w dalszym etapie doborze funkcjonalnych dodatków takich jak: czynniki wzrostu czy peptydy pełniące rolę sygnalizacyjną, których uwalnianie się w czasie będzie wspierało adhezję, proliferację i różnicowanie komórek [Alhattab i wsp. 2023; Cohen i wsp., 2023]. Takie podejście może nie tylko zwiększyć przeżywalność komórek w czasie, ale również przyspieszyć ich adaptację do nowego otoczenia oraz pozwolić na ich integrację z naturalnym środowiskiem, do którego docelowo będą włączone. Aby zapewnić skuteczną rekonstrukcję lub wymianę narządów kluczowe jest również pobudzenie unaczynienia, w tym angiogenezy. Stymulowanie indukcji proangiogennych szlaków sygnałowych jest niezbędne dla prawidłowej aktywności komórek zawartych w rusztowaniu [Oropeza i wsp., 2022]. To z kolei pozwala na zintegrowanie przeszczepionego rusztowania z tkankami biorcy oraz dzięki zachowaniu odpowiedniego tempa angiogenezy, prawidłowego ukrwienia i dotlenienia zregenerowanej tkanki [Saberianpour i wsp., 2018].

Podsumowanie podstawowych wymagań stawianych biotuszom już na pierwszych etapach ich projektowania, z uwzględnieniem podziału na aspekty biologiczne i fizykochemiczne, zostało przedstawione na Rysunku 1.

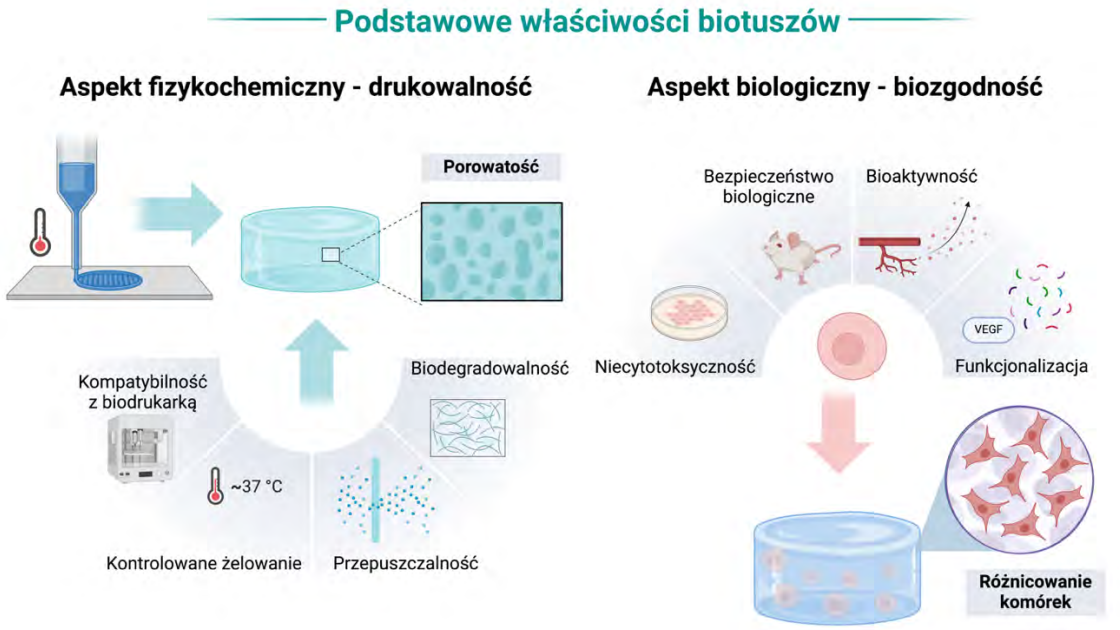

Rysunek 1. Przegląd kluczowych właściwości biotuszów z uwzględnieniem parametrów fizykochemicznych i biologicznych, które mają kluczowe znaczenie przy projektowaniu biotuszów w kontekście inżynierii tkankowej i medycyny regeneracyjnej [opracowano za pomocą narzędzia Biorender.com].

Główny nurt badawczy związany z projektowaniem funkcjonalnych materiałów dedykowanych biodrukowi skoncentrowany jest na wykorzystaniu hydrożeli tworzonych na bazie surowców polimerowych, zwłaszcza tych pochodzenia naturalnego. Podobnie do tkanek składają się one głównie z wody, przez co zdolne są do naśladowania naturalnej macierzy zewnątrzkomórkowej [Fang i wsp., 2023; Das i Basu, 2019]. Podstawowym ograniczeniem większości komercyjnie dostępnych biotuszów, jest spełnienie tylko podstawowych wymagań, takich jak biokompatybilność oraz zapewnienie przeżywalności komórek po wydrukowaniu. Dalsze aspekty, przykładowo różnicowanie komórek w czasie jest pomijane. Takie podejście spowodowało, że obecnie na rynku dostępnych jest wiele uniwersalnych biotuszów [Vijayavenkataraman, 2023] producentów takich jak Cellink i Allevi. Ich produkty, oparte głównie na naturalnych polimerach, są rekomendowane do szerokiego zastosowania w różnych dziedzinach inżynierii tkankowej, w tym w tworzeniu modeli różnych organów, dzięki ich zdolności do wspierania wzrostu i różnicowania wielu typów komórek. Inne podejście stosuje firma Organovo, która oferuje swoim partnerom spersonalizowane układy. W ramach współpracy z takimi firmami jak Merck czy L'Oréal wytwarzane są modele m.in. tkanki skórnej w celu prowadzenia badań przesiewowych leków oraz kosmetyków [Choudhury i wsp., 2018]. Analiza danych literaturowych oraz przegląd komercyjnie dostępnych biotuszów wskazują na najczęstsze zastosowanie polimerów takich jak: alginian, żelatyna oraz kolagen, z czego dwa ostatnie są przeważnie modyfikowane chemicznie do formy

metakrylowanej. Powszechne stosowanie wyżej wymienionych polimerów zarówno w pracach badawczych jak i dostępnych komercyjnie biotuszach wynika z już opracowanych, dobrze poznanych i efektywnych metod sieciowania. W przypadku alginianu proces sieciowania polega na tworzeniu mostków wapniowo-karboksylowych między grupami karboksylowymi występującymi w alginianie a jonami wapnia, które dodawane są najczęściej w formie roztworu chlorku wapnia wraz z przyrostem kolejnych warstw wydruku (Rys. 2A). W przypadku metakrylowanej żelatyny lub kolagenu sieciowanie indukowane jest pod wpływem promieniowania UV, co skutkuje utworzeniem trwałych wiązań kowalencyjnych między grupami metakrylowymi (Rys. 2B) [A5].

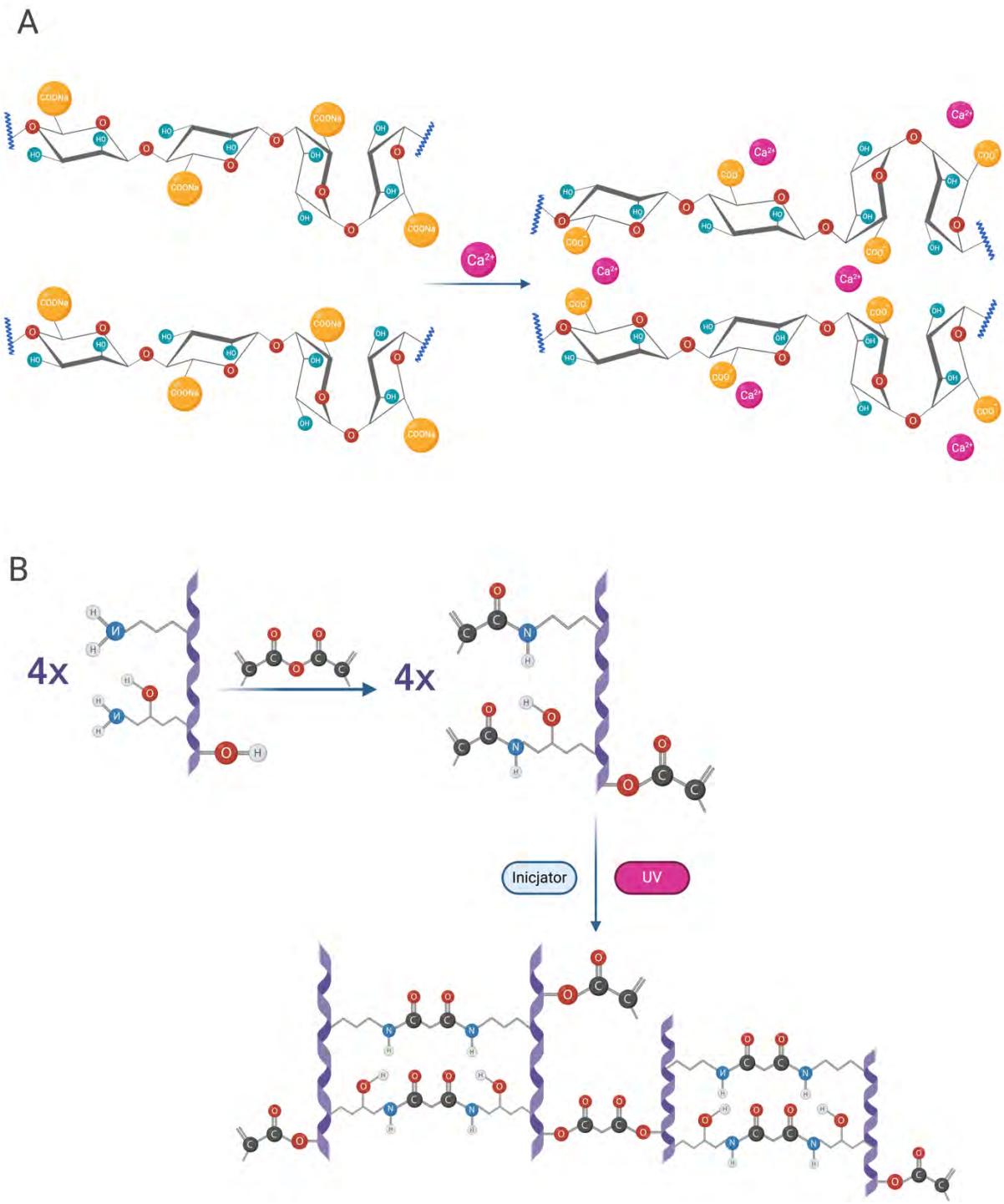

Rysunek 2. Schemat sieciowania A) alginianu za pomocą jonów wapnia oraz B) modyfikowanej żelatyny/kolagenu do metakrylowanych pochodnych z wykorzystaniem inicjatora i światła UV [opracowano za pomocą narzędzia Biorender.com]

W praktyce wybór metody sieciowania jest silnie uzależniony od tego, czy punktem wyjścia jest biodrukarka, czy biotusz o określonym składzie. W przypadku niektórych biodrukarek istnieje możliwość zastosowania różnych metod sieciowania,

co daje większą elastyczność w projektowaniu biotuszów. Ostateczny wybór może być determinowany przez określoną specyfikację urządzenia, wynikającą między innymi z obecności termostatowanego elementu umożliwiającego kontrolowanie temperatury miejsca, w którym umiejscowiony jest biotusz tzw. kartidż, czy stołu roboczego lub źródła światła UV. Mniejszą elastyczność w wyborze metody sieciowania oferuje z kolei sam biotusz o określonym składzie. To właśnie polimery użyte do przygotowania bazy biotuszu, mają główny wpływ na konieczność zastosowania określonej metody sieciowania. To podkreśla, jak kluczową rolę odgrywa decyzja dotycząca wyboru zarówno biotuszu, jak i biodrukarki na wczesnym etapie projektu [A5].

Kolejnym rozwiązaniem stosowanym przez badaczy w projektowaniu biotuszy, jest tworzenie wieloskładnikowych układów, czyli składających się z więcej niż jednego polimeru. Takie podejście pozwala na wykorzystanie pożądanych cech wszystkich wykorzystanych surowców w docelowym materiale, często z towarzyszącym efektem synergii. Jednakże podczas projektowania kompozycji polimerowych konieczne jest dokładne wykluczenie potencjalnie niepożądanych interakcji między składnikami, które mogą ograniczać stabilność materiału oraz jego kompatybilność z warunkami fizjologicznymi. Na przykład chitozan otrzymywany metodą rozpuszczania w kwaśnym środowisku, różnym od fizjologicznego pH, wykazuje właściwości, które mogą prowadzić do niekorzystnych interakcji, takich jak zahamowanie procesu żelowania agarozy, co jest krytyczne dla właściwego uformowania struktury biotuszu po wytłoczeniu. Dlatego alternatywne techniki, jak metoda rozpuszczania chitozanu poprzez saturację, pozwalają na wyeliminowanie tego efektu i uzyskanie materiału o właściwościach synergicznych, w którym chitozan i agaroza zachowują pożądane właściwości [A3].

Chociaż chityna jest drugim co do powszechności występowania polimerem, to wiele badań skupia się na wykorzystywaniu jej zdeacetylowanej pochodnej, czyli chitozanu. Jest to polikationowy polimer, który składa się z D-glukozaminy (70-90%) i połączonych z nią wiązaniem β-1,4-glikozydowm podjednostek N-acetylo-D-glukozaminy (10-30%). To właśnie stopień deacetylacji, czyli udział jednostek D-glukozaminy do N-acetylo-D-glukozaminy determinuje głównie rozpuszczalność chitozanu w rozcieńczonych roztworach kwasów organicznych. Wraz ze wzrostem stopnia deacetylacji, czyli liczby wolnych grup aminowych w strukturze chitozanu, zwiększa się jego rozpuszczalność [Weißpflog i wsp., 2021]. Właściwość ta jest kluczowa, ponieważ rozpuszczalność polimeru ma bezpośredni wpływ na możliwości otrzymywania materiałów hydrożelowych. Wartość pH roztworów chitozanu otrzymywanych klasycznymi metodami rozpuszczania tego polimeru w roztworach kwasu np. mlekowego lub octowego, stanowi poważne ograniczenie z punktu widzenia biozgodności. Zastosowanie hydrożeli o pH niższym niż 7 wywołuje efekt cytotoksyczny względem komórek i na wstępie wyklucza ich zastosowanie w biodruku. Jednakże obecność grup aminowych oraz hydroksylowych w strukturze chitozanu umożliwia jego modyfikacje. Wielu badaczy wykorzystuje tę możliwość, modyfikując chitozan do jego pochodnych,

między innymi do hydroksypropylo-chitozanu [Liu i wsp., 2021] lub karboksymetylo-chitozanu (Rys. 3) [Butler i wsp., 2021; Gu i wsp., 2017].

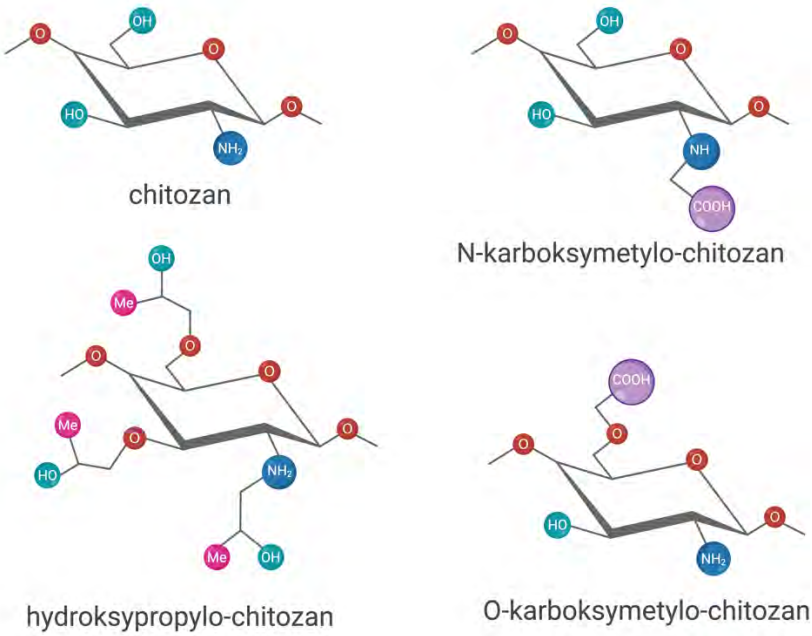

Rysunek 3. Struktury chemiczne chitozanu oraz jego pochodnych [opracowano za pomocą narzędzia Biorender.com]

Powyższe modyfikacje, umożliwiają poprawę rozpuszczalności chitozanu w wodzie i tym samym możliwość otrzymywania roztworów tego polimeru, gdy wartość pH zbliżona jest do 7. Przykładem innego rozwiązania rozszerzającego aplikacyjność chitozanu w branży medycznej i kosmetycznej jest metoda opracowana przez Gorczycę i współpracowników w Politechnice Gdańskiej. Metoda ta polega na otrzymywaniu mikrokrystalicznej formy chitozanu z jego kwaśnego roztworu w wyniku strącenia roztworem wodorotlenku sodu, a następnie ponownemu rozpuszczeniu dokładnie wypłukanego osadu zawieszonego w odpowiedniej ilości wody saturowanej ditlenkiem węgla przy jednoczesnym wspomaganiu mieszaniem mechanicznym. W ten sposób możliwe jest uzyskanie roztworu chitozanu, którego wartość pH wynosi około 6,8. Wykazano, że taka forma roztworu chitozanu jest niecytotoksyczna dla komórek, co umożliwia zastosowanie go także w inżynierii tkankowej [Gorczyca i wsp., 2014]. Pozostałe właściwości chitozanu, które sprawiają, że ma on potencjalne zastosowanie w biodruku i inżynierii tkankowej, to biodegradowalność, biokompatybilność oraz właściwości przeciwdrobnoustrojowe wynikające z obecności grup aminowych. Nadanie biomateriałom właściwości przeciwdrobnoustrojowych stanowi kluczowy postulat ze strony środowiska medycznego, odpowiadając na pilną potrzebę minimalizacji ryzyka zakażeń szpitalnych i tym samym wspierając bezpieczeństwo pacjentów oraz efektywność procedur terapeutycznych [Ke i wsp., 2021]. Liczne badania wykazały, że chitozan wspiera proces gojenia się ran na poszczególnych etapach regeneracji

tkankowej, takich jak inicjacja adhezji i agregacji płytek krwi oraz stymulacja proliferacji fibroblastów [Feng i wsp., 2021]. Jednak głównym wyzwaniem, które należy rozwiązać przy zastosowaniu chitozanu jako hydrożelu w biodruku, jest jego słaba drukowalność oraz ograniczone właściwości mechaniczne [Sadeghianmaryan i wsp., 2020].

Decydując się na opracowanie biotuszu na bazie chitozanu, konieczne jest wytypowanie innego polimeru, który będzie cechować się dobrą drukowalnością, a wydruki na jego bazie będą miały dobre właściwości mechaniczne. Inne polimery pochodzenia naturalnego takie jak: alginian sodu, żelatyna, kolagen, celuloza, karagen mogą tworzyć stabilne materiały hydrożelowe, ale wymagają do tego celu zastosowania czynnika sieciującego lub modyfikacji chemicznej w celu zapewnienia szybkiej przemiany fazowej zol-żel. Wyjątek stanowi agaroza, której szybkie żelowanie silnie zależy od temperatury jej roztworów [A5].

Agaroza otrzymywana jest z agaru w procesie ekstrakcji agaropektyny. Jest to liniowy polimer składający się z naprzemiennie ułożonych podjednostek D-galaktozy i 3,6-anhydro-L-galaktopyranozy połączonych wiązaniami glikozydowymi α-(1→3) i β-(1→4) [Salati i wsp., 2020]. Agaroza jest biologicznie obojętnym polimerem, niewywołującym efektu cytotoksycznego, ale także nieposiadającym żadnych właściwości biologicznych, takich jak promowanie adhezji komórek [Seow i wsp., 2019]. Z perspektywy wymagań stawianych materiałom stosowanym w biodruku, kluczowe kryteria obejmują jej drukowalność, zdolność do formowania stabilnych rusztowań oraz brak cytotoksycznego wpływu na komórki. Te właściwości czynią agarozę optymalnym komponentem strukturalnym w biodruku, umożliwiającym tworzenie trwałych, trójwymiarowych rusztowań komórkowych.

Proces żelowania agarozy przebiega w trzech etapach, czyli indukcji, żelowania oraz osiągnięcia pseudorównowagi. W fazie pierwszej dochodzi do inicjacji formowania struktury helikalnej na skutek utworzonych wiązań wodorowych oraz oddziaływań elektrostatycznych pomiędzy cząsteczkami agarozy, które w dalszych etapach żelowania powodują łączenie się struktur helikalnych i tym samym tworzenie struktury żelowej. Ostatecznie, w stanie pseudorównowagi, sieć ta stabilizuje się, zachowując strukturę dzięki trwałym interakcjom molekularnym [Zarrintaj i wsp., 2018]. Jedną z unikalnych cech agarozy, szczególnie cenną w biodruku, jest jej zdolność do żelowania w temperaturze bliskiej fizjologicznej, co pozwala na tworzenie stabilnych struktur bez ryzyka uszkodzenia komórek. Dodatkowo, proces odwrotny, czyli topnienie, zachodzi dopiero w znacznie wyższej temperaturze, przekraczającej 85°C [Ghebremedhin i wsp., 2021]. Taka różnica w temperaturach żelowania i topnienia zapewnia materiałowi wyjątkową stabilność termiczną, co jest kluczowe w projektowaniu rusztowań komórkowych o wysokiej precyzji i trwałości. Zastosowanie tego rozwiązania pozwala wyeliminować konieczność stosowania dodatkowych związków sieciujących lub żelujących.

Jednakże, aby zapewnić komórkom odpowiednie warunki do proliferacji i różnicowania konieczne jest zagwarantowanie im zarówno prawidłowego środowiska biologicznego jak i strukturalnego. Jednym z ograniczeń agarozy jest brak możliwości

formowania żeli przy pH 3,5 [Toyama i wps., 2011]. Przykładowo, układy oparte na chitozanie rozpuszczonym w kwasach organicznych, takich jak octowy, mlekowy czy hydroksyoctowy, znacząco ograniczają możliwość tworzenia stabilnych żeli w połączeniu z agarozą. W kwaśnym środowisku dochodzi bowiem do zakłócenia interakcji między polimerami, co uniemożliwia uzyskanie jednorodnej i trwałej struktury żelowej. W związku z tym, zastosowanie kwasów do rozpuszczania chitozanu stanowi barierę dla tworzenia kompozycji chitozanowo-agarozowych o optymalnych właściwościach mechanicznych i strukturalnych. Natomiast roztwór chitozanu o pH 6,8, przygotowany metodą saturacji dwutlenkiem węgla, tworzy z agarozą stabilne układy, które wykazują znaczny potencjał jako rusztowania komórkowe.

Głównym utrudnieniem napotykanym w trakcie drukowania materiałami hydrożelowymi, charakteryzującymi się przejściem fazowym pod wpływem obniżenia temperatury, może być ich przedwczesne żelowanie, powodujące zatykanie dyszy i przewodów urządzenia. Problem ten jest często spotykany, gdy temperatura dyszy drukującej jest zbliżona do temperatury przejścia zol-żel i jednocześnie system ogrzewania biotuszu i utrzymania temperatury w martwej przestrzeni biodrukarki nie pozwala na utrzymanie odpowiednich warunków termicznych. W biodruku kluczowe jest utrzymanie stabilnych warunków termicznych, ponieważ nawet niewielki wzrost temperatury może obniżyć żywotność komórek, natomiast zbyt niska temperatura sprzyja przedwczesnemu żelowaniu kompozycji polimerowej, uniemożliwiając jej precyzyjne wytłoczenie. Wynika to z tego, że wahania temperatury, rzędu jednego stopnia wpływają na charakterystykę płynięcia biotuszu, co przekłada się na spadek jakości procesu drukowania. Problem z utrzymaniem ściśle określonej temperatury w biodrukarce i tym samym biotuszu, jest konsekwencją wad konstrukcyjnych biodrukarek, które wyposażone zostały w systemy ogrzewania, jednakże nie są one na tyle wydajne, aby zapobiec ewentualnym wahaniom temperatury [A5].

Aby w pełni zrozumieć specyfikę procesu biodruku i właściwie wybrać odpowiednie parametry dla konkretnych układów i potrzeb, warto przyjrzeć się stosowanym technikom oraz ich unikalnym wymaganiom i ograniczeniom. Podział biodruku obejmuje zazwyczaj następujące techniki: biodruk atramentowy, stereolitograficzny, wspomagany laserem oraz ekstruzyjny, z czego ta ostatnia metoda, oparta na wyciskaniu materiału przez dyszę, jest najczęściej stosowana do hydrożeli. Każda z technik druku ma swoje wady i zalety oraz dedykowana jest do innych rozwiązań materiałowych, różniących się właściwościami reologicznymi i sposobem utwardzania/sieciowania [Deptuła i wsp., 2023]. Dla przykładu, głównym czynnikiem determinującym wybór pomiędzy drukiem atramentowym a ekstruzyjnym, jest lepkość biotuszu. Pierwsza metoda dedykowana jest do płynów o lepkości w zakresie 3-30 $mPa \cdot s^{-1}$ [Li i wsp., 2020], z kolei biodruk ekstruzyjny do roztworów o lepkości do 6×10^7 $mPa \cdot s^{-1}$ [Ramesh i wsp., 2020]. Obie powyższe metody oferują szeroki zakres możliwych do zastosowania sposobów utwardzania/sieciowania. Dodatkowo, ze względu na postępy jakie odniesiono w zakresie druku ekstruzyjnego, takie parametry jak rozdzielczość druku

oraz przeżywalność komórek przestały być już ich ograniczeniem [A5]. Kolejne dwie, bardziej zaawansowane techniki to biodruk stereolitograficzny skupiający się na zastosowaniu fotopolimerowych żywic z fotoinicjatorem, które ulegają utwardzeniu pod wpływem światła ultrafioletowego [Yang i wsp., 2020] oraz biodruk wspomagany laserem polegający na precyzyjnym osadzaniu żywych komórek poprzez wykorzystanie impulsów laserowych do przenoszenia materiału z nośnika donora na docelowe podłoże [Agarwal i wsp., 2023]. Pomimo wysokiej precyzji obu wspomnianych technik, ich zastosowanie ze względu na problem utrzymania wysokiej przeżywalności komórek jest utrudnione. Wymagania, które należy spełnić stosując stereolitografię lub biodruk wspomagany laserowo to konieczność stosowania niecytotoksycznych fotoinicjatorów, optymalizacja czasu naświetlania światłem UV lub lasera, które przy nieodpowiednich parametrach mogłyby wpływać negatywnie na komórki oraz konieczność stosowania dodatkowych warstw ochronnych [A5].

Podsumowując, biodruk reprezentuje nowatorską i intensywnie rozwijającą się dziedzinę o znaczącym potencjale wdrożeniowym, zwłaszcza w kontekście medycyny regeneracyjnej oraz inżynierii tkankowej. Pomimo licznych osiągnięć, kluczowe elementy technologiczne wymagają dalszych usprawnień, aby umożliwić pełne wykorzystanie tej metody w skali przemysłowej. Rozwój technologii addytywnego wytwarzania i integracja polimerów naturalnych stawiają przed naukowcami wyzwania, których przezwyciężenie jest warunkiem koniecznym dla szerokiej adaptacji tej technologii. Kontynuacja prac badawczych będzie miała decydujący wpływ na przyszłość biodruku, prowadząc do stworzenia biomateriałów na masową skalę, co otworzy nowe możliwości w medycynie, czyli od modeli badawczych, przez nowe struktury tkankowe i organoidy, aż po całkowicie funkcjonalne narządy.

2 TEZA, CELE I ZAKRES PRAC BADAWCZYCH

Problem badawczy w przedstawionej rozprawie doktorskiej koncentruje się na opracowaniu i charakterystyce innowacyjnego układu hydrożelowego bazującego na polimerach naturalnych takich jak chitozan i agaroza. Wytypowane polimery mają stanowić bazę biotuszu, posiadającego zastosowanie w inżynierii tkankowej. Ten projekt badawczy wyróżnia się unikalnym połączeniem chitozanu z agarozą bez konieczności stosowania dodatkowych modyfikacji chemicznych polimerów oraz czynników sieciujących lub żelujących. Jest to nowe podejście zarówno w dziedzinie inżynierii tkankowej, jak i biodruku, gdyż w literaturze naukowej brakuje badań dotyczących hydrożeli opartych na agarozie i niemodyfikowanym chitozanie, które mogłyby stanowić bazę dla biotuszy komórkowych. Dzięki zastosowaniu innowacyjnej metody saturacji dwutlenkiem węgla możliwe jest przezwyciężenie tego ograniczenia i tym samym uzyskanie stabilnego hydrożelu chitozanowo-agarozowego, który żeluje pod wpływem zmiany temperatury. Innowacyjny charakter prowadzonych badań podkreśla dodatkowo fakt, że oprócz opracowywania bazy biotuszu, prace ukierunkowane zostały również

na dostosowaniu specyfikacji technicznych drukarki 3D, aby uzyskać pełną kompatybilność z nowym materiałem.

Potwierdzeniem innowacyjności i potencjału aplikacyjnego badań realizowanych w ramach pracy doktorskiej jest zgłoszenie do ochrony patentowej rozwiązania dotyczącego składu, zastosowania oraz sposobu wytwarzania kompozycji chitozanowo-agarozowej jako głównego składnika uniwersalnego biotuszu (P.443403 i EP.23460040). Zgłoszenie patentowe nie tylko chroni nowatorskie podejście do produkcji bazy biotuszowej, ale również podkreśla potencjał komercyjny i naukowy wynikający z możliwości jego zastosowania zarówno w medycynie i jak i w pracach badawczych.

Celem naukowym niniejszej pracy był dobór polimerów stanowiących bazę biotuszu oraz opracowanie metodologii ich utwardzania podczas wytwarzania addytywnego. Ponadto, prace badawcze zostały ukierunkowane na określenie podstawowych właściwości fizykochemicznych i biologicznych wytypowanych polimerów oraz ich kompozycji, a także parametrów reologicznych kluczowych dla potwierdzenia drukowalności układu oraz jego bezpieczeństwa biologicznego.

Celem aplikacyjnym o potencjale wdrożeniowym było wytworzenie rusztowania komórkowego możliwego do zastosowania w inżynierii tkankowej, które zapewni komórkom odpowiednie warunki do proliferacji i różnicowania.

Oczekiwanym efektem końcowym przeprowadzonych prac badawczych było stworzenie innowacyjnego biotuszu z wykorzystaniem polimerów pochodzenia naturalnego i prostej metody utwardzania roztworu hydrożelowego opartej na przejściu zol-żel pod wpływem temperatury, bliskiej tej fizjologicznej. Jednym z założeń projektu było zastosowanie polimerów bez konieczności ich modyfikacji chemicznej oraz stosowania dodatku czynników sprzęgających. Uzyskane wyniki miały nie tylko potwierdzić potencjał aplikacyjny kompozycji chitozanowo-agarozowej, ale również możliwość jej dalszej optymalizacji, zwłaszcza w kontekście ukierunkowywania proliferacji i różnicowania komórek w funkcjonalne i różne tkanki poprzez dodanie czynników wzrostu i bioaktywnych peptydów.

Przedstawiony projekt badawczy wpisuje się w nowoczesne standardy inżynierii tkankowej proponując nie tylko rozwiązanie istotnego problemu medycznego, ale również otwierając nowe perspektywy dla przyszłych badań naukowych i zastosowań w medycynie regeneracyjnej oraz w badaniach farmaceutycznych i biologicznych. Potwierdzenie aplikacyjnego potencjału prowadzonych badań oraz dalsze prace prowadzone nad optymalizacją opracowanego układu chitozanowo-agarozowego mogą przynieść pozytywne efekty dla rozwoju nauki, umacniając rolę biodruku jako kluczowej technologii inżynierii tkankowej.

Zakres prac przeprowadzonych w ramach niniejszej rozprawy doktorskiej:

- Przegląd literatury i wytypowanie polimerów stanowiących podstawę opracowywanej bazy biotuszu jak również określenie stosowanej metody sieciowania **[A5]**.
- Opracowanie metody usuwania endotoksyn z chitozanu w przypadku zagrożenia ich zbyt wysokiego stężenia w surowcu **[A1]**.
- Ocena właściwości fizykochemicznych i biologicznych chitozanu **[A2]**.
- Ocena możliwości zastosowania chitozanu w układzie z agarozą jako środka żelującego oraz określenie wpływu dodatku agarozy na właściwości fizykochemiczne i biologiczne chitozanu oraz układu chitozan-agaroza **[A3]**.
- Ocena możliwości zastosowania kompozycji chitozanowo-agarozowej w biodruku oraz jej aktywności biologicznej, obejmującej biozgodność, wpływ na proliferację i migrację komórek *in vivo* oraz regenerację tkanek *in vitro* **[A4]**.

Zakres prac przeprowadzonych w ramach rozprawy doktorskiej został schematycznie przedstawiony na Rysunku 4. Podzielono go na cztery główne bloki badawcze. Realizacja zadań w ramach bloków drugiego i trzeciego odbywała się równolegle, co wynikało z konieczności zapewnienia, że opracowany biotusz łączy w sobie optymalne właściwości fizykochemiczne oraz biologiczne.

Rysunek 4. Zarys struktury podziału prac badawczych w ramach rozprawy doktorskiej, z uwzględnieniem kluczowych etapów badawczych [opracowano za pomocą narzędzia Biorender.com]

3 REZULTATY BADAŃ

3.1 [A1] Innowacyjna metoda usuwania endotoksyn z hydrożelu chitozanowego jako potencjalnego składnika biotuszu otrzymywanego przez nasycenie dwutlenkiem węgla.

Nadrzędnym wymogiem stawianym surowcom wykorzystywanym w inżynierii tkankowej jest zapewnienie bezpieczeństwa biologicznego materiału. Zastosowanie surowców w sektorze medycznym wymaga bowiem spełnienia rygorystycznych międzynarodowych i krajowych regulacji farmaceutycznych [Sikora i wsp., 2021]. W literaturze naukowej często podkreśla się prostotę i dostępność surowców odpadowych, co może sugerować ich łatwe wdrożenie w praktyce przemysłowej. Jest to jednak nadmierne uproszczenie, pomijające złożone wymagania regulacyjne dotyczące bezpieczeństwa i jakości wyrobów medycznych. Surowce pochodzenia zwierzęcego, w tym morskiego, nie mogą być traktowane jako odpady w kontekście produkcji biomateriałów medycznych. Zgodnie z Rozporządzeniem (WE) nr 1069/2009 Parlamentu Europejskiego i Rady z dnia 21 października 2009 r., w wersji skonsolidowanej z dnia 14 grudnia 2019 r., produkty uboczne pochodzenia zwierzęcego są klasyfikowane w trzech kategoriach pod względem ryzyka dla zdrowia ludzi i zwierząt. W związku z tym, w kontekście medycznym kluczowe jest ich prawidłowe zakwalifikowanie. Tylko materiały należące do kategorii trzeciej mogą być używane w produkcji wyrobów medycznych, farmaceutycznych i kosmetycznych, pod warunkiem eliminacji ryzyka sanitarnego poprzez odpowiednie ich przetworzenie. Natomiast materiały kategorii pierwszej, stanowiące najwyższe ryzyko, są wykluczone z takiego zastosowania. Haładyj (2019) podkreśla, że istotne jest rozróżnienie pojęć odpadu i półproduktu. Otóż, odpady to substancje lub przedmioty, których posiadacz pozbywa się lub jest zobowiązany się pozbyć, zgodnie z Dyrektywą 2008/98/WE Parlamentu Europejskiego i Rady z dnia 19 listopada 2008 r., której aktualna wersja skonsolidowana obowiązuje od 18 lutego 2024 r. Z kolei półprodukty to materiały, które po przetworzeniu mogą być użyte w dalszej produkcji, np. wyrobów medycznych. W związku z powyższym surowce pochodzenia zwierzęcego stosowane w medycynie powinny być traktowane jako półprodukty, które ponadto, muszą spełniać rygorystyczne wymagania dotyczące ich odpowiedniego przetworzenia i oczyszczenia. Procesy te muszą skutecznie eliminować potencjalne zagrożenia biologiczne, w tym wirusy, bakterie i priony, co wymaga zaawansowanych technologii i dokładnej walidacji. Właśnie dlatego Rozporządzenie Komisji (UE) nr 722/2012 z dnia 8 sierpnia 2012 r. nakłada dodatkowe wymogi dla wyrobów medycznych wykorzystujących tkanki pochodzenia zwierzęcego, podkreślając konieczność minimalizacji ryzyka przeniesienia patogenów. Ponadto, nie tylko wyroby medyczne, ale i surowce oraz materiały do nich użyte muszą być kontrolowane zgodnie z aktualnymi normami, takimi jak ISO 10993 dotyczącą oceny biologicznej wyrobów medycznych. Normy te obejmują

m.in. ocenę biokompatybilności, toksyczności i ich pirogenności. Przeprowadzenie takich testów gwarantuje, że surowce spełniają rygorystyczne standardy bezpieczeństwa wymagane w medycynie. Ponadto, wyroby medyczne oraz materiały i surowce wykorzystywane do ich produkcji podlegają szeregowi innych, szczegółowych regulacji, mających na celu zapewnienie bezpieczeństwa pacjentów oraz spełnienie rygorystycznych norm rynkowych. Jednym z kluczowych dokumentów jest Rozporządzenie w sprawie wyrobów medycznych (UE) 2017/745 MDR (Medical Devices Regulation), które obowiązuje od maja 2021 roku i nakłada na producentów obowiązek spełnienia zaostrzonych wymogów dotyczących ich jakości i bezpieczeństwa. W szczególności MDR wymaga, aby materiały stosowane w produkcji, w tym pochodzenia zwierzęcego, były poddawane dokładnej analizie ryzyka oraz szczegółowej ocenie biokompatybilności, co komplikuje proces wprowadzania tych surowców do biomateriałów. Wymóg pełnej identyfikowalności wyrobów i ich składników obejmuje również surowce pochodzenia zwierzęcego, dla których MDR wymaga najwyższej jakości i potwierdzonego bezpieczeństwa. Kompleksowe podejście do spełnienia wymogów jest zatem kluczowe, szczególnie w przypadku biomateriałów, gdzie aspekty technologiczne i regulacyjne muszą być w pełni zharmonizowane, aby umożliwić wdrożenie takich surowców na poziomie przemysłowym.

Jedną z kluczowych kwestii standardów medycznych jest konieczność zapewnienia w surowcu odpowiednio niskiego stężenia endotoksyn, określanego często w specyfikacji produktu jako „wolne od endotoksyn”. Chitozan na tle większości polimerów cechuje się unikalną właściwością jaką jest występowanie w formie polikationu. Wykazuje więc tendencję do interakcji z ujemnie naładowanymi grupami fosforanowymi w lipopolisacharydach, czyli endotoksynach [Lieder i wsp., 2013], które mogą przedostawać się do roztworu również podczas jego przygotowywania między innymi z wody lub ze środowiska. Lipopolisacharydy znajdują się w zewnętrznej membranie komórkowej bakterii Gram-ujemnych, stanowiąc jej integralną część. W związku z tym, że endotoksyny są cząsteczkami termostabilnymi są trudne do usunięcia. Co więcej, w przypadku ich nadmiernego stężenia w krwiobiegu powodują ciężkie zakażenia bakteriami Gram-ujemnymi, posocznicę, a nawet wstrząs septyczny. Śmiertelność pacjentów z zakażeniami endotoksynami waha się w granicach 20-50% [Heine i wsp., 2001]. Zgodnie ze standardami medycznymi w zależności od zastosowania produktu dopuszczalne są dwa różne limity ich występowania w produkcie medycznym, czyli 5,0 EU/kg masy ciała człowieka dla wszystkich wyrobów medycznych i farmaceutycznych z wyjątkiem tych podawanych dootrzewnowo, dla których limit wynosi odpowiednio 0,2 EU/kg masy ciała [Dawson, 2017]. Jednostka biologicznej aktywności endotoksyn (EU), odnosi się do określonej masy standardowej endotoksyny, która w zależności od jej źródła może się różnić. Przykładowo, Amerykańska Agencja ds. Żywności i Leków zdefiniowała tę jednostkę jako aktywność biologiczna 0,2 ng referencyjnego standardu endotoksyny EC-2, co odpowiada 5 EU/ng. Z kolei obecny przelicznik dla standardu EC-6 wynosi około 10 EU/ng. [Kimble i wsp., 2023] W związku z powyższym, za kryterium akceptacji

pozwalające ocenić możliwości zastosowania chitozanu w inżynierii tkankowej postawiono za cel opracowanie alternatywnej metody otrzymywania roztworu tego polimeru z dodatkowym etapem usuwania obecnych w surowcach użytych do jego przygotowania zanieczyszczeń, w tym endotoksyn. Dodatkowym celem przeprowadzonych badań było zbadanie, czy chitozany o różnych masach cząsteczkowych wykazują zróżnicowane powinowactwo do endotoksyn i jaka jest wydajność ich usuwania w zależności od zmienności tego parametru.

Na podstawie dostępnych surowców chitozanowych wytypowano te, dla których zawartość endotoksyn w 1% roztworach chitozanu o niskiej (LMW), średniej (MMW) i wysokiej (HMW) masie cząsteczkowej rozpuszczonych w 0,1M kwasie hydroksyoctowym była największa. Dodatkowo na podstawie przeglądu literaturowego zdefiniowano kluczowe etapy pozwalające na redukcję stężenia endotoksyn. Przykładowo Lebre i wsp. (2019) uzyskali wolne od endotoksyn cząsteczki chitozanu stosując kilkuetapowe oczyszczanie surowca. W pierwszej kolejności, endotoksyny usuwano stosując 1M roztwór KOH. Następnie chitozan rozpuszczono w 1% roztworze kwasu octowego. Oczyszczony surowiec strącono roztworem NaOH i poddano liofilizacji. Po każdym etapie przemywania roztworem zasady, chitozan przemywano kilkukrotnie wodą wolną od pirogenów. W innym badaniu wykazano, że zastosowanie do ekstrakcji endotoksyn chloroformu pozwala na usunięcie z roztworów niekowalencyjnie związanych lipidów, m.in. lipidu A, który jest składnikiem lipopolisacharydów i który stanowi toksyczny element endotoksyn [Morrison i Leive, 1975]. Na tej podstawie, opracowano dwie procedury redukcji stężenia endotoksyn, stanowiące zarazem modyfikację metody otrzymywania roztworów chitozanu z wykorzystaniem saturacji dwutlenkiem węgla [Gorczyca i wsp., 2014] i sprawdzono ich efektywność. Każda z metod zawierała te same etapy oczyszczania, jednakże ich kolejność różniła się. W pierwszym wariancie (Rys. 5A) chitozan rozpuszczony w 0,1M kwasie hydroksyoctowym, został przemyty chloroformem przed etapem jego strącenia w 0,5M wodorotlenku sodu. W wariancie drugim (Rys. 5B), chloroform został użyty po etapie strącenia chitozanu. Wszystkie osady, zostały wielokrotnie przemyte wodą destylowaną wolną od endotoksyn, zawieszone w niej, zhomogenizowane, a następnie wysterylizowane w autoklawie w temperaturze 121°C w czasie 20 min. Kolejnym krokiem była saturacja zawiesiny dwutlenkiem węgla, w celu rozpuszczenia chitozanu.

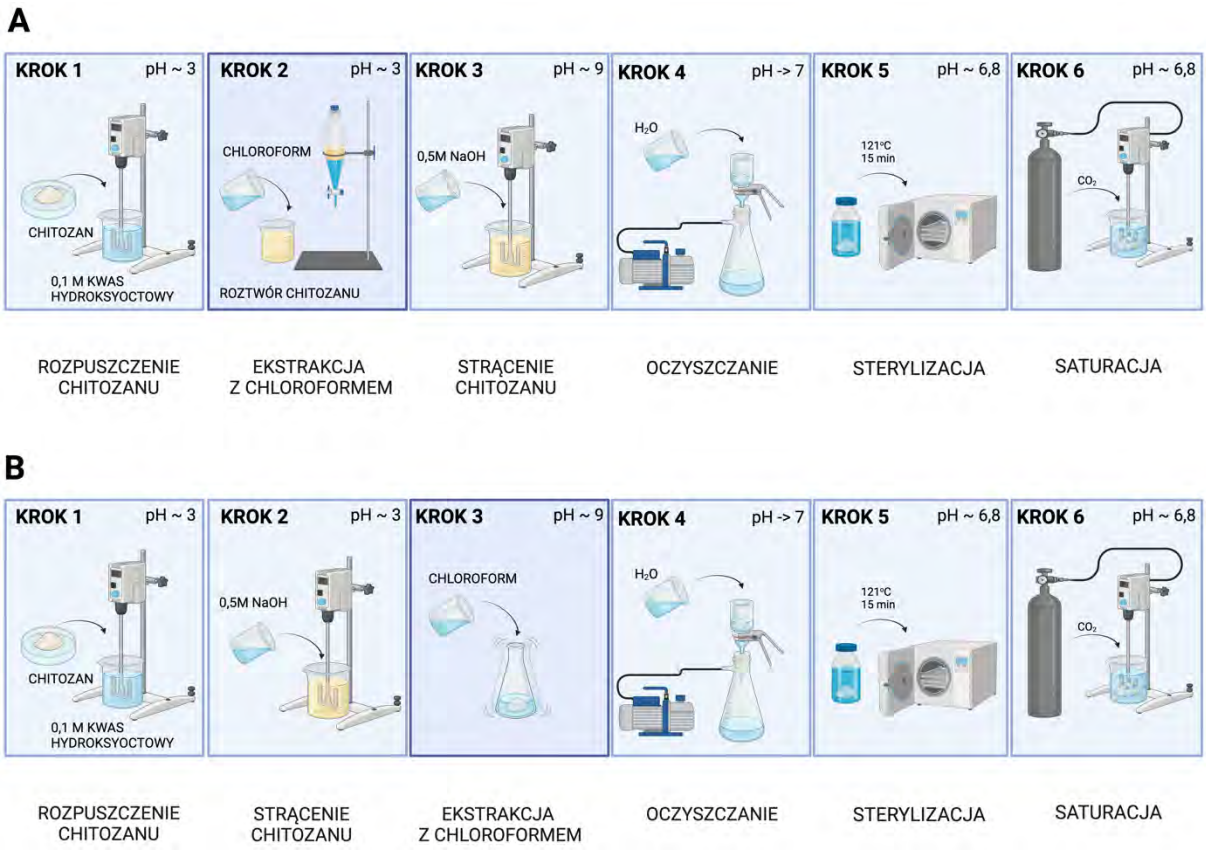

Rysunek 5. Schemat oczyszczania hydrożelu chitozanu przy użyciu metod A) M1 i B) M2 [opracowano z wykorzystaniem Biorender.com]

W celu zbadania wpływu zastosowanych metod oczyszczania roztworów chitozanu i określenia w nich stężenia endotoksyn, do badań użyto test PyroGene rFC Enzymatic Cascade. Istotne jest, że w przeciwieństwie do standardowego i powszechnie stosowanego testu LAL, test rekombinowanego czynnika C (rFC) jest bardziej czuły, powtarzalny i swoisty w oznaczaniu endotoksyn [Reich i Deutschmann, 2020].

Analiza wyników uzyskanych przy użyciu powyżej opisanego testu rFC wykazała, że zawartość endotoksyn zmniejszyła się o 87,9 do 97,6%, względem wartości początkowej mieszczącej się w zakresie od 18,1 do 25,2 EU/mL (Rys. 6A). Wzrost wydajności usuwania endotoksyn zaobserwowano wraz ze wzrostem masy cząsteczkowej chitozanu. Co więcej metoda, w której zanieczyszczenia były ekstrahowane z roztworu chitozanu była o 6-7% bardziej skuteczna, w porównaniu z metodą ekstrakcji zanieczyszczeń z osadu chitozanu po jego strąceniu. Obserwacja ta wynikała ze zwiększonej powierzchni wymiany masy, gdy ekstrakcja odbywała się na granicy faz ciecz-ciecz. Metodą dodatku wzorca potwierdzono także większe powinowactwo endotoksyn do chitozanu LMW, które malało ze wzrostem masy cząsteczkowej tego polimeru.

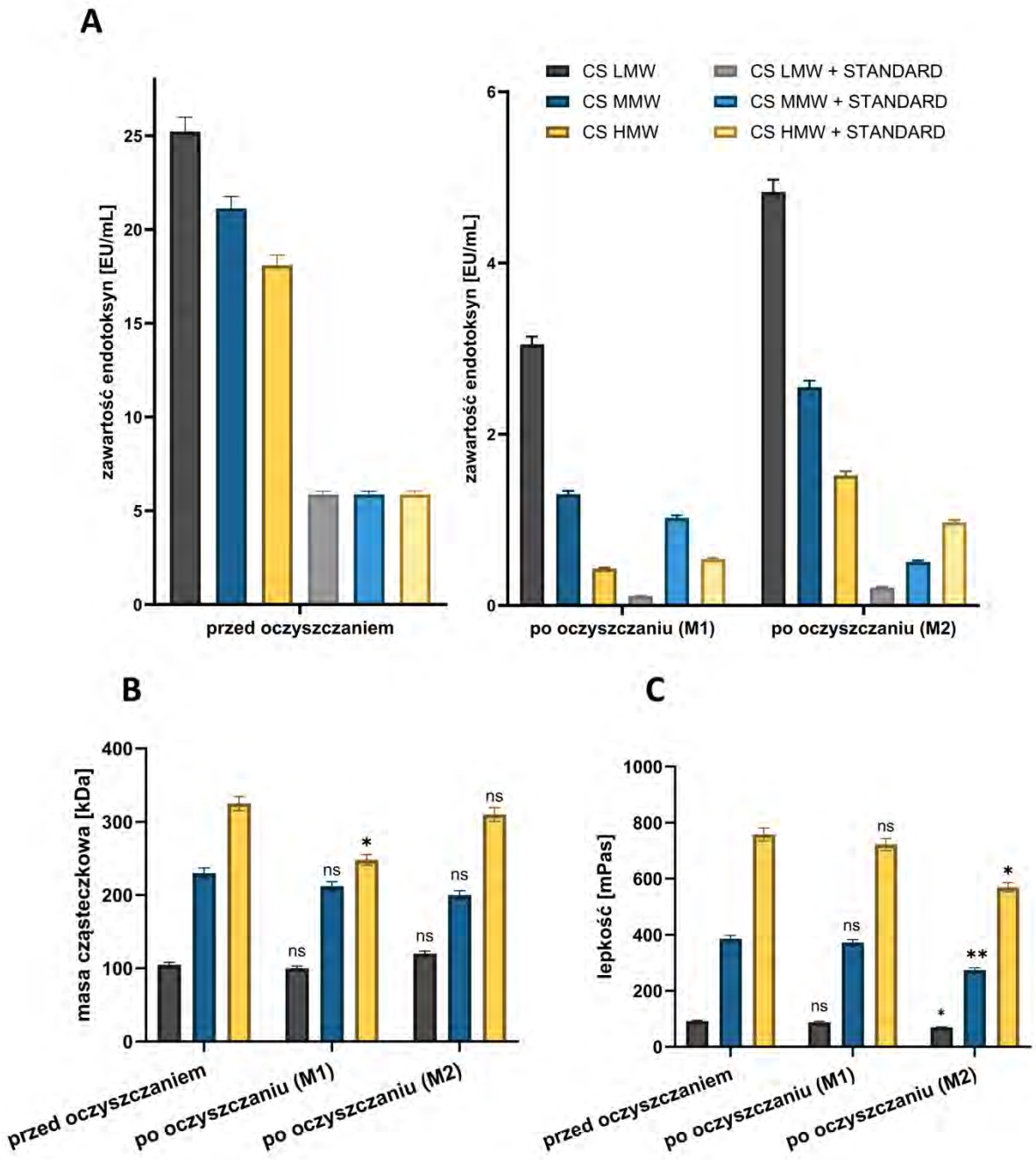

Rysunek 6. Porównanie A) zawartości endotoksyn w hydrożelach chitozanowych (CS) o różnych masach cząsteczkowych: niskiej (LMW), średniej (MMW) i wysokiej (HMW), oraz w standardowych roztworach endotoksyn (STANDARD) po kontakcie z CS o różnych masach cząsteczkowych, B) mas cząsteczkowych chitozanu, oraz C) lepkości hydrożeli chitozanowych przed i po oczyszczeniu metodą M1 lub M2. Wyniki przedstawiono jako średnią ± odchylenie standardowe (SD) na podstawie trzech powtórzeń (n = 3, $p < 0,05$). Wartości na wykresach B i C porównano względem prób kontrolnych (przed oczyszczeniem). Oznaczenia poziomów istotności statystycznej są następujące: ns (nieistotne statystycznie) $p > 0,05$, *$p < 0,05$, **$p < 0,01$.

Opracowaną metodę oczyszczania chitozanu oceniono także pod kątem wpływu na parametry fizykochemiczne takie jak masa cząsteczkowa (Rys. 6B) i lepkość (Rys. 6C) chitozanu. Lepkość dynamiczną roztworów chitozanu o stężeniu 1% zmierzono za pomocą wiskozymetru Brookfield Digital Model DVIII Ultra z termostatowaną komorą pomiarową. Pomiary wykonano przy użyciu wrzeciona SC4-27 i SC4-25 w temperaturze 25°C i naprężeniu ścinającym 22,0 1/s. Średnią masę cząsteczkową oznaczono według metodyki zaproponowanej przez Yacob i wsp. (2013) z wykorzystaniem wiskozymetru kapilarnego Ubbelohde typ 531/10. Wykazano, że metoda ekstrakcji chloroformem endotoksyn z roztworu chitozanu nie tylko zwiększa efektywność usuwania tych zanieczyszczeń, ale również powoduje najmniejsze zmiany w lepkości roztworu chitozanu, zaledwie o 3,6-4,7%. Z kolei druga z metod oczyszczania, choć nie powodowała istotnych zmian w masie cząsteczkowej, to przyczyniała się do zmiany lepkości roztworów nawet o 29%. Tak znacząca zmiana w lepkości roztworu chitozanu, w przypadku przemywania jego osadu chloroformem, wynika najprawdopodobniej z dużych strat chitozanu na tym etapie, spowodowanych naruszeniem strąconego osadu.

W celu określenia bezpieczeństwa biologicznego zaproponowanej metody usuwania endotoksyn przeprowadzono test MTT z wykorzystaniem linii L929 zgodnie z normą ISO 10993-5:2009(E). Test ten przeprowadzono dla 1% roztworów chitozanu MMW otrzymanych metodą rozpuszczenia w kwasie hydroksyoctowym, metodą saturacji dwutlenkiem węgla z i bez uwzględnia w procedurze etapu przemywania chloroformem. Wykazano, że ekstrakty hydrożelu chitozanu rozpuszczonego w kwasie hydroksyoctowym znacząco zahamowały wzrost komórek już przy najniższym jego rozcieńczeniu, tj. 1:1, czyli 0,5% m/v chitozanu (około 20% przeżywalności w porównaniu do kontroli). Porównując ekstrakty z hydrożelu chitozanu nasyconego dwutlenkiem węgla przed i po etapie oczyszczania, zauważono znaczące różnice. Stwierdzono, że ekstrakt z oczyszczonego hydrożelu chitozanowego przy rozcieńczeniu 1:1 (0,5% m/v) spowodował redukcję przeżywalności komórek L929 o około 50% w stosunku do kontroli. W przypadku pozostałych rozcieńczeń, tj. 1:3 i 1:6 (0,33–0,17% m/v chitozanu), żaden z roztworów nie był cytotoksyczny, utrzymując przeżywalność komórek L929 na poziomie ponad 70%. Z kolei ekstrakty z hydrożelu chitozanu rozpuszczonego metodą saturacji dwutlenkiem węgla, nie poddane dodatkowemu etapowi oczyszczania chloroformem, nie wykazywały cytotoksyczności względem tej linii komórkowej przy żadnym z zastosowanych rozcieńczeń, od 1:1 do 1:6 (0,5-0,17% m/v chitozanu).

W celu potwierdzenia potencjału opracowanej metody usuwania endotoksyn wykonano dodatkowo zdjęcia mikroskopowe (Rys. 7) na podstawie których wywnioskowano, że zwiększenie ilości usuwanego chloroformu na etapie ekstrakcji, wydłużenie czasu nasycania dwutlenkiem węgla albo ilość wody płuczącej osad, może przyczynić się do lepszego usunięcia pozostałości chloroformu, który może być główną przyczyną obniżenia żywotności komórek. Morfologia komórek po 24-godzinnym kontakcie z badanym materiałem przy rozcieńczeniu 1:3 (0,33 % m/v chitozanu) potwierdziła, że pomimo przeżywalności fibroblastów powyżej 70% w obecności ekstraktu

z roztworu chitozanu w kwasie hydroksyoctowym, komórki uległy skurczeniu i utraciły swoją charakterystyczną morfologię. W przypadku pozostałych metod, obejmujących chitozan rozpuszczony metodą saturacji dwutlenkiem węgla bez dodatkowego etapu oczyszczania oraz z uwzględnieniem etapu oczyszczania metodą M1, komórki L929 zachowały typowy dla fibroblastów kształt.

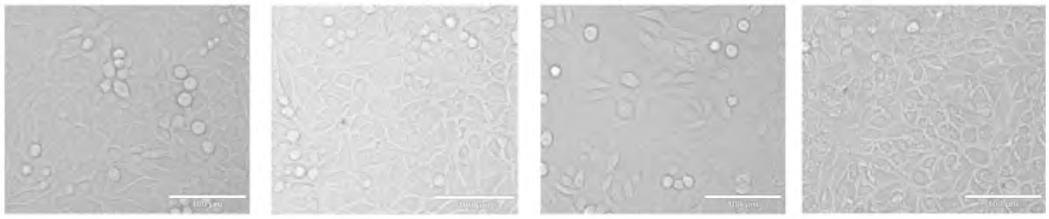

Rysunek 7. Reprezentatywne obrazy (n = 4) morfologii komórek L929 traktowanych ekstraktami 1:3 rozpuszczonymi w pożywce komórkowej: chitozanu po oczyszczeniu pierwszą metodą (M1), chitozanu rozpuszczonego metodą saturacji dwutlenkiem węgla (CO_2) i chitozanu rozpuszczonego w kwasie hydroksyoctowym (HA) przed oczyszczeniem. Skala wynosi 100 µm.

Podsumowując, obniżona przeżywalność komórek po kontakcie z materiałem oczyszczonym metodą przemywania roztworu chitozanu chloroformem wynika z niedostatecznego usunięcia jego pozostałości, co może być skorygowane podczas jednego z trzech etapów przygotowywania roztworu chitozanu tj. ekstrakcji i usunięcia fazy nieorganicznej, etapu przemywania osadu wodą wolną od endotoksyn oraz podczas saturacji dwutlenkiem węgla. Dużą zaletą jest fakt, że opracowana metoda nie powoduje istotnych zmian we właściwościach fizykochemicznych chitozanu oraz nie powoduje zmian w morfologii komórek po ich 24-godzinnym kontakcie z ekstraktem przygotowanym z tego materiału przy rozcieńczeniu 1:3 (0,33% m/v chitozanu). Przedstawione wyniki badań dotyczą chitozanów, dla których ilość zawartych w nich endotoksyn na etapie wytypowania surowców była największa i tym samym możliwe było wykazanie skuteczności opracowanych metod ich usuwania. W związku z tym, że na rynku dostępne są surowce przygotowane zgodnie ze standardami pozwalającymi na zastosowanie chitozanu w inżynierii tkankowej i które zostały użyte w dalszych badaniach, niniejsza metoda stanowi jedynie alternatywę dla surowców nie spełniających standardy medyczne z punktu widzenia zanieczyszczenia endotoksynami. Ma to szczególne znaczenia w przypadku surowców pochodzenia naturalnego, dla których zmienność jest ich standardową cechą.

3.2 [A2] Wpływ masy cząsteczkowej i stopnia deacetylacji kserożeli chitozanowych na ich aktywność przeciwdrobnoustrojową i cytotoksyczność. Porównanie materiałów chitozanowych otrzymanych przy użyciu kwasu mlekowego i nasycania CO_2.

Kluczową kwestią przed rozpoczęciem badań jest określenie podstawowych parametrów używanych surowców, które będą wpływać na właściwości biologiczne jak i fizykochemiczne opracowywanych materiałów. W przypadku kompozycji chitozanowo-agarozowej, to właśnie chitozan, a dokładniej jego parametry takie jak masa cząsteczkowa i stopień deacetylacji (DD), mogą wpływać na biokompatybilność układu, jego właściwości przeciwdrobnoustrojowe, cytotoksyczność, a także na właściwości reologiczne, które będą z kolei decydować o drukowalności biotuszu. W związku z tym, że w specyfikacji dostarczonej przez producenta, są zawarte ogólne informacje na temat masy cząsteczkowej chitozanu jak i jego DD, w pierwszej kolejności dokonano jego szczegółowej charakterystyki. Stosując metodę miareczkowania potencjometrycznego wyznaczono DD chitozanów, czyli procentowy udział wolnych grup aminowych w odniesieniu do sumy obecnych w łańcuchu polimerowym grup aminowych wolnych i zdeacetylowanych. Zgodnie ze specyfikacją chemiczną, DD chitozanów LMW, MMW i HMW były ≥75% i wynosiły odpowiednio około 75,7 ± 5,7%, 81,7 ± 4,8% i 78,8 ± 1,5 % nie różniąc się w sposób statystycznie istotny. Z kolei dla chitozanów HMW otrzymywanych z pancerzy krewetek i krabów DD wynosiły 66,2 ± 3,1% i 83,2 ± 4,6%. Średnie masy cząsteczkowe chitozanów oznaczono metodą pośrednią na podstawie pomiarów lepkości dynamicznej, wykorzystując wiskozymetr Brookfield Digital Model DVIII Ultra z termostatowaną łaźnią. Wiskozymetr skalibrowano przy użyciu wzorcowych olejów mineralnych o lepkościach 10 mPas, 100 mPas i 12500 mPas dla wrzecion SC4-18, SC4-27 i SC4-25, dostosowanych do zakresu lepkości mierzonych roztworów. Lepkość zmierzono dla 1% roztworów chitozanu w 1% roztworze kwasu octowego w temperaturze 25°C, stosując odpowiednie wrzeciono. Na podstawie zależności między lepkością a masą cząsteczkową wyznaczono parametry chitozanów o nieznanych wartościach masy cząsteczkowej, które wyniosły odpowiednio 89, 280, 592 kDa dla LMW, MMW i HMW oraz 545 i 4000 kDa dla chitozanów HMW pozyskanych odpowiednio z pancerzy krewetek oraz krabów.

W dalszym kroku, określono aktywność przeciwdrobnoustrojową pięciu testowanych chitozanów oraz ich cytotoksyczność względem linii komórkowej L929. Bezpieczeństwo biologiczne jest kluczowym kryterium pozwalającym na zastosowanie danego surowca w inżynierii tkankowej. Z kolei wykazanie dodatkowej właściwości jaką jest aktywność przeciwdrobnoustrojowa, stanowi wartość dodaną, która pozwala na samozabezpieczenie materiału przed namnażaniem niepożądanej mikroflory. W związku z tym, że w literaturze dostępnych jest wiele informacji oraz badań potwierdzających wpływ masy cząsteczkowej i DD chitozanu na jego właściwości przeciwdrobnoustrojowe [Chandrasekaran i wsp., 2020; Hosseinnejad i Jafari, 2016],

postawiono za cel sprawdzenie jak powyżej określone parametry będą wpływać na właściwości biologiczne materiałów chitozanowych otrzymanych zastosowaną w niniejszej rozprawie doktorskiej metodą jego rozpuszczenia w kwasie węglowym. Ponadto, właściwości biologiczne roztworów chitozanu otrzymanych powyższą metodą porównano z działaniem chitozanów rozpuszczonych w 0,1M kwasie mlekowym. Aktywność przeciwdrobnoustrojową oznaczono zmodyfikowaną metodą ilościową ASTM E2149 wobec bakterii z grupy Gram-dodatnich *Staphylococcus aureus* i Gram-ujemnych *Escherichia coli.* W tym celu kserożelowe próby chitozanów inkubowano przez 24-godziny z odpowiednio wcześniej przygotowanym inokulum, a następnie po wyekstrahowaniu komórek bakterii do roztworu PBS wykonano seryjne rozcieńczenia i posiewy metodą zalewową. Przeprowadzone doświadczenie wykazało, że metoda przygotowania roztworu chitozanu w sposób istotny wpływa na jego aktywność przeciwdrobnoustrojową (Rys. 8). Wszystkie próby chitozanu otrzymane poprzez jego rozpuszczenie w 0,1M kwasie mlekowym charakteryzowały się wysoką aktywnością przeciwdrobnoustrojową, nie różniąc się w sposób statystycznie istotny pomiędzy poszczególnymi masami cząsteczkowymi i DD. Co więcej, wykazano silny efekt bakteriobójczy, o którym świadczy redukcja komórek bakteryjnych wynosząca ponad 5 rzędów w skali logarytmicznej. Tak wysoka aktywność jest wynikiem obecności pozostałości kwasu mlekowego w materiałach po ich liofilizacji, który niezbędny jest do rozpuszczenia chitozanu w klasycznych i dobrze poznanych metodach jego przetwarzania. Sprawdzając kolejno pH zawiesin kserożeli chitozanowych wykazano, że wynosi ono około 3,5, potwierdzając tym samym obecność kwasu w materiałach, który przyczynił się do degradacji błon komórkowych i wycieku składników wewnątrzkomórkowych na zewnątrz komórki. Zróżnicowaną aktywność przeciwdrobnoustrojową wykazano z kolei dla chitozanów otrzymanych metodą saturacji dwutlenkiem węgla. Dla prób chitozanu MMW i HMW o DD 83%, otrzymanych z wykorzystaniem metody saturacji dwutlenkiem węgla, redukcja liczby bakterii *E. coli* wyniosła około 1 rzędu logarytmicznego. W przypadku pozostałych prób aktywność ta była porównywalna z uzyskaną dla chitozanu rozpuszczonego w kwasie mlekowym. Redukcja liczby kolonii bakterii *S. aureus* przez materiały chitozanowe, uzyskane techniką saturacji dwutlenkiem węgla, była znacznie niższa niż dla materiałów z pozostałością kwasu mlekowego; np. 4,5 i 3 rzędy logarytmiczne redukcji stwierdzono dla chitozanu LMW i HMW o DD 66.

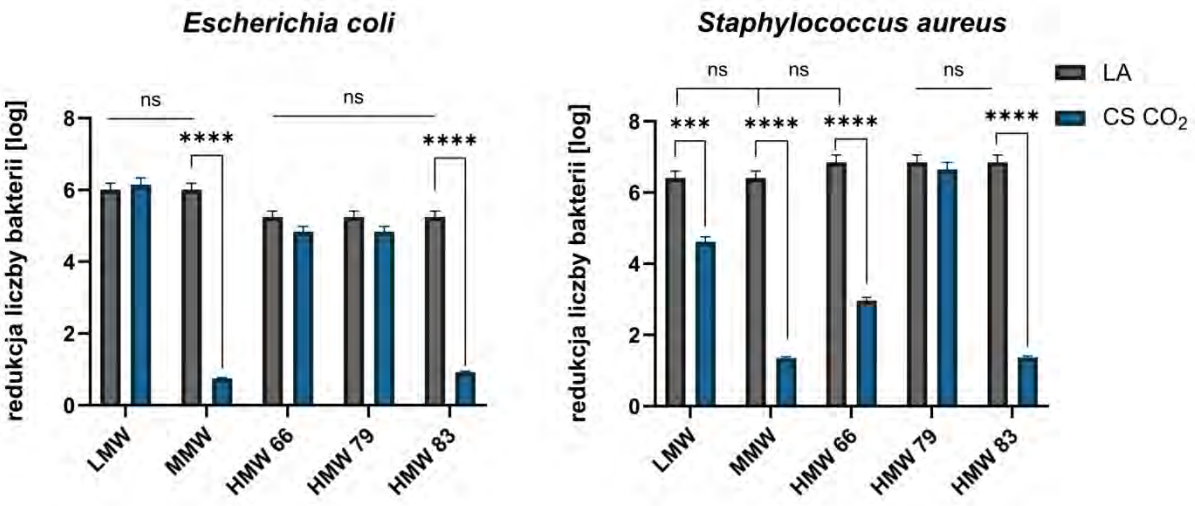

Rysunek 8. Aktywność przeciwdrobnoustrojowa wobec *Escherichia coli* i *Staphylococcus aureus* dla chitozanów o różnej masie cząsteczkowej: niskiej (LMW), średniej (MMW) i wysokiej (HMW) oraz chitozanów HMW o różnym stopniu deacetylacji 66, 79 i 83 rozpuszczonych w kwasie mlekowym (LA) oraz chitozanów rozpuszczonych metodą saturacji dwutlenkiem węgla (CS CO_2). Wyniki przedstawiono jako średnią ± odchylenie standardowe (SD) na podstawie trzech powtórzeń (n = 3, $p<0,05$). Istotność statystyczną różnic między poszczególnymi grupami oznaczono odpowiednio jako: ns (nieistotne statystycznie) $p > 0,05$, ***$p < 0,001$, ****$p < 0,0001$.

Brak ścisłego związku pomiędzy masą cząsteczkową i DD a aktywnością przeciwdrobnoustrojową wynika nie tylko z różnic w budowie ścian bakterii Gram-dodatnich i Gram-ujemnych, ale także z różnych mechanizmów, opisywanych w literaturze dla chitozanów różniących się wspomnianymi powyżej parametrami. Chitozany o LMW, w przypadku bakterii Gram-ujemnych, zdolne są przenikać przez ich ścianę komórkową, a chitozany o większej masie cząsteczkowej wykazują tendencję do tworzenia błony polimerowej na powierzchni komórek [Feng i wsp., 2021; Zheng i Zhu, 2003]. W przypadku DD, wraz z jego wzrostem, przy jednoczesnym spadku pH, poprawiają się właściwości przeciwdrobnoustrojowe. Jeśli pH roztworu chitozanu jest poniżej jego pKa, czyli 6,3, to sprotonowane grupy aminowe oddziałują z ujemnie naładowanymi błonami komórek bakteryjnych powodując ich destabilizację i śmierć [Helander i wsp., 2001]. W przypadku chitozanu otrzymanego z wykorzystaniem metody nasycania dwutlenkiem węgla, dodatni ładunek na jego grupach jest znikomy, przez co interakcje elektrostatyczne pomiędzy polimerem a błoną są znacznie słabsze. Prawdopodobny mechanizm aktywności przeciwdrobnoustrojowej chitozanów przetwarzanych z wykorzystaniem metody saturacji dwutlenkiem węgla, może być rezultatem zdolności do chelatowania jonów metali zlokalizowanych na powierzchni komórki. Mechanizm ten jest dodatkowo intensyfikowany, przy pH 6,5. Na tym etapie następuje deprotonowanie grup aminowych, poprzez oddawanie wolnej pary elektronowej zlokalizowanej na atomie azotu [Goy i wsp., 2006].

Przeprowadzając dalsze badania nad wpływem MW i DD chitozanów na cytotoksyczność względem komórek L929 wykazano, że ekstrakty roztworów chitozanu otrzymanych metodą ich rozpuszczania w 0,1M kwasie mlekowym, przy rozcieńczeniu 1:1 (0,5% m/v chitozanu) wykazują silny efekt cytotoksyczny. Również morfologia komórek po 24-godzinnym kontakcie była nieprawidłowa, a ich liczba znacznie mniejsza w odniesieniu do kontroli, co wskazuje na zahamowanie ich proliferacji. W przypadku prób chitozanów otrzymanych metodą saturacji dwutlenkiem węgla przy rozcieńczeniu 1:1 (0,5% m/v chitozanu) również stwierdzono obniżoną przeżywalność komórek L929. Są to wyniki sprzeczne z danymi uzyskanymi podczas opracowywania metody redukcji stężenia endotoksyn z roztworów chitozanu. W tym badaniu wykazano, że przeżywalność komórek w obecności ekstraktów z roztworu chitozanu rozpuszczonego w kwasie węglowym przy rozcieńczeniu 1:1, co odpowiada 0,5% m/v chitozanu, wynosi powyżej 80% [A2]. Analizując dokładnie powyższe wyniki oraz etapy otrzymywania chitozanu metodą saturacji dwutlenkiem węgla jedynym powodem, który mógł mieć wpływ na wywołanie efektu cytotoksycznego była pozostałość soli sodowej kwasu hydroksyoctowego. Po etapie rozpuszczenia chitozanu w kwasie, polimer zostaje strącony wodorotlenkiem sodu, a następnie przemywany. Podczas usuwania endotoksyn zwiększono ilość wody płuczącej, celem wypłukania jak największej ilości chloroformu, stanowiącego potencjalne zanieczyszczenie. W związku z tym, że w zależności od masy cząsteczkowej, struktura osadu różni się, możliwe jest, że również w przypadku LMW i HMW istnieje konieczność zwiększenia ilości wody płuczącej, celem wypłukania uwięzionych zanieczyszczeń w formie resztek soli kwasu hydroksyoctowego. W związku z powyższym przeprowadzono ponowną analizę wpływu masy cząsteczkowej i DD na aktywność przeciwdrobnoustrojową chitozanu otrzymanego metodą saturacji dwutlenkiem węgla, w kolejnej publikacji stanowiącej część cyklu publikacyjnego [A3].

Podsumowując, nie stwierdzono ścisłego związku między aktywnością przeciwdrobnoustrojową chitozanu, a ich DD. Tylko w przypadku bakterii Gram-ujemnych zaobserwowano malejący trend aktywności przeciwdrobnoustrojowej wraz ze wzrostem DD. Interesujący przykład stanowi próba HMW o DD 66, która wykazuje dwa różne efekty tj. bakteriobójczy wobec *E. coli* i bakteriostatyczny wobec *S. aureus*. Wyniki te dowodzą, że stopień oczyszczenia chitozanu z pozostałości soli powstałych podczas jego strącania w procedurze ma ogromne znaczenie. Przeprowadzone badania dowodzą, że konieczne jest zastosowanie nieznacznej modyfikacji opracowywanej metody otrzymywania roztworów chitozanu poprzez ich rozpuszczenie w kwasie węglowym, polegającej na zwiększeniu ilości wody płuczącej osadu polimeru, tak aby móc uzyskać materiały o wysokim stopniu bezpieczeństwa biologicznego.

3.3 [A3] Potencjał nowej, termoczułej kompozycji przeciwdrobnoustrojowej na bazie agarozy i chitozanu nasyconego CO_2 dla technologii biodruku.

Jednym z pierwszych, ale i zarazem głównych wyzwań podczas prac badawczych nad biodrukiem jest wytypowanie surowców stanowiących bazę biotuszu. Ich właściwości fizykochemiczne oraz biologiczne to główne czynniki warunkujące ich właściwości użytkowe, m. in charakterystykę płynięcia, czyli drukowalność, a w konsekwencji teksturę wydruków, czy też czas ich biodegradacji. Co więcej, dobór surowców będzie determinował konieczność zastosowania odpowiedniego mechanizmu sieciowania oraz ustalenia określonego zakresu parametrów procesu biodruku.

Połączenie dwóch lub większej ilości składników nie zawsze prowadzi do uzyskania mieszaniny charakteryzującej się wyłącznie korzystnymi cechami połączonych surowców. Zasada ta także dotyczy materiałów polimerowych, łączonych w kompozycje podczas otrzymywania biotuszy. Jednym z negatywnych skutków łączenia hydrożeli agarozy i chitozanu jest pogorszenie zdolności żelowania w odniesieniu do czystego hydrożelu agarozowego na skutek zaburzenia interakcji pomiędzy cząsteczkami agarozy. Efektem tego jest dłuższy czas żelowania i/lub obniżenie temperatury żelowania. Kolejnym negatywnym aspektem jest możliwość uzyskania kompozycji pozbawionej właściwości przeciwdrobnoustrojowych, pomimo obecności w niej chitozanu. Właściwość ta nie jest kluczowa i wymagana dla tego typu układów, ale jest jednym z powodów, dla których chitozan został wytypowany z szeregu innych polimerów naturalnych jako główny składnik biotuszu. Właściwości przeciwdrobnoustrojowe biotuszu pozwalają na ograniczenie ryzyka jego kontaminacji podczas przygotowywania, drukowania oraz podczas inkubacji wydruku zasiedlonego komórkami. Znając zalety i wady stosowanych polimerów oraz możliwe zagrożenia i korzyści płynące z ich połączenia, konieczne było przeprowadzenie badań, które potwierdzą możliwość zastosowania kompozycji chitozanowo-agarozowej w biodruku oraz określenie optymalnego udziału obu polimerów w niej zawartych. Proces przygotowania kompozycji chitozanowo-agarozowej, jak również schemat metody otrzymywania chitozanu metodą saturacji dwutlenkiem węgla, został przedstawiony na Rysunku 9.

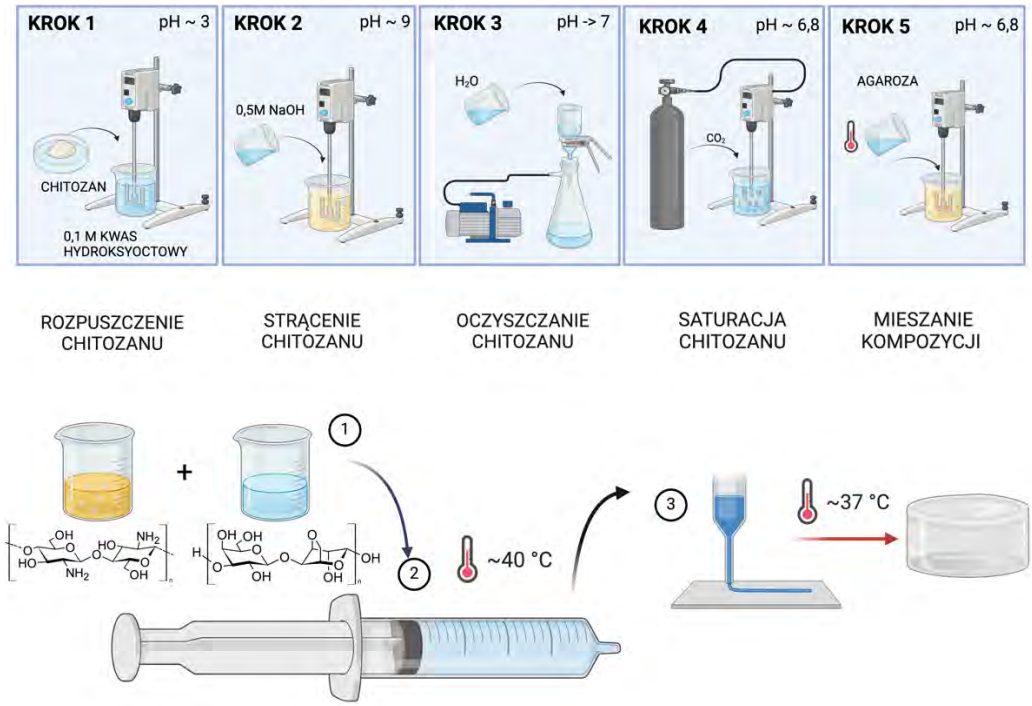

Rysunek 9. Schemat przygotowania kompozycji chitozanowo-agarozowej wraz z metodą otrzymywania chitozanu metodą saturacji dwutlenkiem węgla [opracowano z wykorzystaniem Biorender.com]

W ramach prowadzonych badań scharakteryzowano kompozycje chitozanowo-agarozowe różniące się udziałem obu polimerów oraz masami cząsteczkowymi użytych do ich wytworzenia chitozanów. Po przeprowadzeniu charakterystyki mas cząsteczkowych oraz DD chitozanów [A2] i stwierdzeniu, że pozostałość soli kwasu hydroksyoctowego może wpływać na aktywność przeciwdrobnoustrojową chitozanu, zdecydowano o ponownym zbadaniu tej aktywności, ale już tylko dla chitozanu rozpuszczonego w kwasie węglowym. Wykazując, że DD nie ma istotnego wpływu na właściwości biologiczne chitozanu, zdecydowano się pominąć ocenę wpływu tego parametru na właściwości kompozycji polimerowej w dalszych badaniach. Jednakże, pomiary uwzględniające zmienność masy cząsteczkowej zostały przeprowadzone, mając na uwadze, że masa cząsteczkowa stanowi kluczowy parametr wpływający na właściwości reologiczne roztworów chitozanu, a tym samym na właściwości kompozycji polimerowych z agarozą. Ponadto, komercyjna dostępność chitozanów spełniających standardy medyczne oraz dodatkowo różniących się DD dla LMW i MMW jest znacznie ograniczona. W związku z tym, dalsze badania zostały przeprowadzone tylko na chitozanach o określonym DD.

W pierwszej kolejności przeprowadzono ponowną analizę wpływu DD i masy cząsteczkowej na aktywność przeciwdrobnoustrojową (Rys. 10A) roztworów chitozanu otrzymanych metodą saturacji dwutlenkiem węgla oraz na ich cytotoksyczność, z tą zmianą, że osad przemywano do momentu uzyskania stabilnego pH przesączu wody płuczącej. Ostateczne wyniki wykazały, że intensyfikacja procesu wypłukiwania prowadzi

do istotnego spadku aktywności przeciwdrobnoustrojowej chitozanu, co można przypisać redukcji pozostałości soli w osadzie przed jego ponownym rozpuszczeniem. W przypadku chitozanów MMW aktywność ta nie zmieniła się w sposób istotny statystycznie. Znacznemu obniżeniu redukcji liczby bakterii, do poziomu zbliżonego dla chitozanu MMW uległy z kolei próby LMW. Również aktywność przeciwdrobnoustrojowa chitozanów HMW, za wyjątkiem HMW o DD 66 względem bakterii Gram-ujemnych, dla którego redukcja w skali log wynosiła około 4 uległa znacznemu obniżeniu. Podsumowując, wszystkie materiały chitozanowe otrzymane metodą saturacji dwutlenkiem węgla z wyjątkiem HMW DD66 wykazały aktywność przeciwdrobnoustrojową, ale nie większą niż 2 rzędy log tj. 1,61-1,72 i znacząco niższą, niż dla prób chitozanów rozpuszczonych w 1% kwasie mlekowym [A2]. W przypadku bakterii Gram-dodatnich aktywność ta była mniejsza i dla chitozanów LMW, MMW i HMW poniżej 75% DD nie przekroczyła 1 rzędu log. Z kolei dla dwóch pozostałych chitozanów HMW o DD 79 i 83 log rząd redukcji wyniósł między 1 a 2 dla dwóch badanych szczepów bakterii. Wyższa skuteczność przeciwdrobnoustrojowa chitozanu o HMW i DD 66 może być związana z jego zwiększoną hydrofobowością wynikającą z wyższej zawartości grup acetylowych. Grupy te przyczyniają się do lepszej interakcji chitozanu z hydrofobowymi obszarami błony komórkowej bakterii Gram-ujemnych, która jest bogata w lipopolisacharydy. Interakcje hydrofobowe pomiędzy chitozanem HMW DD 66 a błoną bakterii Gram-ujemnych mogą prowadzić do zaburzenia integralności błony, zwiększenia jej przepuszczalności, a w konsekwencji do śmierci komórek bakteryjnych [Yang & Yang, 2008].

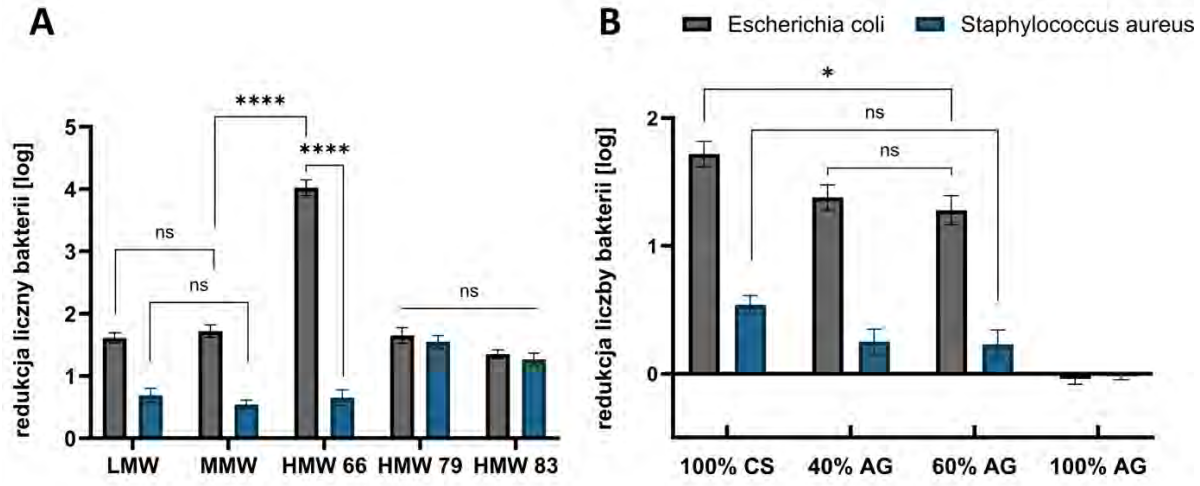

Rysunek 10. Aktywność przeciwdrobnoustrojowa wobec *Escherichia coli* i *Staphylococcus aureus* dla A) chitozanów o różnej masie cząsteczkowej: niskiej (LMW), średniej (MMW) i wysokiej (HMW) oraz chitozanów HMW o różnym stopniu deacetylacji 66, 79 i 83 rozpuszczonych metodą saturacji dwutlenkiem węgla; B) kompozycji chitozanowo-agarozowych. Wyniki przedstawiono jako średnią ± odchylenie standardowe (SD) na podstawie trzech powtórzeń (n = 3, $p < 0,05$). Istotność statystyczną różnic między poszczególnymi grupami oznaczono odpowiednio jako: ns (nieistotne statystycznie) $p > 0,05$, *$p < 0,05$, ****$p < 0,0001$.

Dodatkowo, ponownie zbadano wpływ ekstraktów badanych materiałów na ich cytotoksyczny wpływ względem komórek L929, celem potwierdzenia wyciągniętej na podstawie poprzednich badań hipotezy (Rys. 11). Żaden z badanych materiałów, bez względu na masę cząsteczkową i DD, nie wykazał efektu cytotoksycznego, a przeżywalność komórek wyniosła powyżej 80% względem kontroli. Brak cytotoksycznego efektu potwierdziły również zdjęcia mikroskopowe wykonane po 24-godzinnym kontakcie komórek z ekstraktami badanych polimerów. Morfologia komórek była zachowana, a ich liczba porównywalna, co wskazuje na brak zahamowanej proliferacji. Dodatkowo, w tym samym badaniu określono również bezpieczeństwo biologiczne agarozy. Na podstawie przeprowadzonego testu MTT nie wykazano efektu cytotoksycznego ani nieprawidłowości w morfologii komórek L929 po ich kontakcie z badanym materiałem.

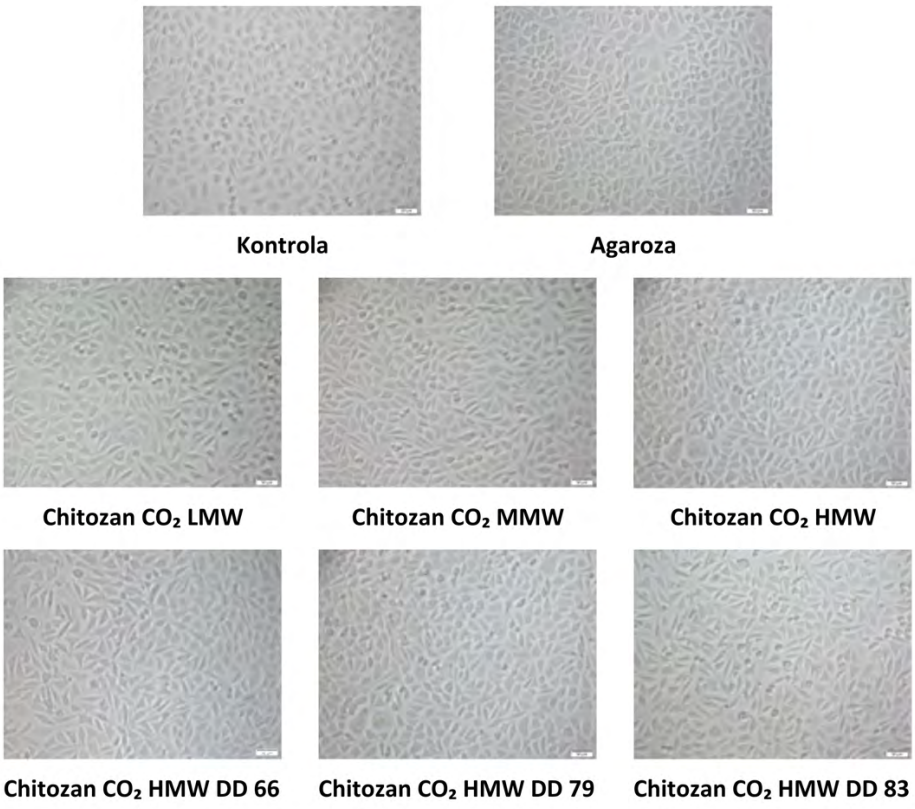

Rysunek 11. Reprezentatywne obrazy (n = 4) morfologii komórek L929 traktowanych rozpuszczonymi w pożywce komórkowej przy rozcieńczeniu 1:1 ekstraktami: agarozy, chitozanów o różnej masie cząsteczkowej: niskiej (LMW), średniej (MMW), wysokiej (HMW), oraz chitozanów HMW o różnym stopniu deacetylacji: 66, 79 i 83, rozpuszczonych metodą saturacji dwutlenkiem węgla. Zdjęcia wykonano po 24-godzinnym kontakcie komórek z ekstraktami w rozcieńczeniu 1:1. Skala wynosi 50 µm, powiększenie 200×.

Jednym z analizowanych zagrożeń było pogorszenie właściwości biologicznych chitozanu wynikające z faktu, że do wytworzenia kompozycji polimerowej wykorzystana została agaroza nie będąca nośnikiem funkcji biologicznych. W celu zbadania wpływu

udziału agarozy na wybrane właściwości biologiczne przeprowadzono ocenę aktywności przeciwdrobnoustrojowej materiałów (Rys. 10B). W tym celu zastosowano procedurę ASTM E2149 z modyfikacjami. Zgodnie z danymi literaturowi wykazano, że agaroza nie wykazuje właściwości przeciwdrobnoustrojowych [Jiang i wsp., 2023]. Co więcej, wraz ze wzrostem jej udziału w kompozycji chitozanowo-agarozowej aktywność ta maleje. Obserwowana zależność wynika z malejącego stężenia chitozanu, który posiada aktywność przeciwdrobnoustrojową i co zostało wykazane w przeprowadzonych badaniach. Zgodnie z wcześniejszymi testami [A2] aktywność przeciwdrobnoustrojowa chitozanu MMW względem bakterii Gram-ujemnych jest większa niż dla bakterii Gram-dodatnich. W przypadku układów zawierających 40 i 60% agarozy, wyniki redukcji liczby bakterii w skali log nie różnią się w sposób istotny statystycznie wskazując na efekt bakteriostyatyczny, wynoszący około 95% dla *E. coli* i 45% dla *S. aureus*.

W dalszej kolejności, aby zrozumieć interakcje jakie zachodzą pomiędzy chitozanem a agarozą przeprowadzono identyfikację poszczególnych grup chemicznych w polimerach jak również w ich kompozycji polimerowej metodą spektroskopii w podczerwieni z transformacją Fouriera (FTIR). Na podstawie charakterystyki pasm przy określonych liczbach falowych zbadano charakter oddziaływań między chitozanem a agarozą w ich kompozycji, zawierającej ten sam ułamek masowy obu polimerów. Zarówno w widmach chitozanu, agarozy, jaki i ich kompozycji wykryto pasma charakterystyczne dla obu polimerów, które różniły się intensywnościami. Różnice te były wynikiem wymieszania obu polimerów. W widmach kompozycji polimerowej nie zaobserwowano jakościowych zmian w pasmach, stąd wniosek, że kompozycje chitozanowo-agarozowa jest wyłącznie dwuskładnikową, fizyczną mieszaniną. Układ chitozanowo-agarozowy, pomimo możliwości tworzenia polielektrolitycznego kompleksu wynikającego z obecności polikationowego polimeru, czyli chitozanu i polianionowego agarozy, stanowi fizyczną mieszaninę polimerów o bardzo słabych oddziaływaniach międzycząsteczkowych. W przypadku tworzenia się wiązań wodorowych lub oddziaływań polielektrostatycznych między chitozanem a agarozą, zaobserwowano by zmiany w pasmach odpowiadających za rozciąganie O-H, N-H, C=O oraz C-O-C. Zmiany te obejmowałyby przesunięcie pasm w kierunku niższych częstotliwości, zmiany ich intensywności oraz poszerzenia pasm.

Znając interakcje zachodzące pomiędzy polimerami w badanym układzie, w kolejnym kroku określono wpływ masy cząsteczkowej chitozanów oraz ich udziału w kompozycji na proces żelowania w odniesieniu do charakterystyki żelowania agarozy, jako jednego ze wskaźników drukowalności docelowego biotuszu. Pomiary wykonano przy użyciu wiskozymetru Brookfield Digital Model DVIII Ultra z termostatowaną komorą pomiarową, badając zarówno czas jak i temperaturę przejścia fazowego zol-żel (SGPT) oraz wykonując pomiar krzywych płynięcia (FC). Mierząc zmiany lepkości dynamicznej roztworów w zakresie temperatur od 40 do 20°C, przy szybkości chłodzenia 1°C $min^{-1,}$ szybkości ścinania 5 1/s, z wykorzystaniem wrzeciona SC4-25 wyznaczono SGPT dla 1% roztworu agarozy, jak i dla kompozycji chitozanowo-agarozowych. Na podstawie

uzyskanych wyników stwierdzono, że dodatek chitozanu do agarozy zmienia zarówno temperaturę jak i czas żelowania w porównaniu z czystą agarozą. Ponadto, wykazano, że masa cząsteczkowa jak i udział chitozanu znacząco wpływa na SGPT. W przypadku 1% roztworu agarozy, proces żelowania rozpoczyna się w temperaturze 36,5°C i zachodzi natychmiast, o czym świadczy niski kąt nachylenia krzywej. Gwałtowny wzrost lepkości w danej temperaturze, jest następstwem żelowania roztworu tego polimeru (Rys. 12 A).

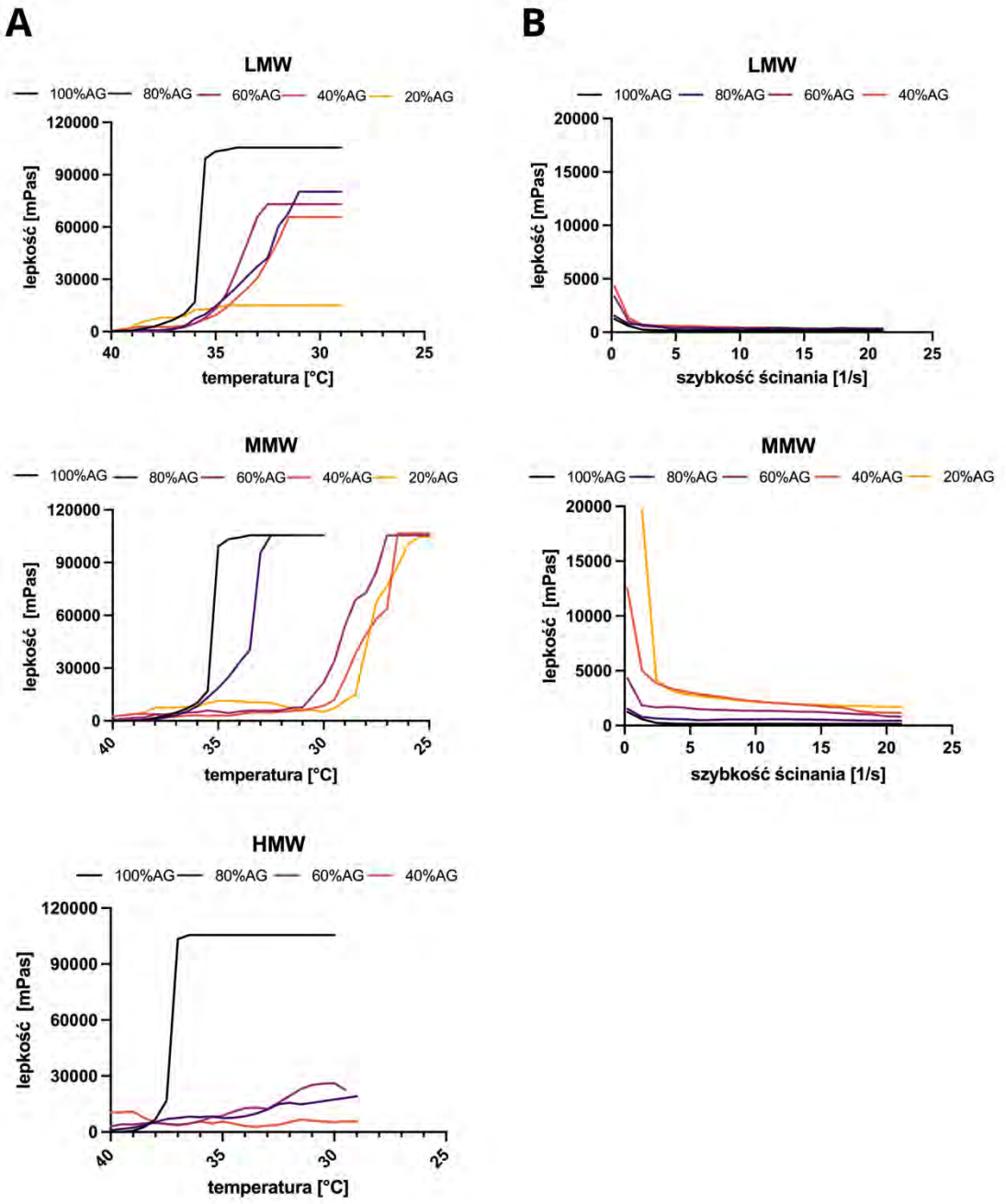

Rysunek 12. Właściwości reologiczne kompozycji chitozanowo-agarozowej (CS/AG) dla CS o różnych masach cząsteczkowych: niskiej (LMW), średniej (MMW) i wysokiej (HMW). A) Charakterystyka reologiczna przejścia fazowego zol-żel oraz B) krzywe płynięcia kompozycji CS/AG (n = 3, $p<0,05$).

Porównując krzywą uzyskaną dla 1% roztworu agarozy, z krzywą kompozycji polimerowych na bazie agarozy i chitozanu LMW zaobserwowano zbliżoną temperaturę żelowania, z tą różnicą, że zakres temperatur ich przejścia fazowego był znacznie szerszy i wynosił od 3 do 5°C. Porównując lepkości prób przed całkowitym zżelowaniem, to wraz ze wzrostem udziału LMW chitozanu w kompozycji parametr ten malał. Całkowicie inną zależność wykazywał chitozan HMW. W przypadku jego kompozycji z agarozą stwierdzono, że uzyskanie biotuszu o odpowiednich parametrach reologicznych niezbędnych do zastosowania w biodruku jest niemożliwe. Te kompozycje polimerowe cechuje brak ostrego przejścia fazowego, za wyjątkiem mieszaniny zawierającej 80% agarozy, która wręcz odwrotnie, zżelowała natychmiast po zmieszaniu obu polimerów. Brak obserwacji natychmiastowego lub bardzo szybkiego przejścia fazowego pod wpływem obniżania temperatury sugeruje bardzo niską drukowalność. Kolejna obserwacja świadcząca o słabej drukowalności to nieznaczny wzrost lepkości pod wpływem obniżenia temperatury. W związku z powyższym, już na tym etapie kompozycje zawierające HMW chitozan zostały wykluczone z dalszych badań. Chitozan MMW, w przeciwieństwie do LMW i HMW, jako jedyny w kompozycji z agarozą cechował się SGPT wskazującą na potencjalne zastosowanie w biodruku. Zwiększenie udziału MMW chitozanu w kompozycji nie wpłynęło na wartość lepkości dynamicznej przed jego żelowaniem, a jedynie na zmniejszenie zakresu temperatur, w którym ono zachodziło. W porównaniu do 1% roztworu agarozy, żelującego natychmiast po obniżeniu temperatury o 0,5°C w zakresie temperatur 36,0-36,5°C, zakres temperatur żelowania kompozycji polimerowych na bazie chitozanu MMW wynosił od 26,5-33,1°C do 30,5-36,5°C. Tym samym, w celu osiągnięcia pełnego zżelowania tych kompozycji polimerowych, konieczne było obniżenie temperatury o dodatkowe 3,4-4,0°C. W związku z tym, że mechanizm żelowania agarozy zakłada dwa główne etapy, takie jak tworzenie się podwójnych helis w temperaturze około 45°C, a następnie dalsze twardnienie na skutek ich agregacji w temperaturze około 30°C zakłada się, że poszczególne masy cząsteczkowe chitozanów mogą mieć znaczący wpływ na proces żelowania agarozy. Po pierwsze, obserwowane zmniejszenie lepkości zolu chitozanowo-agarozowego przed całkowitym żelowaniem kompozycji polimerowej wraz ze wzrostem udziału LMW chitozanu sugeruje, że jego obecność może zakłócać formowanie helis agarozowych, przez co proces ten jest wydłużony w czasie. Z kolei, obecność w kompozycji chitozanu HMW może dodatkowo zakłócać formowanie helis poprzez tworzenie przeszkód sterycznych. W konsekwencji takie działanie może przyczynić się do tego, że przejście zol-żel nie jest obserwowane. W przypadku dodania MMW chitozanu do agarozy następuje jedynie nieznaczne wydłużenie czasu żelowania kompozycji oraz obniżenie temperatury żelowania. Może to wynikać z faktu, że MMW chitozan wpływa na organizację cząsteczek agarozowych w bardziej uporządkowane helisy, opóźniając tym samych ich późniejszą agregację. Powyższe przypuszczenia zdają się być zgodne z wnioskami wysuniętymi przez Russ i wsp. (2013), którzy wykazali, że żelowanie agarozy zarówno w obecności alginanu jak i ksantanu następuje w niższych temperaturach.

Wynika to, z obniżenia efektywnego stężenia agarozy, stanowiącej główny czynnik odpowiedzialny za tworzenie struktury żelowej oraz interakcji między polimerami. Jednakże w przypadku ksantanu, którego łańcuch polimerowy charakteryzuje się wysoką sztywnością wynikającą z ograniczonej elastyczności molekularnej, tworzy się złożona i heterogeniczna sieć polimerowa. Zjawisko to wynika z unieruchomienia segmentów łańcucha przy wyższych temperaturach, jeszcze przed rozpoczęciem procesu żelowania agarozy. To sprawia, że działa on jako fizyczna przeszkoda ograniczając ruchliwość łańcuchów agarozy i utrudniając ich agregację w helisy uzyskując tym samym mniejszą liczbę stref połączeń. Alginian będący elastycznym polimerem, działa z kolei jako wypełniacz, zwiększając elastyczność powstałego żelu i integrując się z siecią agarozy, stabilizując jej strukturę. Chociaż badania te dotyczyły innych polimerów, można stwierdzić, że chitozan LMW wykazuje zbliżone działanie do alginianu, HMW do ksantanu, a MMW najprawdopodobniej stabilizuje strukturę żelu bez znaczącego obniżenia temperatury żelowania. Pomimo tego, że są to tylko przypuszczenia o możliwych mechanizmach wpływu chitozanów różniących się masą cząsteczkową na proces żelowania agarozy tj. temperatury i czasu, to uzyskane wyniki wskazują na potencjalne zastosowanie chitozanów LMW i MMW w biodruku.

Kolejnym istotnym parametrem reologicznym w ocenie drukowalności biotuszu, jest określenie jego krzywej lepkości, czyli zależności lepkości dynamicznej w funkcji szybkości ścinania. Wyznaczenie tej zależności w biodruku pozwala na określenie rodzaju płynu, wartości lepkości biotuszu w czasie, a także jego stabilności przetłaczania w zmiennych warunkach działania naprężenia ścinającego [Habib i Khoda, 2022]. Pomiary krzywych lepkości (FC) wykonano dla kompozycji chitozanowo-agarozowych na bazie chitozanów LMW i MMW z wykorzystaniem wrzeciona SC4-25, z szybkością ścinania w zakresie od 0,1 s^{-1} do 25,0 s^{-1} w temperaturze 37°C (Rys. 12B). Stwierdzono, że lepkość kompozycji chitozanowo-agarozowych maleje wraz ze wzrostem szybkości ścinania, co potwierdza, że są to płyny pseudoplastyczne. Jednakże, w przypadku układów na bazie LMW chitozanu, spadek lepkości pod wpływem naprężenia ścinającego był mniejszy niż dla wariantu MMW. Dodatkowo, zależność ta malała wraz ze wzrostem zawartości agarozy w kompozycji polimerowej. Krzywe lepkości charakteryzowały się stałą wartością lepkości po przekroczeniu wartości szybkości ścinania równej 3 1/s. Taka informacja wskazuje na możliwość stabilnego przetłaczania kompozycji polimerowej w szerokim zakresie szybkości ścinania.

W ocenie drukowalności układów chitozanowo-agarozowych uwzględniono także inne parametry, takie jak: średnica dyszy tłoczącej oraz temperatura elementu grzejnego strzykawki z biotuszem, przeprowadzając empiryczny test symulacji ekstruzji (EFT) imitującego wytłaczanie biotuszu w trakcie drukowania (Rys. 13). W tym celu zaadaptowano uniwersalną maszynę do testowania Instron 5543 z oprogramowaniem "Merlin" V 4.42. Między stolikiem a głowicą urządzenia zamocowano strzykawkę owiniętą matą grzewczą, której zadaniem było utrzymanie stałej temperatury kompozycji polimerowej w strzykawce, wynoszącej 37°C. W pierwszej kolejności przeprowadzono

testy ekstruzji dla 1% roztworu agarozy z użyciem wybranych średnic dysz wylotowych, tj. 0,84, 0,58, 041 mm (Rys. 13A). Po napełnieniu strzykawki 30 mL badaną kompozycją, inkubowano ją w jej wnętrzu przez 10 min. Następnie tłok strzykawki był przesuwany w dół ze stałą prędkością przemieszczenia równą 0,25 mm/s, do całkowitego jej opróżnienia, w czasie około 3,5 min.

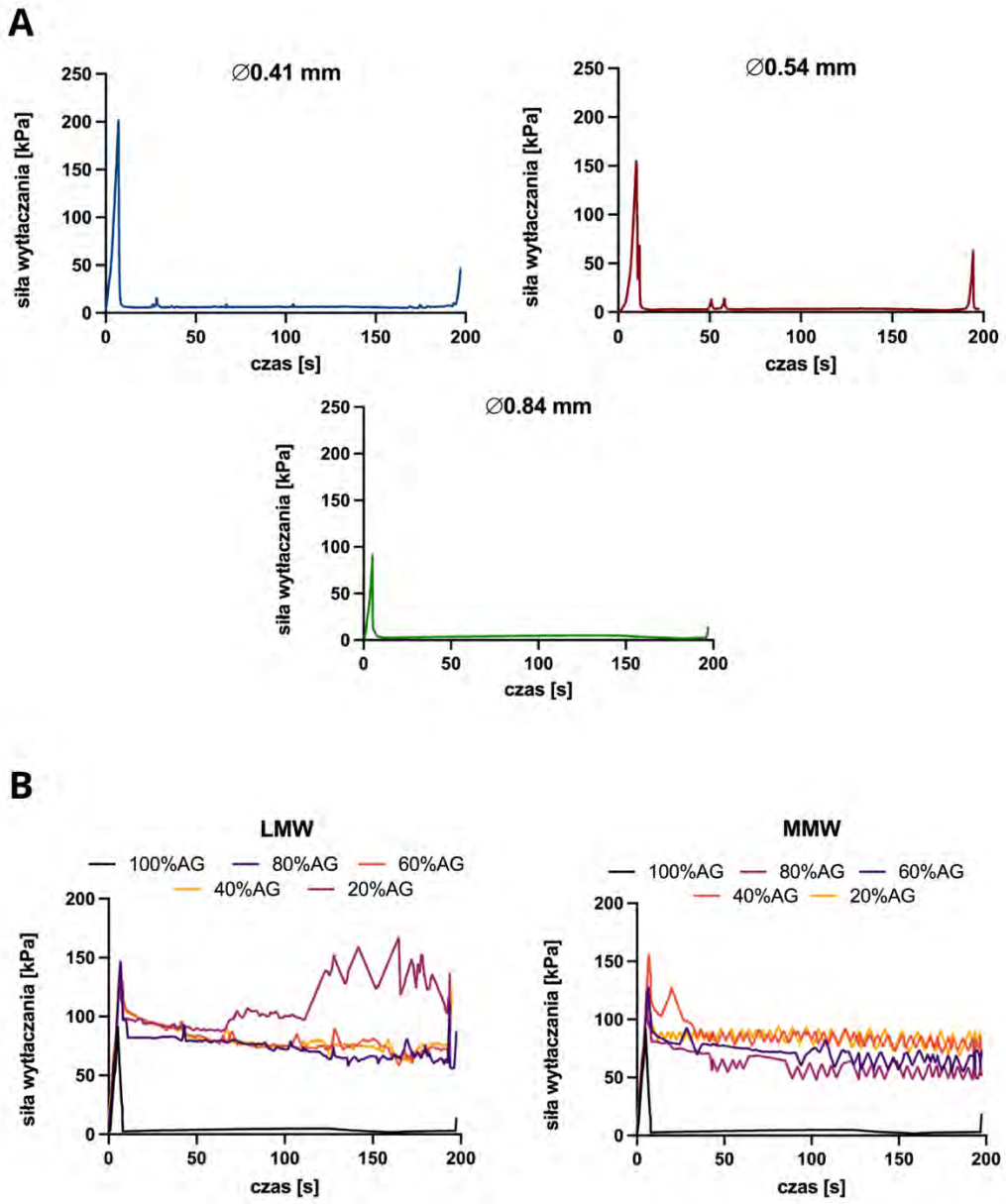

Rysunek 13. Wynik testu siły wyciskania dla A) 1% roztworu agarozy przy średnicy dyszy tłoczącej 0,41, 0,54 oraz 0,84 mm i B) kompozycji chitozanowo-agarozowych CS/AG w temperaturze 37 °C przy średnicy dyszy tłoczącej 0,84 mm (n = 3, $p<0,05$)

W pierwszej kolejności, stosując wybrane średnice dysz, możliwe było stwierdzenie, jaka siła potrzebna jest do zainicjowania przepływu, czyli do rozrzedzenia układu co jest typowe dla płynów pseudoplastycznych. Dla dysz o średnicy 0,84,

0,580 i 0,41 mm siła ta wynosiła odpowiednio 200 kPa, 250 kPa i 100 kPa. Po osiągnięciu wartości maksymalnej, siła ekstruzji gwałtownie malała, a następnie ulegała stabilizacji. Taka obserwacja wskazuje na osiągnięcie równowagi dynamicznej w przepływie, gdzie lepkość materiału przystosowuje się do warunków przepływu przez dyszę. W związku z tym, że najbardziej stabilny przepływ zaobserwowano dla średnicy 0,84 mm, która była największą badaną średnicą, gdzie krzywa nie wykazywała żadnych odchyleń podczas testu, ta średnica dyszy została wytypowana do dalszych badań jako optymalna. Gdy podczas testu obserwowane były fluktuacje, to dodatnie piki na wykresie wskazywały najprawdopodobniej na obecność lokalnie tworzących się agregatów żelu kompozycji polimerowej, natomiast ujemne na obecność pęcherzyków powietrza, które mogły zostać zassane do strzykawki podczas jej napełniania. W przypadku kompozycji chitozanowo-agarozowych (Rys. 13B) obecność fluktuacji spowodowana była także uwalnianiem się z nich dwutlenku węgla wykorzystywanego do rozpuszczania chitozanu i jego niestabilności w czasie. Na skutek uwalniania się dwutlenku węgla tworzą się agregaty polimerowe w pobliżu przejścia fazowego. Efekt ten jednak jest na tyle powolny, że nie stanowi ograniczenia w zastosowaniu kompozycji polimerowej jako potencjalnego biotuszu. W przypadku układów chitozanowo-agarozowych siła ekstruzji zmniejszała się wraz ze wzrostem udziału agarozy w kompozycji, co wskazuje na niższą lepkość roztworu agarozy w temperaturze pomiaru, a tym samym obniżanie przez agarozę siły potrzebnej do ekstruzji materiału w trakcie drukowania.

Porównując układ LMW i MMW chitozanowo-agarozowy, większe fluktuacje siły ekstruzji obserwuje się w przypadku tego pierwszego, co może wskazywać na mniej jednolity przepływ materiału przez dyszę. Natomiast w przypadku kompozycji z chitozanem MMW proces wytłaczania jest bardziej stabilny, co stanowi kolejny argument za potencjalnym wykorzystaniem go w układzie z agarozą, zapewniając lepszą drukowalność biotuszu. Przeprowadzone testy potwierdziły możliwość uzyskania kompozycji LMW i MMW chitozanowo-agarozowych charakteryzujących się odpowiednimi dla biodruku właściwościami reologicznymi. Na dodatek, niewielka szybkość ścinania, wynosząca 3 1/s, która wprawia hydrożelową mieszaninę w stabilny przepływ, wskazuje nie tylko na łatwość jego ekstruzji ze strzykawki, ale także na stworzenie warunków zapewniających przeżywalność komórek na poziomie uznawanym za akceptowalny, czyli powyżej 70% [Mohammadrezaei i wsp., 2024]. Ze względu na najbardziej przewidywalny i najszybszy profil żelowania zdecydowano się na przeprowadzeniu dalszych badań nad układami MMW chitozanowo-agarozowymi, różniącymi się proporcją obu polimerów. Badane były układy o zawartości 100%, 80%, 60%, 40%, 20% chitozanu oraz 100% agarozy.

W kolejnym kroku określono także wpływ kompozycji chitozanowo-agarozowych na bezpieczeństwo biologiczne komórek eukariotycznych, które będą osadzane w biotuszu. W testach wykorzystano skórne linie komórkowe, czyli fibroblasty 46Br.1N oraz keratynocyty HaCaT (Rys. 14). W pierwszej kolejności wykonano oznaczenie wpływu ekstraktów badanych materiałów, czyli agarozy, chitozanu oraz ich kompozycji

zawierających oba polimery w stosunku masowym 1:1 na cytotoksyczność (Rys. 14A) i proliferację (Rys. 14B) względem komórek skóry. W celu określenia wpływu materiałów na proliferację zbadano aktywność metaboliczną komórek poprzez test oznaczenia zdolności żywych komórek do redukcji soli tetrazolowej XTT do formazanu pod wpływem obecnego w mitochondriach enzymu dehydrogenzay. Z kolei cytotoksyczność została określona poprzez wykonanie testu LDH i pomiarze ilości uwolnionej dehydrogenazy mleczanowej, na skutek uszkodzenia błony komórkowej. Tak jak w przypadku komórek L929, nie wykazano, aby jakikolwiek z badanych materiałów wykazał efekt cytotoksyczny. Spadek przeżywalności, wynoszący jednak poniżej 10% względem kontroli pozytywnej, został zarejestrowany dla ekstraktów agarozowych i chitozanowych, dla których stężenie materiału w trakcie ekstrakcji wynosiło 100mg/mL, czyli dla ekstraktu 100%. W przypadku komórek fibroblastów 46BR.1N, zaobserwowano ich zwiększoną proliferację względem kontroli pozytywnej, w porównaniu z komórkami keratynocytów. Największy wzrost liczby komórek względem kontroli, powyżej 30% odnotowano dla ekstraktów chitozanowych i agarozowych przy stężeniu 10mg/mL i 25mg/mL. Z kolei wszystkie ekstrakty chitozanowo-agarozowe cechowała zdolność wzrostu liczby komórek o 20%, a przy stężeniu 25mg/mL o 25% większą.

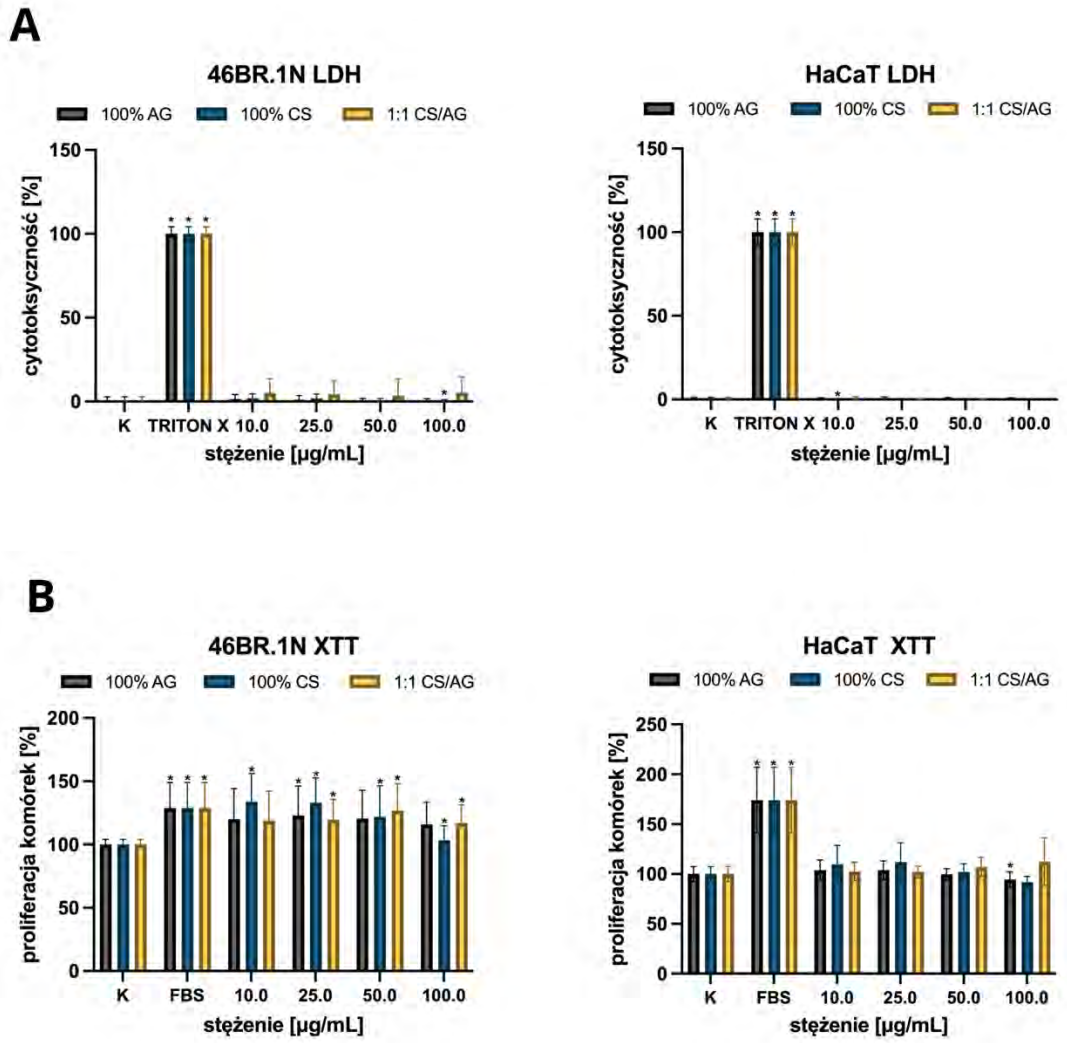

Rysunek 14. Wpływ kserożeli chitozanowych (CS), agarozowych (AG) oraz ich kompozycji (CS/AG) na komórki ludzkiej skóry: keratynocyty HaCaT i fibroblasty 46BR.1 N, po 48 godzinach inkubacji. A) Oddziaływanie kserożeli na proliferację komórek i B) analiza cytotoksyczności kserożeli. Wyniki przedstawiono jako średnią ± odchylenie standardowe (SD) na podstawie trzech powtórzeń (n = 3). Istotność statystyczną różnic w porównaniu do kontroli oznaczono odpowiednio jako: *p < 0,05.

Badając wpływ chitozanu, agarozy oraz ich kompozycji na bezpieczeństwo biologiczne względem wymienionych wyżej linii komórkowych przeprowadzono test oceny przeżywalności komórek po ich umieszczeniu w badanym materiale, wytłoczeniu i inkubacji w medium hodowlanym przez 48 godz. Wykazano, że zarówno fibroblasty 46Br.1N jak i keratynocyty HaCaT charakteryzuje wysoka przeżywalność. W przypadku 1% hydrożelu agarozowego, przeżywalność obu linii komórkowej wynosiła ponad 80%, a dla kompozycji chitozanowo-agarozowej zawierającego oba polimeru w stosunku masowym 1:1 ponad 90%. Tak wysokie wskaźniki przeżywalności po 48 godz. inkubacji potwierdzają pozytywną interakcję między badanymi komórkami a bazą docelowego biotuszu oraz brak negatywnego wpływu temperatury wytłaczania na przeżywalność komórek.

W związku z tym, kolejnym krokiem w przyszłych badaniach nad oceną możliwości wykorzystania kompozycji polimerowej w hodowli komórkowej będzie określenie przeżywalności komórkowej w dłuższym przedziale czasu, w celu określenia możliwości badanych komórek do dalszej proliferacji.

3.4 [A4] Od biotuszu do tkanki: Badanie kompozycji chitozanowo-agarozowej w kontekście drukowalności i aktywności biologicznej.

Analiza właściwości reologicznych badanych kompozycji polimerowych jest kluczowa podczas ich charakterystyki, ponieważ ma ona bezpośredni wpływ nie tylko na zachowanie biotuszu podczas wytłaczania, ale i na przeżywalność komórek. Symulację warunków ekstruzji kompozycji chitozanowo-agarozowej z głowicy drukarki w temperaturze 37°C przeprowadzono z wykorzystaniem trzyetapowego testu tiksotropowego w wersji oscylacyjno-rotacyjno-oscylacyjnej. Dzięki temu możliwa była ocena, w jaki sposób kompozycja oraz poszczególne polimery reagują na obciążenie dynamiczne i jak szybko odbudowują swoją strukturę. Na podstawie uzyskanych zależności zmian lepkości zespolonej, która uwzględnia zarówno właściwości lepkościowe jak i sprężyste materiału, oraz lepkości dynamicznej, opisującej jedynie opór materiału wobec jednokierunkowegp płynięcia, stwierdzono, że procesy degradacji i regeneracji struktury badanych układów zachodzą i odgrywają kluczową rolę w ocenie ich przydatności do biodruku (Rys. 15). Kompozycje polimerowe z 20% i 40% zawartością chitozanu wykazały największy potencjał, ponieważ po fazie rotacyjnej szybko odbudowywały swoją trójwymiarową strukturę, co czyni je szczególnie obiecującymi materiałami do biodruku, gdzie zdolność do regeneracji struktury jest kluczową właściwością dla stabilności wydrukowanych konstrukcji.

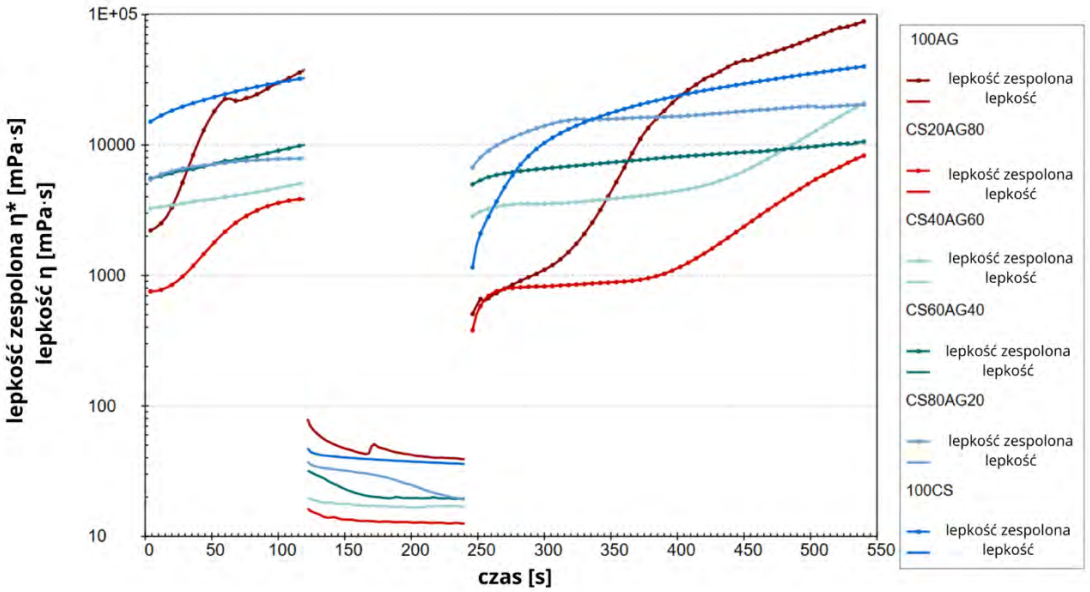

Rysunek 15. Porównanie lepkości zespolonej oraz dynamicznej podczas testu oscylacyjno-rotacyjno-oscylacyjnego (ORO) (n=3, p<0,05)

Określając dalsze możliwości aplikacyjne kompozycji chitozanowo-agarozowej, poza weryfikacją podstawowych kryteriów akceptacji, takich jak brak efektu cytotoksycznego oraz drukowalności, konieczna była weryfikacja przepuszczalności modelowych związków imitujących składniki odżywcze i metabolity wtórne komórek. Jest to uzasadnione, ponieważ komórki osadzone w hydrożelu znajdują się nie tylko na jego powierzchni, ale także wewnątrz każdego wydrukowanego filamentu. Dlatego efektywna dyfuzja składników odżywczych i bioaktywnych molekuł do wnętrza rusztowania i hydrożelu jest kluczowa dla ich prawidłowego funkcjonowania. Do tego, w kontekście przyszłej funkcjonalizacji biotuszu poprzez dodanie czynników wzrostu czy peptydów, istotne jest, aby te związki mogły swobodnie przenikać przez strukturę hydrożelu. Na podstawie średnicy dyfuzji barwników w czasie stwierdzono, że zarówno proporcja chitozanu do agarozy, jak i masa cząsteczkowa dyfundujących substancji znacząco wpływają na to zjawisko. Dyfuzja zachodziła szybciej w przypadku membran agarozowych niż chitozanowych, co wynika z mniejszej gęstości usieciowania i większej porowatości tych pierwszych. W przypadku kompozycji chitozanowo-agarozowych zaobserwowano, że wzrost udziału chitozanu w membranie ogranicza szybkość dyfuzji, a wzrost masy cząsteczkowej dyfundującej substancji dodatkowo zwiększał ten efekt. Zjawisko to można przypisać silniejszym wiązaniom międzycząsteczkowym chitozanu, co z kolei wpływa na jego niższą przepuszczalność. Porównując wpływ masy cząsteczkowej barwnika na dyfuzję przez membranę agarozową, stwierdzono, że średnica obszaru dyfuzji była 1,6 razy mniejsza dla nigrozyny o masie cząsteczkowej 616,49 g/mol niż dla rezazuryny o masie cząsteczkowej 251,17 g/mol. Kolejnym krokiem była ocena szybkości dyfuzji modelowego składnika pokarmowego dla komórek, czyli glukozy. Badając wszystkie opracowane warianty membran, nie stwierdzono, aby dyfuzja przez nie glukozy o masie cząsteczkowej 180,17 g/mol znacząco się różniła. Zdolność do efektywnego transportu glukozy potwierdza możliwość zastosowania opracowanej kompozycji chitozanowo-agarozowej w inżynierii tkankowej, zwłaszcza w obszarach wymagających precyzyjnego dostarczania składników odżywczych. Na podstawie przeprowadzonych badań można również wywnioskować, że zmieniając udziały poszczególnych polimerów w biotuszu, można regulować porowatość i gęstość usieciowania membran, pozwalając na modyfikację szybkości dyfuzji, bez wpływu na przenikanie glukozy. Takie właściwości membran otwierają możliwości ich zastosowania w wielu dziedzinach, od biotechnologii po medycynę regeneracyjną, gdzie kontrola dyfuzji substancji przez membrany jest kluczowa.

W kontekście potencjalnych zastosowań w medycynie regeneracyjnej, oprócz optymalizacji parametrów dyfuzji przez dostosowanie porowatości i gęstości usieciowania membran, istotne jest także zrozumienie wpływu opracowanych materiałów na zachowanie komórek w ich otoczeniu. Jednym z kluczowych aspektów tego oddziaływania jest zdolność biotuszu do stymulacji migracji komórek, co jest fundamentalne dla procesów regeneracyjnych i prawidłowego gojenia tkanek. W związku z tym, przeprowadzono testy migracji komórek, wykorzystując test Ibidi wound healing,

aby ocenić wpływ ekstraktów badanych materiałów na zdolność komórek do migracji (Rys. 16). Test ten polega na stworzeniu kontrolowanej przerwy „rany" w monowarstwie komórek, co umożliwia analizę tempa zamykania tej przerwy przez migrujące komórki. Wykazano znaczną migrację komórek HaCaT pod wpływem ekstraktów chitozanowych i chitozanowo-agarozowych. Takiej właściwości nie potwierdzono dla ekstraktów z materiałów agarozowych. W przypadku komórek 46BR.1N, istotne statystycznie różnice w porównaniu do kontroli zaobserwowano tylko dla jednej próby kompozycji chitozanowo-agarozowej, co wskazuje na umiarkowany efekt pro-migracyjny. Brak stymulacji przez FBS sugeruje, że te komórki mają specyficzne wymagania środowiskowe.

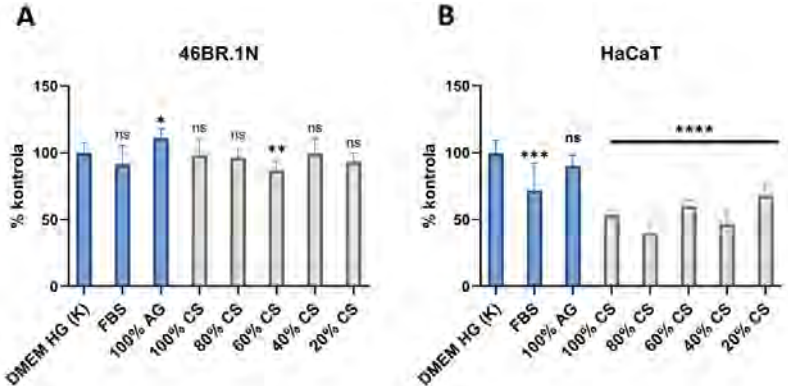

Rysunek 16. Wpływ MMW chitozanu (CS), agarozy (AG) i ich kompozycji na migrację A) fibroblastów 46BR.1N i B) keratynocytów HaCaT. Wyniki przedstawiono jako średnią ± odchylenie standardowe (SD) na podstawie co najmniej trzech powtórzeń (n = 3). Istotność statystyczną różnic w porównaniu do kontroli (DMEM HG) oznaczono odpowiednio jako: ns (nieistotne statystycznie) $p > 0,05$, *$p < 0,05$, **** $p < 0,0001$.

Zgodnie z wytycznymi dotyczącymi oceny wyrobów medycznych, przeprowadzone badania obejmowały ocenę wpływu ekstraktów z badanych materiałów na proliferację, cytotoksyczność oraz migrację komórek. Aby przeprowadzić kompleksową ocenę oddziaływania kompozycji polimerowej, przeanalizowano również jej wpływ na komórki bezpośrednio umieszczone w hydrożelowym materiale. W związku z tym oceniono przeżywalność komórek linii 46BR.1N oraz HaCaT podczas 14-dniowej inkubacji w 1% hydrożelu agarozowym oraz w kompozycji 0,5% chitozanu i 0,5% agarozy, po ich wytłoczeniu za pomocą strzykawki na płytki wielodołkowe w formie rusztowania (Rys. 17). Wysoki wskaźnik przeżywalności komórek w układzie chitozan-agaroza, wynoszący około 100% drugiego dnia, od 70 do 78% siódmego dnia i od 117 do 129% czternastego dnia dla kolejno 46BR.1N i HaCaT potwierdził brak efektu cytotoksycznego oraz wzmożoną proliferację komórek w czasie. W przypadku komórek umieszczonych w agarozowym hydrożelu również nie stwierdzono efektu cytotoksycznego. Jednakże, po czternastu dniach, liczebność żywych komórek utrzymała się na podobnym poziomie, a komórki cechowała tendencja do gromadzenia się poza obszarem rusztowania. Wyniki te są zgodne z danymi literaturowymi, które sugerują, że agaroza ma słabe właściwości biologiczne wspierające proliferację komórek [Kim and Lee, 2016].

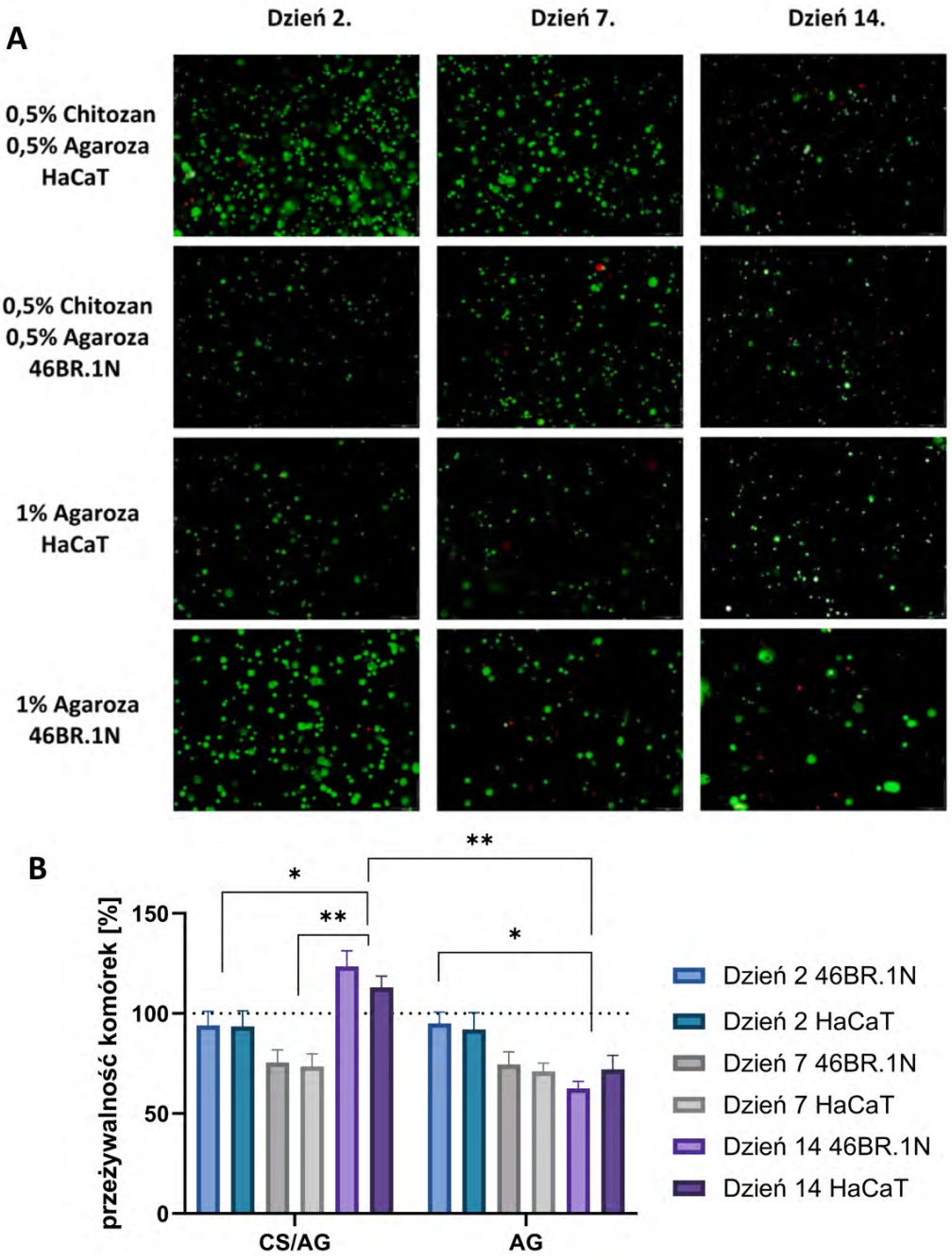

Rysunek 17. Żywotność fibroblastów 46BR.1N i keratynocytów HaCaT osadzonych w kompozycji chitozanowo-agarozowej (CS/AG) i w samej agarozie (AG). A) Rysunek przedstawia fluorescencyjne obrazy mikroskopowe pokazujące barwienie żywych i martwych komórek w rusztowaniach w dniach 2, 7 i 14-dniu hodowli. Żywe komórki są zabarwione na zielono kalceiną, podczas gdy martwe komórki są zabarwione na czerwono jodkiem propidyny; pasek skali 250 µm. B) Wykres zmian wskaźników przeżywalności obu linii komórkowych w czasie. Wyniki przedstawiono jako średnią ± odchylenie standardowe (SD) na podstawie trzech powtórzeń ($n = 3$, $p < 0,05$). Wartości na wykresie B porównano między sobą. Oznaczenia poziomów istotności statystycznej są następujące: *$p < 0,05$, **$p < 0,01$.

Na podstawie powyższych wyników dotyczących przeżywalności komórek fibroblastów i keratynocytów w kompozycji chitozanowo-agarozowej i agarozie, uzyskano cenne informacje na temat długoterminowego wpływu biotuszu na ich żywotność. Aby jednak ocenić pełne bezpieczeństwo biologiczne opracowanej kompozycji polimerowej i potwierdzić jej przydatność do zastosowań biomedycznych, wykonano dodatkowe, szczegółowe badania zgodne z wytycznymi dotyczącymi oceny wyrobów medycznych. W ramach tych działań przeprowadzono testy MTT, tym razem z wykorzystaniem linii komórkowych dedykowanych do tego biotuszu, tj. fibroblastów 46BR.1N oraz keratynocytów HaCaT. Wysoka żywotność komórek (85-112% dla linii 46.BR.1N i 90-137% dla linii HaCaT) po ich 24-godzinnym kontakcie z ekstraktami badanych materiałów (2,5% m/v) ponownie potwierdziła brak efektu cytotoksycznego i bezpieczeństwo biologiczne dla wybranych komórek.

Po uzyskaniu pozytywnych wyników dotyczących biozgodności, w tym bezpieczeństwa biologicznego badanej kompozycji chitozanowo-agarozowej, kolejnym etapem było przejście do bardziej zaawansowanych metod badawczych, takich jak test błony kosmówkowo-omoczniowej CAM (chorioallantoic membrane assay) z wykorzystaniem zarodka jaja kurzego. Test CAM, rekomendowany przez FDA (Food and Drug Administration), umożliwia m.in. ocenę wpływu biomateriałów na procesy regeneracyjne, w tym rozwój angiogenezy w warunkach *in vivo*. Proces angiogenezy, czyli tworzenie nowych naczyń krwionośnych z już istniejących, jest kluczowy dla dostarczenia tlenu, składników odżywczych oraz czynników wzrostu do regenerującej się tkanki. Prawidłowa, szybko zachodząca angiogeneza nie tylko wspiera proces gojenia, lecz także zapobiega martwicy, która może nastąpić podczas regeneracji tkanki [Guo et al., 2022]. Co istotne, w krajach europejskich, zgodnie z dyrektywą UE 2010/63, oraz w USA, metoda CAM nie jest klasyfikowana jako eksperyment na zwierzętach, ponieważ zarodek kurzy rozwija się poza organizmem macierzystym, a test musi zostać zakończony do osiemnastego dnia inkubacji, zanim zarodek osiągnie pełną zdolność odczuwania bodźców bólowych (nocycepcji). Test CAM wpisuje się w zasady 3R (replace, reduce, refine), które zmierzają do ograniczenia eksperymentów na zwierzętach. Jest to kluczowy element etyki w przemyśle biomedycznym i farmaceutycznym, a także priorytet dla organów regulacyjnych takich jak EMA i Komisja Europejska, które promują metody minimalizujące cierpienie zwierząt i zwiększające wartość badań przedklinicznych [Fischer i wsp., 2022]. W związku z powyższym, badając ilość nowo powstałych rozgałęzień naczyń krwionośnych, ich długość, grubość oraz całkowitą powierzchnię stwierdzono, że tylko w przypadku układów na bazie chitozanu oraz chitozanu i agarozy następuje promowanie niewielkiego wzrostu powyższych parametrów naczyniowych w porównaniu z kontrolą, czyli obojętnym materiałem jakim jest zanurzona w 0,9% roztworze soli fizjologicznej bibuła Whatmana (Rys. 18). Hydrożelowe membrany na bazie chitozanu wykazały najbardziej spójne działanie proangiogenne, pod względem długości naczyń i liczby rozgałęzień, w przeciwieństwie do membrany agarozowej.

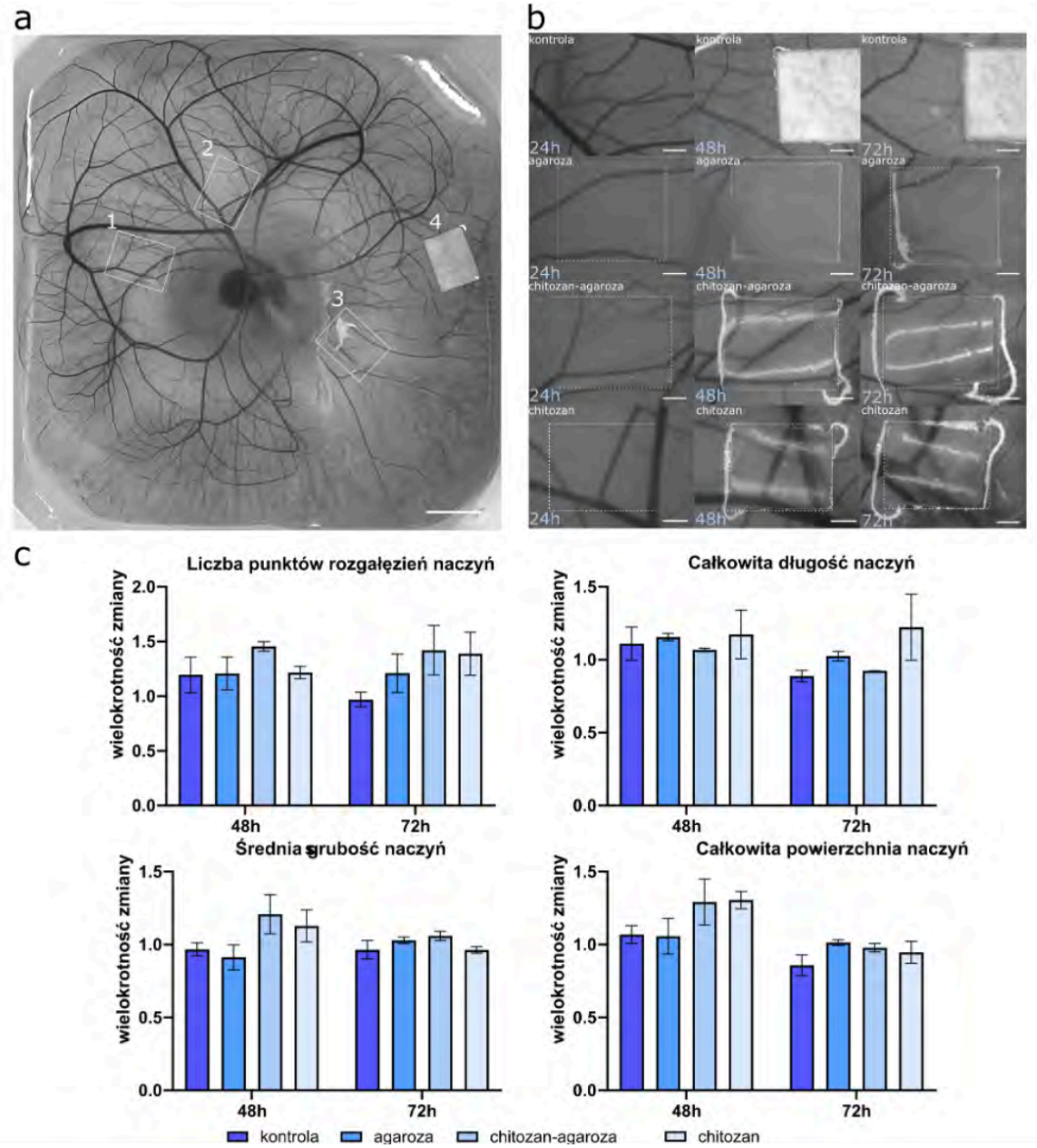

Rysunek 18. Test angiogenezy CAM *ex-ovo*. A) Reprezentatywny obraz zarodka jaja kurzego hodowanego *ex-ovo* z różnymi testowanymi materiałami w 9. dniu rozwoju embrionalnego. Materiały są oznaczone w następujący sposób: 1 - agaroza + chitozan, 2 - chitozan, 3 - agaroza, 4 - bibuła filtracyjna Whatman. Pasek skali = 5 mm. B) Reprezentatywne obrazy mikroskopowe pokazujące angiogenezę indukowaną materiałem po 24, 48 i 72 godzinach inkubacji. Pasek skali = 1 mm. Analiza zmian w sieci naczyniowej, w tym liczba punktów rozgałęzień naczyń (C), całkowita długość naczyń (D), średnia grubość naczyń (E) i całkowita powierzchnia naczyń (F), przedstawione jako zmiany krotności w stosunku do 24-godzinnej inkubacji Wyniki przedstawiono jako średnią ± odchylenie standardowe (SD) z co najmniej dwóch niezależnych eksperymentów.

Po zakończeniu badań w modelu CAM, które umożliwiły szybką ocenę pro-regeneracyjnych właściwości badanych kompozycji polimerowych, kolejny etap prac obejmował zastosowanie modelu zwierzęcego, stanowiącego bardziej złożone środowisko biologiczne. W badaniach tych przeanalizowano wpływ opracowanego rusztowania na proces gojenia się ran, wykorzystując zwierzęcy model rany u myszy. Tego typu badania stanowią pierwszy krok umożliwiający przeprowadzenie badań klinicznych, które decydują o przydatności rusztowania w zastosowaniach medycznych.

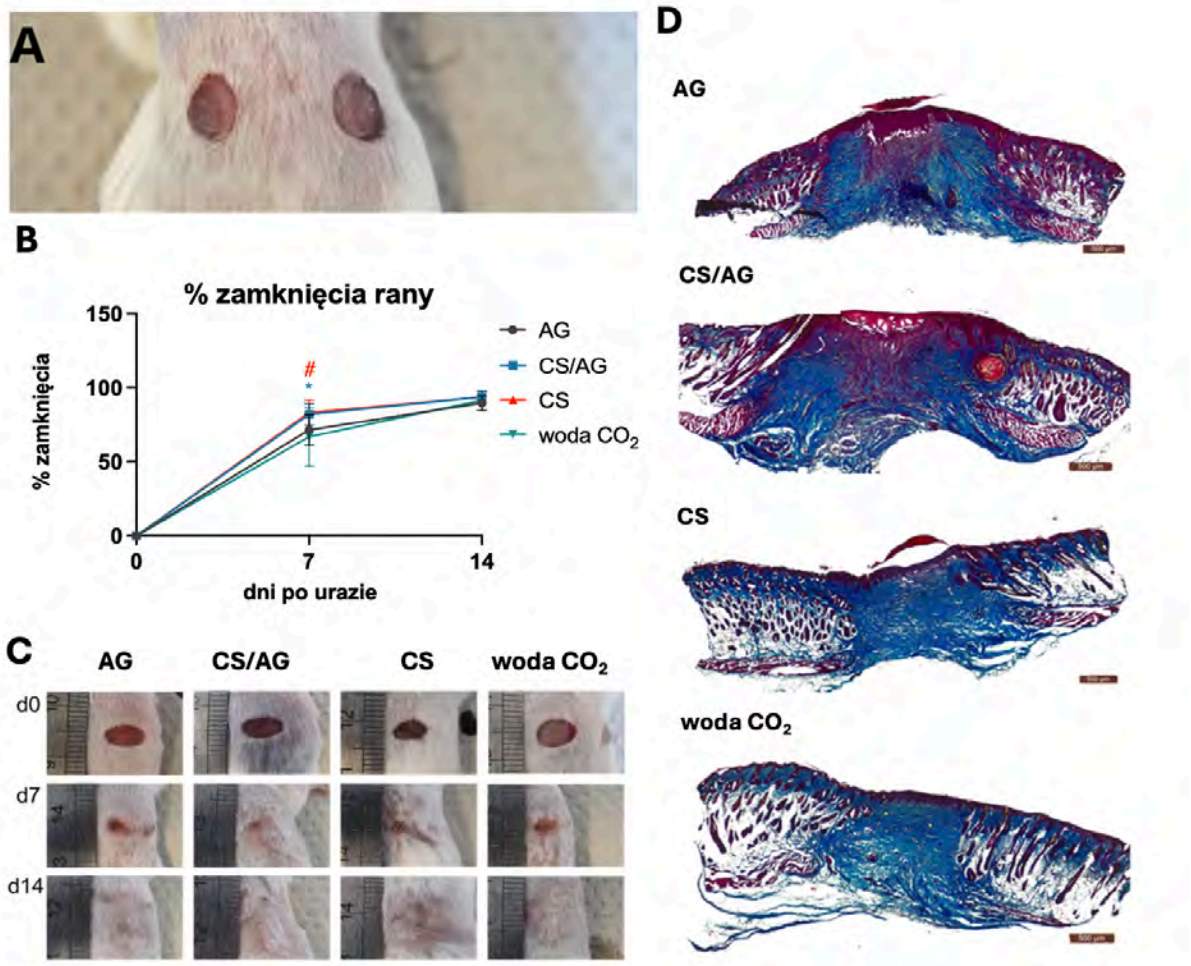

Rysunek 19. Wpływ badanych hydrożeli na gojenie się ran skóry u myszy. A) przykładowe zdjęcie krążków hydrożelowych nałożonych na rany skóry grzbietowej; B) średni procent zamknięcia rany; słupki błędów reprezentują SD, n = 12 - liczba ran reprezentujących 6 myszy w każdej grupie; istotność statystyczną w stosunku do kontroli woda z CO_2 określono za pomocą dwustronnego testu Manna-Whitneya i oznaczono gwiazdką „*” dla CS/AG i hasztagiem „#” dla samego CS; C) reprezentatywne obrazy ran w dniu (d) 0, 7 i 14; D) reprezentatywne wycinki skóry pobrano w 14 dniu po urazie i wybarwiono trichromem Massona w celu wizualizacji architektury tkanki: czerwony - mięśnie i keratyna; niebieski - kolagen; różowy - cytoplazma; brązowy - jądra.

W ramach badań nad wpływem hydrożelowych rusztowań w formie walca zastosowano różne układy: kompozycję zawierającą 0,5% chitozanu i 0,5% agarozy, 1% agarozy, 1% roztworu chitozanu nasyconego dwutlenkiem węgla oraz kontrolny, czyli nasyconą dwutlenkiem węgla wodę destylowaną. Wyniki wykazały, że metoda aplikacji materiału na ranę ma istotny wpływ na proces gojenia (Rys. 19). Naniesienie płynnej warstwy hydrożelu chitozanu, spowodowało jej szybkie wyschnięcie. Kompozycja chitozanowo-agarozowa, pozwoliła z kolei na dłuższe utrzymanie wilgotnego środowiska, chroniąc ranę przed wyschnięciem. Udział agarozy w materiale przyczynia się do tworzenia stabilnego i trwałego rusztowania, które naśladuje naturalne środowisko tkankowe, sprzyjające procesowi gojenia się ran. Po 7 dniach leczenia ran badanymi kompozycjami chitozanowo-agarozowymi zaobserwowano zmniejszenie się jej powierzchni do 33%, co stanowiło 40-50% szybsze gojenie się ran niż w pozostałych badanych grupach. Dodatkowo na podstawie badań histologicznych zauważono integrację chitozanu ze strukturą skóry podczas regeneracji oraz znaczny wzrost liczby keratynocytów. Podsumowując, wyniki te wskazują na wyraźną przewagę kompozycji chitozanowo-agarozowej nad jej poszczególnymi składnikami z osobna oraz wodą nasyconą CO_2 w kontekście wspomagania procesu gojenia ran. Potwierdzono pozytywny wpływ kompozycji chitozanowo-agarozowegona kilka wybranych ważnych dla procesów regeneracyjnych parametrów biologicznych, otwierając nowe możliwości jej zastosowania w inżynierii tkankowej.

4 PODSUMOWANIE

Przeprowadzone badania, integrujące wiedzę z zakresu chemii, inżynierii materiałowej oraz biologii medycznej, pozwoliły na opracowanie biotuszu o unikalnych właściwościach aplikacyjnych, stanowiącego wkład w rozwój technologii biodruku oraz inżynierii tkankowej. Opracowana kompozycja hydrożelowa, bazująca na chitozanie otrzymanym metodą saturacji dwutlenkiem węgla, w połączeniu z agarozą, posiada optymalne właściwości fizykochemiczne i biologiczne, spełniając kluczowe kryteria drukowalności oraz biozgodności. Te właściwości czynią ten materiał szczególnie przydatnym w regeneracji tkanki skórnej, co stanowi bezpośrednią odpowiedź na postawione cele badawcze i potwierdza jego szeroki potencjał aplikacyjny w medycynie regeneracyjnej oraz technologiach inżynierii tkankowej.

Rozwiązanie problemu badawczego osiągnięto poprzez opracowanie kompozycji chitozanowo-agarozowej o zdolności do natychmiastowego żelowania w warunkach temperatury fizjologicznej, eliminując tym samym konieczność stosowania dodatkowych modyfikacji chemicznych oraz czynników sieciujących. Dzięki temu uzyskano materiał o wysokim poziomie bezpieczeństwa biologicznego oraz prostocie zastosowania w warunkach przemysłowych. Unikalny charakter opracowanego biotuszu został zabezpieczony zgłoszeniami patentowymi (P.443403 i EP.23460040).

Do głównych dokonań badawczych niniejszej rozprawy należą:

- **Optymalizacja procesu usuwania endotoksyn z roztworów chitozanowych** bez wpływu na masę cząsteczkową i stopień deacetylacji tego polimeru, co jest kluczowe dla zachowania jego parametrów fizykochemicznych.
- **Wykazanie, że masa cząsteczkowa i DD chitozanu nie miały istotnego wpływu na jego właściwości przeciwdrobnoustrojowe ani cytotoksyczność,** pozwoliło to skupić się na ocenie wpływu masy cząsteczkowej na drukowalność oraz właściwości żelujące kompozycji z agarozą.
- **Opracowanie innowacyjnej metody wytwarzania termoczułej kompozycji chitozanowo-agarozowej**, która może być stosowana jako baza biotuszu. Materiał ten, żelujący pod wpływem temperatury fizjologicznej, umożliwia szybkie i skuteczne wytwarzanie rusztowań komórkowych bez użycia dodatkowych czynników sieciujących.
- **Spełnienie podstawowych kryteriów akceptacji, takich jak drukowalność i biozgodność**. Właściwości reologiczne kompozycji polimerowej obejmują zdolność do odbudowy struktury po zadziałaniu sił mechanicznych, jest to niezbędne dla zachowania integralności geometrycznej w procesie druku warstwowego. Dodatkowo, biozgodność kompozycji została zweryfikowana na liniach komórkowych L929, 46BR.1N oraz HaCaT, co potwierdza jej potencjalne zastosowanie w inżynierii tkankowej i biomedycynie.

- **Ocena wpływu kompozycji chitozanowo-agarozowej wykazała, że materiał wspiera migrację, proliferację i przeżywalność komórek,** co stanowi solidną podstawę do potencjalnych zastosowań w inżynierii tkankowej. Wyniki sugerują, że opracowana kompozycja może efektywnie wspierać procesy regeneracyjne w uszkodzonych tkankach, sprzyjając tworzeniu funkcjonalnych struktur niezbędnych do skutecznej regeneracji.
- **Brak negatywnego wpływu na angiogenezę i wspieranie procesu gojenia ran**, co stanowi podstawę do potencjalnych zastosowań w inżynierii tkankowej. Stwierdzono, że kompozycja może wspierać procesy regeneracyjne w uszkodzonych tkankach.

Podsumowując, opracowana kompozycja chitozanowo-agarozowa stanowi istotny postęp w dziedzinie biodruku i inżynierii tkankowej. Eliminując konieczność stosowania dodatkowych czynników sieciujących, znacząco upraszcza proces produkcji i zwiększa bezpieczeństwo aplikacyjne. Materiał ten zachowuje kluczowe właściwości, takie jak drukowalność, biozgodność oraz właściwości przeciwdrobnoustrojowe, które są odpowiedzią na specyficzne wymagania sektora medycznego, szczególnie w kontekście zastosowań klinicznych i biomedycznych.

Kolejne etapy badań będą koncentrować się nie tylko na biologicznych właściwościach materiału, ale także na kompleksowym opracowaniu i optymalizacji całego procesu biodruku, z uwzględnieniem jego różnych wariantów. Planowane jest również skupienie się na druku robotycznym, co pozwoli na uzyskanie jeszcze bardziej precyzyjnych struktur trójwymiarowych, o zoptymalizowanych parametrach, kluczowych dla efektywnej regeneracji tkankowej. Dodatkowo, istotną rolę odegrają technologie sztucznej inteligencji, które będą wykorzystane do szczegółowej analizy parametrów reologicznych i strukturalnych kompozycji, jak również do modelowania, przewidywania zachowania materiału w trakcie procesu biodruku, a także w badaniach biologicznych, takich jak ocena efektów proangiogennych w modelu CAM. Optymalizacja procesu biodruku będzie obejmowała badania nad kluczowymi parametrami technologicznymi, uwzględniającymi aspekty takie jak przepływ materiału, gradient ciśnienia oraz warunki termiczne wpływające na proces żelowania, szczególnie w kontekście porowatości, drukowalności oraz metod osadzania materiału. Wykorzystanie algorytmów uczenia maszynowego umożliwi symulacje procesu biodruku oraz precyzyjne dostosowanie właściwości biotuszu do specyficznych wymagań medycznych. Wprowadzenie peptydów proangiogennych w celu zwiększenia bioaktywności kompozycji będzie kolejnym istotnym krokiem w rozwoju kompozycji polimerowych, zwłaszcza w kontekście wspierania procesów angiogenezy, które są kluczowe dla regeneracji tkankowej.

Przyszłe badania będą skoncentrowane na dalszej optymalizacji opracowanej kompozycji polimerowej, która już spełnia wysokie wymagania inżynierii tkankowej, lecz wciąż kryje w sobie ogromny potencjał rozwoju. Celem jest dostosowanie jej do specyficznych zastosowań. Pozwoli to na poszerzenie jej funkcjonalności i efektywności w zróżnicowanych obszarach medycyny regeneracyjnej, farmacji i biologii.

5 BIBLIOGRAFIA

1. [A2] Mania S., Banach-Kopeć A., Staszczyk K., Kulesza J., Augustin E., & Tylingo R. (2023). An influence of molecular weight, deacetylation degree of chitosan xerogels on their antimicrobial activity and cytotoxicity. Comparison of chitosan materials obtained using lactic acid and CO_2 saturation. Carbohydrate Research, 534, 108973.
2. [A3] Banach-Kopeć A., Mania S., Tylingo R., Wawrzynowicz A., Pawłowska M., Czerwiec K., Deptuła M., Pikuła M. (2024). Thermosensitive composite based on agarose and chitosan saturated with carbon dioxide. Preliminary study of requirements for production of new CSAG bioink. Carbohydrate Polymers, 336, 122120.
3. [A5] Banach-Kopeć A., Mania S., & Tylingo R. (2024). Marine polymers in tissue bioprinting: Current achievements and challenges. Reviews on Advanced Materials Science, 63(1), 20230180.
4. Agarwal, K., Srinivasan, V., Lather, V., Pandita, D., & Vasanthan, K. S. (2023). Insights of 3D bioprinting and focusing the paradigm shift towards 4D printing for biomedical applications. Journal of Materials Research, 38(1), 112-141.
5. Alhattab D. M., Khan Z., Alshehri S., Susapto H. H., & Hauser C. A. (2023). 3D bioprinting of ultrashort self-assembling peptides to engineer scaffolds with different matrix stiffness for chondrogenesis. International Journal of Bioprinting, 9(4).
6. Butler H. M., Naseri E., MacDonald D. S., Tasker R. A., & Ahmadi A. (2021). Investigation of rheology, printability, and biocompatibility of N, O-carboxymethyl chitosan and agarose bioinks for 3D bioprinting of neuron cells. Materialia, 18, 101169.
7. Chandrasekaran M., Kim K. D., & Chun S. C. (2020). Antibacterial activity of chitosan nanoparticles: A review. Processes, 8(9), 1173.
8. Choudhury D., Anand S., & Naing M. W. (2018). The arrival of commercial bioprinters–Towards 3D bioprinting revolution! International Journal of Bioprinting, 4(2).
9. Cohen R., Baruch E. S., Cabilly I., Shapira A., & Dvir T. (2023). Modified ECM-based bioink for 3D printing of multi-scale vascular networks. Gels, 9(10), 792.
10. Das S., & Basu B. (2019). An overview of hydrogel-based bioinks for 3D bioprinting of soft tissues. Journal of the Indian Institute of Science, 99, 405-428.
11. Dawson M. (2017). Endotoxin limits for parenteral drug products. BET White Paper, 1(2), 1-7.

12. Deptuła M., Zawrzykraj M., Sawicka J., Banach-Kopeć A., Tylingo R., & Pikuła M. (2023). Application of 3D-printed hydrogels in wound healing and regenerative medicine. Biomedicine & Pharmacotherapy, 167, 115416.
13. Dyrektywa 2008/98/WE Parlamentu Europejskiego i Rady z dnia 19 listopada 2008 r. w sprawie odpadów, aktualna wersja skonsolidowana obowiązująca od 18 lutego 2024 r. Dziennik Urzędowy Unii Europejskiej L 312, s. 3–30.
14. Fang W., Yang M., Wang L., Li W., Liu M., Jin Y., Hou X., Tang J., & Fu Q. (2023). Hydrogels for 3D bioprinting in tissue engineering and regenerative medicine: Current progress and challenges. International Journal of Bioprinting, 9(5).
15. Feng P., Luo Y., Ke C., Qiu H., Wang W., Zhu Y., Shuai C., Peng S., & Wu S. (2021). Chitosan-based functional materials for skin wound repair: Mechanisms and applications. Frontiers in Bioengineering and Biotechnology, 9, 650598.
16. Fischer D., Fluegen G., Garcia P., Ghaffari-Tabrizi-Wizsy N., Gribaldo L., Huang R. Y. J., Rasche V., Ribatti D., Rousset X., Pinto M. T., Viallet J., Wang Y., & Schneider-Stock, R. (2022). The CAM model—Q&A with experts. Cancers, *15*(1), 191.
17. Gao G., Ahn M., Cho W. W., Kim B. S., & Cho D. W. (2021). 3D printing of pharmaceutical application: drug screening and drug delivery. Pharmaceutics, 13(9), 1373.
18. Ghebremedhin M., Seiffert S., & Vilgis T. A. (2021). Physics of agarose fluid gels: Rheological properties and microstructure. Current Research in Food Science, 4, 436-448.
19. Gorczyca G., Tylingo R., Szweda P., Augustin E., Sadowska M., & Milewski S. (2014). Preparation and characterization of genipin cross-linked porous chitosan–collagen–gelatin scaffolds using chitosan–CO_2 solution. Carbohydrate Polymers, 102, 901-911.
20. Goy R. C., Britto D. D., & Assis O. B. (2009). A review of the antimicrobial activity of chitosan. Polímeros, 19, 241-247.
21. Gu Q., Tomaskovic-Crook E., Wallace G. G., & Crook J. M. (2017). 3D bioprinting human induced pluripotent stem cell constructs for in situ cell proliferation and successive multilineage differentiation. Advanced Healthcare Materials, 6(17), 1700175.
22. Guo Y., Huang J., Fang Y., Huang H., & Wu J. (2022). 1D, 2D, and 3D scaffolds promoting angiogenesis for enhanced wound healing. Chemical Engineering Journal, 437, 134690.
23. Habib M. A., & Khoda B. (2022). Rheological analysis of bio-ink for 3D bio-printing processes. Journal of Manufacturing Processes, 76, 708-718.
24. Haładyj A. (2019). Uznanie produktu ubocznego pochodzenia zwierzęcego za odpad–kryteria i skutki. Roczniki Nauk Prawnych, 29(3), 21-39.
25. He P., et al. (2018). Bioprinting of skin constructs for wound healing. Burns & Trauma, 6.

26. Heine H., Rietschel E. T., & Ulmer A. J. (2001). The biology of endotoxin. Molecular biotechnology, 19, 279-296.
27. Helander I. M., Nurmiaho-Lassila E. L., Ahvenainen R., Rhoades J., & Roller S. (2001). Chitosan disrupts the barrier properties of the outer membrane of Gram-negative bacteria. International Journal of Food Microbiology, 71(2-3), 235-244.
28. Hosseinnejad M. ,& Jafari S. M. (2016). Evaluation of different factors affecting antimicrobial properties of chitosan. International journal of biological macromolecules, 85, 467-475.
29. Huang G., Zhao Y., Chen D., Wei L., Hu Z., Li J., Feng Y., Zhang Y., & Chen Z. (2024). Applications, advancements, and challenges of 3D bioprinting in organ transplantation. Biomaterials Science, 12(6), 1425-1448.
30. ISO 10993 – Ocena biologiczna wyrobów medycznych – Części 1–20. Międzynarodowa Organizacja Normalizacyjna, Genewa, 2018.
31. Jiang F, Xu X-W, Chen F-Q, Weng H-F, Chen J, Ru Y, Xiao Q, & Xiao A-F. (2023). Extraction, Modification and Biomedical Application of Agarose Hydrogels: A Review. Marine Drugs, 21(5), 299.
32. Kačarević Ž. P., Rider P. M., Alkildani S., Retnasingh S., Smeets R., Jung O., Schnettler R., & Barbeck M. (2018). An introduction to 3D bioprinting: possibilities, challenges and future aspects. Materials, 11(11), 2199.
33. Ke C. L., Deng F. S., Chuang C. Y., & Lin C. H. (2021). Antimicrobial actions and applications of chitosan. Polymers, 13(6), 904.
34. Kim H., & Lee J. (2016). Strategies to maximize the potential of marine biomaterials as a platform for cell therapy. Marine Drugs, 14(2), 29.
35. Kimble A., Hauschild J., & McDonnell G. (2023). Affinity and inactivation of bacterial endotoxins for medical device materials. Biomedical Instrumentation & Technology, *57*(4), 153-162.
36. Levato R., Jungst T., Scheuring R. G., Blunk T., Groll J., & Malda J. (2020). From shape to function: the next step in bioprinting. Advanced Materials, 32(12), 1906423.
37. Li X., Liu B., Pei B., Chen J., Zhou D., Peng J., Zhang X., Jia W., & Xu T. (2020). Inkjet bioprinting of biomaterials. Chemical Reviews, 120(19), 10793-10833.
38. Lieder R., Gaware V. S., Thormodsson F., Einarsson J. M., Ng C. H., Gislason J., Masson M., Petersen P. H., & Sigurjonsson O. E. (2013). Endotoxins affect bioactivity of chitosan derivatives in cultures of bone marrow-derived human mesenchymal stem cells. Acta biomaterialia, 9(1), 4771-4778.
39. Liu X., Hao M., Chen Z., Zhang T., Huang J., Dai J., & Zhang Z. (2021). 3D bioprinted neural tissue constructs for spinal cord injury repair. Biomaterials, 272, 120771.

40. Malekpour A., & Chen X. (2022). Printability and cell viability in extrusion-based bioprinting from experimental, computational, and machine learning views. Journal of Functional Biomaterials, 13(2), 40.
41. Mohammadrezaei D., Podina L., De Silva J., & Kohandel M. (2024). Cell viability prediction and optimization in extrusion-based bioprinting via neural network-based Bayesian optimization models. Biofabrication, 16(2), 025016.
42. Morrison D. C., & Leive L. (1975). Fractions of lipopolysaccharide from Escherichia coli O111: B4 prepared by two extraction procedures. Journal of Biological Chemistry, 250(8), 2911-2919.
43. Murphy S. V., & Atala A. (2014). 3D bioprinting of tissues and organs. Nature Biotechnology, 32(8), 773-785.
44. Ng W. L., Chua C. K., & Shen Y. F. (2019). Print me an organ! Why we are not there yet. Progress in Polymer Science, 97, 101145.
45. Oropeza B. P., Serna C., Furth M. E., Solis L. H., Gonzalez C. E., Altamirano V., Acevedo R., Ramirez M., & Boland T. (2022). Assessment of angiogenesis and cell survivability of an inkjet bioprinted biological implant in an animal model. Materials, 15(13), 4468.
46. Ouyang L. (2022). Pushing the rheological and mechanical boundaries of extrusion-based 3D bioprinting. Trends in Biotechnology, 40(7), 891-902.
47. Ramesh S., Harrysson O. L., Rao P. K., Tamayol A., Cormier D. R., Zhang Y., & Rivero I. V. (2021). Extrusion bioprinting: Recent Progres, challenges, and future opportunities. Bioprinting, 21, e00116.
48. Reich J., & Deutschmann S. (2020). General chapter on the rFC test adopted by the European Pharmacopoeia Commission. European Pharmaceutical Review. Retrieved September 2, 2024, from https://www.europeanpharmaceuticalreview.com/article/113332/general-chapter-on-the-rfc-test-adopted-by-the-european-pharmacopoeia-commission/ (data dostępu 02.08.2024).
49. Rozporządzenie (WE) nr 1069/2009 Parlamentu Europejskiego i Rady z dnia 21 października 2009 r. w sprawie przepisów sanitarnych dotyczących produktów ubocznych pochodzenia zwierzęcego, nieprzeznaczonych do spożycia przez ludzi, w wersji skonsolidowanej z dnia 14 grudnia 2019 r. Dziennik Urzędowy Unii Europejskiej L 300, s. 1–33.
50. Rozporządzenie Komisji (UE) nr 722/2012 z dnia 8 sierpnia 2012 r. dotyczące szczególnych wymagań odnoszących się do wymagań ustanowionych w dyrektywach Rady 90/385/EWG i 93/42/EWG dla aktywnych wyrobów medycznych do implantacji oraz wyrobów medycznych produkowanych z wykorzystaniem tkanek pochodzenia zwierzęcego. Dziennik Urzędowy Unii Europejskiej L 212, s. 3–12.

51. Rozporządzenie (UE) 2017/745 Parlamentu Europejskiego i Rady z dnia 5 kwietnia 2017 r. w sprawie wyrobów medycznych (MDR). Dziennik Urzędowy Unii Europejskiej L 117, s. 1–175.
52. Russ N., Zielbauer B. I., Koynov K., & Vilgis T. A. (2013). Influence of nongelling hydrocolloids on the gelation of agarose. Biomacromolecules, 14(11), 4116-4124.
53. Saberianpour S., Heidarzadeh M., Geranmayeh M. H., Hosseinkhani H., Rahbarghazi R., & Nouri M. (2018). Tissue engineering strategies for the induction of angiogenesis using biomaterials. Journal of Biological Engineering, 12, 1-15.
54. Sadeghianmaryan A., Naghieh S., Sardroud H. A., Yazdanpanah Z., Soltani Y. A., Sernaglia J., & Chen X. (2020). Extrusion-based printing of chitosan scaffolds and their in vitro characterization for cartilage tissue engineering. International Journal of Biological Macromolecules, 164, 3179-3192.
55. Seow W. Y., Kandasamy K., Peh G. S., Mehta J. S., & Sun W. (2019). Ultrathin, strong, and cell-adhesive agarose-based membranes engineered as substrates for corneal endothelial cells. ACS Biomaterials Science & Engineering, 5(8), 4067-4076.
56. Sikora M., Wiśniewska-Wrona M., & Arabski M. (2021). Biomedyczne właściwości chitozanu – zastosowanie w inżynierii tkankowej. Postępy Higieny i Medycyny Doświadczalnej, 75(1), 1020-1037.
57. Salati M. A., Khazai J., Tahmuri A. M., Samadi A., Taghizadeh A., Taghizadeh M., Kadirvelu K., & Mozafari M. (2020). Agarose-based biomaterials: opportunities and challenges in cartilage tissue engineering. Polymers, 12(5), 1150.
58. Toyama Y., Sahara R., Iino Y., & Kubota K. (2011). pH dependence of rheological properties of gelatin gel mixed with agar or agarose. Transactions of the Materials Research Society of Japan, 36(3), 383-386.
59. Yacob N., Talip N., Mahmud M., Aizam Aisam Idayu Mat Sani N., & Akma Samsuddin N. (2013). Determination of viscosity-average molecular weight of chitosan using intrinsic viscosity measurement. J. Nucl. Relat. Technol., 10, 39-44.
60. Yang F., & Yang X. (2008). Kinetic analysis of interaction between lipopolysaccharide and biomolecules. Frontiers of Chemistry in China, 3, 14-17.
61. Yang, X., Mohseni, M., Bas, O., Meinert, C., New, E. J., & Castro, N. J. (2020). Type II photoinitiator and tuneable poly (Ethylene Glycol)-based materials library for visible light photolithography. Tissue Engineering Part A, 26(5-6), 292-304.
62. Vijayavenkataraman S. (2023). 3D bioprinting: challenges in commercialization and clinical translation. Journal of 3D Printing in Medicine, 7(2), 3DP8.
63. Wang X., Zhang D., Singh Y. P., Yeo M., Deng G., Lai J., Lin F., Wu J., & Yu Y. (2024). Progress in organ bioprinting for regenerative medicine. Engineering.

64. Weißpflog J., Vehlow D., Müller M., Kohn B., Scheler,U., Boye S., & Schwarz S. (2021). Characterization of chitosan with different degree of deacetylation and equal viscosity in dissolved and solid state–Insights by various complimentary methods. *International Journal of Biological Macromolecules*, *171*, 242-261
65. Xu H. Q., Liu J. C., Zhang Z. Y., & Xu C. X. (2022). A review on cell damage, viability, and functionality during 3D bioprinting. Military Medical Research, 9(1), 70.
66. Zarrintaj P., Manouchehri S., Ahmadi Z., Saeb M. R., Urbanska A. M., Kaplan D. L., & Mozafari M. (2018). Agarose-based biomaterials for tissue engineering. Carbohydrate Polymers, 187, 66-84.
67. Zheng L. Y., & Zhu, J. F. (2003). Study on antimicrobial activity of chitosan with different molecular weights. Carbohydrate polymers, 54(4), 527-530.

6 TREŚĆ ARTYKUŁÓW Z OPISEM WKŁADU PRACY DOKTORANTA

6.1 [A1] A Novel Method of Endotoxins Removal from Chitosan Hydrogel as a Potential Bioink Component Obtained by CO_2 Saturation.

6.1.1 Wkład pracy doktoranta

Tytuł: A Novel Method of Endotoxins Removal from Chitosan Hydrogel as a Potential Bioink Component Obtained by CO_2 Saturation
Autorzy: Adrianna Banach-Kopeć, Szymon Mania, Joanna Pilch,
Ewa Augustin, Iwona Gabriel, Robert Tylingo
Czasopismo: INTERNATIONAL JOURNAL OF MOLECULAR SCIENCES
Rok wydania: 2022
Impact factor: 5,6 (2022)
Liczba punktów wg MNiSW: 140
DOI: 10.3390/ijms23105505
Procentowy wkład pracy doktoranta: 28%

Byłam jedną z kluczowych osób odpowiedzialnych za opracowanie koncepcji badań, które stanowią podstawę niniejszej pracy. Wspólnie z pozostałymi autorami zaprojektowałam oraz przeprowadziłam eksperymenty. Moim zadaniem było opracowanie metody usuwania endotoksyn, oznaczenia ich stężenia, przeprowadzenie badań czystości mikrobiologicznej, jak również przygotowanie prób do dalszych testów z wykorzystaniem tej metody. Brałam aktywny udział w badaniach nad lepkością oraz oznaczaniu masy cząsteczkowej analizowanych prób. Wspólnie z głównymi autorami pełniłam funkcję zarządzającą projektem, nadzorując jego realizację i koordynując prace zespołu. Byłam odpowiedzialna za opracowanie wstępnych wersji manuskryptu oraz brałam aktywny udział w jego edycji. Ponadto koordynowałam przygotowanie odpowiedzi na recenzje, a także finalizację ostatecznej wersji manuskryptu do publikacji.

6.1.2 Treść artykułu

International Journal of *Molecular Sciences*

MDPI

Article

A Novel Method of Endotoxins Removal from Chitosan Hydrogel as a Potential Bioink Component Obtained by CO_2 Saturation

Adrianna Banach-Kopeć [1], Szymon Mania [1,*], Joanna Pilch [2], Ewa Augustin [2], Iwona Gabriel [2] and Robert Tylingo [1]

1 Department of Chemistry, Technology, and Biotechnology of Food, Faculty of Chemistry, Gdańsk University of Technology, 11/12 G.Narutowicza Str., 80-233 Gdansk, Poland; adrianna.banach@pg.edu.pl (A.B.-K.); robertt@pg.edu.pl (R.T.)

2 Department of Pharmaceutical Technology and Biochemistry, Faculty of Chemistry, Gdańsk University of Technology, 11/12 G.Narutowicza Str., 80-233 Gdansk, Poland; joapilch@pg.edu.pl (J.P.); ewa.augustin@pg.edu.pl (E.A.); iwona.gabriel@pg.edu.pl (I.G.)

* Correspondence: szymon.mania@pg.edu.pl; Tel.: +48-58-347-28-56

Abstract: The article presents a new approach in the purification of chitosan (CS) hydrogel in order to remove a significant amount of endotoxins without changing its molecular weight and viscosity. Two variants of the method used to purify CS hydrogels from endotoxins were investigated using the PyroGene rFC Enzymatic Cascade assay kit. The effect of the CS purification method was assessed in terms of changes in the dynamic viscosity of its hydrogels, the molecular weight of the polymer, microbiological purity after refrigerated storage and cytotoxicity against L929 cells based on the ISO 10993-5:2009(E) standard. The proposed purification method 1 (M1) allows for the removal of significant amounts of endotoxins: 87.9–97.6% in relation to their initial concentration in the CS hydrogel without affecting the solution viscosity. Moreover, the final solutions were sterile and microbiologically stable during storage. The M1 purification method did not change the morphology of the L929 cells.

Keywords: chitosan hydrogel; CO_2 saturation; endotoxin; cytotoxicity; microbiological purity; molecular weight; viscosity

check for updates

Citation: Banach-Kopeć, A.; Mania, S.; Pilch, J.; Augustin, E.; Gabriel, I.; Tylingo, R. A Novel Method of Endotoxins Removal from Chitosan Hydrogel as a Potential Bioink Component Obtained by CO_2 Saturation. *Int. J. Mol. Sci.* **2022**, *23*, 5505. https://doi.org/10.3390/ijms23105505

Academic Editor: Ylenia Zambito

Received: 25 April 2022
Accepted: 13 May 2022
Published: 14 May 2022

Publisher's Note: MDPI stays neutral with regard to jurisdictional claims in published maps and institutional affiliations.

1. Introduction

Bioprinting is an additive manufacturing method in which thermoplastic materials and hydrogels filled with cells and distributed layer-by-layer are used to obtain a three-dimensional scaffold [1,2]. The bioinks used in bioprinting must fulfil a number of criteria, that is, biodegradable, non-cytotoxic, biocompatible, and porous, to allow the formation of new tissues and support cell growth throughout the regeneration period. In addition, cellular scaffolds must be adherent, allow for the exchange of gases and metabolites, and have adequate mechanical properties [3]. Polysaccharides of marine origin are raw materials that meet most of the 3D printing requirements and medical guidelines. Compared with polysaccharides obtained from mammals, there is a lower risk of transmitting infectious diseases. In contrast, natural polysaccharides exhibit a low immune response and good biocompatibility [4].

Chitosan (CS) is a polycationic polymer produced by the deacetylation of chitin, a part of the exoskeletons of marine invertebrates, insects, and fungal cell walls. It consists of d-glucosamine (70–90%) and *N*-acetyl-d-glucosamine (10–30%), which are linked to each other by random or block β-1,4-glycosidic bonds. The solubility of CS is determined by both the molecular weight and degree of deacetylation, which is defined as the ratio of the number of glucosamine groups to the total number of *N*-acetylglucosamine and glucosamine groups. CS is a bioactive biopolymer that is biocompatible, biodegradable,

bioactive, has good mechanical strength, and can be easily modified. Additionally, the presence of amino groups in the polymer structure affects its antimicrobial properties [5]. CS has a stable and stiff crystalline structure, which makes the polymer insoluble in water, solutions at pH above 7, and in most organic solvents. In contrast, in diluted acidic solutions, the amine groups of CS become protonated and the molecules of this compound become soluble below pH 5 [6]. The problem of insufficient biocompatibility of CS, resulting from the presence of acid in its solutions, which is necessary to dissolve the polymer, has already been solved by our research team and consists of the use of saturation of microcrystalline CS sediment with the use of carbon dioxide [7]. One limitation of using CS in 3D printing is the presence of endotoxins. An additional complication is that the endotoxin content of the raw material varies, even within CS from the same manufacturer [8].

Endotoxins, also called lipopolysaccharides (LPS), are the main components of the outer cell membranes of gram-negative bacteria. In contrast to the thermolabile exotoxins produced by Vibrio cholerae, they are characterised by high thermal stability. Endotoxins, because of their excessive concentration in the bloodstream, are responsible for severe gram-negative bacterial infections, sepsis, and septic shock, which is associated with a mortality rate of 20–50%. LPS is released during cell death and cell growth and division. Despite the wide variation in endotoxin composition, owing to different bacterial stereotypes, there is one common scheme to describe them. LPS are amphiphilic molecules consisting of a hydrophilic polysaccharide moiety divided into a core and an O-specific chain, and a covalently bound hydrophobic lipid component known as lipid A. The essential structural elements that provide cytotoxic activity are 2-keto-3-deoxy-octulosonic acid (kdo), which are present in the core and lipid A [9]. Endotoxins are resistant to extreme temperature and pH conditions. Consequently, the removal of endotoxins by separation is more difficult than sterilisation. To inactivate endotoxins, it is recommended to expose them to 250 °C for a minimum of 30 min or 180 °C for at least 3 h [10]. There is a relationship between the concentration of endotoxins present in the product administered to the patient and the effects of endotoxins. Depending on the intended use of such a product, 2 limits are set: 5.0 EU/kg body weight for all preparations except those administered intraperitoneally, for which the limit is 0.2 EU/kg body weight [11]. The term EU denotes the biological activity of the endotoxins, which corresponds to 1 EU for 100 pg of standard endotoxin EC-5, 200 pg of EC-2, and 120 pg of endotoxin from *Escherichia coli* O111:B4 [10]. Owing to the unique and specific biological characteristics of endotoxins, various methods have been proposed for their removal. Currently, techniques based on the removal of endotoxins by size are used, such as gel permeation chromatography, ultrafiltration, or sucrose gradient centrifugation. Other methods are based on specific binding using ion-exchange and affinity chromatography techniques or extraction [12]. However, most of these methods have their drawbacks and limitations. Therefore, there is a need for research to develop new methods for the purification of polymers, considering their chemical structure and surface properties [13]. The limulus amoebocyte lysate (LAL) assay is currently the gold standard for endotoxin determination. This assay is used for the specific in vitro determination of endotoxins, based on a clotting cascade mediated by endotoxin activated factor C. The disadvantage of this method is that other alternative mediating pathways, such as factor G, may affect the test results only if they are activated in the presence of beta-glucans. Consequently, the use of this method for CS solutions is difficult because beta-glucan blockers present in the solution are required. Otherwise, CS will bind to the reagent, resulting in a false positive test result. In addition, the lack of defined quantities of the blocker used means that if too much is used, the compound will bind not only to the CS but also to the endotoxin, and a false positive result will be obtained [14]. In contrast to LAL, the recombinant factor C (rFC) test is more sensitive and specific for the determination of endotoxins. The reaction mechanism involves the binding of the endotoxin to rFC and its activation, which leads to the cleavage of the synthetic fluorogenic substrate, causing the solution to fluoresce [15].

The above test was used to evaluate the effectiveness of endotoxin removal from CS obtained by the carbon dioxide saturation method as a component of the cell bioink dedicated for bioprinting. The potential of the proposed purification method was also tested to ensure the microbiological purity of the CS solution, as well as its cytotoxic effect on murine fibroblasts (L929).

2. Results and Discussion

Considering the physicochemical and biological properties of CS, this polymer seems to be a very good candidate for producing cell bioinks for 3D printing technology. This is especially true for features such as biodegradability, biocompatibility, nontoxicity, immunogenicity, and antimicrobial activity [16]. CS in composites with collagen allows appropriate mechanical properties of cell scaffolds to be obtained while maintaining cell adhesion and proliferation [17]. Controlled dosing of bioink in a 3D printer requires liquid CS. Unfortunately, to dissolve the polymer, it is necessary to use an acid that significantly reduces the biocompatibility of the CS hydrogels. Such a limitation for this form of CS can be overcome by saturating the suspension of microcrystalline CS sediment with carbon dioxide, which increases the pH of the obtained hydrogels from 3–4 to 6.5, thus increasing their biocompatibility [7]. This method uses sodium hydroxide precipitation and autoclaving to obtain a sterile CS-CO_2. Alkaline environments and high temperatures are also factors used in the removal of bacterial toxins from raw materials [18]. Therefore, in this work, we present two variants of a common method of obtaining CS with increased biocompatibility and, at the same time, devoid of bacterial toxins (2.1). We assessed their effectiveness in terms of efficiency of toxin purification, changes in molecular weight, microbiological purity, and cytotoxicity against L929 mouse fibroblasts.

2.1. Effect of the Method of Chitosan Hydrogel Purification on LPS Content

The content of bacterial endotoxins in the LMW, MMW and HMW CS hydrogels ranged from 18.1–25.2 EU/mL (Figure 1). The use of the M1 method for their purification reduced the endotoxin content by 87.9%, 93.8%, and 97.6%, respectively, in relation to their initial concentration in the CS hydrogel. Purification by M2 lowered the endotoxin levels in the hydrogels of the LMW, MMW, and HMW samples by 80.9%, 87.9%, and 91.6%, respectively. This indicates a higher toxin removal efficiency with the M1 method (6–7%). The visual effect of treatment with the M1 method is shown in Figure 2. It confirms that the purification by this method does not affect the appearance of the chitosan hydrogel. It may also appear that the purification efficiency increases with increasing molecular weight. This dependence was observed for both the purification methods. The higher efficiency of LPS extraction in the M1 method may have resulted from the increased contact of the polymer with chloroform. This solvent was used here to wash the hydrogel and not the CS sediment, as is the case for M2 (Figure 1). In the scientific literature, CS, due to its polycationic nature, is instead perceived as a compound that catches bacterial toxins with a negative charge [19]. Therefore, the phenomenon of a higher affinity of endotoxin for low molecular weight CS was confirmed in the test with its standard (S) (Figure 1). The addition of the same mass sample of LMW, MMW, and HMW CS to the LPS standard solution at a 5.87% concentration resulted in the binding of the toxin with a similar effect. This means that the reduction in the LPS concentration of the standard solution was 90.7%, 96.0%, and 98.1% for M1 and 83.6%, 91.3%, and 96.3% for M2, respectively.

In comparison, Lebre et al. proposed a method for purification of CS particles based on dissolution and precipitation of the solution under strongly acidic and basic conditions. Based on the gel-clot LAL assay with a detection limit of 0.125 EU/mL, it was shown that the method can be used for endotoxin removal; however, due to its limitations, follow-up tests are needed to confirm the test result [18].

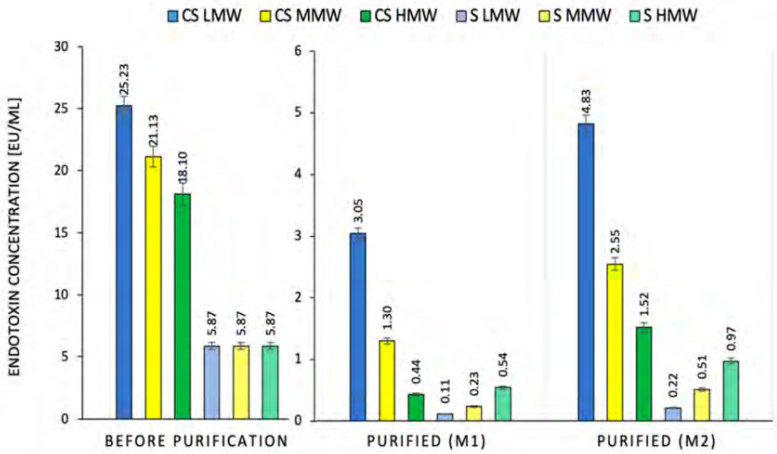

Figure 1. Comparison of endotoxin concentration in CS hydrogels: low molecular weight (LMW), medium molecular weight (MMW), and high molecular weight (HMW) and standard endotoxin solutions (S) after contact with CS of different molecular weights, before and after purification using M1 or M2 method ($n = 3$, $p < 0.05$).

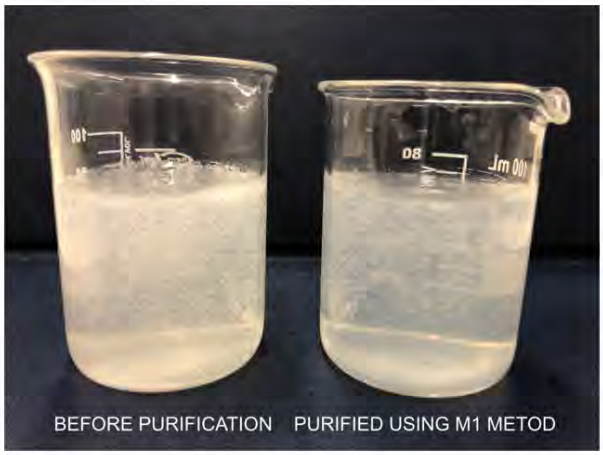

Figure 2. Comparison of the appearance of chitosan hydrogel samples before and after treatment with M1 method.

Similar results were obtained by Davydova et al., who confirmed that CS with a molecular mass of 20 kDa had a higher affinity for LPS than chitosan with a molecular mass of 140 kDa. However, precise determination of the molecular mechanism of the interaction between CS and endotoxins is difficult because of the variability of both raw materials. Endotoxins are heterogeneous and capable of forming polydisperse aggregates of high molecular weight in aqueous solutions, and their organization depends on the length of O-specific lipopolysaccharide chains [20].

2.2. Effect of the Method of Chitosan Hydrogel Purification on the Molecular Weight of Polymer and Hydrogel Viscosity

Figure 3 shows the effect of the purification methods on the change in the molecular weight of CS and the viscosity of the hydrogels. Regardless of the purification method used, the molecular mass of the CS did not significantly change. This applies to the low, medium, and high molecular weights of the polymers (Figure 3A). It was observed that the M1 purification method reduced the viscosity of the CS hydrogel by 3.6–4.7%. In contrast, for the M2 method, the losses were much greater, ranging from 24.8% to 29% (Figure 3B). The obtained results indicate that the CS chain did not degrade during purification, which could be initiated by the action of high temperature (Figure 6). A significant reduction in the viscosity of the hydrogels after M2 purification was due to the loss of CS during the washing of the sediment with chloroform. Chloroform physically delaminated the CS precipitate obtained by precipitation with NaOH. In the M1 method, this was not the case because the extraction of the toxins with chloroform occurred immediately after the dissolution of CS in the hydroxyacetic acid solution. Under these conditions, chloroform spontaneously separates from the aqueous layer containing the polymer.

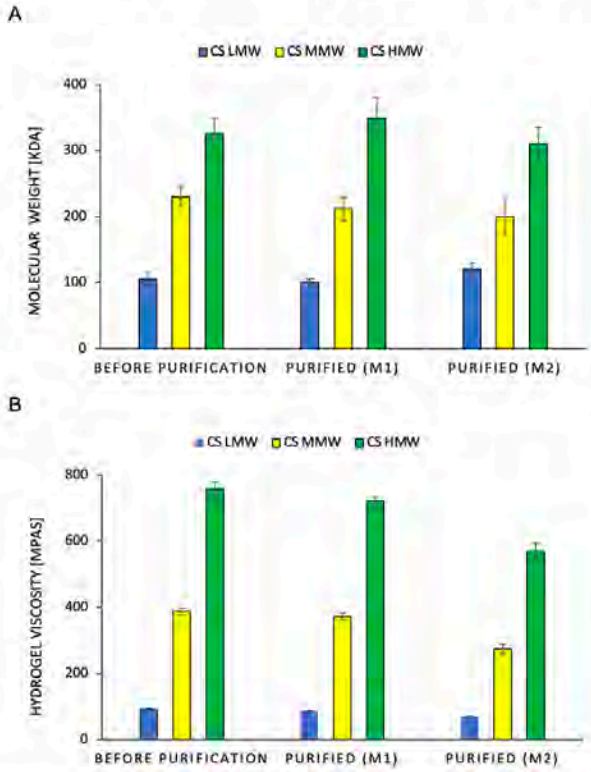

Figure 3. Comparison of molecular weight of chitosan polymer (**A**) and chitosan hydrogel. viscosity (**B**) with LMW, MMW and HMW, before and after purification using M1 or M2 method ($n = 3$, $p < 0.05$).

Martini et al. measured the degradation rate of different CS hydrogels in dynamic sweep test mode by monitoring several parameters, such as temperature, CS concentration, dynamic viscosity, and polymer molecular weight, and concluded a clear dependence between these parameters. The results demonstrate that there is a direct relationship between

solvating conditions and CS backbone integrity overtime in an acidic environment [21]. On the other hand, in the proposed CS purification procedure, the temperature treatment (12 °C, 15 min) was subjected to the CS sediment suspended in an appropriate amount of distilled water and no degradation of the polymer chain was observed. It is highly probable that the rate of CS degradation is mainly determined by the presence of acid in the environment and only by other factors such as concentration and molecular weight. The presence of acid in CS materials mainly causes the hydrolysis of the polymer to lower molecular weight without significantly affecting the degree of deacetylation and polydispersity [22]. We observed a similar phenomenon during the attempt to thermally degrade dry CS-poly(vinyl acid) composites, in which the elimination of the acid from the CS material significantly increases its stability during thermal treatment, even when it is used as a filler for thermoplastic materials [1].

2.3. *Effect of the Method of Chitosan Hydrogel Preparation on Microbiological Purity*

TVC is a microbiological parameter commonly used to assess the total number of bacteria, yeasts, and molds. The sterilization step applied by autoclaving the chitosan solutions in the M1 and M2 methods yielded sterile solutions, for which no colony growth was observed (Table 1).

Table 1. Effect of Purification Method on Total Viable Count during the 30-Days Storage Period at 4 °C ($n = 3$).

Storage Period (d)	Total Viable Count (CFU/g)		
	Control	M1	M2
0	1.6×10^3	ND	ND
15	2.5×10^3	ND	ND
30	3.3×10^4	ND	ND

ND = not detected.

In addition, the solutions showed microbiological stability when stored at 4 °C for 1 month. On the other hand, for the control sample, which was an unsterilised and unpurified chitosan solution, an increase in TVC was observed, which was 1.6×10^3 CFU/g (colony-forming unit per gram) was observed on the first day. After 2 weeks and 1 month of storage at 4 °C, the number increased to 2.5×10^3 and 3.3×10^4 CFU/g, respectively. The results showed that the chitosan hydrogels obtained by the M1 and M2 methods could be successfully stored for further distribution without the need for reserialization.

The applied storage conditions of chitosan hydrogels, such as 4 °C temperature and previous sterilization, are a consequence of problems regarding the stability of chitosan products which limits their further application. The rate of hydrolysis of chitosan chains is consistent with first-order kinetics; therefore, storage at low temperatures of 2–8 °C is recommended [23]. In addition, despite the broad-spectrum antimicrobial activity of chitosan, its activity is dependent on its physicochemical properties, such as pH, degree of deacetylation, molecular weight, derivatives, and the type of microorganism [24]. Therefore, there is a need for sterilization to ensure the safety of chitosan hydrogels. Based on the study by San Juan et al., it was found that autoclaving physical chitosan hydrogels did not significantly change the macromolecular structure of the polymer. In addition, as it is one of the most convenient sterilisation procedures, it can be used to sterilise physical chitosan hydrogels after preparation [25]. Sterilisation by autoclaving can be successfully applied to the M2 method of chitosan purification because it does not significantly affect the depolymerisation of chitosan, as evidenced by small changes in the viscosity of the solutions during purification.

2.4. Effect of the Method of Chitosan Hydrogel Preparation on Cytotoxicity

The MTT assay was used to investigate the cytotoxicity of the chitosan hydrogels against adult mouse fibroblast L929 cells at different dilutions (1:1, 1:3, and 1:6). The obtained results were expressed as the percentage of viable cells compared to the control without the materials. The cytotoxic effect was determined for MMW CS-AC, CS-CO_2 [7], and chitosan hydrogel purified by M1 method, defined as the optimal purification procedure based on previous results (CS-CO_2-P). According to Huang et al., molecular weight does not affect the cytotoxicity of chitosan; therefore, only a polymer with an average molecular weight was used for the determination [26]. The data presented in Figure 4 clearly shows that the CS-CO_2 hydrogel was not toxic to L929 cells, regardless of the dilution used. According to ISO 10993-5:2009(E), this material exhibits good biocompatibility. Significant cell growth inhibition of the CS-AC sample was observed only at a dilution 1:1 (80% compared to the control). In turn, CS-CO_2-P at the same dilution inhibited L929 cell growth by approximately 50% compared to cells without the hydrogel. The remaining diluent fractions (1:3 and 1:6) of the CS-AC and CS-CO_2-P samples were non-toxic (>70% viability) to L929 cells. However, these materials inhibited cell growth more efficiently than CS-CO_2 did at the same diluent fraction. This proves that chitosan dissolved in carbonic acid demonstrated good biocompatibility.

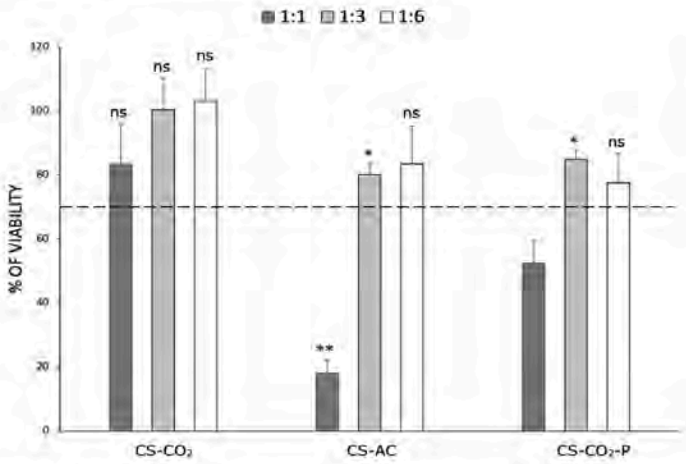

Figure 4. The cytotoxicity of chitosan hydrogels: chitosan dissolved by CO_2 saturation method (CS-CO_2), chitosan dissolved in hydroxyacetic acid (CS-AC), and chitosan hydrogel purified by M1 method (CS-CO_2-P) following 24 h of incubation at different dilution factors (1:1, 1:3, and 1:6) against L929 cells. Data are expressed as the mean ± standard deviation of three independent experiments. The results were analyzed by two-way ANOVA with Dunnett's multiple comparisons vs. Control: ns (not statistically significant, $p > 0.05$), * $p < 0.01$, ** $p < 0.001$.

The cytotoxicity data were confirmed by morphological examination of L929 cells treated with the studied chitosan derivatives diluted at 1:3 for 24 h. This dilution was chosen because the viability of the cells reached 70% following treatment with chitosan derivatives compared to that of the control. Figure 5 shows that L929 cells presented unchanged morphology (maintaining their fibroblast shape) following treatment with CS-CO_2-P and CS-CO_2 chitosan hydrogels compared to the control. In contrast, treatment with the CS-AS hydrogel resulted in morphological changes (the cells were shrunken and did not retain their fibroblast morphology). Endotoxins have a variety of effects on cell cultures that can result in pyrogenic responses ranging from fever and chills to irreversible and fatal septic shock, and may result from endotoxin levels in final products and the influence of

endotoxins on the expression system. Nalbantsoy et al. showed that endotoxins do not equally affect cell cultures. Some cell cultures lack the appropriate endotoxin receptors and may only be sensitive to very high levels of LPS. Therefore, such a risk must be eliminated in the case of chitosan hydrogels, which must meet the requirements for bioinks in the production of cell scaffolds using the bioprinting method [27].

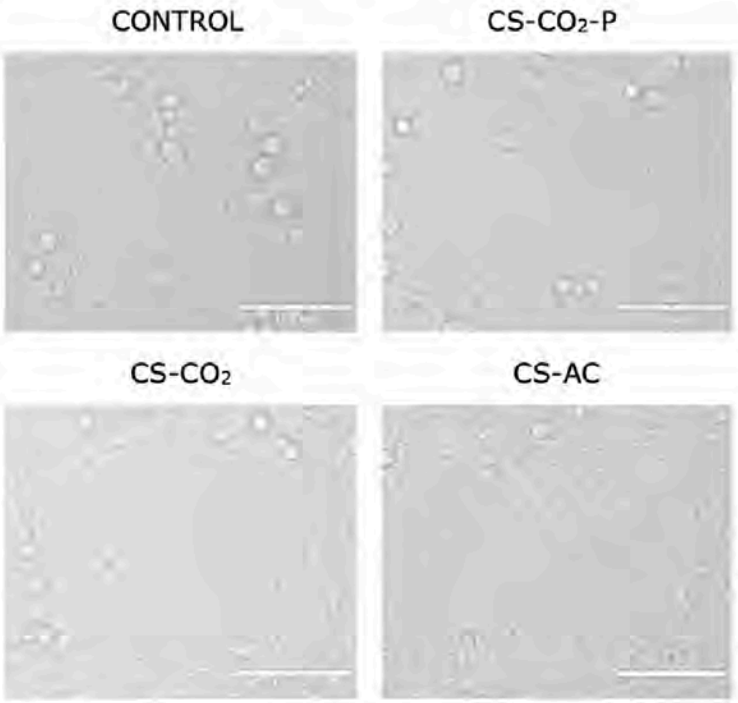

Figure 5. Representative image at 200× magnification of L929 cells following 24 h of treatment with chitosan hydrogels: CS-CO_2, CS-AC, and CS-CO_2-*p* at 1:3 diluent factor. The scale bar is 100 µm.

3. Materials and Methods

3.1. Materials

Low molecular weight CS (LMW) with 50–190 kDa molecular weight and 75–85% deacetylation degree, medium molecular weight CS (MMW) with 190–310 kDa molecular weight and 75–85% deacetylation degree, and high molecular weight CS (HMW) with 310–390 kDa molecular weight and above 75% deacetylation degree were purchased from Merck (Darmstadt, Germany). 3-(4,5-dimethylthiazol-2-yl)-2,5-diphenyltetrazolium bromide (MTT), streptomycin, and penicillin were purchased from Sigma-Aldrich, St. Louis, MO, USA. IPA was purchased from POCH (Gliwice, Poland). MilliQ water was used to prepare all the aqueous solutions (Milli-Q® IQ 7005 Water Purification System, Millipore, Boston, MA, USA). All other reagents were of analytical grade or higher. Chloroform, hydroxyacetic acid, and sodium hydroxide were purchased from Avantor Performance Materials Poland S. A. (Gliwice, Poland). The carbon dioxide used to saturate the CS precipitate was obtained from Linde Gaz Polska Sp. z o. o. (Gdańsk, Poland). Tryptic soy agar (TSA) medium was purchased from Merck (Darmstadt, Germany).

3.2. Chitosan Hydrogels Preparation and Purification

CS hydrogels were prepared with three molecular weight variants: low (LMW), medium (MMW), and high (HMW). The concentration of endotoxins before purification was determined in 1% (*m*/*v*) CS hydrogels obtained by direct dissolution of the polymer in 0.1 M hydroxyacetic acid solution during mechanical stirring at 300 RPM (RA 2020, Heidolph Instruments GmbH & Co. KG, Kelheim, Germany). The effectiveness of endotoxin removal from hydrogels was assessed after their purification using the M1 and M2 methods presented in Figure 6. Both purification methods constitute a modification of the CS dissolution method by saturating the water suspension of the microcrystalline sediment with carbon dioxide [7].

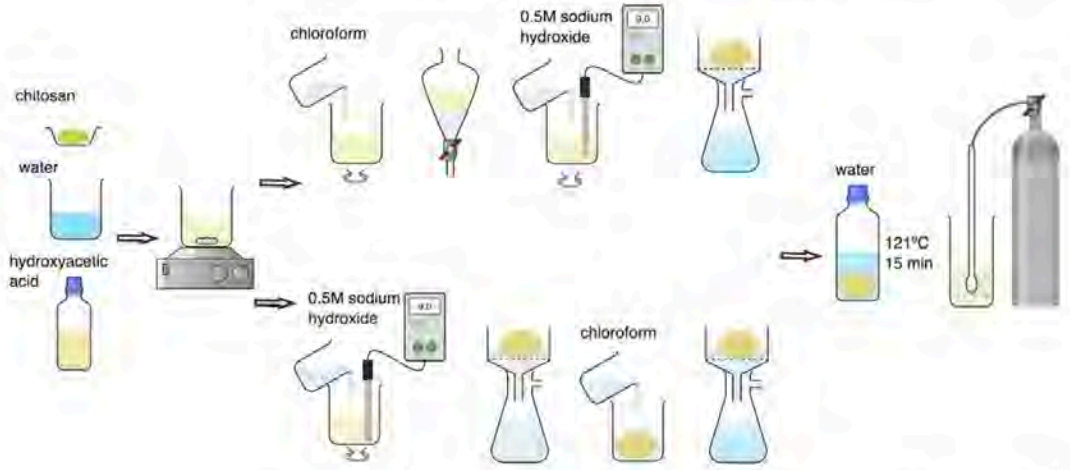

Figure 6. Scheme of chitosan (CS) hydrogel purification using M1 (top) and M2 (bottom) methods.

In the M1 purification method, 100 mL of CS dissolved in hydroxyacetic acid was transferred to a 250 mL separating funnel and washed 3 times with 50 mL of chloroform. After separation of chloroform, the CS hydrogel was transferred to a beaker, a 0.5 M sodium hydroxide solution was added during mixing until a pH value in the range of 9–10 was reached. This was equivalent to the complete precipitation of CS in the microcrystalline form. The precipitated CS was filtered using a seepage kit under reduced pressure and washed several times with distilled water until the pH of the rinsing water reached a value equal to 7.0. Finally, the precipitated CS was weighed, sterilised at 121 °C for 15 min (Systec VB-50, De Ville, Raszyn, Poland), and suspended in an amount of free endotoxin distilled water to obtain a 1% (*m*/*v*) CS solution. The CS suspension was homogenized at 10,000 rpm for 3 min (Silent Crusher M, Heidolph Instruments GmbH & Co. KG, Kelheim, Germany) and then saturated with CO_2 by simultaneous mechanical mixing using a hollow shaft stirrer for gas saturation (BIO-MIXBMX-10, Gdańsk, Poland) until completely dissolved.

In the M2 purification method, 100 mL of CS dissolved in hydroxyacetic acid was first treated with 0.5 M sodium hydroxide solution during mixing until a pH value in the range of 9–10 was reached. The precipitated CS was then filtered using a seepage kit under reduced pressure, washed 3 times with 50 mL of chloroform, and several times with distilled water until the pH of the rinsing water reached a value equal to 7.0. Finally, the precipitated CS was weighed, sterilised at 121 °C for 15 min (Systec VB-50, De Ville, Raszyn, Poland), and suspended in an amount of free endotoxin distilled water to obtain a 1% (*m*/*v*) CS solution. The CS suspension was homogenized at 10,000 rpm for 3 min (Silent Crusher M, Heidolph Instruments GmbH & Co. KG, Kelheim, Germany) and then saturated with

CO_2 by simultaneous mechanical mixing using a hollow shaft stirrer for gas saturation (BIOMIXBMX-10, Gdańsk, Poland) until completely dissolved.

3.3. Determination of Endotoxins Concentration

The endotoxin concentration in CS hydrogels was determined using the PyroGene rFC Enzymatic Cascade assay (Lonza Group Ltd., Visp, Switzerland). The solutions for testing endotoxin concentrations were applied to a 96-well plate, which was incubated in a microplate reader at 37 °C. The fluorescence of the solution was measured at an excitation/emission wavelength of 380/440 nm (Spark® multimode, microplate reader, TEKAN, Maennedorf, Switzerland). The endotoxin concentration in solutions was determined based on a previously determined sight curve in the range of concentration 0.5–5.0 EU/mL of *E. coli* 055: B5, E50-643 endotoxin. This assay was used to perform two tests. First, 1% CS solutions in hydroxyacetic acid (before purification) and 1% CS solutions purified using the M1 and M2 methods were tested. The second part of the test was used to evaluate the endotoxin binding capacity of unpurified and purified 1% CS solution using the M1 and M2 methods. For this purpose, a standard solution of endotoxin *E. coli* 055: B5, E50-643 with a concentration of 5.87 EU/mL was prepared. Next, 100 mg of the tested CS was added to o 2 mL of the standard solution and shaken for 15 min at 25 °C (Unimax 1010 with Incubator 1000, Heidolph Instruments GmbH & Co. KG, Kelheim, Germany). The assay solution was taken from the insoluble precipitate of the polymer after centrifuging the samples at 3000× *g* for 5 min. (MPW-260; Labfunk, Kluczbork, Poland). Dry CS preparations after purification used for this determination were obtained by freeze-drying: 0.94 mbar, condenser temperature: −78 °C (Christ Alpha 2-4 LD Plus, Donserv, Warsaw, Poland).

3.4. Determination of Chitosan Molecular Weight and Hydrogel Viscosity

To determine the dynamic viscosity of 1%, CS solutions were introduced into a measuring cell equipped with a temperature-controlled bath (Brookfield Digital Model DVIII Ultra viscometer (Middleborough, MA, USA). The measurements were carried out using SC4-27 and SC4-25 spindles at a temperature of 25 °C and shear stress of 22.00 1/s. All rheological measurements were performed in triplicate. The viscosity average molecular weight was identified by viscosimetric measurements using a Ubbelohde capillary viscometer type 531/10 according to the method proposed by Yacob et al. [28]. This value was calculated from $[\eta] = KM\alpha$ equation, where $K = 9.66 \times 10^{-5}$ (dm^3/g) and $a = 0.742$ determined in 0.15 M ammonium acetate and 0.2 M acetic acid solutions at 25 °C.

3.5. Purity and Microbiological Stability

A control sample of 1% CS (MMW) in hydroxyacetic acid and 1% CS (MMW) purified using the M1 and M2 methods was stored at 4 °C for 1 month. Total viable count (TVC) was determined immediately after the preparation of the solutions and after 14 and 30 days of storage. To determine the TVC, serial dilutions were made and samples from each tube were plated on a solid TSA medium using the pour plate method. Plates were incubated at 37 °C for 48 h. After incubation, bacterial colonies grown on Petri dishes were counted.

3.6. Determination of Cytotoxicity

3.6.1. Cell Culture

The adult mouse fibroblast L929 cell line was purchased from the American Type Culture Collection (ATCC; Manassas, VA, USA) and tested for mycoplasma using a Universal Mycoplasma Detection Kit, ATCC-30-1012 K (ATCC). The L929 cell line was cultured in low-glucose Dulbecco's modified Eagle's medium (DMEM; Sigma-Aldrich, St. Louis, MO, USA) supplemented with 10% foetal bovine serum (FBS; Biowest, Riverside, MO, USA), 100 $\mu g \times mL^{-1}$ streptomycin, and 100 units $\times mL^{-1}$ penicillin. Cells were incubated in a humidified atmosphere containing 5% CO_2 at 37 °C. All of the experiments were performed with cells in the exponential growth phase.

3.6.2. Cell Viability and Morphology Assessment

The in vitro cytotoxicity of the foams was assessed using the 3-(4,5-dimethylthiazol-2-yl)-2,5-diphenyltetrazolium bromide (MTT) assay, according to ISO 10993-5:2009(E). Briefly, L929 cells (1×10^4 cells/well) were seeded in 96-well plates, and 100 µL of culture medium only (blank) was dispensed into the peripheral wells. After 24 h of preincubation at 37 °C in a humidified 5% CO_2 atmosphere, the culture medium was removed and replaced with a fresh medium containing different concentrations of sample, positive control, or blank. Following 24 h of incubation, the culture medium was removed, and 50 µL of the MTT solution (1 mg × mL^{-1} in medium without supplements and phenol red) was added to each well and incubated for the next 2 h at 37 °C in a humidified 5% CO_2 atmosphere. Furthermore, media containing the MTT solution were removed, and the formazan crystals were dissolved in 100 µL of isopropanol and shaken for 10 min. Absorbance at 540 nm was measured using a microplate reader (iMark™, Bio-Rad, Warsaw, Poland). The results were repeated at least three times. was obtained from three independent experiments ($n = 3$).

The morphology of L929 cells following treatment with the CS compounds was evaluated using a light microscope. Briefly, L929 cells were seeded at a 60 mm plate with coverslips at a density of 1×10^6 and incubated overnight. Then, the culture medium was removed and replaced with fresh medium containing CS compounds such as: chitosan hydrogel in CO_2 (CS-CO_2), chitosan dissolved in hydroxyacetic acid (CS-AC) and purified chitosan hydrogel (CS-CO_2-P) at a 1:3 dilution factor for 24 h. Finally, the cells were observed using a light microscope (Olympus IX83, Tokyo, Japan; objective 200× magnification).

3.7. *Statistical Analysis of the Data*

STATISTICA software (StatSoft, Inc., Tulsa, OK, USA) was used for all of the analyses. Statistical significance was set at $p < 0.05$. All of the data reported are based on the means of 3 replicates ($n = 3$) or 5 replicates ($n = 5$) in the case of mechanical tests. Experimental results are expressed as mean ± standard deviation (SD). Student's t-test and one-way analysis of variance (ANOVA) were applied. Differences were considered statistically significant at $p < 0.05$.

4. Conclusions

In line with this hypothesis, we assumed that the procedure of obtaining a chitosan hydrogel by saturating the aqueous suspension of its microcrystalline sediment, combined with the stages of washing out toxins with chloroform, will allow for the preparation of biocompatible and endotoxin-free solutions, which can be used as the main component in the preparation of bioinks for creating personalised cell scaffolds using the bioprinting method. The obtained results confirmed that 1 of the proposed methods (M1) is characterised by a high purification efficiency of the chitosan hydrogel (88–98%) without affecting the solution viscosity after purification, as well as the molecular weight of the polymer. The method also allowed us to obtain a microbiologically pure hydrogel immediately after treatment and after 30 days of refrigerated storage. The results of cytotoxicity tests were also promising. They clearly showed that the method of CO_2 saturation (CS-CO_2) allows for the production of a non-cytotoxic chitosan hydrogel against mouse fibroblast cells. The addition of chloroform slightly reduced the viability of the cells, which was evident in the samples with the lowest dilution. However, the lack of changes in cell morphology and the higher survival of the L929 line in the CS-CO_2-P sample compared to the CS-AS sample indicate that the method seems to be promising. Increasing the viability of cells in contact with the CS-CO_2-P sample will probably be achieved by extending the duration of carbon dioxide sowing. The results obtained will be the basis for further tests on the regeneration of skin tissue with the use of chitosan.

Author Contributions: A.B.-K. and S.M. conceived the study. A.B.-K., S.M., J.P., E.A. and R.T. designed and performed the experiments described in the manuscript. I.G. helped with experimental work related with fluorescent measurements, A.B.-K., S.M., and R.T. provided overall management and supervision for the project. A.B.-K., S.M., J.P., E.A. and R.T. wrote the initial drafts of the manuscript and all authors participated in the editing process for the manuscript. All authors have read and agreed to the published version of the manuscript.

Funding: The purchase of research materials was supported by the internal minigrant No. 032408T103 funded by the Dean of the Chemical Faculty of the Gdansk University of Technology.

Institutional Review Board Statement: Not applicable.

Informed Consent Statement: Not applicable.

Data Availability Statement: Not applicable.

Conflicts of Interest: The authors declare no conflict of interest.

References

1. Tylingo, R.; Kempa, P.; Banach-Kopeć, A.; Mania, S. A novel method of creating thermoplastic chitosan blends to produce cell scaffolds by FDM additive manufacturing. *Carbohydr. Polym.* **2022**, *280*, 119028. [CrossRef] [PubMed]
2. Zhang, B.; Gao, L.; Ma, L.; Luo, Y.; Yang, H.; Cui, Z. 3D Bioprinting: A novel avenue for manufacturing tissues and organs. *Engineering* **2019**, *5*, 777–794. [CrossRef]
3. Laurenti, M.; Cauda, V. ZnO Nanostructures for tissue engineering applications. *Nanomaterials* **2017**, *7*, 374. [CrossRef] [PubMed]
4. Heidenreich, A.C.; Pérez-Recalde, M.; González Wusener, A.; Hermida, É.B. Collagen and chitosan blends for 3D bioprinting: A rheological and printability approach. *Polym. Test.* **2020**, *82*, 106297. [CrossRef]
5. Cheung, R.C.F.; Ng, T.B.; Wong, J.H.; Chan, W.Y. Chitosan: An update on potential biomedical and pharmaceutical applications. *Mar. Drugs* **2015**, *13*, 5156–5186. [CrossRef]
6. Francis Suh, J.K.; Matthew, H.W.T. Application of Chitosan-Based polysaccharide biomaterials in cartilage tissue engineering: A review. *Biomaterials* **2000**, *21*, 2589–2598. [CrossRef]
7. Gorczyca, G.; Tylingo, R.; Szweda, P.; Augustin, E.; Sadowska, M.; Milewski, S. Preparation and characterization of genipin cross-linked porous chitosan–collagen–gelatin scaffolds using chitosan–CO_2 solution. *Carbohydr. Polym.* **2014**, *102*, 901–911. [CrossRef] [PubMed]
8. Ravindranathan, S.; Koppolu, B.P.; Smith, S.G.; Zaharoff, D.A. Effect of chitosan properties on immunoreactivity. *Mar. Drugs* **2016**, *14*, 91. [CrossRef]
9. Heine, H.; Rietschel, E.T.; Ulmer, A.J. The biology of endotoxin. *Mol. Biotechnol.* **2001**, *19*, 279–296. [CrossRef]
10. Miyamoto, T.; Okano, S.; Kasai, N. Inactivation of Escherichia coli endotoxin by soft hydrothermal processing. *Appl. Environ. Microbiol.* **2009**, *75*, 5058. [CrossRef]
11. Dawson, M. Endotoxin limits for parenteral drug products. *BET White Pap.* **2017**, *1*, 1–7.
12. Serdakowski London, A.; Kerins, B.; Tschantz, W.R.; Mackay, K. Endotoxin removal and prevention for pre-clinical biologics production. *Biotechnol. J.* **2012**, *7*, 1509–1516. [CrossRef] [PubMed]
13. Lieder, R.; Petersen, P.H.; Sigurjónsson, Ó.E. Endotoxins-the invisible companion in biomaterials research. *Tissue Eng. Part B Rev.* **2013**, *19*, 391–402. [CrossRef] [PubMed]
14. Piehler, M.; Roeder, R.; Blessing, S.; Reich, J. Comparison of LAL and RFC assays—Participation in a proficiency test program between 2014 and 2019. *Microorganisms* **2020**, *8*, 418. [CrossRef]
15. Ding, J.L.; Ho, B. A new era in pyrogen testing. *Trends Biotechnol.* **2001**, *19*, 277–281. [CrossRef]
16. Rodríguez-Vázquez, M.; Vega-Ruiz, B.; Ramos-Zúñiga, R.; Saldaña-Koppel, D.A.; Quiñones-Olvera, L.F. Chitosan and its potential use as a scaffold for tissue engineering in regenerative medicine. *BioMed Res. Int.* **2015**, 1–15. [CrossRef]
17. Pezeshki-Modaress, M.; Zandi, M.; Rajabi, S. Tailoring the Gelatin/Chitosan electrospun scaffold for application in skin tissue engineering: An in vitro study. *Prog. Biomater.* **2018**, *7*, 207–218. [CrossRef]
18. Lebre, F.; Lavelle, E.C.; Borges, O. Easy and effective method to generate endotoxin-free chitosan particles for immunotoxicology and immunopharmacology studies. *J. Pharm. Pharmacol.* **2019**, *71*, 920–928. [CrossRef]
19. Yang, Q.; Li, Y.; Tuohuti, P.; Qin, Z.; Zhang, Z.; Zhao, W.; Su, B. Advances in the development of biomaterials for endotoxin adsorption in sepsis. *Front. Bioeng. Biotechnol.* **2021**, *9*, 646. [CrossRef]
20. Davydova, V.N.; Yermak, I.M.; Gorbach, V.I.; Krasikova, I.N.; Solov'eva, T.F. Interaction of bacterial endotoxins with chitosan. Effect of endotoxin structure, chitosan molecular mass, and ionic strength of the solution on the formation of the complex. *Biochem. Biokhimiia* **2000**, *65*, 1082–1090.
21. Martini, B.; Dimida, S.; de Benedetto, E.; Madaghiele, M.; Demitri, C. Study on the degradation of chitosan slurries. *Results Phys.* **2016**, *6*, 728–729. [CrossRef]
22. Sikorski, D.; Gzyra-Jagieła, K.; Draczyński, Z. The kinetics of chitosan degradation in organic acid solutions. *Mar. Drugs* **2021**, *19*, 236. [CrossRef] [PubMed]

23. Szymańska, E.; Winnicka, K. Stability of chitosan-A challenge for pharmaceutical and biomedical applications. *Mar. Drugs* **2015**, *13*, 1819–1846. [CrossRef] [PubMed]
24. Ke, C.-L.; Deng, F.-S.; Chuang, C.-Y.; Lin, C.-H.; Bardosova, M. Polymers antimicrobial actions and applications of chitosan. *Polymers* **2021**, *13*, 904. [CrossRef]
25. San Juan, A.; Montembault, A.; Gillet, D.; Say, J.P.; Rouif, S.; Bouet, T.; Royaud, I.; David, L. Degradation of chitosan-based materials after different sterilization treatments. In *IOP Conference Series: Materials Science and Engineering*; IOP Publishing: Tokyo, Japan, 2012; Volume 31.
26. Huang, M.; Khor, E.; Lim, L.Y. Uptake and cytotoxicity of chitosan molecules and nanoparticles: Effects of Molecular weight and degree of deacetylation. *Pharm. Res.* **2004**, *21*, 344–353. [CrossRef]
27. Nalbantsoy, A.; Karabay-Yavasoglu, N.U.; Deliloglu-Gurhan, I. Food and Agricultural immunology determination of in vivo toxicity and in vitro cytotoxicity of lipopolysaccharide isolated from salmonella enteritidis and its potential use for production of polyclonal antibody. *Food Agric. Immunol.* **2011**, *22*, 271–281. [CrossRef]
28. Yacob, N.; Talip, N.; Mahmud, M.; Aizam Aisam Idayu Mat Sani, N.; Akma Samsuddin, N.; Fabillah, N.A. Determination of viscosity-average molecular weight of chitosan using intrinsic viscosity measurement. *J. Nucl. Relat. Technol.* **2013**, *10*, 39–44.

6.2 [A2] An influence of molecular weight, deacetylation degree of chitosan xerogels on their antimicrobial activity and cytotoxicity. Comparison of chitosan materials obtained using lactic acid and CO_2 saturation.

6.2.1 Wkład pracy doktoranta

Tytuł: An influence of molecular weight, deacetylation degree of chitosan xerogels on their antimicrobial activity and cytotoxicity. Comparison of chitosan materials obtained using lactic acid and CO_2 saturation

Autorzy: Szymon Mania, Adrianna Banach-Kopeć, Karol Staszczyk, Jolanta Kulesza, Ewa Augustin, Robert Tylingo

Czasopismo: CARBOHYDRATE RESEARCH

Rok wydania: 2024

Impact factor: 3,1

Liczba punktów wg MNiSW: 100

DOI: 10.1016/j.carres.2023.108973

Procentowy wkład pracy doktoranta: 30%

W ramach współautorstwa tej publikacji byłam zaangażowana w kluczowe etapy realizacji badań naukowych. Wspólnie z pozostałymi autorami uczestniczyłam w opracowywaniu metodologii oraz zarządzaniu danymi, co obejmowało ich zbieranie, organizację oraz przygotowanie do analizy. W ramach badań eksperymentalnych brałam udział w ocenie aktywności przeciwdrobnoustrojowej oraz przygotowaniu prób do dalszych testów. Wspierałam zarządzanie zasobami projektu, w tym organizację niezbędnych materiałów i narzędzi badawczych. Brałam udział w walidacji wyników, a także współtworzyłam wstępną wersję manuskryptu, aktywnie uczestnicząc w jego dalszej edycji.

6.2.2 Treść artykułu

Carbohydrate Research 534 (2023) 108973

Contents lists available at ScienceDirect

Carbohydrate Research

journal homepage: www.elsevier.com/locate/carres

An influence of molecular weight, deacetylation degree of chitosan xerogels on their antimicrobial activity and cytotoxicity. Comparison of chitosan materials obtained using lactic acid and CO_2 saturation

Szymon Mania [a,*], Adrianna Banach-Kopeć [a], Karol Staszczyk [a], Jolanta Kulesza [b], Ewa Augustin [b], Robert Tylingo [a]

[a] Department of Chemistry, Technology and Biotechnology of Food, Faculty of Chemistry, Gdansk University of Technology, 11/12 G. Narutowicza Street, 80-233, Gdansk, Poland

[b] Department of Pharmaceutical Technology and Biochemistry, Faculty of Chemistry, Gdansk University of Technology, 11/12 G. Narutowicza Street, 80-233, Gdansk, Poland

ARTICLE INFO

Keywords:
Chitosan
Antimicrobial properties
Cytotoxicity
Molecular weight
Deacetylation degree

ABSTRACT

This paper presents a comparison of the antimicrobial activity and cytotoxicity against L929 cells of chitosan xerogels prepared by dissolving the polymer in a solution of lactic acid (LA) or carbonic acid (CO_2) and then freeze-drying. There was no simple relationship between the antimicrobial activity and cytotoxicity of the samples obtained using both techniques (LA and CO_2). Chitosan materials obtained by the LA method in a 1:1 dilution were characterized by the highest cytotoxicity against L929 cells (~20%). For the same diluted samples prepared using the CO_2 saturation method, the viability of L929 cells was approximately 2.5 times greater. Some of the tested chitosan materials obtained by the innovative method were characterized by significantly lower antimicrobial activity, for example, reduction of *E. coli* bacteria for MMW-LA and MMW-CO_2 samples by 6.00 and 0.75 logarithmic order, respectively. This clearly indicates that in many applications, the presence of the acid necessary to dissolve chitosan is responsible for the antimicrobial activity of the polymer solution and its products.

1. Introduction

Chitosan is a natural polysaccharide with a positive charge, and is a derivative of chitin. It consists of the monomers N-acetyl-D-glucosamine and D-glucosamine linked by β-1,4-glycosidic bonds [1]. Chitosan occurs sporadic in the biosphere, therefore this polymer is obtained from chitin, which is one of the main components of the exoskeletons of arthropods such as shrimp, crabs, lobsters and arachnids [2]. The most common method for obtaining chitosan is the deacetylation of chitin, which is a two-stage nucleophilic substitution reaction that takes place in an alkaline solution. Depending on the origin of chitin and parameters of the deacetylation process, chitosan can be obtained with different molecular weights (MW) and degrees of deacetylation (DD). These parameters affect the physicochemical and biological properties of biopolymer-based materials based on this biopolymer [1–4].

The properties of chitosan, such as biocompatibility, biodegradability, non-toxicity, antimicrobial activity, hemostatic properties, and ability to accelerate wound healing, make it an object of research and application in designing dressing materials [5], scaffolds [6], and carriers for the controlled release of drugs and other biologically active pathways [7]. Chitosan can also be used as a component of food packaging or as a food additive, inhibiting the development of microorganisms and thus prolonging the freshness of the product u [8].

One of the most significant features of the potential action of chitosan is the antimicrobial activity of the polymer, which is the result of many different factors, including DD and MW [9]. Zheng and Zhu [9] and Tavaria et al. [10] reported an increase in the antimicrobial activity of chitosan against Staph. aureus bacteria with increasing MW [9,10]. Despite the relatively well-determined effect of the MW of chitosan on its antimicrobial activity against Gram-positive bacteria, many inconsistent results of its activity against Gram-negative bacteria can be found [11]. Some studies on *E. coli* and *Salmonella* have indicated an increase

* Corresponding author.
E-mail addresses: szymon.mania@pg.edu.pl (S. Mania), adrianna.banach@pg.edu.pl (A. Banach-Kopeć), karol.staszczyk@pg.edu.pl (K. Staszczyk), jolanta.kulesza@pg.edu.pl (J. Kulesza), ewa.augustin@pg.edu.pl (E. Augustin), robertt@pg.edu.pl (R. Tylingo).

https://doi.org/10.1016/j.carres.2023.108973
Received 6 May 2023; Received in revised form 3 October 2023; Accepted 10 October 2023
Available online 14 October 2023

in antimicrobial activity with decreasing MW [9,12,13]. Other results for the same class of bacteria showed an increase in performance as the MW increased to the determined value and then decreased with increasing MW, or different performances for different MW and different types of bacteria of the same class ([14,15], n.d.). The justification for these differences is the method of processing the chitosan material, the pH of the solution, or the DD [16]. In addition, the source of chitin from which chitosan was produced, as well as the method of processing, play an important role in the antimicrobial activity of chitosan materials [17–19].

Several models have suggested that the antimicrobial activity of chitosan is due to its cationic nature. The electrostatic interaction between positively charged polymers and negatively charged microbial cell membranes is predicted to be responsible for cellular lysis, and is assumed to be the main antimicrobial mechanism [20].

The second mechanism is based on the binding of chitosan to bacterial DNA, which leads to the inhibition of protein synthesis as a result of chitosan penetration inside the cells of microorganisms. This model assumes that chitosan can pass through the walls and/or membranes of bacterial cells, as confirmed by scanning techniques [2].

The third mechanism of the antimicrobial activity of chitosan is related to its ability to chelate metal ions. It consists of binding the polymer to nutrients necessary for the growth of microorganisms [20]. This mechanism applies in particular to the alkaline environment because the amino groups are in the unprotonated state, and the electron pair present on the nitrogen of these groups can interact with cations [21,22].

Chitosan is generally considered safe, which has been confirmed by numerous studies presenting in vitro tests carried out on cell lines [23–25], and in vivo tests carried out on model organisms living ([26,27], 1997b). Despite the proven harmlessness of chitosan, some studies have indicated the possible cytotoxicity of materials produced through its participation [28,29]. It is assumed that the cytotoxicity may depend indirectly on the method of processing and the origin of chitin because the influence of the DD and the MW of chitosan on the cytotoxicity phenomenon was observed. The lower molecular weight (LMW) chitosan showed less cell-damaging effects than its higher molecular weight (HMW) counterpart. This phenomenon is probably correlated with the surface charge density distribution and amount of free amino groups. Their greater amount in the case of chitosan with a higher MW results in stronger electrostatic interactions between the chitosan chains, and thus the formation of a more developed polycation molecule that attaches more easily to the cell [30,31].

There is a lot of information in the scientific literature on the biological properties of chitosan, but finding an answer to the relationship between the cytotoxic effect and antimicrobial activity of chitosan materials is practically impossible. The biological properties of these materials are subject to high variability resulting from the source of the polymer, method of extraction and processing, and different conditions of freezing and freeze-drying to obtain porous materials [32–34]. This paper presents the change in antimicrobial activity and cytotoxicity of xerogel chitosan materials resulting from the difference in the DD and MW of the polymer, and the technique of its dissolution. The influence of the use of an innovative procedure for obtaining chitosan xerogel materials consisting of dissolving the polymer by saturation of its suspension with carbon dioxide (CO_2) [35] on the above parameters is presented. To date, no attempt has been made in the scientific literature to assess these relationships, taking into account the above variables.

According to the research hypothesis, the lack of acid residues in xerogel chitosan materials obtained by the innovative method of saturation with gaseous CO_2 will allow the actual assessment of the antimicrobial activity of chitosans resulting from the structures of the polymer itself and differences in MW and DD. In addition to maintaining this activity, the prepared materials will be characterized by lower cytotoxicity in relation to the L929 model cell line in comparison to xerogels created by classical chitosan dissolution in acid, freezing and lyophilization.

Standard methods of producing chitosan xerogels involve predissolving the polymer in an acid solution, freezing the solution and freeze-drying it. During this operation, water is removed from the material by sublimation, and acid anhydrides are formed, which remain in the material in an amount depending on its volatility and boiling point. After contact with water, acid is formed again in the chitosan xerogel, i. e. hydrogen cations and anions of the acid residues used to dissolve the polymer are present. In the CO_2 saturation method, chitosan is initially dissolved in a solution of hydroxyacetic acid (hydrogen cations, hydroxyacetic anions), then precipitated with sodium hydroxide, as a result of which chitosan is precipitated in a microxystalline form to produce sodium hydroxyacetate and water as a result of reaction. The precipitate is washed thoroughly until the pH is neutral (removal of sodium cations and hydroxyacetic anions). In the last stage, the chitosan precipitate is suspended in distilled water and saturated with carbon dioxide gas, which acidifies the environment (production of weak carbonic acid), which dissolves the polymer. Carbonic acid is a weak acid that dissociates only slightly and is unstable, decomposing fast into carbon dioxide and water, which means that the chitosan hydrogel ready for freeze drying does not contain any additional compounds that would affect the biological properties of the chitosan xerogels created.

2. Experimental section

2.1. Materials

Chitosan polymers with low (20–300 cps, DD ≥ 75%, Cat. No.:102473649, LOT: BCCG5629), medium (200–800 cps, DD ≥ 75%, Cat. No.:102466463, LOT: BCCG9377), high (800–2000 cps, DD ≥ 75%, Cat. No.:102515456, LOT: BCCH4876) MW, chitosan isolated from crab (Cat. No.:101167160, LOT: BCBH3811V) and shrimp shells (DD ≥ 75%, Cat. No.:1003507957, LOT: SLCP5257),phosphate buffer saline (PBS, Cat. No.:1002795530, LOT: SLBZ3711), Tryptic Soy Agar (TSA, Cat. No.:1.05458.0500, LOT: VM1009758 216), Tryptic Soy Broth (TSB, Cat. No.:1.05459.0500, LOT: VM899959 942), Lactic acid (LA; Cat. No.:1003429706, LOT:SHBP4889), hydroxyacetic acid (Cat. No.:102527954, LOT: STBK8247) were purchased from Merck. Chitosan with MW of 150 kDa (Cat. No.: 22741, LOT: 407568/1) was purchased form Fluka.Peptone K (Cat. No.:S-0011, LOT: S011130306) was purchased from BTL Sp. Z o.o.(Poland). Acetic acid (Cat. No.:568760114, LOT:1024/04/19), hydrochloric acid (Cat. No.: 115752837 LOT:210305322), and sodium hydroxide (Cat. No.: 115752837 LOT:210305322) were purchased from Avantor Performance Materials Poland S.A. (Gliwice, Poland). Viscosity standards in the form of mineral oils for viscosimeter calibration were purchased from IKA (10 mPas Cat. No.: 25000398, LOT: 280038/1, 100 mPas (Cat. No.: 25000434, LOT: 07040, 1000 mPas (Cat. No.: 25000436, LOT: 07119) (Warsaw, Poland) Viscosimeter standards – poly(ethylene glycol) with MW of 200 kDa (Cat. No.: 102511497 LOT:BCCG7893, 400 kDa Cat. No.: 102550289 LOT:BCCH5871, 1000 kDa (Cat. No.: 8.07488.1000 LOT:S8283588 247. The CO_2 used to saturate the chitosan precipitate was obtained from Linde Gaz Polska Sp. Z o. o. (Gdansk, Poland). For microbiological tests, the following bacterial species were used: Gram-negative *Escherichia coli* (ATCC 25922) and Gram-positive *Staphylococcus aureus* (ATCC 29213) from the Polish Collection of Microorganisms, Ludwik Hirszfeld Institute of Immunology and Experimental Therapy of the Polish Academy of Sciences (Wroclaw, Poland). 3-(4,5-dimethylthiazol-2-yl)-2,5-diphenyltetrazolium bromide (MTT; Cat. No.:1003404689, LOT: MKCR748), medium, antibiotics, and supplements necessary for cell culture were obtained from Merck (Germany). MilliQ water was used to prepare all the aqueous solutions (Milli-Q® IQ 7005 Water Purification System, Millipore, USA). All other reagents were of analytical grade or higher.

2.2. Chitosan characterization

2.2.1. Degree of deacetylation

The DD of chitosan was determined using the potentiometric titration method [36]. The titration solution was prepared by dissolving 0.25 g of chitosan in 10 mL of 0.3 M hydrochloric acid and filled up to 200 mL). It was titrated with a 1 M solution of sodium hydroxide, which allowed the pH vs. amount of added NaOH titration curve to be plotted. Then, using MatLab software (R2022a, The MathWorks, Inc.), the inflection points of the titration curve were determined. The mass of used chitosan (M), value of measured pH for the first inflection point (x), and value for the second inflection point (y) were applied in equation (1) to calculate the percentage of chitosan-free amino groups (%NH_2).

$$\% NH_2 = 16.1\,(y - x)/M \quad (1)$$

2.2.2. Molecular weight

The MW of the chitosan polymers was determined by an indirect method using dynamic viscosity measurements with a Brookfield Digital Model DVIII Ultra viscometer equipped with a temperature-controlled bath (Middleboro, MA, USA). The viscometer was calibrated using viscosity standards in the form of mineral oils with viscosities of 10 mPas, 100 mPas, and 12500 mPas (IKA, Warsaw, Poland) to measure spindles SC4-18, SC4-27, and SC4-25, respectively, whose measuring range corresponds to the viscosity of the measured chitosan solutions. Then, the viscosity dependence of the standard glycol solutions and chitosan solution with a defined MW (150 kDa; 1% m/v solutions in 1% v/v acetic acid) as a function of shear rate at 25 °C was determined. In order to determine the MW of chitosans, a 1% solution (m/v) in 1% acetic acid (v/v) was prepared from each of them, and their viscosities were measured at 25 °C using an appropriate measuring spindle adjusted based on the generated strain as a result of shear stresses between the liquid layers during the measurement. For each of the measuring spindles, the relationship between MW and dynamic viscosity was used to determine the MW of chitosans with unknown MW. All rheological measurements were performed in triplicate.

2.3. Chitosan xerogels preparation

Xerogel materials based on chitosan were prepared using two dissolution methods: the classic method using a 0.1 M LA solution [37] and the method of CO_2 saturation, an aqueous suspension of chitosan in the microcrystalline form [35]. The chitosan concentration in the solution was 1% v/v. The solutions in LA were prepared by systematically pouring chitosan powder into a LA solution during mechanical mixing at a speed of 300 RPM (RA 2020, Heidolph Instruments GmbH & Co. KG, Kelheim, Germany) and stirred until the polymer was completely dissolved (approximately 1 h). The chitosan solution was prepared by CO_2 saturation, as follows: In the first step, a 1,5% chitosan solution in 0.1 M hydroxyacetic acid was obtained by indirect dissolution of the polymer in a proper acid solution during mechanical stirring at a speed of 300 RPM (RA 2020, Heidolph Instruments GmbH & Co. KG, Kelheim, Germany). Then, during mixing 0.5 M solution of sodium hydroxide solution was added until a pH value in the range of 9–10 was reached. This was equivalent to the complete precipitation of chitosan in the microcrystalline form. The precipitated chitosan was filtered using a seepage kit under reduced pressure and washed five times with distilled water. Finally, the precipitated chitosan was weighed and suspended in distilled water to obtain a solution of 1% relative to the dry matter of the polymer. The suspension was homogenized at 10000 RPM for 3 min (Silent Crusher M, Heidolph Instruments GmbH & Co. KG, Kelheim, Germany), and then saturated with CO_2 with simultaneous mechanical mixing using a hollow shaft stirrer for gas saturation (BIOMIX BMX-10, Gdansk, Poland) until completely dissolved. The obtained solutions were poured into flat forms of 10 × 20 cm size to a height of 5 mm, frozen at −80 °C, and then freeze-dryed (Pressure: 0.94 mbar, Condenser temperature: −80 °C, Sample shelf temperature: 50 °C). Before use in the tests, the samples were stored in a dry, tight package under cool conditions.

2.4. Solubility test with visualization

To compare the behavior of chitosans xerogel immersed in water, 0.5 g was suspended in 50 mL of distilled water for 24h at 37 °C. Subsequently, the samples were imaged using the TOP Show 3D automatic rotation system (Wroclaw, Poland).

2.5. Antimicrobial activity

The antimicrobial properties of the xerogel materials were evaluated according to the quantitative ASTM E2149 method with slight modifications using *E. coli* and *S. aureus* species [38]. Colonies of bacteria were first subcultured in TSB for 24 h at 37 °C. Then, from cultured bacteria test medium in TSB were prepared by adjusting the number of bacterial cells in the range 1.0–5.0 × 10^7 CFU/mL with a spectrophotometer, measuring the absorbance at 600 nm (optical density 0.1). The change in absorbance of a bacterial culture is proportional to the number of bacteria present in the sample. This is a relationship that describes how absorbance (A) changes as a function of the number of bacterial cells in the sample. This relationship can be described by the general equation: A (Absorbance) = ε absorption coefficient) *b (length of the light path through the sample) *c (concentration of absorbing substances in the sample). The more bacterial cells there are, the more light they absorb, leading to a higher absorbance value. The value of the absorption coefficient (ε) is specific to a given type of bacteria and the wavelength of light used for measurement.The materials for the study were prepared by cutting squares with a side of 4 cm from the chitosan xerogels. Polyethylene foil of the same dimensions was used as the control sample, which showed no antimicrobial activity. The cut materials were sterilized with UV radiation for 30 min on each side. Then, 0.4 mL of diluted bacterial inoculum was applied to the surface of the samples. Each square of the inoculated surface was covered with a sterile polyethylene film with the same dimensions to ensure contact of the cell suspension with the material on the surface of 16 cm^2. After 24 h incubation at 37 °C, samples were placed separately in 10 mL of PBS solution and vortexed intensively for 25 s. Next ten-fold serial dilutions were prepared, then seeded on TSA plates, and incubated for 48 h at 37 °C. After incubation, only plates containing 30 CFU–300 CFU were counted. When no colonies were recovered in non dilluted sample, the number of bacteria was recorded as "10." The viable count of bacteria (CFU/mL) was recorded using the following formula:

$$V_C = N \bullet D \quad (2)$$

where Vc is the bacterial concentration in colony forming units per mL (CFU/mL), N is the average value in colony forming units (CFU) from Petri dishes, and D is the dilution factor from the counted plates. The antimicrobial activity on a logarithmic scale was calculated using the following formula:

$$R = \log(B/A) \quad (6)$$

where A is the average of the number of viable cells on the test sample after 24 h incubation at 37 °C (CFU/mL) and B is the average of the number of viable cells in the control sample after 24 h incubation at 37 °C (CFU/mL). A percentage reduction of bacteria on logarithmic (R) scale equal to 1, 2, and 3 corresponded to a reduction of 90%, 99%, and 99.9%, respectively.

2.6. Cytotoxicity

2.6.1. Cell culture

Adult mouse fibroblast L929 cells were purchased from the American

Type Culture Collection (ATCC, Manassas, VA, USA) and tested negative for mycoplasma using a Universal Mycoplasma Detection Kit (ATCC, Manassas, VA, USA). The L929 cell line was cultured in low-glucose Dulbecco's modified Eagle's medium (DMEM; Sigma-Aldrich, St. Louis, MO, USA) supplemented with 10% heat-inactivated fetal bovine serum (FBS; Biowest, Nuaille, France), 100 μg/mL streptomycin, and 100 U/mL penicillin. Cells were incubated at 37 °C in a 5% CO_2 atmosphere. All experiments were performed using cells in the exponential phase of growth.

2.6.2. Cell viability and morphology assessment

To estimate the in vitro cytotoxicity of the extracts, the 3-(4,5-dimethylthiazol-2-yl)-2,5-diphenyltetrazolium bromide (MTT) assay was used, according to ISO 10993–5:2009(E). Briefly, L929 cells were seeded in 96-well plates at a density of 1×10^4 cells/well and 100 μL of culture medium (blank) was dispensed into the peripheral wells. After 24h of incubation at 37 °C in a 5% CO_2 atmosphere, the culture medium was removed and replaced with either fresh medium (positive control and blank) or fresh medium containing samples (1:1 v/v, 1:5 v/v, and 1:9 v/v of chitosan extract). Samples for cytotoxicity studies were prepared by suspending 0.5 g of the chitosan xerogel in 50 mL of distilled water for 24h at 37 °C. After this time, the liquid part of the sample (extract) was passed through a 0.22 μm filter. Following 24h incubation, images of cells were taken using a 20× objective in an OLYMPUS 1×83 inverted microscope with an XC 50 camera and cellSens Dimension software. The culture medium was then removed, and 50 μL of the MTT solution (1 mg/mL in medium without supplements and phenol red) was added to each well and incubated for 2h at 37 °C in a 5% CO_2 atmosphere. Next, the MTT solution was removed, and the formazan crystals were dissolved in 100 μL isopropanol and shaken for 10 min. Absorbance was measured at 540 nm using a microplate reader (iMarkTM, Bio-Rad, Hercules, CA, USA). The results were obtained from four independent experiments (n = 4).

2.7. Statistical analysis

STATISTICA software (StatSoft, Inc., Tulsa, OK, USA) was used for all the analyses. Statistical significance was set at $P < 0.05$. All data reported are based on the means of four replicates (n = 4). Experimental results are expressed as mean ± standard deviation (SD). Student's t-test and one-way analysis of variance (ANOVA) were applied. The Mann-Whitney *U* test was used to analyze the differences between the results of the cytotoxicity assay for LA and CO2—obtained materials (*$p < 0.05$).

3. Results and discussion

3.1. Chitosan characteristic parameters

Five different chitosan polymers were used to evaluate the relationship between the antimicrobial properties and cytotoxicity of the materials prepared using two different methods. Table 1 shows the results of the DD measurements and their MW.

The indirect measurement of the MW by viscometry confirmed the information provided by the chitosan manufacturer. The values for low molecular weight (LMW), medium molecular weight (MMW), and high molecular weight chitosan (HMW) are consistent with literature data, for which the MW range are 50–150 kDa, 150–500 kDa and 500–2000 kDa, respectively [37,39,40]. Data from the specification of chitosan from shrimp shells and crab shells indicate that these are HMW polymers, which is also confirmed by our results. In addition, the manufacturer described chitosan from crab shells as highly viscous. This is consistent with the results, as the mass of chitosan was as high as 4000 kDa. The highest measured MW of chitosan reported in literature is approximately 10 million dalton [41]. However, the MW of chitosan can vary depending on its source, method of preparation, and DD. The LMW, MMW and HMW chitosans do not differ significantly in the DD. Significant differences were observed only for chitosans with HMW (Table 1).

Table 1
Description of the tested chitosan samples, their DD and MW (n = 3, $p < 0.05$).

Seller chitosan name	DD [%]	MW [kDa]	Given symbol
Low molecular weight	75.7 ± 5.7^{a}	89 ± 4^{a}	LMW
Medium molecular weight	81.7 ± 4.8^{a}	289 ± 10^{b}	MMW
High molecular weight	78.8 ± 1.5^{a}	591 ± 26^{c}	HMW/H79
From shrimp shells	66.2 ± 3.1^{c}	545 ± 22^{c}	HMW/H66
From crab shells	83.2 ± 4.6^{b}	4000 ± 142^{d}	HMW/H83

[a] High molecular weight chitosan.

Therefore, the results were used to determine the variability of the biological properties of chitosan materials (antimicrobial activity and cytotoxicity) depending on the MW with the same DD (LMW, MMW, HMW) and the DD with the same HMW (H66, H79, H83). Chitosan materials were obtained by the classical method using LA dissolved in water (Fig. 1. B). This indicates that their preparation method, which includes a lyophilization step, retains the acid in the final product. The acid trapped in the dried material causes it to re-dissolve when immersed in water. Photographs in Fig. 1 indicate that the chitosan materials obtained by CO_2 saturation did not dissolve in water because they did not contain acid. Only swelling of the materials can be observed, which is a well known characteristic of this polymer. According to literature, chitosan materials can absorb liquids 30 times their own weight or more. ([42]; Zhang et al., 2019).

3.2. Antimicrobial activity

The antimicrobial activity of the obtained chitosan xerogels was determined using the modified ASTM E2149 method because of its high accuracy in relation to the given form of material [38]. Fig. 2 shows the antimicrobial properties of chitosan xerogels as a function of MW and DD against *E. coli* and *S. aureus*. The antimicrobial activity of all chitosans dissolved in lactic acid, for both Gram-positive and Gram-negative bacteria, was greater than 99.99%. The reduction of bacteria by more than five logarithmic orders proved the bactericidal activity of the materials. It can be seen that such high activity is caused by one factor, i.e. the presence of LA in the samples. The mechanism of action of this acid is based on the degradation of the cell membrane, causing leakage of proteins from the inside of the cell and, thus, cell death [43]. Stanojević-Nikolić and co workers conducted a study to investigate the antimicrobial effect of lactic acid against different pathogen and spoilage microorganisms [powinno by]. They the determined minimal inhibitory concentration (MIC) and minimal bactericidal concentration (MBC) against *E. coli* and *S. aureus*. For both species, the MIC and MBC were 0.25% and 0.50%, respectively [44,45]. The methodology of the antimicrobial test (number of samples, volume of applied inoculum) shows that the concentration of lactic acid in our test system was approximately 0.36%, which results in a registered killing effect (at least 3 logarithmic orders of reduction), which could also be intensified by the synergistic effect of the lactic acid and chitosan. Chitosan materials produced by the CO_2 saturation method were characterized by lower antimicrobial activity in relation to the same samples prepared using the classical method (Fig. 2), and were more effective in inhibiting the growth of the *S. aureus* than *E. coli*. Considering the MW, the antimicrobial activity against both bacterial species was similar to that obtained for materials produced using LA. MMW was characterized by the lowest antimicrobial activity, amounting to 1.35 and 0.75 logarithmic for *S. aureus* and *E. coli*, respectively, which concern materials obtained by CO_2 saturation.

Chung and Chen investigated the antibacterial activity of LMW chitosan (30 kDa) by assessing the mortality rates of *E. coli* and *S. aureus*, and demonstrated that chitosan can destroy the cell structure of both bacterial cells, resulting in the leakage of enzymes and nucleotides from

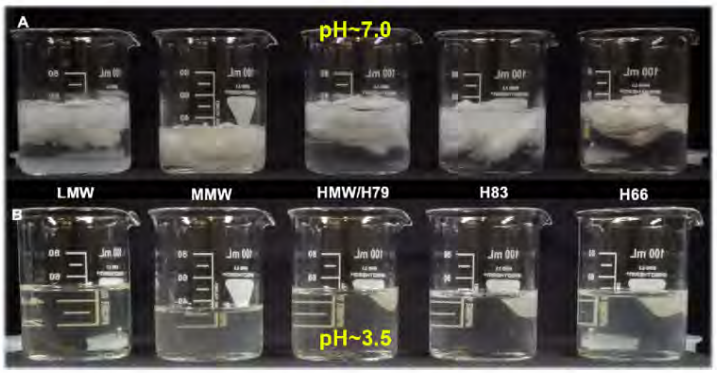

Fig. 1. Results of water extraction of xerogel materials prepared A) by CO_2 saturation, B) by dissolving with LA.

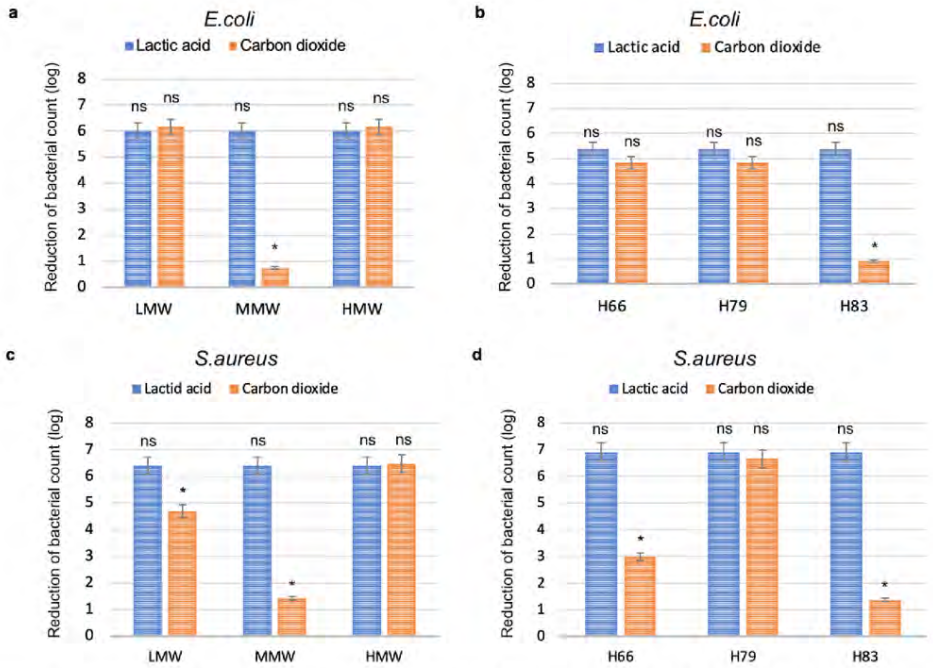

Fig. 2. Antimicrobial properties of chitosan xerogels of a) different MW against *E. coli*, b) different DD against *E. coli*, c) different MW against *S. aureus*, d) different DD against *S. aureus*. The results were analyzed by one-way ANOVA with comparisons vs. control: ns (not statistically significant, $p > 0.05$), *$p < 0.05$.

different cell locations [44]. Jeon et al. used fluorescence-labeled chitosans and monitored changes in zeta potential values of bacteria with chitosan coating, confirming the flocculation and adsorption behavior of this polymer (Jeon et al., 2001). Zheng et al. reported that the antimicrobial activity of chitosan against Gram-positive *S. aureus* increased with an increase in the MW. In addition, for Gram-negative *E. coli*, the antimicrobial activity of chitosan increased with a decrease in MW. The authors suggested the following two mechanisms for the antimicrobial activity. In the case of *S.aureus*, chitosan on the cell surface can form a polymer membrane, which inhibits nutrients from entering the cell. For *E. coli*, activity, especially in the case of low MW, is related to the penetration of chitosan into the cell [9]. If so, the antimicrobial effect must be the result of several mechanisms (Fig. 3). Moreover, differences in antimicrobial activity were also observed between chitosans H66 and H83. A bactericidal effect was achieved for both bacterial species and materials obtained using lactic acid. H83 produced by CO_2 saturation showed the lowest activity compared to H66 and H79, but it was also the chitosan with the highest viscosity and molecular weight. The H66 sample produced by the CO_2 saturation method was characterized by lower activity against S.aureus than H79 and higher than H83, which in turn could be the result of weak protonation and, at the same time, the amount of amino groups in chitosan, which determine the strength of

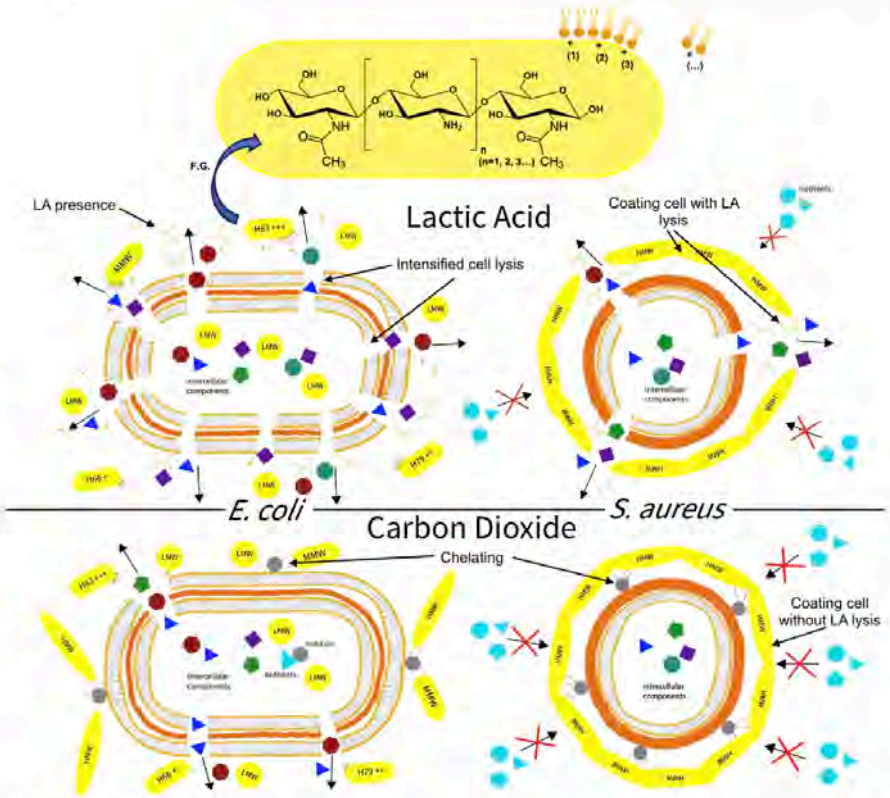

Fig. 3. Schematic showing the proposed mechanism of antimicrobial activity of chitosan depending on the method on polymer dissolution method (LA and CO_2), MW and DD against Gram-positive and Gram-negative bacteria.

the antimicrobial effect.

There is a significant difference in the structure of the cell walls of Gram-positive and Gram-negative bacteria, which leads to differences in their charge. Gram-positive bacteria have a thicker layer of peptidoglycan in their cell walls, which is surrounded by a polysaccharide and lipid layer. Peptidoglycan contains a large amount of positively charged amino acids such as lysine, which makes the cell wall of Gram-positive bacteria highly positively charged. Gram-negative bacteria are surrounded by a cell membrane composed of two lipid layers, the outer layer of which contains lipopolysaccharides (LPS). LPS is a complex molecule that consists of lipids, polysaccharides, and proteins. LPS also includes many carboxyl groups, which are responsible for the negative charge on the outer membrane of Gram-positive bacteria [46]. The positive charge of the amino group ($NH3+$) at pH values lower than pKa (pH < 6.3), at which this functional group carries 50% of its total electrical charge, allows interactions with the negatively charged microbial cell of the membrane, which is prone to the leakage of intracellular components [47]. In the case of chitosan prepared using CO_2 saturation (above pKa), the positive charge transfer of chitosan was negligible. This results in very limited electrostatic interactions between the polymer and cell.

Most studies have shown that an increase in DD and a decrease in pH improves the antimicrobial properties of chitosan (Jeon et al., 2001). The dependence of the increase in antimicrobial activity on the increase in DD should also be maintained for materials prepared using the innovative method of CO_2 saturation. A greater DD means a greater amount of free amino groups capable of carrying a charge, even at pH values lower than pKa (pH < 6.3).

In the case of materials prepared with LA, the change in the DD does not affect the antimicrobial activity of chitosan, which is a very high - reduction of bacteria by five and seven logarithmic orders for *E. coli* and *S. aureus*, respectively (Fig. 2b and d). There was no strict relationship between antimicrobial activity and the DD of chitosans obtained by CO_2 saturation. This may mean that DD has a lower priority in imparting activity to the materials than the MW because samples H66, H79, and H83 are high-molecular chitosans. However, the MW of H83 was significantly higher than those of the other two chitosans (H66 and H79). This may mean that molecules that are too large lose their antimicrobial activity due to the formation of aggregates (intramolecular hydrogen interactions).

For acid-free chitosans, it is highly likely that a third antimicrobial mechanism may occur, involving chelation of metal ions found on the surface of the bacteria or in its nutrients. According to the literature, this mechanism occurs more often at pH > 6.5, owing to the ability of the deprotonated amino group to donate the nitrogen lone pair. At pH values of 7–9, metal ion chelation occurs through both the amine groups and the two deprotonated hydroxyl groups, forming a more stable complex than the two $-NH_2$ receptor groups at lower pH [20].

Fig. 3 shows a diagram of the proposed mechanism of antimicrobial activity of chitosans, differentiated by the method of dissolution, MW,

DD, and type of bacteria. In the case of Gram-negative bacteria and the LA environment, the cell membrane is lysed under the influence of this acid and LMW chitosan. This causes migration of intracellular components from the cell. For Gram-positive bacteria in the same environment, there is a hybrid mechanism consisting of coating the cell with HMW, thus preventing the uptake of nutrients and damage to the cell membrane. In the case of chitosans dissolved by CO_2 saturation and Gram-positive bacteria, the cell membrane was not lysed, and only the surface of the cells was coated with HMW chitosan. For LMW chitosan and Gram-negative bacteria, membrane lysis should be limited. In addition, for all chitosans obtained by CO_2 saturation, the mechanism of chelation of ions constituting the components of the cell membranes is activated. This difference may also be due to the influence of the environment on the activity of chitosans differing in the DD, where the presence of acid enhances the interaction of polymers with the cell membrane in a series of increasing activities: H83(CO_2) < H66(CO_2) < H79(CO_2) < H66(LA); H79 (LA); H83(LA).

3.3. *Cytotoxicity*

The MTT assay was used to investigate the cytotoxicity of the studied chitosan xerogels against adult mouse fibroblast L929 cells at different dilutions (1:1 v/v, 1:5 v/v, and 1:9 v/v).

The obtained results were expressed as the percentage of viable cells compared to the control without the materials. The data presented in Fig. 4 clearly show that chitosan materials obtained by the LA method in a 1:1 dilution are characterized by the highest cytotoxicity against L929 cells (~20%). For the same dilution and samples prepared using the CO_2 saturation method, the viability of L929 cells was approximately 2.5 times higher (~50%). aStatistical analysis showed lower cytotoxicity of tests performed using the CO_2 method for all chitosan extracts with the lowest dilution of the extract (1:1 v/v) administered to cells. For samples with the highest dilution of chitosan extract (1:9 vv/v), no statistically significant differences were found (Fig. 4).

Hismiogullari and colleagues conducted a study to investigate the effects of organic acids, including lactic acid, on murine fibroblast cells from the NIH 3T3 cell line. Their research showed a similar relationship despite the use of different cell types. For samples administered to cells

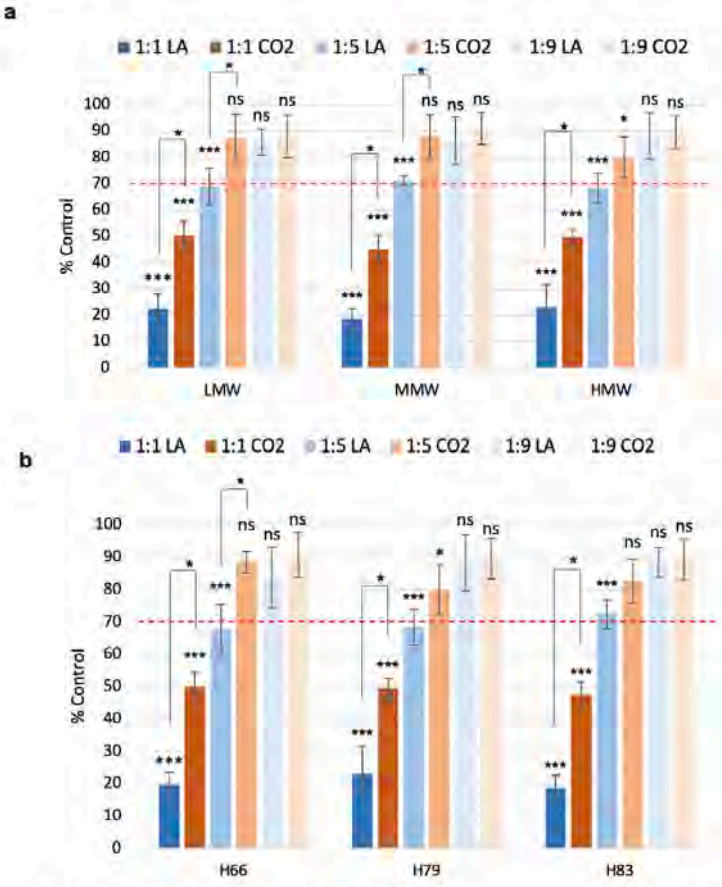

Fig. 4. The cytotoxicity of chitosan materials following 24 h incubation at different dilution factors (1:1 v/v, 1:5 v/v, and 1:9 v/v) against L929 cells. Data are expressed as the mean ± standard deviation of four independent experiments. The results were analyzed by one-way ANOVA with comparisons vs. control: ns (not statistically significant, $p > 0.05$), *$p < 0.05$, **$p < 0.01$, ***$p < 0.001$. The Mann-Whitney *U* test was used to analyze the differences between the results of the cytotoxicity assay for LA and CO2—obtained materials (*$p < 0.05$).

with lactic acid concentrations of 0.5%, 0.25% and 0.1%, cell survival was ~20%, ~70% and 90–100%, respectively [48]. Comparable results were achieved for sample extracts from chitosan materials produced using lactic acid, in which the concentration of this acid was: 0.45%, 0.15%, 0.09%. Therefore, for both lines of mouse fibroblasts, the cytotoxic effect of drug acid was very similar.

Cell viability improved with increasing dilutions of extracts prepared from chitosan materials. The same trend was observed for all materials, regardless of the MW and DD of chitosan. Huang et al. also confirmed that the MW does not affect the cytotoxicity of chitosan [31]. On the other hand, cytotoxicity studies of chitosan with different MW (17 kDa, 45 kDa, and 240 kDa) by Zhang et al. showed an increase in cytotoxicity with a decrease in MW of <40%, ~60%, and >90%, respectively [49].

Results reported by Jeon et al. showed that chitosan oligosaccharides with a higher DD exhibited higher cytotoxicity against L929 cells [50]. The exact mechanism of chitosan-induced cytotoxicity in L929 cells is not fully understood and may involve multiple factors, such as cell membrane disruption through the interaction of positively charged chitosan particles with negatively charged cell membranes, induction of reactive oxygen species (ROS) generation by chitosan, activation of

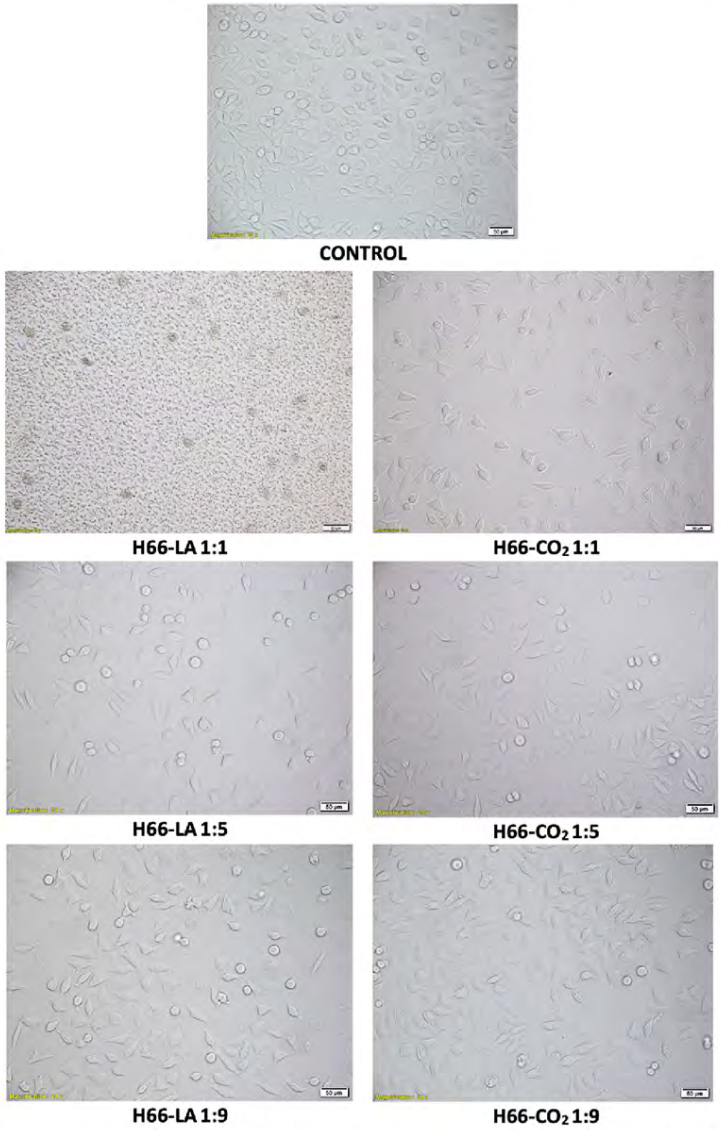

Fig. 5. Representative images at 200 × magnification of L929 cells following 24 h treatment with chitosan materials. The scale bar is 50 μm (LA-samples prepared with lactic acid, CO_2-samples prepared with CO_2 technology).

pro-apoptotic pathways or inhibition of anti-apoptotic pathways, and induction of cell cycle arrest at different stages, depending on the cell type and chitosan concentration or mitochondrial dysfunction leading to the release of pro-apoptotic factors and subsequent cell death [51,52]. The cytotoxicity data obtained here were confirmed by a morphological study of L929 cells treated with the tested chitosan extracts for 24 h (Fig. 5). Owing to the very similar cytotoxicity of all tested chitosans, the imaging results are presented in a comparison of tested dilutions only for the selected sample, H66. Fig. 5 clearly shows that as the dilution of the tested extracts increases, there is a marked increase in the number of cells visible in the microscopic images. Moreover, L929 cells showed unchanged morphology (retained their fibroblast shape) after treatment with extracts at 1:5 and 1:9 dilutions, relative to the control sample. Significant differences were observed in the morphology of cells treated with chitosan extracts at 1:1 v/v dilution. In the case of cells treated with the chitosan extract obtained by the innovative method of CO_2 saturation, the morphology of the majority of the L929 cells was preserved. The cells were oval and elongated in shape (H66-CO_2 1:1). For the H66-LA 1:1 sample, two observations were made. First, the microscopic image is blurred. Chitosan LA-extracts diluted 1:1 were characterized by the highest viscosity, resulting from the increased solubility of the polymer under such conditions, making it difficult to visualize the cell morphology. Second, the number of cells in the H66-LA 1:1 sample in the same measuring field of the microscope was lower than that in the other images, indicating substantial inhibition of cell proliferation and induction of cell death of a significant number of cells. Contours of cells with only spherical shapes are visible, revealing a change in L929 cell morphology. Undoubtedly, the cytotoxic effect of lactic acid was evident. This acid affects the function and viability of the cells, which has been confirmed in many studies. The cytotoxic effect of lactic acid is attributed to mechanisms such as the generation of free radicals, which affect the activity of intracellular enzymes, such as dehydrogenases (causing disturbances in energy metabolism), and gene expression (disruption of DNA replication and transcription) [52–54].

In vitro methods, which are crucial when evaluating medical devices such as implants, cannot capture all the complexities of the human body. Therefore, standardized tests for biosafety evaluation have been developed, as described in ISO 109933 "Biological Evaluation of Medical Devices." In the section that provides a set of recommendations, parameters and conditions for conducting the test ISO 10993–5:2009 recommends testing on a cell line derived from mouse fibroblasts L929 [55]. Accordingly, many authors in their studies focus precisely on using the L929 line as a model, a benchmark. However, in cases where authors focus their studies on a specific tissue, organ, or site of action of a compound in the body, they conduct additional studies confirming the biosafety of a given implant, on target cell lines, in order to confirm this cytotoxic effect or lack thereof.

As an example, Dodero et al. compared the effect of the method used to crosslink electrospun chitosan-based membranes on their biosafety. The toxicity of the methods was tested on three cell lines, i.e. L929, HaCaT and human Saos-2 osteoblasts. For both chemical and physical crosslinking of the test material, the survival rate of L929 cells after 24 h of contact was the highest and significantly higher than for the other cells. Moreover, only the L929 cells showed no cytotoxic effect of the samples tested. In addition, comparing the other two lines with each other, HaCaT cells had a higher survival rate after exposure to the test materials than Saos-2 cells [56]. In another study conducted by Castellano et al. the biological safety of electrospun chitosan-collagen nanofibers was also examined by MTT for two cell lines, i.e. L929 and human HaCaT keratinocytes. The study showed differential behavior of these two cell lines in interaction with different substrates over time. In the case of L929 cells, for all tested materials, a decrease in cell counts was observed after 48h, followed by an increase after 72h. Moreover, the survival rate of this cell line, compared to HaCaT cells, after 24h contact with the tested material was higher in most samples. In the case of HaCaT cells, cell abundance decreased with increasing exposure time up to 120 h [57]. The biocompatibility of the manufactured titanium alloy materials was also evaluated using the MTT test with L929 fibroblast cells and MG-63 osteoblasts. Analysis of the MTT test data showed that the survival rate of L929 cells after 120 h of incubation was significantly higher than that of MG-63 osteoblasts [58]. In contrast, bioassessment of the Ti17Mg composite material showed no difference in the abundance of viable cells of both L929 and hDPSC dental pulp stem cells, which was comparable in both cases [59]. However, in the case of cancer cells, their sensitivity is different. For example, Elsayed et al. examined the effects of Moringa oleifera seed essential oil on HeLa, human cervical cancer; HepG2, human hepatocellular carcinoma; MCF-7, human breast cancer; CACO-2, Caucasian colon adenocarcinoma and L929, mouse fibroblast cell lines. The researchers showed that cytotoxicity depended not only on the concentration of the test compound, but also on the cell line. HeLa proved to be the most sensitive cells, followed by HepG2, MCF-7, L929 and CACO-2 [60]. Similar conclusions were reached by Samarghandian, who observed that the cytotoxic effect of ethanolic saffron extract on the human non-small lung cancer cells (A549) was significantly greater than on L929 cells [61].

In conclusion, the use of the L929 line in the MTT assay to assess the biosafety of a given material is a standardized method that allows a preliminary assessment of the cytotoxic effect. One of the main reasons for using fibroblasts as a model line is that they are cells present in every tissue except blood. Therefore, if a particular compound has a detrimental effect on a fibroblast line then its use will adversely affect the entire body. In addition, these are the most commonly used cell lines in experiments which is due to their simple culture [62]. This approach makes it possible to compare specific materials, composites or compounds with each other. However, when conducting further research to evaluate the applicability of a given composite, it is necessary to conduct extended studies on their effects on specific cell lines.

4. Conclusions

Chitosan is a well-known and widely studied compound. Several of its advantages are often pointed out, such as biocompatibility, biodegradability, bioadhesiveness, coating ability, and antimicrobial activity. Due to the many mechanisms determining the resultant antimicrobial activity of chitosan and its cytotoxicity, it remains a challenge to precisely identify and link those properties.

However, it can certainly be unequivocally stated that the use of innovative technology for CO_2 saturation in the production of chitosan materials significantly expands the application possibilities of this polymer owing to the reduction of its cytotoxic effect, regardless of the MW and DD, compared to the classical method of dissolution in LA and certainly in other acid solutions. The results of the antimicrobial activity measurements indicate that the acid present in the chitosan materials, which is necessary for the dissolution and processing of this polymer, is partly responsible for its high antibacterial activity. In the next work, we plan to perform an additional test confirming the absence of the sodium salt of hydroxyacetic acid in the rinsed chitosan suspension to completely exclude the potential impact of this compound on the activity of the polymer.The results showed that the same materials produced by the CO_2 saturation technique may show much lower antimicrobial activity against microorganisms, which results from the resultant mechanisms related to the MW of the polymer and the DD. Nevertheless, the antimicrobial effect of materials produced by CO_2 saturation is still sufficient to design bacteriostatic or even bactericidal materials.

The results indicate that chitosan is a safe raw material and can be used in many industries, even in the food industry (registered as a food additive in some countries), as well as in the packaging industry. However, it is an organic compound of natural origin, which is often difficult to process technologically and ensure appropriate mechanical properties of the final products. This creates the need to use it as an additive and not the main raw material, which still requires strict

control, including potential cytotoxic effects.

Author contributions

Conceptualization: S.M., Data curation: S.M., A.B–K., K.S., J.K., E.A., and R.T., Formal analysis: S.M., J.K., Funding acquisition: S.M., Investigation: S.M., A.B–K., K.S., J.K., Methodology: S.M., A.B–K., K.S., J.K., E.A., and R.T., Project administration: S.M., Resources: S.M., A.B–K., K. S., J.K., E.A., and R.T., Software: S.M., A.B–K., K.S., J.K., Supervision: S. M., E.A. and R.T., Validation: S.M., A.B–K., K.S., J.K., E.A., and R.T., Visualization S.M., K.S., J.K., Writing—original draft preparation: S.M., A.B–K., K.S., J.K., E.A., and R.T, Writing—review and editing: S.M., A. B–K., K.S., J.K., E.A., and R.T All authors have read and agreed to the published version of the manuscript.

Declaration of competing interest

The authors declare that they have no known competing financial interests or personal relationships that could have appeared to influence the work reported in this paper.

Data availability

Data will be made available on request.

Acknowledgement

This study was supported by NCN Miniatura 6 grant (2022/06/X/ST8/00096). The visualizations shown in Fig. 1 were made using TOP Show 3D automatic rotation system (Wroclaw, Poland) purchased thanks to Argentum Triggering Research Grants - 'Excellence Initiative - Research University' (DEC-10/2021/IDUB/I.3.3) and Agisoft Metashape Professional EDU software (Softnow, Warszawa, Poland) financed form RADIUM LEARNING THROUGH RESEARCH PROGRAMS (DEC-25/2022/IDUB/III. 1/Ra).

References

[1] G. Martina Mathew, S. Bill Ulaeto, R. Kumar Sukumaran, P. Binod, A. Pandey, R. Sindhu, Chitosan Derivatives: Properties and Applications, 2021.
[2] C.V. Stevens, J. Dewulf, H. Van, L. Biofuels, W. Soetaert, E. Vandamme, T. Bechtold, R. Mussak, M. Kjellin, I. Johansson, C. Bergeron, D.J. Cartier, S. Ramaswamy, C.E. Wyman, S. Kabasci, D.D. Stokke, Q. Wu, G. Han, D.I. Kaiten, F. Deswarte, Chitin and Chitosan Wiley Series in Renewable Resources Handbook of Natural Colorants Surfactants from Renewable Resources Aqueous Pretreatment of Plant Biomass for Biological and Chemical Conversion to Fuels and Chemicals Introduction to Wood and Natural Fiber Composites Introduction to Chemicals from Biomass, second ed., 2020.
[3] L.J.R. Foster, S. Ho, J. Hook, M. Basuki, H. Marçal, Chitosan as a biomaterial: influence of degree of deacetylation on its physiochemical, material and biological properties, PLoS One 10 (8) (2015), https://doi.org/10.1371/journal.pone.0135153.
[4] M. Prostiolli, R. Jenwithisuk, K. Kongsuwan, N. Damrongchai, P. Watts, Cellular Responses to Chitosan In Vitro: the Importance of Deacetylation, 2000.
[5] I. Bano, M. Arshad, T. Yasin, M.A. Ghauri, M. Younus, Chitosan: a potential biopolymer for wound management, Int. J. Biol. Macromol. 102 (2017) 380–383, https://doi.org/10.1016/j.ijbiomac.2017.04.047. Elsevier B.V.
[6] U. Chadha, P. Bhardwaj, S.K. Selvaraj, K. Kumari, T.S. Isaac, M. Panjwani, K. Kulkarni, R.M. Mathew, A.M. Satheesh, A. Pal, N. Gunreddy, O. Dubey, S. Singh, S. Latha, A. Chakravorty, B. Badoni, M. Banavoth, P. Sonar, M. Manoharan, V. Paramasivam, Advances in chitosan biopolymer composite materials: from bioengineering, wastewater treatment to agricultural applications, Mater. Res. Express 9 (5) (2022), https://doi.org/10.1088/2053-1591/ac5a9d.
[7] I. Aranaz, A.R. Alcántara, M.C. Civera, C. Arias, B. Elorza, A.H. Caballero, N. Acosta, Chitosan: an overview of its properties and applications, Polymers 13 (19) (2021), https://doi.org/10.3390/polym13193256. MDPI.
[8] A.G. Mitelut, E. Tănase, V.I. Popa, M.E. Popa, Sustainable Alternative For Food Packaging: Chitosan Biopolymer A Review, 2015.
[9] L.Y. Zheng, J.F. Zhu, Study on antimicrobial activity of chitosan with different molecular weights, Carbohydr. Polym. 54 (4) (2003) 527–530, https://doi.org/10.1016/j.carbpol.2003.07.009.
[10] F.K. Tavaria, J.C. Soares, I.L. Reis, M.H. Paulo, F.X. Malcata, M.E. Pintado, Chitosan: antimicrobial action upon staphylococci after impregnation onto cotton fabric, J. Appl. Microbiol. 112 (5) (2012) 1034–1041, https://doi.org/10.1111/j.1365-2672.2012.05274.x.
[11] N.N. Irmandar, V. Monrya, 6 Chitosan and Low-Molecular Weight Chitosan: Biological and Biomedical Applications, 2014.
[12] L. Jiang, F. Wang, F. Han, W. Prinyawiwatkul, H.K. No, B. Ge, Evaluation of diffusion and dilution methods to determine the antimicrobial activity of water-soluble chitosan derivatives, J. Appl. Microbiol. 114 (4) (2013) 956–963, https://doi.org/10.1111/jam.12111.
[13] N. Liu, X.G. Chen, H.J. Park, C.G. Liu, C.S. Liu, X.H. Meng, L.J. Yu, Effect of MW and concentration of chitosan on antibacterial activity of Escherichia coli, Carbohydr. Polym. 64 (1) (2006) 60–65, https://doi.org/10.1016/j.carbpol.2005.10.028.
[14] X. Fei Liu, Y. Lin Guan, D. Zhi Yang, K.D.K. Yao, Antibacterial Action of Chitosan and Carboxymethylated Chitosan, 2000.
[15] KyoonNo, H., Park, N. Y., Lee, S. H., & Meyers, S. P. (n.d.). Antibacterial activity of chitosans and chitosan oligomers with different molecular weights. www.elsevier.com/locate/ijfoodmicro.
[16] P. Chhabra, Y.-W. Huang, J.F. Frank, R. Chmielewski, K. Gates, Fate of Staphylococcus aureus, Salmonella enterica serovar typhimurium, and Vibrio vulnificus in raw oysters treated with chitosan, J. Food Protect. 69 (Issue 7) (2006). https://meridian.allenpress.com/jfp/article-pdf/69/7/1600/1677708/0362-028x-69_7_1600.pdf.
[17] M. Kong, X.G. Chen, K. Xing, H.J. Park, Antimicrobial properties of chitosan and mode of action: a state of the art review, Int. J. Food Microbiol. 144 (1) (2010) 51–63, https://doi.org/10.1016/j.ijfoodmicro.2010.09.012.
[18] S. Mania, R. Tylingo, E. Augustin, K. Guewa, J. Szwacki, H. Staroszczyk, Investigation of an elutable N-propylphosphonic acid chitosan derivative composition with a chitosan matrix prepared from carbonic acid solution, Carbohydr. Polym. 179 (2018) 196–206, https://doi.org/10.1016/j.carbpol.2017.09.082.
[19] R. Tylingo, P. Kempa, A. Banach-Kopeć, S. Mania, A novel method of creating thermoplastic chitosan blends to produce cell scaffolds by FDM additive manufacturing, Carbohydr. Polym. 280 (2022), https://doi.org/10.1016/j.carbpol.2021.119028.
[20] Rejane C. Goy, D. de B. O.B. G, A review of the antimicrobial activity of chitosan, Polímeros - Ciência Tecnol. 19 (3) (2009) 241–247.
[21] M. Hosseinnejad, S.M. Jafari, Evaluation of different factors affecting antimicrobial properties of chitosan, Int. J. Biol. Macromol. 85 (2016) 467–475, https://doi.org/10.1016/j.ijbiomac.2016.01.022. Elsevier B.V.
[22] J. Li, S. Zhuang, Antibacterial activity of chitosan and its derivatives and their interaction mechanism with bacteria: current state and perspectives, Eur. Polym. J. 138 (2020), https://doi.org/10.1016/j.eurpolymj.2020.109984. Elsevier Ltd.
[23] I. Adekogbe, A. Ghanem, Fabrication and characterization of DTBP-crosslinked chitosan scaffolds for skin tissue engineering, Biomaterials 26 (35) (2005) 7241–7250, https://doi.org/10.1016/j.biomaterials.2005.05.043.
[24] A.S. Hoffm, I.C. Kwong, I. Zainol, A. Hazri, A. Rashid, Biocompatibility and Biodegradation of Chitosan and Derivatives, 2012.
[25] A. Lauto, J. Hook, M. Doran, F. Camacho, L.A. Poole-Warren, A. Avolio, L.J. R. Foster, Chitosan adhesive for laser tissue repair: in vitro characterization, Laser Surg. Med. 36 (3) (2005) 193–201, https://doi.org/10.1002/lsm.20145.
[26] M. Kurniasih, Purwati, R.S. Dewi, Toxicity tests, antioxidant activity, and antimicrobial activity of chitosan, IOP Conf. Ser. Mater. Sci. Eng. 349 (1) (2018), https://doi.org/10.1088/1757-899X/349/1/012037.
[27] S.B. Rao, C.P. Sharma, Use of chitosan as a biomaterial: studies on its safety and hemostatic potential, J. Biomed. Mater. Res. 34 (1) (1997) 21–28, https://doi.org/10.1002/(SICI)1097-4636(199701)34:1<21::AID-JBM4>3.0.CO;2-P.
[28] A. Mafica, G. Menighin, V. Ostafe, Toxicity of chitosan based products, Porta Ann West Univ. Timisoara – Ser. Chem. 26 (1) (2017) 65–74.
[29] M. Otterlei, K.M. Ytrum, L. Ryan, T. Espevik, Characterization of Binding and TNF-Inducing Ability of Chitosans on Monocytes: the Involvement of CD14, 1994.
[30] A. Domard, C. Chatelet, O. Damour, A. Domard, Influence of the degree of acetylation on some biological properties of chitosan films, Biomaterials 22 (2001).
[31] M. Huang, E. Khor, L.-Y. Lim, Uptake and Cytotoxicity of Chitosan Molecules and Nanoparticles: Effects of Molecular Weight and Degree of Deacetylation, 2004.
[32] S.K.L. Levengood, M. Zhang, Chitosan-based scaffolds for bone tissue engineering, J. Mater. Chem. B 2 (21) (2014) 3161–3184, https://doi.org/10.1039/c4tb00027g.
[33] S.V. Madihally, H.W.T. Matthew, Porous chitosan scaffolds for tissue engineering, Biomaterials 20 (1999).
[34] B. Yang, X.Y. Li, S. Shi, X.Y. Kong, G. Guo, M.J. Huang, F. Luo, Y.Q. Wei, X. Zhao, Z.Y. Qian, Preparation and characterization of a novel chitosan scaffold, Carbohydr. Polym. 80 (3) (2010) 860–865, https://doi.org/10.1016/j.carbpol.2009.12.044.
[35] G. Gorczyca, R. Tylingo, P. Szweda, E. Augustin, M. Sadowska, S. Milewski, Preparation and characterization of genipin cross-linked porous chitosan-collagen-gelatin scaffolds using chitosan-CO2 solution, Carbohydr. Polym. 102 (1) (2014) 901–911, https://doi.org/10.1016/j.carbpol.2013.10.060.
[36] Y. Yuan, B.M. Chesnutt, W.O. Haggard, J.D. Bumgardner, Deacetylation of chitosan: material characterization and in vitro evaluation via albumin adsorption and pre-osteoblastic cell cultures, Materials 4 (8) (2011) 1399–1416, https://doi.org/10.3390/ma4081399.
[37] M. Rinaudo, Chitin and chitosan: properties and applications, Prog. Polym. Sci. 31 (7) (2006) 603–632, https://doi.org/10.1016/j.progpolymsci.2006.06.001. Oxford.

[38] L. Damian, S. Patachia, Method for testing the antimicrobial character of the materials and their fitting to the scope, Bull. Transilvania Univ. Brasov 7 (Issue 56) (2014).
[39] I. Kaur, A.K. Chopra, A. Saini, Molecular weight determination of chitosan, Int. J. Pharmaceut. Sci. Res. 5 (6) (2014) 2126–2135.
[40] K. Kofuji, H. Kishimura, Characteristics and applications of chitin and chitosan, Curr. Org. Chem. 23 (1) (2019) 74–95.
[41] S. Mao, B. Xu, Progress in the preparation and application of high molecular weight chitosan, J. Contr. Release 139 (1) (2009) 1–11.
[42] R. Tylingo, G. Gorczyca, S. Mania, P. Szweda, S. Milewski, Preparation and characterization of porous scaffolds from chitosan-collagen-gelatin composite, React. Funct. Polym. 103 (2016) 131–140, https://doi.org/10.1016/j.reactfunctpolym.2016.04.008.
[43] C. Wang, T. Chang, H. Yang, M. Cui, Antibacterial mechanism of lactic acid on physiological and morphological properties of Salmonella Enteritidis, Escherichia coli and Listeria monocytogenes, Food Control 47 (2015) 231–236, https://doi.org/10.1016/j.foodcont.2014.06.034.
[44] Y.C. Chung, C.Y. Chen, Antibacterial characteristics and activity of acid-soluble chitosan, Bioresour. Technol. 99 (8) (2008) 2806–2814, https://doi.org/10.1016/j.biortech.2007.06.044.
[45] S. Stanojević Nikolić, G. Dimić, L. Mojović, J. Pejin, A. Djukić-Vuković, S. Kocić-Tanackov, Antimicrobial acitivity of lactic acid against PAthogen and spoilage microorganisms, J. Food Process. Preserv. 40 (5) (2015) 990–998.
[46] B. Alberts, Molecular Biology of the Cell, sixth ed., Garland Science, 2015. 6th ed.
[47] I.M. Helander, E.-L. Nurmiaho-Lassila, R. Ahvenainen, J. Rhoades, S. Roller, Chitosan disrupts the barrier properties of the outer membrane of Gram-negative bacteria, Int. J. Food Microbiol. 71 (2001). www.elsevier.com/locate/ijfoodmicro.
[48] S. Hismiogullari, A. Hismiogullari, F. Sahin, E.B.R.U. Toksoy Öner, S. Yenice, D. Karasartova, Investigation of antibacterial and cytotoxic effects of organic acids including ascorbic acid, lactic acid and acetic acids on mammalian cells, J. Anim. Vet. Adv. 7 (6) (2008).
[49] X. Zhang, Y. Zhang, J. Wang, P. Li, Cytotoxicity of chitosan with different molecular weights on L929 fibroblast cells, Mater. Med. 26 (4) (2015) 1–7.
[50] Y. Jeon, P.J. Park, S.K. Kim, H.G. Byun, Effect of degree of deacetylation on the antitumor activity of chitosan oligosaccharides, Int. J. Mol. Med. 12 (1) (2003) 141–144.
[51] Y. Qiao, S. Zhang, S. Zhou, S. Li, J. Chen, Advances in the mechanism of chitosan-induced cytotoxicity, J. Funct.Foods 81 (2021).
[52] L. Li, et al., Lactic acid induces apoptosis in L929 cells through a ROS-dependent pathway, Front. Pharmacol. 11 (2020).
[53] H. Yang, Lactic acid triggers mitochondrial apoptosis in L929 fibroblast cells via the caspase-9-dependent pathway, J. Biochem. Mol. Toxicol. 35 (8) (2021).
[54] Y. Jia, et al., Lactic acid induces apoptosis in L929 cells by disrupting the mitochondrial membrane potential and increasing reactive oxygen species production, J. Biochem. Mol. Toxicol. 32 (1) (2018).
[55] P. Jablonská, J. Kubásek, D. Vojtěch, T. Ruml, J. Lipov, Test conditions can significantly affect the results of in vitro cytotoxicity testing of degradable metallic biomaterials, Sci. Rep. 11 (1) (2021) 6628.
[56] A. Dodero, S. Scarfi, S. Mirata, A. Sionkowska, S. Vicini, M. Alloisio, M. Castellano, Effect of crosslinking type on the physical-chemical properties and biocompatibility of chitosan-based electrospun membranes, Polymers 13 (5) (2021) 831.
[57] M. Castellano, A. Dodero, S. Scarfi, S. Mirata, M. Pozzolini, E. Tassara, S. Vicini, Chitosan–collagen electrospun nanofibers loaded with curcumin as wound-healing patches, Polymers 15 (13) (2023) 2931.
[58] A. Radtke, M. Grodzicka, M. Ehlert, T. Jędrzejewski, M. Wypij, P. Golińska, "To be microbiocidal and not to be cytotoxic at the same time…"—silver nanoparticles and their main role on the surface of titanium alloy implants, J. Clin. Med. 8 (3) (2019) 334.
[59] Y. Cetin, A.M.H. Ibrahim, A. Gungor, Y. Yildizhan, M. Bulog, P. Krizik, In vitro evaluation of a partially biodegradable TiMg dental implant: the cytotoxicity, genotoxicity, and oxidative stress, Materialia 14 (2020), 100899.
[60] E.A. Elsayed, M.A. Sharaf-Eldin, M. Wadaan, In vitro evaluation of cytotoxic activities of essential oil from Moringa oleifera seeds on Hela, HepG2, MCF-7, CACO-2 and L929 cell lines, Asian Pac. J. Cancer Prev. APJCP 16 (11) (2015) 4671–4675.
[61] S. Samarghandian, M.H. Boskabady, S. Davoodi, Use of in vitro assays to assess the potential antiproliferative and cytotoxic effects of saffron (Crocus sativus L.) in human lung cancer cell line, Phcog. Mag. 6 (24) (2010) 309.
[62] S. Ranjitkar, D. Zhang, F. Sun, S. Salman, W. He, K. Venkitanarayanan, X. Tian, Cytotoxic effects on cancerous and non-cancerous cells of trans-cinnamaldehyde, carvacrol, and eugenol, Sci. Rep. 11 (1) (2021), 16281.

6.3 [A3] Thermosensitive composite based on agarose and chitosan saturated with carbon dioxide. Preliminary study of requirements for production of new CSAG bioink.

6.3.1 Wkład pracy doktoranta

Tytuł: Thermosensitive composite based on agarose and chitosan saturated with carbon dioxide. Preliminary study of requirements for production of new CSAG bioink.
Autorzy: Adrianna Banach-Kopeć, Szymon Mania, Robert Tylingo, Agata Wawrzynowicz, Monika Pawłowska, Katarzyna Czerwiec, Milena Deptuła, Michał Pikuła
Czasopismo: CARBOHYDRATE POLYMERS
Rok wydania: 2024
Impact factor: 11,2 (2022)
Liczba punktów wg MNiSW: 140
DOI: 10.1016/j.carbpol.2024.122120
Procentowy wkład pracy doktoranta: 27%

Moje zaangażowanie w przygotowanie tego artykułu polegało na pełnieniu roli jednego z głównych twórców koncepcji i planu badawczego, które były fundamentem projektu, oraz na organizacji zasobów niezbędnych do jego realizacji. Aktywnie uczestniczyłam w przeprowadzaniu badań eksperymentalnych, w tym w przygotowywaniu prób do dalszej analizy. Samodzielnie przeprowadziłam badania oceny właściwości reologicznych badanych kompozycji oraz ich aktywności przeciwdrobnoustrojowej. Brałam udział w badaniach nad oceną sił wytłaczania kompozycji chitozanowo-agarozowych oraz w eksperymentach oceny żywotności komórek w wytłoczonych kompozycjach polimerowych, jak również w procesie ich drukowania. Przygotowałam próby do testów biologicznych oceniających biozgodność kompozycji polimerowych. Moje obowiązki obejmowały także zarządzanie danymi (ich zbieranie, organizację oraz przygotowanie do analizy) oraz formalną analizę większości wyników. Odpowiadałam za przygotowanie większości wykresów oraz walidację wyników. Byłam również zaangażowana w przygotowanie pierwszej wersji manuskryptu, jego edycję oraz przygotowanie odpowiedzi dla recenzentów.

6.3.2 Treść artykułu

Carbohydrate Polymers 336 (2024) 122120

Contents lists available at ScienceDirect

Carbohydrate Polymers

journal homepage: www.elsevier.com/locate/carbpol

Thermosensitive composite based on agarose and chitosan saturated with carbon dioxide. Preliminary study of requirements for production of new CSAG bioink

Adrianna Banach-Kopeć [a,1], Szymon Mania [a,*,1], Robert Tylingo [a], Agata Wawrzynowicz [a], Monika Pawłowska [b], Katarzyna Czerwiec [c], Milena Deptuła [d], Michał Pikuła [d]

[a] Department of Chemistry, Technology and Biotechnology of Food, Faculty of Chemistry, Advanced Materials Center, Gdańsk University of Technology, G. Narutowicza 11/12 Str., 80-233 Gdansk, Poland
[b] Department of Pharmaceutical Technology and Biochemistry, Faculty of Chemistry, Gdańsk University of Technology, G. Narutowicza 11/12 Str., 80-233 Gdansk, Poland
[c] Division of Clinical Anatomy, Medical University of Gdańsk, M. Skłodowskiej-Curie 3a Str., 80-210 Gdańsk, Poland
[d] Laboratory of Tissue Engineering and Regenerative Medicine, Division of Embryology, Medical University of Gdansk, M. Skłodowskiej-Curie 3a Str., 80-210 Gdańsk, Poland

ARTICLE INFO

Keywords:
Agarose
Bioink
Biosafety, chitosan
3D printing, antimicrobial properties

ABSTRACT

This study introduces a method for producing printable, thermosensitive bioink formulated from agarose (AG) and carbon dioxide-saturated chitosan (CS) hydrogels. The research identified medium molecular weight chitosan as optimal for bioink production, with a preferred chitosan hydrogel content of 40–60 %. Rheological analysis reveals the bioink's pseudoplastic behavior and a sol-gel phase transition between 27.0 and 31.5 °C. The MMW chitosan-based bioink showed also the most stable extrusion characteristic. The choice of chitosan for the production of bioink was also based on the assessment of the antimicrobial activity of the polymer as a function of its molecular weight and the degree of deacetylation, noting significant cell reduction rates for *E. coli* and *S. aureus* of 1.72 and 0.54 for optimal bioink composition, respectively. Cytotoxicity assessments via MTT and LDH tests confirm the bioink's safety for L929, HaCaT, and 46BR.1 N cell lines. Additionally, XTT proliferation assay proved the stimulating effect of the bioink on the proliferation of 46BR.1 N fibroblasts, comparable to that observed with Fetal Bovine Serum (FBS). FTIR spectroscopy confirms the bioink as a physical polymer blend. In conclusion, the CS/AG bioink demonstrates the promising potential for advanced spatial cell cultures in tissue engineering applications including skin regeneration.

1. Introduction

Tissue engineering (TE) is a promising field that addresses the shortage of tissue donors and organs through the development of cellular scaffolds (Mandrycky, Phong, & Zheng, 2017). Several basic methods exist for producing materials for this industry, including solvent casting, particle leaching, freeze-drying, thermal-induced phase separation (TIPS), electrospinning, and gas foaming. However, significant potential lies in additive manufacturing techniques (Arifin, Sudin, Ngadiman, & Ishak, 2022). Among the available 3D printing techniques, such as fused deposition modeling (FDM), stereolithography (SLA), selective laser sintering (SLS), and bioprinting (BP), the latter appears most suitable in terms of the raw materials used and the microenvironment for living cells formed in a 3D functional object (Zaszczyńska, Moczulska-Heljak, Gradys, & Sajkiewicz, 2021). A key concept in tissue engineering is developing cell scaffolds that act as an artificial extracellular matrix (ECM) until new tissue forms, promoting cell survival, proliferation, and differentiation (Zhang et al., 2021). Recent scientific works demonstrate that the best ECM reproduction is achievable through the combination of BP technology and the use of natural

* Corresponding author.
E-mail addresses: adrianna.banach@pg.edu.pl (A. Banach-Kopeć), szymon.mania@pg.edu.pl (S. Mania), robert1@pg.edu.pl (R. Tylingo), s172385@student.pg.edu.pl (A. Wawrzynowicz), monika.pawlowska@pg.edu.pl (M. Pawłowska), katarzyna.czerwiec@gumed.edu.pl (K. Czerwiec), milena.deptula@gumed.edu.pl (M. Deptuła), michal.pikula@gumed.edu.pl (M. Pikuła).
[1] These authors contributed equally to this paper.

https://doi.org/10.1016/j.carbpol.2024.122120
Received 24 January 2024; Received in revised form 4 March 2024; Accepted 31 March 2024
Available online 2 April 2024

polymer materials in hydrogel form (Chakrabarty, Majumder, Sharma, Prasad, & Ghosh, 2022; Gao, Li, Liu, Huang, & Zhang, 2023; Himanshu, Sandeep, Avanish, & Shilpi, 2022; Wu et al., 2022). Bioprinting is the only method allowing for the distribution of living cells directly in the bioink and their precise embedding in the matrix, maintaining the cells' vital functions and high print resolution (Unagolla & Jayasuriya, 2020). Bioprinting live cell scaffolds requires meeting many criteria. Scaffolds must be biocompatible, biodegradable, non-cytotoxic, and mechanically stable. The size of the pores and the scaffold's porosity should facilitate gas exchange and the transport of nutrients and metabolites (Tan, Ngo, Sci, Leavesley, & Liang, 2022). The process also necessitates a rapid sol-gel phase transition (SGPT) that is non-invasive for cells, converting the bioink into a 3D bioprint during the creation of successive two-dimensional layers. This transformation's induction stems from the materials used for scaffold production and the phase transition effect may arise from physical factors like temperature or pH changes or chemical factors, such as using a coupling reagent (Innocenzi, 2020).

Marine organisms provide various polymers, including CS and AG, essential for tissue engineering. Compared to mammalian sources, they offer a lower risk of transmitting infectious diseases compared to mammalian sources. This is due to the lower biological relationship between humans and marine organisms, which reduces the possibility of cross-transmission of pathogens. The use of marine-derived materials avoids potential religious and cultural restrictions associated with the use of products derived from mammals such as pigs or cattle, which may be important in the context of the global use of biomaterials (Zhang et al., 2019). Chitosan is a cationic polymer constructed from β-1,4 glycosidic bonds of D-glucosamine and *N*-acetyl-d-glucosamine, derived from chitin through the deacetylation process. Chitin's primary sources are marine invertebrates' exoskeletons, insects, and fungi cell walls. Chitosan is bioactive, biocompatible, and biodegradable, possessing anticancer and antioxidant effects (Rinaudo, 2006). Due to amino groups in its structure, it also has antimicrobial properties (Cheung, Ng, Wong, & Chan, 2015). Consequently, chitosan is insoluble in water, solutions with a pH above 7, and most organic solvents. However, in acidic solutions, chitosan's amino groups become protonated, and the molecules dissolve. This fact significantly limits chitosan's use, especially in tissue engineering, due to the acid's toxic effect on living cells, reducing the material's biocompatibility. Another disadvantage of chitosan, despite its promising properties, is its poor printability and limited mechanical properties (Sadeghianmaryan et al., 2020). Thus, it's common to combine it with other polymers, like agarose, to enhance its properties. Agarose is a polysaccharide extracted from seaweed and algae, consisting of alternating D-galactose and 3,6-anhydro-L-galactopyranose linked by α-(1 → 3) and β-(1 → 4) glycosidic bonds (Salati et al., 2020). Unlike chitosan, agarose has a low capacity for promoting cell adhesion but can gel swiftly in a narrow temperature range, optimal for most living cells without requiring cross-linking agents (Zarrintaj et al., 2018). Additionally, the gel remains mechanically stable at physiological temperatures due to phase transition hysteresis, making agarose's primary bioprinting applications its use as a support material for other bioprinting components (Gu et al., 2020).

Only two solutions exist in the literature regarding bioink production using chitosan and agarose. Gu and co-authors presented a bioink based on carboxymethyl chitosan, agarose, and sodium alginate for the proliferation and differentiation of induced pluripotent stem cells from three germ layers—endoderm, ectoderm, and mesoderm (Gu et al., 2020). Bioprinting with these polymers relies on alginate cross-linking using calcium ions in the egg-box model. Butler and co-authors proposed a thermosensitive bioink based on *N,O* carboxymethyl chitosan and agarose. Here, agarose stabilizes subsequent bioprint layers through sol-gel transformation resulting from bioink cooling (Butler, Naseri, MacDonald, Tasker, & Ahmadi, 2021). The *N,O*-carboxymethyl chitosan base's good water solubility eliminates the acid from the system, enhancing its biocompatibility. However, derivatization requires organic solvents and is time-intensive. Inadequate derivative purification might lead to cytotoxic effects. The presence of acid in the chitosan-agarose composite system is a significant limitation, as it hinders the composite's gelation, considerably prolongs its gelation time, or produces gels with weak mechanical properties. Due to these constraints, using the chitosan-agarose hydrogel composite in additive manufacturing is unfeasible, as it doesn't support the rapid formation of successive two-dimensional object layers (Graham, Marina, & Blencowe, 2019; Gu et al., 2020).

According to the research hypothesis, the use of chitosan hydrogel obtained as a result of CO_2 saturation and agarose hydrogel will enable the creation of a thermosensitive chitosan-agarose composite without the need for modification of either polymer, meeting the basic rheological and biological requirements to function as the main ingredient of bio-inks dedicated to bioprinting technology. In this approach, an unstable over time chitosan hydrogel formed by saturating carbon dioxide in an aqueous suspension containing microcrystalline sediment of this polymer, with a pH of ~6.5, is used. The concept of this idea is described in one of our previous works (Gorczyca et al., 2014). The higher pH value of materials based on chitosan devoid of acids significantly increases its application potential and removes many barriers related to the design of antimicrobial chitosan materials, which has been confirmed by our earlier works (Mania et al., 2018; Tylingo, Kempa, Banach-Kopeć, & Mania, 2022).

This publication, as the first in the scientific literature, presents a thermosensitive CSAG composite dedicated to bioprinting technology, which has antibacterial properties, does not cause a cytotoxic effect. Moreover, its production is based on the use of unmodified chitosan and agarose polymers, whose participation in the composite determines the sol-gel transition temperature. This material seems to be a universal medium for culturing many different cell lines.

2. Experimental

2.1. Materials

Chitosan (CS) with low (20–300 cps, DD ≥ 75 %, Cat. No.:102473649, LOT: BCCG5629), medium (200–800 cps, DD ≥ 75 %, Cat. No.:102466463, LOT: BCCG9377), high (800–2000 cps, DD ≥ 75 %, Cat. No.:102515456, LOT: BCCH4876) MW, chitosan isolated from crab (Cat. No.:101167160, LOT: BCBH3811V) and shrimp shells (DD ≥ 75 %, Cat. No.:1003507957, LOT: SLCP5257), and agarose (AG) with low EEO, 34.5–37.5 °C gel point, phosphate buffer saline (PBS) triptic soy agar (TSA), triptic soy broth (TSB), sodium chloride, peptone K, and glycolic acid were purchased from Merck (Germany). Sodium hydroxide was produced by Avantor Performance Materials Poland S.A (Gliwice, Poland). The carbon dioxide used to saturate the chitosan precipitate was derived from Linde Gaz Polska Sp. z o. o. (Gdańsk, Poland). For microbiological tests, the following bacterial strains were used: Gram (−) *Escherichia coli* (ATCC 25922) and Gram (+) *Staphylococcus aureus* (ATCC 29213) from the Polish Collection of Microorganisms, Ludwik Hirszfeld Institute of Immunology and Experimental Therapy of the Polish Academy of Sciences (Wrocław, Poland). Mouse fibroblast L929 cells were purchased from the American Type Culture Collection (ATCC, Manassas, VA, USA). Immortalized human keratinocyte HaCaT cells were purchased from the German Cancer Research Center (DKFZ, Heidelberg, Germany). Human skin fibroblast cell line 46BR.1 N obtained from the European Collection of Authenticated Cell Cultures (ECACC, Sigma Aldrich, St. Louis, MO, USA). The 3-(4,5-dimethylthiazol-2-yl)-2,5-diphenyltetrazolium bromide (MTT), Low-glucose Dulbecco's modified Eagle's medium (DMEM), antibiotics, and supplements necessary for cell culture were obtained from Sigma-Aldrich (St. Louis, MO, USA). Fetal bovine serum (FBS) was purchased from Biowest (Nuaille, France), MilliQ water was used for the preparation of all aqueous solutions. All other reagents were of analytical grade or higher.

The chitosans used in this work were thoroughly characterized in terms of molecular weight and degree of deacetylation in our previous

work. The table below summarizes these characteristics (Table 1).

2.2. CSAG composite bioink preparation

CS was dissolved in 0.1 M hydroxyacetic acid at a concentration of 1.5 % (w/w) with using mechanical stirrer at 200 RPM (RA 2020, Heidolph Instruments GmbH & Co. KG, Kelheim, Germany) until a homogeneous solution with no undissolved solids was obtained. To prepared CS solution, during mixing, 0.5 M solution of sodium hydroxide was added until the pH value in the range of 9–10 was reached. This was equivalent to complete precipitation of chitosan in the microcrystalline form. The precipitated chitosan was filtered with the use of vacuum filtration kit and washed several times with distilled water until the pH of the rinsing water reached a value equal 7.0. Finally, the precipitated chitosan was weighed and suspended in such an amount of distilled water to obtain a solution of 1 % (w/v) in relation to the dry matter of the polymer. The CS suspension was homogenized at 10000 RPM for 3 min (Silent Crusher M, Heidolph Instruments GmbH & Co. KG, Kelheim, Germany) and then saturated with CO_2 with simultaneously mechanical mixing using of with a hollow shaft stirrer for gas saturation (BIOMIX BMX-10, Gdańsk, Poland). Saturation and mixing were carried out until a homogeneous and transparent solution was obtained. This was a sign of complete dissolution of the CS.

A 1 % (m/m) AG solution was prepared as follows. AG was added in portions to water at 80 °C while maintaining stirring at 200 RPM (RA 2020, Heidolph Instruments GmbH & Co. KG, Kelheim, Germany) until the polymer was completely dissolved. Composites of CS and AG hydrogels were prepared by pre-cooling the hot AG solution to 45 °C and quickly combining it with the CS solution prepared according to the above description using a mechanical stirrer at 300 RPM for 2 min (BIOMIXBMX-10, Gdańsk, Poland), in this way so that the temperature of the polymer mixture does not drop below 40 °C until rheological and extrusion force measurements begin. To carry out FTIR tests and biological tests, CS, AG and their composites were frozen at −24 °C and then freeze-dried for 72 h (p = 0.94 mbar, sample temperature 20 °C, condenser temperature − 80 °C; Christ Alpha 12–4 LD Plus, Osterode am Harz, Germany).

2.3. Rheological properties

Rheological factors of the compositions affecting printability were investigated with the help of a Brookfield Viscometer (Brookfield DV-III Ultra AMETEK rheometer, Warsaw, Poland). Time and temperature of the SGPT, measurement of flow curves (FC) were investigated. SGPT was determined by measuring changes in the dynamic viscosity of the AG solution or CSAG bioinks during temperature changes in the range of 40–20 °C, at a cooling rate of 1 °C min^{-1} and at 5 rpm, on an SC4-25 spindle. The FC were determined by measuring the relationship between dynamic viscosity of AG solution or CSAG bioinks and shear rate at 37 °C. The shear rate was measured with SC4–25 spindle in the range of 0.1/s to 25.0 s^{-1}.

Table 1
Description of the tested chitosan samples, their DD and MW (n = 3, $p < 0.05$) (Mania et al., 2023). Values marked with different letters in each column differ significantly.

Seller chitosan name	DD [%]	MW [kDa]	Given symbol
Low molecular weight	75.7 ± 5.7a	89 ± 4a	LMW
Medium molecular weight	81.7 ± 4.8a	280 ± 10b	MMW
High molecular weight	78.8 ± 1.5a	591 ± 26c	HMW/H79
From shrimp shells*	66.2 ± 3.1c	545 ± 22c	HMW/H66
From crab shells*	83.2 ± 4.6b	4000 ± 142d	HMW/H83

* High molecular weight chitosan.

2.4. Extrusion force test

The extrusion force test (EFT) required to extrude the hydrogel composition were carried out on a universal testing machine (Instron model 5543 with "Merlin" V 4.42. software, Warsaw, Poland). First, extrusion tests were carried out for the 100 % AG system, in order to select from among three needles with 840, 580, 410 μm outlet diameters, the one with which further extrusion tests were carried out. For this purpose, a 60 mL syringe was filled with the appropriate ink and placed in a holder with a heating mat attached. The total volume of ink in the cartridges was 30 mL, and the incubation time at 37 °C to stabilize the temperature throughout the syringe volume was 10 min. The syringe plunger was then pushed down at a constant displacement speed of 0.25 mm/s, until all the ink was extruded from the syringe.

2.5. Antimicrobial activity

The evaluation of the antimicrobial properties of the materials was conducted according to the ASTM E2149 method with slight modifications using *E. coli* and *S. aureus* strains. Bacterial colonies were first subcultured in TSB and incubated for 24 h at 37 °C. Microbial suspensions were prepared in the test medium by adjusting the bacterial cell count to between 1.5×10^7 and 5×10^7 CFU/mL with a spectrophotometer (Merck Spectroquant Pharo 100, Germany) by measuring the absorbance at a wavelength of 600 nm (optical density between 0.08 and 0.1). To determine the antimicrobial activity of composites, 4 cm squares were cut from the test materials. The materials were sterilized under UV radiation for 30 min on each side. Subsequently, 0.4 mL of the inoculum was applied to each square. Immediately after inoculation, the materials labeled as '0 h exposure time' were transferred to 10 mL of PBS solution and shaken five times for 5 s using a vortex. Ten-fold serial dilutions and inoculations on TSA medium were performed. Plates were incubated for 24 h at 37 °C. The remaining materials labeled as '24 h exposure time' were incubated with the inoculum at 37 °C for 24 hs (Heidolph Incubator 1000, Merck Sp. z o.o., Warsaw, Poland), after which the same procedure was followed as for the '0 hs exposure time'. After incubation, bacterial colonies that grew on the Petri plates were counted. To calculate the number of cells per mL of the initial suspension, the results from the colony counts were used, with numbers ranging from 30 to 300 units, according to the equation:

$$Vc = N \times D,$$

where Vc is the bacteria concentration, in colony forming units per mL (CFU/mL), N is the average value, in colony forming units (CFU), from Petri dishes, D is the dilution factor from the plates counted. Antimicrobial activity was calculated according to the formula:

$$R = log|og \frac{B}{C},$$

where B is the average of the number of viable cells on the control sample after 24 h incubation at 37 °C (CFU/mL), C is the average of the number of viable cells on the tested sample after 24 h incubation at 37 °C (CFU/mL). A percentage reduction of bacteria/fungi on a logarithmic scale (R) equal to 1, 2, and 3 corresponds to a reduction of 90 %, 99 %, and 99.9 %, respectively.

2.6. Cytotoxicity against L929

2.6.1. Cell culture

Adult mouse fibroblast L929 cells were purchased from the American Type Culture Collection (ATCC, Manassas, VA, USA) and tested negative for mycoplasma using a Universal Mycoplasma Detection Kit (ATCC, Manassas, VA, USA). The L929 cell line was cultured in DMEM supplemented with 10 % heat-inactivated FBS, 100 μg/mL streptomycin, and 100 U/mL penicillin. Cells were incubated at 37 °C in a 5 % CO_2

atmosphere. All experiments were performed using cells in the exponential phase of growth.

2.6.2. Cell viability and morphology assessment

To estimate the in vitro cytotoxicity of the extracts, MTT assay was used, according to ISO 10993–5:2009(E). Briefly, L929 cells were seeded in 96-well plates at a density of 1×10^4 cells/well and 100 μL of culture medium (blank) was dispensed into the peripheral wells. After 24 h of incubation at 37 °C in a 5 % CO_2 atmosphere, the culture medium was removed and replaced with either fresh medium (positive control and blank) or fresh medium containing samples (1:1 v/v, 1:5 v/v, and 1:9 v/v of chitosan or agarose extract). Samples for cytotoxicity studies were prepared by suspending 0.1 g of the CS or AG xerogel in 10 mL of DMEM for 24 h at 37 °C. After this time, the liquid part of the sample (extract) was passed through a 0.22 μm filter. Following 24 h incubation, images of cells were taken using a 20× objective in an OLYMPUS I × 83 inverted microscope with an XC 50 camera and cellSens Dimension software. The culture medium was then removed, and 50 μL of the MTT solution (1 mg/mL in medium without supplements and phenol red) was added to each well and incubated for 2 h at 37 °C in a 5 % CO_2 atmosphere. Next, the MTT solution was removed, and the formazan crystals were dissolved in 100 μL isopropanol and shaken for 10 min. Absorbance was measured at 540 nm using a microplate reader (iMarkTM, Bio-Rad, Hercules, CA, USA). The results were obtained from four independent experiments ($n = 4$).

2.7. Biocompatibility analysis with XTT and LDH and live dead assays

2.7.1. Cell culture

Analysis of biocompatibility was performed with the use of human cell lines: HaCaT keratinocytes (ATCC, Manassas, VA, USA) and 46BR.1 N fibroblast (ECACC, Sigma Aldrich Co.) Cells were routinely cultured in 25 cm^2 T flask in standard conditions (5%CO_2, 37 °C) in DMEM HG medium (Sigma Aldrich) supplemented with 10 % FBS and antibiotics (100 U/mL of penicillin and 100 μg/mL streptomycin). Cells were passaged twice a week.

2.7.2. Extract preparation

The analysis was performed according to ISO 10993-5:2009 standard by the evaluation of extract activity. Extracts were prepared by incubation of xerogels (25 mg per 1 mL of culture medium) with DMEM HG culture medium for 24 h in 37 °C. After the time of incubation, the medium was collected, centrifuged (1500 rpm) and immediately used for cell stimulation. The following concentrations of extracts were used for cell stimulation: 100 % (undiluted) and 50, 25, 10 % (diluted with DMEM HG medium).

2.7.3. Cytotoxicity (LDH) and cell proliferation (XTT) assay

Lactate dehydrogenase (LDH, Roche) and XTT (Roche) tests were used to analyze cytotoxicity and the effect on cell viability respectively. Cells were seeded into 96-well plates (5000 cells per well) in DMEM HG medium with 10 % FBS and placed in standard condition for 24 h. Next, the medium was changed for extracts prepared by incubation of DMEM HG medium with xerogels. In both tests, cells cultured in DMEM HG medium constituted negative control. Cells cultured with DMEM HG supplemented with 10 % FBS and cells stimulated with 1 % TRITON X-100 (maximum cytotoxicity) were used as positive controls in XTT and LDH assay respectively. After 24 h hs of incubation, both tests were performed according to the manufacturer's instructions.

2.7.4. Live-dead assay

To investigate the efficacy of the newly developed bio-ink in maintaining cell viability, an experiment was conducted using a mixture of chitosan (1 % w/v) of medium molecular weight and agarose (1 % w/v) in a 1:1 ratio, and agarose (1 % w/v) alone as a control. These components were combined in equal proportions and incubated at 37 °C to prevent the composition from gelling. Cells, at a concentration of 1×10^6 cells/mL, were integrated with the prepared bio-ink and then applied to 24-well culture plates using a syringe, forming 3D structures. After the scaffolding gelled at temperatures below 37 °C, the wells were filled with the appropriate medium and placed in an incubator (37 °C, 5 % CO_2). To assess the cell viability in the produced structures after two days of incubation, selective staining was conducted to stain live cells green and dead cells red. After the removal of the medium, the scaffolds were cleansed with phosphate-buffered saline. Then, 3 mL of PBS solution with the addition of calcein and propidium iodide was added to each well. The incubation of scaffolds with the dyes was carried out in darkness at a constant temperature of 37 °C in a 5 % CO_2 environment for a period of 45 min. After incubation, the staining solution was removed, and observations were made using fluorescence microscopy (Nikon Eclipse TE300).

2.8. Chemical structure

FT-IR spectra of freeze-dried composite samples have been recorded using a spectrometer (Nicolet 8700; Thermo Electron Corp., Waltham, MA, USA) equipped with GoldenGate (Specac Corp., Oprington, UK) with a single-reflection diamond. The temperature of the crystal was maintained at 25.0 ± 0.1 °C during measurement. 64 scans were obtained with a resolution of 4 cm^{-1} within the wavelength range from 4000 to 550 cm^{-1}. The spectrum of each material was measured, averaged and corrected by background removal. Spectragryph *V* 1.2.10 software was used to process the obtained spectra (Oberstdorf, Germany).

2.9. 3D bioprinting

The printability of the thermosensitive CSAG bioink was verified empirically using the syringe heating system (37 °C) of the CSAG 3D bioprinter created as part of the DEC-10/2021/IDUB/I.3.3 project in Faculty of Chemistry, Gdańsk University of Technology. A detailed description can be found in supplementary materials. Subsequently, the samples were imaged using the TOP Show 3D automatic rotation system (Wroclaw, Poland).

2.10. Statistical analysis

The Prism 10 V10.0.3 (GraphPad software, Boston, MA, USA) was used for analyzing the results. The statistical significance was determined at $p < 0.05$. All data reported were based on the means of three replicates ($n = 3$) or four ($n = 4$) replicates in case of MTT tests. Experimental results were expressed as mean ± standard deviation (SD). The differences were considered to be statistically significant at $p < 0.05$. Statistical analysis of biocompatibility cell culture date was performed with one-way ANOVA ($p < 0.05$) and Mann-Whitney *U* test, ($p < 0.05$) in case of LDH and XTT tests.

3. Results and discussion

The results below present the only way to use chemically unmodified chitosan as a component of a universal cellular bioink, which can be successfully used in new research paths related to tissue regeneration (Ramiah du Toit, Choonara, Kondiah, & Pillay, 2020).

3.1. Rheological evaluation

The main components of the developed composite as a potential bioink are CS and AG, where the second component is a factor ensuring its gelation. In order to determine the share of both polymers in the composite and the type of chitosan in terms of molecular weight, rheological tests were carried out SGPT (Fig. 1A), FC (Fig. 1B) and EFT (Fig. 2).

A

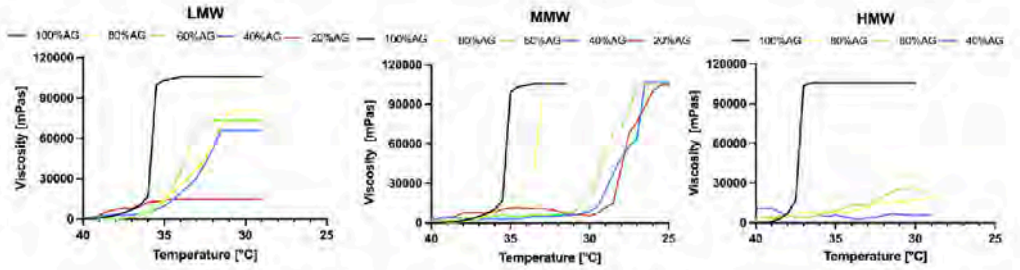

Sample	SGPT temperature range [°C]		Viscosity after SGPT [mPas]
100%AG	36.0	36.5	105557 ± 467
80%AG	31.5	36.5	80249 ± 76
60%AG	33.7	36.5	73136 ± 65
40%AG	32.6	36.7	65746 ± 72
20%AG	-	-	15068 ± 58

Sample	SGPT temperature range [°C]		Viscosity after SGPT [mPas]
100%AG	36.0	36.5	105557 ± 467
80%AG	33.1	36.5	105557 ± 289
60%AG	27.5	31.5	105602 ± 355
40%AG	27.0	30.5	105598 ± 402
20%AG	26.5	30.5	105623 ± 381

Sample	SGPT temperature range [°C]		Viscosity after SGPT [mPas]
100%AG	36.0	36.5	105557 ± 467
80%AG	-	-	19131 ± 87
60%AG	-	-	22459 ± 122
40%AG	-	-	5374 ± 140
20%AG	-	-	-

B

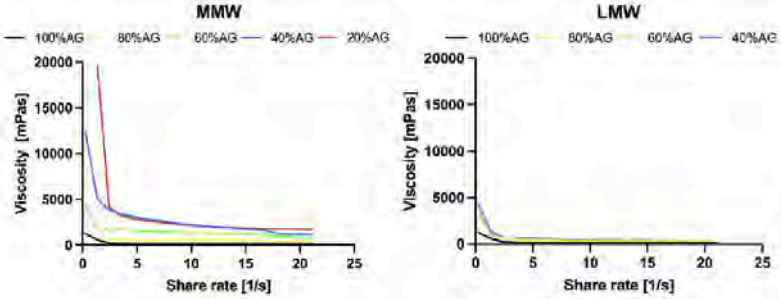

Fig. 1. Rheological properties of CSAG composition for chitosans of different molecular weights: low (LMW), medium (MMW), and high (HMW). (A) The rheological characteristic of the sol-gel phase transition and (B) flow curves of the CSAG composites (n 3, $p < 0.05$).

Fig. 1 shows the results of the measurement of the sol-gel phase transition characteristics of hydrogels differing in the share of chitosan and agarose, which was performed for chitosan with low (LMW), medium (MMW), and high molecular weight (HMW). A clear influence of chitosan on the phase transition of the CSAG composite can be observed. SGPT for agarose begins at 36.5 °C and occurs the fastest - the lowest slope of the curve and the sharpest increase in viscosity caused by gelation of this polymer. Composites based on AG and LMW CS begin to gel at the same temperature as pure agarose, but the temperature range of their phase transition is much wider than for pure agarose (from 3 to 5 °C). The intrinsic viscosity of the sol measured before complete gelation decreased with the increase in the proportion of LMW CS in composite (Fig. 1A). For the HMW CSAG composite, no sharp phase transition was recorded, but only a slight increase in the viscosity during measurements for samples containing from 20 % to 60 % of CS hydrogel. It was impossible to perform measurements for the HMW CSAG composite marked as 20%AG. The most predictable SGPT characteristics were obtained from AG and CS of medium molecular weight. In this system, the increase in the share of chitosan in the composite did not affect the value of the intrinsic viscosity before gelation of the composite and caused a decrease in the temperature range in which it occurred.

Huang et al. (2018) in their studies of the phase transition temperature of two-component hydrogels prepared using CS and AG in the presence of 1 % citric acid demonstrated the same relationships. Compared to pure AG (0.5 °C), the gelation temperature of MMW CS based composites was in the range of 3.4–4 °C (Fig. 1A.). The gelation process during the cooling of pure agarose samples contains two major steps. The first is the formation of double helices upon cooling. So called "hardening step" at around 45 °C is assigned to the formation of "cross-links", i.e., the helices. Further hardening in the temperature range around 30 °C is likely to correspond to the aggregation of several helices (Norddqvist & Vilgis, 2011). The decrease in the viscosity of the sol before complete gelation with an increase in CS molecular weight suggests that LMW CS may interfere with the formation of agarose helices, leading to a more gradual and extended gelation process. In the case of HMW CS, the larger CS molecules interfere more significantly with the AG network formation, possibly by steric hindrance or by forming less efficient cross-links with AG. This effect disrupts the typical two-step gelation process of AG, leading to a less defined phase transition. In turn, MMW CS may facilitate more ordered or efficient packing of agarose molecules into helices and their subsequent aggregation and shift this process towards lower temperatures.

Due to the fact that HMW CSAG composites do not show a sharp SGPT, LMW and MMW CSs were used for further investigations (Figs. 1B, 2). Fig. 1B shows the viscosity of CSAG composites decreases exponentially with the increase in the shear rate, showing that in all

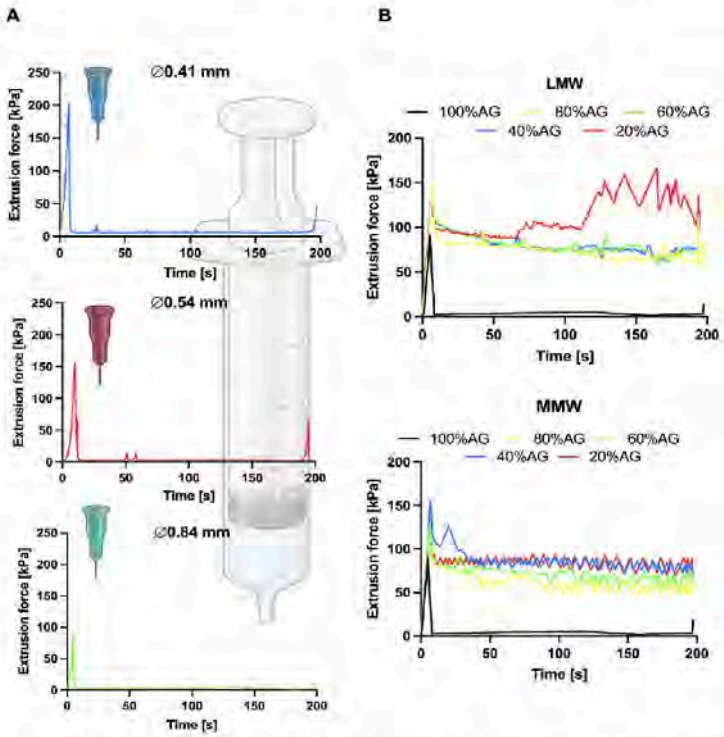

Fig. 2. The result of extrusion force test for (A) 1 % AG solution and (B) CSAG composites at 37 °C (n = 3, $p < 0.05$).

cases the fluids are pseudoplastic. The shear thinning effect of the CSAG composites is identical to that of CS hydrogels alone, i.e., both CSs (LMW and MMW) in the composites show shear thinning, but the degree of viscosity reduction under shear stress is less pronounced for low molecular weight chitosan than for the MMW variant. It also decreases with increasing agarose content in the CSAG composites. The explanation for this behavior is given in terms of the destruction of polymeric entanglement with consequent alignment of the chains in the direction of the shear flow (do Amaral Sobral et al., 2022). For all tested systems, it is possible to quickly achieve a steady flow of the potential bioink. A clear decrease in viscosity is observed after exceeding a shear rate of 3 1/s. The low shear rate will ensure easier flow control during printing and high cell viability, as the action of shear forces leads to cell disintegration (Smith & Doe, 2022).

The charts in Fig. 2 present the relationships of the extrusion force of polymeric hydrogels as a function of time. Section A pertains to the comparison of the extrusion curve for a 1 % AG solution at 37 °C, from a syringe ending in needles of 3 different diameters.

All charts are characterized by an initial rapid increase in the extrusion force necessary for thinning the system and initiating flow, which is typical for pseudoplastic fluids (Doe & Smith, 2021). After reaching the maximum value, the extrusion force drops sharply and stabilizes, suggesting that the material flows more easily through the nozzle after overcoming the initial resistance. The peak height decreases with the increase in needle diameter. The curves around 200 s of the test are ended by a sudden increase in force related to the moment the syringe plunger contacts its bottom. The most stable flow was observed for a diameter of 0.84 mm, in which the curve did not show any deviations during the test (Fig. 2A). The fluctuation of the extrusion force can indicate the presence of aggregates by a positive peak, whereas on the other hand, air introduced during the cartridge filling procedure is indicated by a negative peak in the extrusion force (Miller et al., 2019). In the case of AG and CSAG composites, fluctuations may also indicate the commencement of a phase transition if the measurement is conducted at a temperature close to that transition. For AG, regardless of the needle diameter, no negative peaks were registered, which means that the solution was not aerated during production (Fig. 2A). Section B presents the results for CSAG composites obtained based on LMW and MMW CSs (Fig. 2B). It is evident that the extrusion force decreases with an increasing proportion of AG in the composite for both types of chitosan with the studied molecular weights. This suggests that AG can be extruded with less force than CS. This statement is valid because the chitosan hydrogel itself in carbonic acid is unstable over time and will always show positive and negative fluctuations, associated with the escape of carbon dioxide from the gel trapped in excess and the formation of polymer aggregates near the phase transition. LMW CSAG composites show greater fluctuations in extrusion force, which may indicate less uniform material flow through the nozzle compared to MMW CSAG composites, which have a more uniform and stable extrusion force profile, considered in this work as optimal, taking into account the specifics of the designed bioink (Fig. 2B).

3.2. Biological properties

3.2.1. Antimicrobial activity

To evaluate the antimicrobial activity of materials based on CS, AG, and their composites, ASTM Method E2149 was employed with minor modifications suitable for water-insoluble samples. Fig. 3 illustrates the

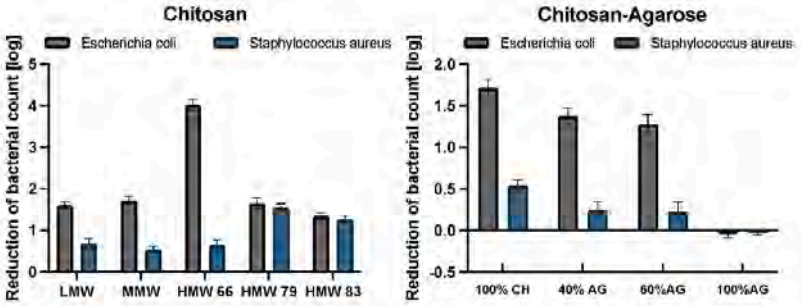

Fig. 3. The antimicrobial activity against *E. coli* and *S. aureus* for (A) CS materials with different MW and DD and (B) CSAG composites according to Standard ASTM: E2149.

antimicrobial activity, expressed as a logarithmic reduction degree after 24 h of interaction between the *Staphylococcus aureus* and *Escherichia coli* inoculum and the materials tested.

The initial phase of the study involved analyzing the impact of CS molecular weight on its antimicrobial effectiveness. This stage aimed to select a potential base material for subsequent investigations into the antimicrobial properties of CSAG composites. Our previous research indicated that CS molecular weight significantly influences its capability to suppress microbial growth (Mania et al., 2023). However, we highlighted that the activity observed might be attributable to sodium hydroxyacetate residues, which notably hinder microbial growth. To confirm these findings, the current study replicated the research with certain modifications. The CS precipitate, acquired through precipitation, underwent a rinse to stable pH of washing water rather than a threefold rinse to potentially remove any sodium hydroxyacetate residues.

The results presented in Fig. 3 reveal globally the higher antimicrobial activity of CSs against Gram-negative than Gram-positive bacteria. The reduction degree for CSs differing the molecular mass (LMW, MMW, and HMW79 with similar DD) is comparably about 1.61–1.72 log against Gram-negative bacteria, and 0.64, 0.59, and 1.55 log reduction for Gram-positive, respectively. In our previous work, we also failed to find a strict relationship between the antimicrobial activity of CSs and their DD (Mania et al., 2023). However, the results in Fig. 3A indicate a trend of decreasing antimicrobial activity with an increasing degree of deacetylation against *E. coli* bacteria. No such trend was observed in the case of *S. aureus*. In the same section, the HMW63 sample is characteristic, demonstrating bactericidal action against *E. coli* and bacteriostatic effect towards *S. aureus*, as a result of the effect of coating bacterial cells with HMW CS, particularly efficient between the cationic polymer and the negatively charged components of the Gram-negative bacterial cell membrane, as well as the chelation mechanism of ions that are part of the cell membranes. According to the literature, this mechanism occurs more frequently at pH > 6.5, due to the ability of the deprotonated amino group to donate a free pair of nitrogen. At pH values of 7–9, the chelation of metal ions occurs both through amino groups and two deprotonated hydroxyl groups, forming a more stable complex than two NH_2 receptor groups at lower pH (Goy, Britto, & Assis, 2009, Mania et al., 2023). The results prove that the degree of purification of CS from the residual salts formed during its precipitation in the procedure is of great importance. There is no strict relationship between the effect of molecular weight and antimicrobial activity, which may result from the existence of several competing mechanisms of this activity, the effect of which results from the method of preparing the chitosan material and the environment in which this material was placed. In most cases, the effect of pure chitosan can be described as bacteriostatic.

These findings and rheological results led to the selection of MMW CS for further study on CSAG composite activity due to its consistent reduction effect on bacteria. Composite analysis indicated that increasing AG content in the samples correlates with diminished antimicrobial action against both bacterial strains. The CS-based materials exhibited cell reduction rates for *E. coli* and *S. aureus* of 1.72 and 0.54 (98.24 % and 70.71 %), respectively, on a logarithmic scale. At 60 % agarose content, the activity reduced to 1.28 and 0.23 log, equating to 95.88 % and 45.44 %, respectively. Furthermore, it was verified that xerogel materials composed solely of agarose lacked antimicrobial activity (Fig. 3B). The observed decline in activity with increasing agarose is attributed to the diminished chitosan concentration in the final product, the sole polymer with the inherent ability to inhibit both Gram-negative and Gram-positive bacteria in this study.

3.2.2. Biological safety

The biological safety of raw materials/biomaterials used in bioprinting is an entry criterion that permits their application in tissue engineering. In the evaluation of medical devices such as implants and other medical or pharmaceutical products, standardized tests for biological safety assessment are employed to capture the entire complexity of the human body. In accordance with the ISO 10993 standard "Biological evaluation of medical devices," a series of recommendations, parameters, and conditions for conducting the test ISO 10993-5:2009 are described, in which the recommended cell line for cell viability studies is the mouse fibroblasts L929 (Jablonská, Rubášek, Vojtěch, Ruml, & Lipov, 2021).

3.2.2.1. MTT assay. Fig. 4A indicates that CS of various molecular weights and DD, as well as AG at each dilution, i.e., 1:1 v/v, 1:5 v/v, and 1:9 v/v, do not exhibit a cytotoxic effect on L929 cells. The only significant difference was registered for the sample of high molecular weight chitosan with a DD of 83 %, for which the lowest survival rate was obtained, namely 80 % relative to the control.

HMW83 was characterized by an approximately 7-fold higher molecular weight than the other two high molecular weight chitosans, so such an effect may result from, among other things, different aggregation of the polymer chain, more difficult washing out of hydroxyacetate residues due to the high viscosity of the solution and the nature of the formation of the microcrystalline CS precipitate during its precipitation from the solution (Gorczyca et al., 2014).

These results confirm our earlier hypothesis, as well as the fact that the degree of washing out of the CS precipitate significantly affects the cytotoxicity of the biomaterial, which results from the residues of sodium salts of hydroxyacetic acid (Mania et al., 2013). Control untreated L929 cells and treated with agarose and chitosan extracts resembled the typical morphology (Fig. 4B). Cells exhibited heterogeneous shapes, including: spindle-like, epithelial-like, stellate, and rounded. Some of the cells were bigger and flattened. The morphology of the L929 cells did not change upon treatment with CS and AG extracts. They also did not

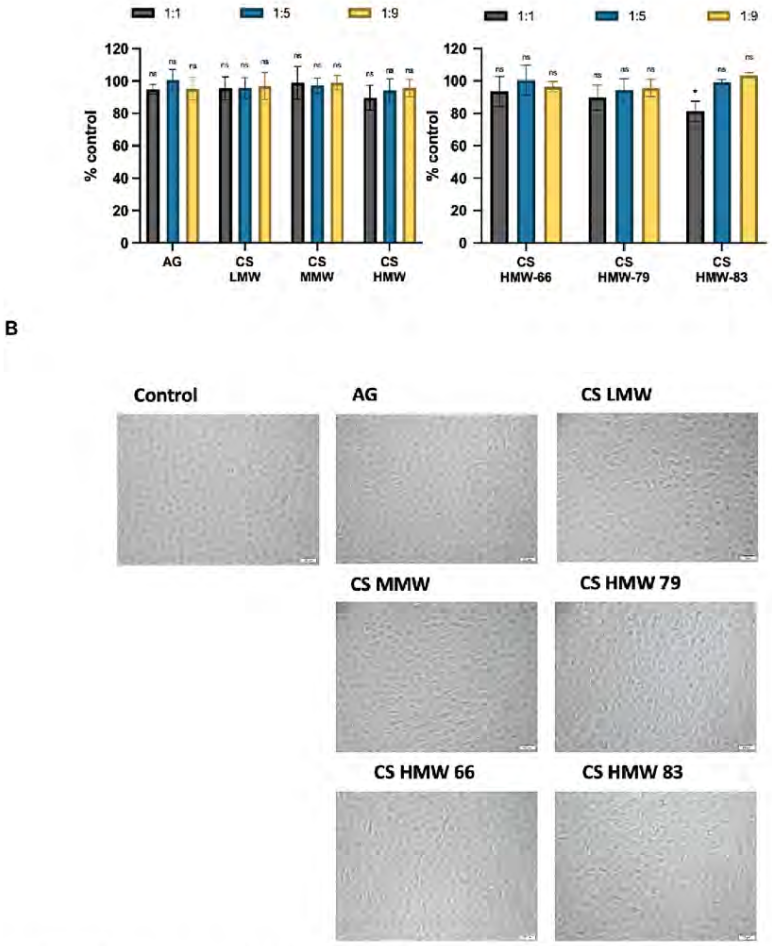

Fig. 4. (A) The cytotoxicity of CS of different molecular weights and AG and (B) CS of different deacetylation degree: 66, 79 and 83 following 24 h incubation against L929 cells. Data are expressed as the mean ± standard deviation of four independent experiments. The results were analyzed by one-way ANOVA with comparisons vs. control: ns (not statistically significant, $p > 0.05$), *$p < 0.05$. B) Representative images (n 4) of the morphology of L929 cells treated with agarose and chitosan extracts dissolved in cell medium. Pictures were taken after 24 h treatment of cells with agarose and chitosan extracts at diluent factor 1:1. Scale bar is 50 μm, magnification 200×.

affect the proliferation of cells. In presented images it is easy to recognize cells undergoing mitosis – they are rounded and more convex, and some of them are still closely situated to each other. In summary, the CS extracts are not harmful to L929 cells. More photos of all dilutions are available in Supplementary materials.

The obtained results are also consistent with our earlier studies, which examined how the developed method for removing endotoxins from chitosan affects the cytotoxicity of its solution. At a 1:1 *v/v* dilution, the survival relative to the control was about 80 % for uncleaned CS of MMW (Banach-Kopeć et al., 2022). In summary, the survival of L929 cells after 24-h contact with CS material obtained by the innovative carbon dioxide saturation method is at least 2.5 times greater, approximately 50 % compared to the control, than in the case of chitosan obtained by dissolving it in 0.1 M lactic acid (Mania et al., 2023). In accordance with ISO standard 10,993–5:2009(E), both materials, i.e., chitosan and agarose, are not cytotoxic and can be safely used in tissue engineering.

3.2.2.2. XTT/LDH assays. Results presented in Fig. 5 confirmed the overall safety and biocompatibility of the analyzed materials. The LDH analysis indicated that CS, AG and CSAG composite did not elicit a cytotoxic effect on human skin cells (HaCaT keratinocytes and 46BR.1 N fibroblasts). In the XTT assay, only the highest concentration (100 %) of AG and CS extracts slightly reduced cell viability (<10 %) in HaCaT keratinocytes. Interestingly, for 46BR.1 N fibroblasts, a significant increase in cell viability was observed. The most pronounced effect (>30 % compared to the control) was noted for CS at 10 % and 25 % concentrations. AG enhanced cell viability by approximately 20 % across all tested concentrations. For CSAG, a 25 % increase in cell viability was observed at a 25 % extract concentration, while all other tested concentrations resulted in a 20 % increase in cell viability.

The absence of cytotoxic effects from agarose-based scaffolds was

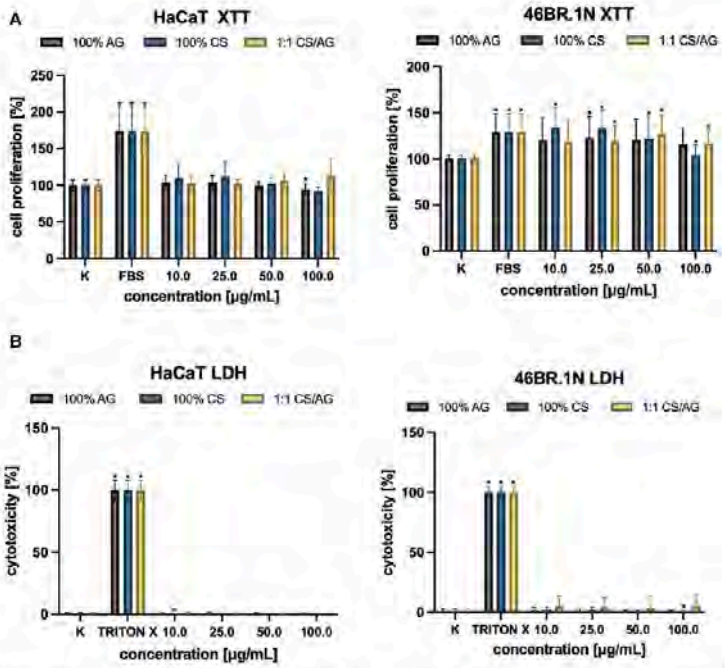

Fig. 5. Effect of CS, AG and CSAG on human skin cells after 48 h of incubation. (A) Xerogels effect on proliferation of HaCaT keratinocytes and 46BR.1 N fibroblasts. (B) Cytotoxicity of the scaffolds towards HaCaT keratinocytes and 46BR.1 N fibroblasts. The graphs show results from three independent experiments. Results are presented as mean with SEM. * - statistically significant differences compared to control, Mann-Whitney *U* test, $p < 0.05$.

also corroborated in the study by Witzler group, where MTT assays on MG-63 osteosarcoma cell lines and Lw35 primary hMSCs revealed no toxic effects of AG (Witzler et al., 2019). However, more extensive research on the biocompatible effects on skin cells has been conducted for chitosan. Indeed, this polymer and its derivatives are crucial in the first three stages of wound healing, notably in promoting the growth of granulation tissue, which consists of inflammatory cells, capillaries, and fibroblasts. The effectiveness varies with the degree of deacetylation and molecular weight, with those possessing a high degree of deacetylation and low molecular weight exhibiting the most beneficial properties. Moreover, fibroblasts can be categorized into two phenotypes: chitosan-responsive and chitosan-non-responsive, which are not influenced by the donor's sex, age, or anatomical site. As for keratinocyte cells, the polymer's effect on their proliferation can be either inhibitory or non-inhibitory, depending on the degree of deacetylation; an increase in deacetylation tends to exhibit an inhibitory effect (Howling et al., 2001). In summary, this study supports our previous assumptions that highly biocompatible materials such as chitosan and agarose can lead to the development of biologically safe biomaterials with potential applications in wound healing, including for burn injuries.

3.2.2.3. Live-dead assay. For an in-depth exploration of the biological safety of the investigated system, additional studies on the viability of HaCaT and 46BR.1 N cell lines were conducted upon integrating them with the bioink base, specifically the CSAG composition at 1:1 mass ratio and 100 % AG serving as the control. The primary objective was to validate the non-cytotoxic nature of the CSAG setup, a finding previously corroborated through research that assessed how extracts from the polymers under investigation affect cytotoxicity and cell proliferation. In this method, the effects of the hydrogel bioink base and thus the hydrogel scaffold on cells after extrusion and after a 48-h incubation period were analyzed. After staining, cell viability was found to remain significantly high in all samples assessed, exceeding 80 % for the 100 % AG formulation and above 90 % for the CS/AG composition (Fig. 6).

This high rate of survival underlines a positive interaction between the studied cells and the bio-ink base, thus confirming the absence of cytotoxic effects. A further step in research to optimise the use of a bio-ink base in cell culture will be to determine how cells proliferate, migrate and survive in the long term. However, achieving this will depend on several variables, such as scaffold porosity, nutrient access and thus scaffold size and geometry. These will be key aspects that will be investigated in the next phase of the research to further understand the interactions between the bio-inks tested and the cells in the context of their biomedical applications.

3.3. Chemical structure

The infrared spectroscopy was used to identify individual chemical groups in pure CS and AG as well as to register structural changes in composites of both polymers (Fig. 7). The CS spectrum shows the labels of the characteristic bands for chitosan. Intense signals at wavelengths of 1151 cm^{-1}, 1064 cm^{-1},1028 cm^{-1} and 898 cm^{-1} indicate the presence of a saccharide structure. Another characteristic bands at 3356 cm^{-1} and 3290 cm^{-1} are the signals coming from the hydroxyl group of the chitosan molecule. A series of signals at 1586 cm^{-1}, 1467 cm^{-1}, 1373 cm^{-1}, and 1317 cm^{-1} correspond to amides I, II and III. The remaining marked signal come from groups $-CH_2-$ (Mania et al., 2018; Staroszczyk, Sztuka, Wolska, Wojtasz-Pajak, & Kołodziejska, 2014). The FTIR spectrum of AG shows a wide band at 3362 cm^{-1}, which is attributed to the stretching vibrations of the -OH groups. The band at 2899 cm^{-1} corresponds to the symmetrical vibrations of the C—H groups. The vibrations at wave numbers 1637 cm^{-1} and 1370 cm^{-1} are bending vibrations -OH and

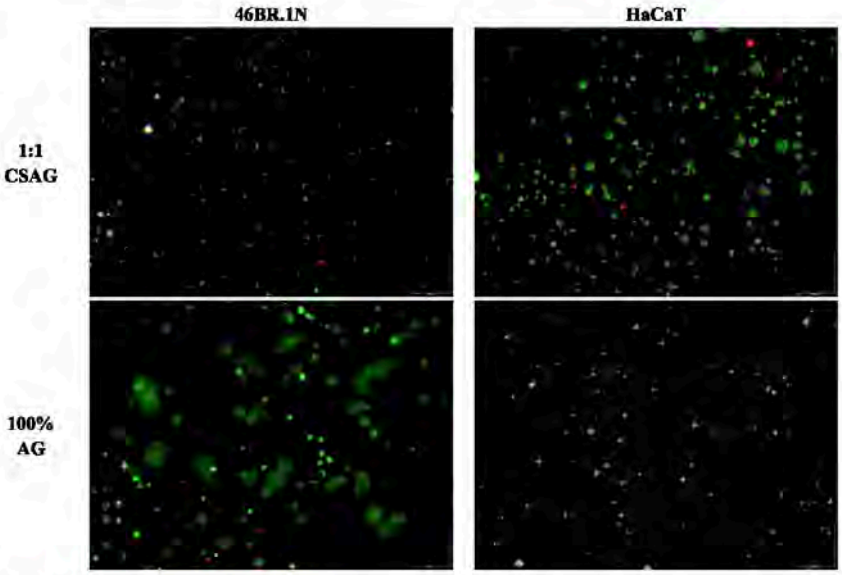

Fig. 6. Viability of 46BR.1 N fibroblasts and HaCaT keratinocytes embedded in CSAG composite and in AG alone. This figure presents fluorescent microscope images showing live-dead staining of cells in the scaffolds at day 2 of cultivation. Viable cells are stained green with calcein, while dead cells are stained red with propidium iodide; the scale bar 250 μm.

C—C, respectively.

The most intense band can be seen at 1039 cm $^{-1}$. This band is assigned to deformation vibrations of C—O groups in saccharide molecules. The peak at 890 cm $^{-1}$ is attributed to the C—H angular strain of the anomeric carbon of β-galactose and about 930 cm $^{-1}$ to 3,6-anhydrogalactose (Gómez-Mascaraque, Méndez, Fernández-Gutiérrez, Vázquez, & San Román, 2014; Sivashankari & Prabaharan, 2020). The nature of the interactions between CS and AG in their composite containing the same mass fraction of both polymers was also examined. The characteristic peaks were detected as in the spectra of individual components of this composite. The intensity of individual bands is the value resulting from mixing both components in equal proportion. According to literature, some bands of CSAG composite can be shifted against the bands of pure components. This mainly concerns the shift of the chitosan amide II band towards longer wavenumbers, which may be caused by the formation of intermolecular hydrogen bonds between chitosan amino groups and agarose hydroxyl groups (Sivashankari & Prabaharan, 2020; Zamora-Mora, Velasco, Hernández, Mijangos, & Kumacheva, 2014). The spectrum of the composite shows that despite the cationic nature of chitosan and the anionic nature of agarose, mixing their hydrogels allowed to obtain a physical mixture of polymers with very weak hydrogen interactions in the form of physical mixture. The FTIR measurement results also confirm that the presence of agarose in the CSAG composite does not significantly impair its antimicrobial properties resulting from the presence of chitosan due to the presence of weak hydrogen bonds between these polymers. The decrease in the antimicrobial activity of the composite with increasing agarose content is primarily due to the reduced chitosan concentration in the final composite. The hydrogen bonds between chitosan and agarose are insufficiently strong to block the interaction of chitosan with the membranes of both Gram-positive and Gram-negative bacteria.

3.4. 3D bioprinting

In Fig. 8, an attempt to create a 3-layer print in the form of a lattice structure is depicted. The print attempt using chitosan hydrogel was unsuccessful due to the lack of a phase transition in the temperature range defined in rheological studies (Fig. 1A).

Already a 20 % inclusion of AG hydrogel in the bioink was sufficient for successful application of subsequent layers. The increase in agarose content in the bioink was not significant in visual assessment. Only for samples containing at least 80 % agarose hydrogel does the granularity of the print become visible, which may be due to the narrow temperature range of AG phase transition and the beginning of its gelling during flow in the conducted empirical test. However, the same test confirms the possibility of using the proposed CSAG bioink in 3D bioprinting technology.

4. Conclusion

This study successfully develops a printable, thermosensitive bioink composed of medium molecular weight chitosan hydrogel obtained by CO_2 saturation method and agarose hydrogel as a fast-gelling agent. The bioink exhibits pseudoplastic behavior and a favorable sol-gel phase transition temperature, ideal for bioprinting applications. Its antimicrobial properties, demonstrated through significant reduction in *E. coli* and *S. aureus* populations, coupled with its non-cytotoxic nature to various cell lines, establish its potential in advanced spatial cell cultures and tissue engineering. This is the first publication that presents a change in the antimicrobial activity of processed chitosan and, at the same time, free from any acid residues necessary for its dissolution, which is of great importance in the design of new solutions based on this polymer. The research notably advances the field by presenting a novel, safe, and efficient bioink, suitable for creating complex structures in tissue engineering, particularly for skin regeneration. This bioink's characteristics open new avenues for 3D bioprinting technologies, emphasizing the importance of material selection and composition in developing future biomedical applications.

In the context of further perspectives, our research on CSAG bioink in tissue engineering will continue to deeply understand the gelation

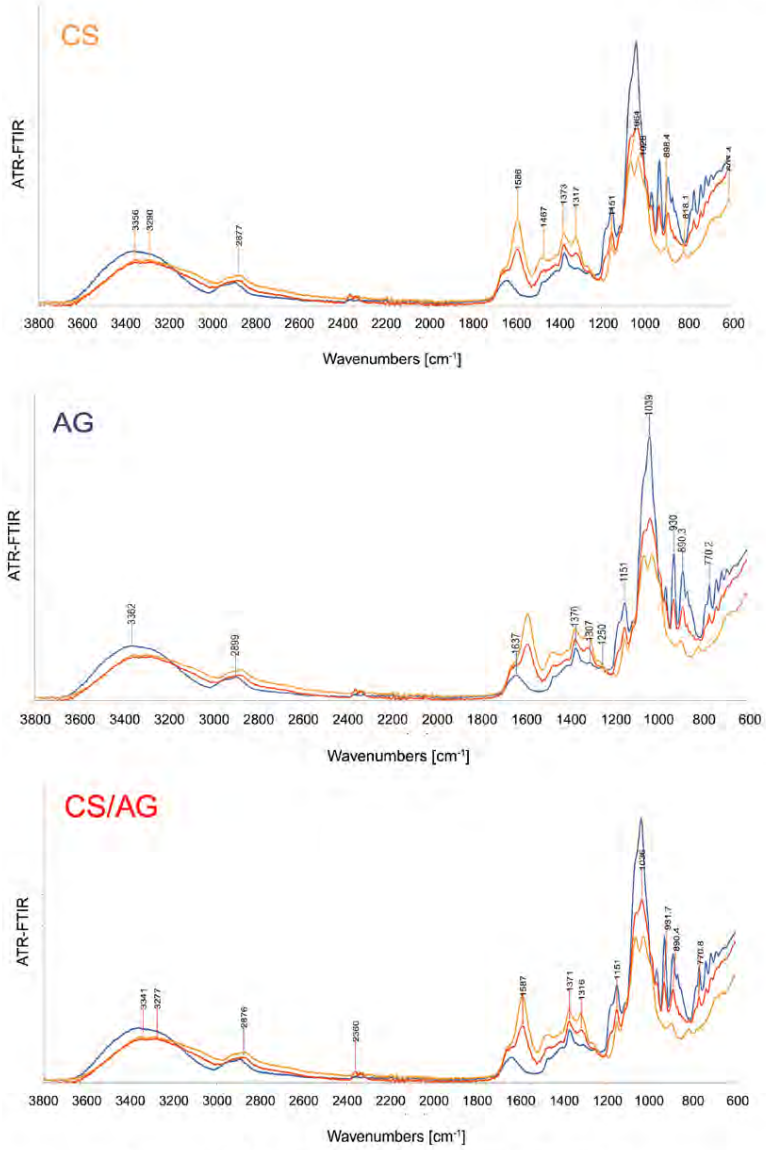

Fig. 7. The ATR-FTIR spectra with labeled signals for CS, AG, and CSAG.

mechanism of agarose in the presence of chitosan. It is necessary to confirm the hypothesis that chitosan contributes to the formation of a more ordered agarose gel structure, which may delay the gelation process and thereby lower the gelation temperature. Additionally, we plan to expand the research to evaluate the applicability of the discussed bioink base in cell cultures by determining the impact of key parameters on both the survivability and printability of the bioink. The next stage will involve advanced studies, both in vivo and in vitro, aimed at a detailed understanding of the interactions between the bioink components and living cells, and their impact on regenerative processes in tissues. Such a comprehensive research program will enable the optimization of the bio-ink composition, which is crucial for its future clinical and industrial applications, ensuring safety and efficacy in creating functional tissue structures.

Funding

Financial support of these studies from Gdańsk University of Technology by the DEC-10/2021/IDUB/I.3.3 grant under the Argentum Triggering Research Grants - 'Excellence Initiative - Research

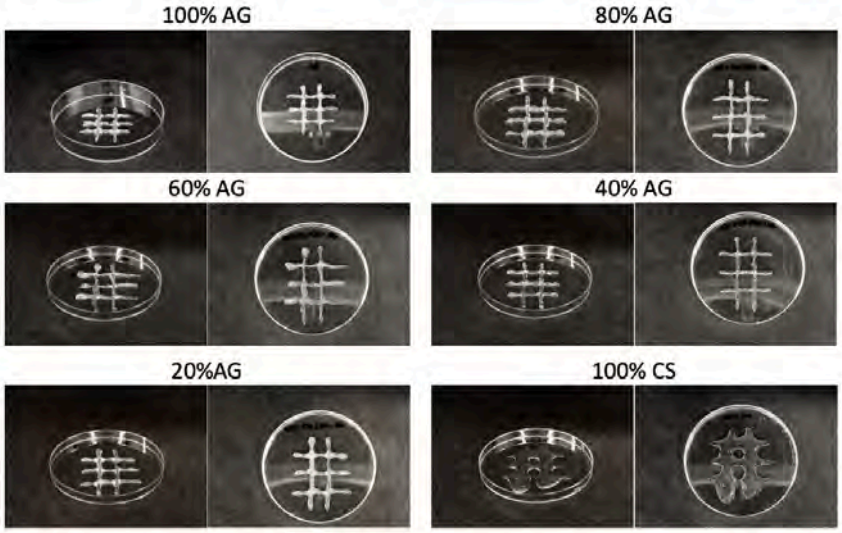

Fig. 8. Results of three-layer 3D prints using CS, AG, and CSAG.

University' program is gratefully acknowledged.

CRediT authorship contribution statement

Adrianna Banach-Kopeć: Writing – review & editing, Writing – original draft, Visualization, Validation, Software, Resources, Methodology, Investigation, Formal analysis, Data curation, Conceptualization. **Szymon Mania:** Project administration, Methodology, Investigation, Funding acquisition, Formal analysis, Data curation, Conceptualization, Resources, Software, Supervision, Validation, Visualization, Writing – original draft, Writing – review & editing. **Robert Tylingo:** Writing – review & editing, Writing – original draft, Validation, Supervision, Software, Methodology, Investigation, Formal analysis, Data curation. **Agata Wawrzynowicz:** Investigation, Data curation. **Monika Pawłowska:** Writing – review & editing, Writing – original draft, Visualization, Validation, Software, Resources, Methodology, Investigation, Data curation. **Katarzyna Czerwiec:** Methodology, Investigation, Data curation, Resources, Software, Validation, Visualization, Writing – original draft, Writing – review & editing. **Milena Deptuła:** Data curation, Investigation, Methodology, Resources, Software, Supervision, Validation, Visualization, Writing – original draft, Writing – review & editing. **Michał Pikuła:** Data curation, Investigation, Methodology, Software, Supervision, Validation, Writing – original draft, Writing – review & editing.

Declaration of competing interest

The authors declare the following financial interests/personal relationships which may be considered as potential competing interests: Szymon Mania reports financial support was provided by Gdansk University of Technology. If there are other authors, they declare that they have no known competing financial interests or personal relationships that could have appeared to influence the work reported in this paper.

Data availability

Data will be made available on request.

Appendix A. Supplementary data

Supplementary data to this article can be found online at https://doi.org/10.1016/j.carbpol.2024.122120.

References

Arifin, M., Sudin, I., Ngadiman, N. H. A., & Ishak, M. S. A. (2022). A comprehensive review of biopolymer fabrication in additive manufacturing processing for 3D-tissue-engineering scaffolds. *Polymers, 14*(10), 2119.

Banach-Kopeć, A., Mania, S., Pilch, J., Augustin, E., Gabriel, I., & Tylingo, R. (2022). A novel method of endotoxins removal from chitosan hydrogel as a potential bioink component obtained by CO2 saturation. *International Journal of Molecular Sciences, 23*, 5505.

Butler, H. M., Naseri, E., MacDonald, D. S., Tasker, R. A., & Ahmadi, A. (2021). Investigation of rheology, printability, and biocompatibility of N,O-carboxymethyl chitosan and agarose bioinks for 3D bioprinting of neuron cells. *Materialia, 18*.

Chakraborty, J., Majumder, H., Sharma, A., Prasad, S., & Ghosh, S. (2022). 3D bioprinted silk-reinforced alginate-gellan gum constructs for cartilage regeneration. *Bioprinting, 28*.

Cheung, R. C. F., Ng, T. B., Wong, J. H., & Chan, W. Y. (2015). Chitosan: An update on potential biomedical and pharmaceutical applications. *Marine Drugs, 13*(8), 5156–5186.

do Amaral Sobral, P. J., Gebremariam, G., Drudi, F., De Aguiar Saldanha Pinheiro, A. C., Romani, S., Rocculi, P., & Dalla Rosa, M. (2022). Rheological and viscoelastic properties of chitosan solutions prepared with different chitosan or acetic acid concentrations. *Foods, 11*(17), 2692.

Doe, J., & Smith, A. (2021). Rheological properties of chitosan and its applications as a pseudoplastic fluid in biomedical engineering: A review. *International Journal of Biological Macromolecules, 165*(Part B), 2185–2197.

Gao, C., Li, Y., Liu, X., Huang, J., & Zhang, Z. (2023). 3D bioprinted conductive spinal cord biomimetic scaffolds for promoting neuronal differentiation of neural stem cells and repairing of spinal cord injury. *Chemical Engineering Journal, 451*.

Gómez-Mascaraque, L. G., Méndez, J. A., Fernández Gutiérrez, M., Vázquez, B., & San Román, J. (2014). Oxidized dextrins as alternative ecosinking agents for polysaccharides: Application to hydrogels of agarose-chitosan. *Acta Biomaterialia, 10*(2), 798–811.

Gorczyca, G., Tylingo, R., Szweda, P., Augustin, E., Sadowska, M., & Milewski, S. (2014). Preparation and characterization of genipin ecoss-linked porous chitosan–collagen–gelatin scaffolds using chitosan–CO2 solution. *Carbohydrate Polymers, 102*(15), 901–911.

Goy, R. C., Britto, D., & Assis, O. B. G. (2009). A review of the antimicrobial activity of chitosan. *Polímeros: Ciência e Tecnologia, 19*(3), 241–247.

Graham, S., Marina, P. F., & Blencowe, A. (2019). Thermoresponsive polysaccharides and their thermoreversible physical hydrogel networks. *Carbohydrate Polymers, 207*, 143–159.

Gu, Y., Schwarz, B., Forget, A., Barbero, A., Martin, I., & Prasad Shastri, V. (2020). Advanced bioink for 3D bioprinting of complex free-standing structures with high stiffness. *Bioengineering, 7*(4), 1–15.

Himanshu, T., Sandeep, S. M., Avanish, S. P., & Shilpi, C. (2022). Hydrogel based 3D printing: Bio ink for tissue engineering. *Journal of Molecular Liquids, 367*, Article 120390.

Howling, G. I., Dettmar, P. W., Goddard, P. A., Hampson, F. C., Dornish, M., & Wood, E. J. (2001). The effect of chitin and chitosan on the proliferation of human skin fibroblasts and keratinocytes in vitro. *Biomaterials, 22*(22), 2959–2966.

Huang, D.-Y., Zhang, Y., Liu, H., Wu, J.-J., Pan, L.-H., Wu, Y., … Tu, T. (2018). Preparation of chitosan/agarose two-component hydrogels and its water holding and sustained release properties. *Modern Food Science and Technology, 34*(11), 145–150.

Innocenzi, P. (2020). Understanding sol–gel transition through a picture: A short tutorial. *Journal of Sol-Gel Science and Technology, 94*, 544–550.

Jablonska, E., Kubásek, J., Vojtěch, D., Ruml, T., & Lipov, J. (2021). Test conditions can significantly affect the results of in vitro cytotoxicity testing of degradable metallic biomaterials. *Scientific Reports, 11*(1), 6628.

Mandrycky, C., Phong, K., & Zheng, Y. (2017). Tissue engineering toward organ-specific regeneration and disease modeling. *MRS Communications, 7*(3), 332–347.

Mania, S., Banach-Kopeć, A., Staszczyk, K., Kulesza, J., Augustin, E., & Tylingo, R. (2023). An influence of molecular weight, deacetylation degree of chitosan xerogels on their antimicrobial activity and cytotoxicity. Comparison of chitosan materials obtained using lactic acid and CO2 saturation. *Carbohydrate Research, 534*, Article 108973.

Mania, S., Tylingo, R., Augustin, E., Guewa, K. M., Szwacki, J., & Staroszczyk, H. (2018). Investigation of an elutable N-propylphosphonic acid chitosan derivative composition with a chitosan matrix prepared from carbonic acid solution. *Carbohydrate Polymers, 179*, 196–206.

Müller, M., Fisch, P., Molnar, M., Eggert, S., Binelli, M., Maniura-Weber, K., & Zenobi-Wong, M. (2019). Development and thorough characterization of the processing steps of an ink for 3D printing for bone tissue engineering. *Materials Science and Engineering. C*, Article 110510.

Nordqvist, D., & Vilgis, T. A. (2011). Rheological study of the gelation process of agarose-based solutions. *Food Biophysics, 6*(4), 450–460.

Ramiah, R., du Toit, L., Choonara, Y. E., Kondiah, P. P. D., & Pillay, V. (2020). Hydrogel-based bioinks for 3D bioprinting in tissue regeneration. *Frontiers in Materials, 7*, 76.

Rinaudo, M. (2006). Chitin and chitosan: Properties and applications. *Progress in Polymer Science, 31*(7), 603–632.

Sadeghianmaryan, A., Naghieh, S., Alizadeh Sardroud, H., Yazdanpanah, Z., Afzal Soltani, Y., Sernaglia, J., & Chen, X. (2020). Extrusion-based printing of chitosan scaffolds and their in vitro characterization for cartilage tissue engineering. *International Journal of Biological Macromolecules, 164*, 3179–3192.

Salati, M. A., Khazai, J., Tahmuri, A. M., Samadi, A., Taghizadeh, A., Taghizadeh, M., … Mozafari, M. (2020). *Polymers agarose-based biomaterials: Opportunities and challenges in cartilage tissue engineering.*

Sivashankari, P. R., & Prabaharan, M. (2020). Three-dimensional porous scaffolds based on agarose/chitosan/graphene oxide composite for tissue engineering. *International Journal of Biological Macromolecules, 146*, 222–231.

Smith, J., & Doe, A. (2022). The impact of shear rate on bio-ink printability and cell viability in 3D bioprinting. *Journal of Biomedical Materials Research, 58*(4).

Staroszczyk, H., Sztuka, K., Wolska, J., Wojtasz-Pająk, A., & Kołodziejska, I. (2014). Interactions of fish gelatin and chitosan in uncrosslinked and crosslinked with EDC films: FT-IR study. *Spectrochimica Acta Part A-Molecular and Biomolecular Spectroscopy, 117*, 707–712.

Tan, S. H., Ngo, Z. H., Sci, D. B., Leavesley, D., & Liang, K. (2022, February). Recent advances in the design of three-dimensional and bioprinted scaffolds for full thickness wound healing. *Tissue Engineering Part B: Reviews, 2022*, 160–181.

Tylingo, R., Kempa, P., Banach-Kopeć, A., & Mania, S. (2022). A novel method of creating thermoplastic chitosan blends to produce cell scaffolds by FDM additive manufacturing. *Carbohydrate Polymers, 280*, Article 119028.

Unagolla, J. M., & Jayasuriya, A. C. (2020). Hydrogel-based 3D bioprinting: A comprehensive review on cell-laden hydrogels, bioink formulations, and future perspectives. In , *Vol. 18. Applied materials today*. Elsevier Ltd.

Witzler, M., Ottensmeyer, P. F., Gericke, M., Heinze, T., Tobiasch, E., & Schulze, M. (2019). Non-cytotoxic agarose/hydroxyapatite composite scaffolds for drug release. *International Journal of Molecular Sciences, 20*(14), 3565.

Wu, J., Han, Y., Fu, Q., Hong, Y., Li, L., Cao, J., … Qian, Q. (2022). Application of tissue-derived bioink for articular cartilage lesion repair. *Chemical Engineering Journal, 450*.

Zamora-Mora, V., Velasco, D., Hernández, R., Mijangos, C., & Kumacheva, E. (2014). Chitosan/agarose hydrogels: Cooperative properties and microfluidic preparation. *Carbohydrate Polymers, 111*, 348–355.

Zarrintaj, P., Manouchehri, S., Ahmadi, Z., Saeb, M. R., Urbanska, A. M., Kaplan, D. L., & Mozafari, M. (2018). Agarose-based biomaterials for tissue engineering. *Carbohydrate Polymers, 187*, 66–84.

Zaszczyńska, A., Moczulska-Heljak, M., Gradys, A., & Sajkiewicz, P. (2021). Advances in 3D printing for tissue engineering. *Materials, 14*(12), 3149.

Zhang, X., Chen, X., Hong, H., Hu, R., Liu, J., & Liu, C. (2021). Decellularized extracellular matrix scaffolds: Recent trends and emerging strategies in tissue engineering. *Bioactive Materials, 10*, 15–31.

Zhang, Y., Zhou, D., Chen, J., Zhang, X., Li, X., Zhao, W., & Xu, T. (2019). Biomaterials based on marine resources for 3D bioprinting applications. *Marine Drugs, 17*(10), 555.

6.4 [A4] From Bioink to Tissue: Exploring Chitosan-Agarose Composition in the Context of Printability and Cellular Behaviour.

6.4.1 Wkład pracy doktoranta

Tytuł: From Bioink to Tissue: Exploring Chitosan-Agarose Composite in the Context of Printability and Cellular Behaviour
Autorzy: Szymon Mania, Adrianna Banach-Kopeć, Natalia Maciejewska, Katarzyna Czerwiec, Paulina Słonimska, Milena Deptuła, Michał Pikuła, Jakub Baczyński-Keller, Paweł Sachadyn, Robert Tylingo
Czasopismo: Molecules
Rok wydania: 2024
Impact factor: 4,2
Liczba punktów wg MNiSW: 140
DOI: 10.3390/molecules29194648
Procentowy wkład pracy doktoranta: 25%

Mój udział w przygotowaniu tego artykułu obejmował pełnienie roli jednej z głównych osób odpowiedzialnych za opracowanie koncepcji i planu badawczego, które stanowiły fundament projektu, a także organizację zasobów niezbędnych do jego realizacji. Ponadto aktywnie uczestniczyłam w przeprowadzaniu badań eksperymentalnych, w tym w przygotowywaniu próbek do dalszej analizy. Samodzielnie przeprowadziłam badania oceny stopnia dyfuzji i przepuszczalności oraz współpracowałam przy badaniach oceny właściwości reologicznych, ocenie przeżywalności komórek w kompozycjach polimerowych, a także w ocenie stopnia angiogenezy. Przygotowałam również wszystkie próby do testów biologicznych oceniających biozgodność badanych układów, w tym testów przeprowadzonych z użyciem zwierząt. Moje obowiązki obejmowały także zarządzanie danymi (ich zbieranie, organizację oraz przygotowanie do analizy) oraz formalną analizę większości wyników. Dokonałam analizy większości uzyskanych wyników przeprowadzonych badań. Odpowiadałam za przygotowanie większości wykresów oraz walidację wyników. Byłam główną osobą odpowiedzialną za przygotowanie pierwszej wersji manuskryptu oraz jego dalszą edycję. Pełniłam rolę autora korespondencyjnego oraz byłam główną osobą zajmującą się przygotowaniem odpowiedzi na recenzje.

6.4.2 Treść artykułu

molecules

MDPI

Article

From Bioink to Tissue: Exploring Chitosan-Agarose Composite in the Context of Printability and Cellular Behaviour

Szymon Mania [1,†], Adrianna Banach-Kopeć [1,*,†], Natalia Maciejewska [2], Katarzyna Czerwiec [3], Paulina Słonimska [4], Milena Deptuła [5], Jakub Baczyński-Keller [4], Michał Pikuła [5], Paweł Sachadyn [4] and Robert Tylingo [1]

1. Department of Chemistry, Technology and Biotechnology of Food, Faculty of Chemistry, Gdańsk University of Technology, 80-233 Gdańsk, Poland; szymon.mania@pg.edu.pl (S.M.); robertt@pg.edu.pl (R.T.)
2. Department of Pharmaceutical Technology and Biochemistry, Gdańsk University of Technology, 80-233 Gdańsk, Poland; natalia.maciejewska@pg.edu.pl
3. Division of Clinical Anatomy, Medical University of Gdańsk, 80-210 Gdańsk, Poland; katarzyna.czerwiec@gumed.edu.pl
4. Laboratory for Regenerative Biotechnology, Gdańsk University of Technology, 80-233 Gdańsk, Poland; paulina.slonimska@pg.edu.pl (P.S.); jakub.keller@pg.edu.pl (J.B.-K.); psach@pg.edu.pl (P.S.)
5. Laboratory of Tissue Engineering and Regenerative Medicine, Division of Embryology, Medical University of Gdańsk, 80-210 Gdańsk, Poland; milena.deptula@gumed.edu.pl (M.D.); michal.pikula@gumed.edu.pl (M.P.)

* Correspondence: adrianna.banach@pg.edu.pl

† These authors contributed equally to this work.

Abstract: This study presents an innovative method for producing thermosensitive bioink from chitosan hydrogels saturated with carbon dioxide and agarose. It focuses on a detailed characterisation of their physicochemical properties and potential applications in biomedicine and tissue engineering. The ORO test approved the rapid regeneration of the three-dimensional structure of chitosan–agarose composites in a unidirectional bench press simulation test. The diffusion of dyes through the chitosan–agarose hydrogel membranes strongly depended on the share of both polymers in the composite and the molecular weight of the dyes. Glucose, as a nutrient marker, also diffused through all membranes regardless of composition. Biocompatibility assessment using MTT tests on 46BR.1N fibroblasts and HaCaT keratinocytes confirmed the safety of the bioink. The regenerative potential of the bioink was confirmed by efficient cell migration, especially HaCaT. Long-term viability studies showed that chitosan–agarose scaffolds, unlike the agarose ones, support cell proliferation and survival, especially 14 days after bioink extrusion. Experiments in a skin wound model in mice confirmed the biocompatibility of the tested dressing and the beneficial action of chitosan on healing. Studies on vessel formation in chicken embryos highlight the potential of the chitosan–agarose composition to enhance proangiogenic effects. This composition meets all entry criteria and possesses excellent biological properties.

Keywords: chitosan; agarose; bioprinting; natural polymers; tissue engineering; biocompatibility

check for updates

Citation: Mania, S.; Banach-Kopeć, A.; Maciejewska, N.; Czerwiec, K.; Słonimska, P.; Deptuła, M.; Baczyński-Keller, J.; Pikuła, M.; Sachadyn, P.; Tylingo, R. From Bioink to Tissue: Exploring Chitosan-Agarose Composite in the Context of Printability and Cellular Behaviour. *Molecules* **2024**, *29*, 4648. https://doi.org/10.3390/molecules29194648

Academic Editor: Katarzyna Lewandowska

Received: 22 August 2024
Revised: 19 September 2024
Accepted: 26 September 2024
Published: 30 September 2024

1. Introduction

Bioprinting is an excellent tool for the production and study of artificial tissues, and is thus a potential tool in skin regeneration [1]. Compared to typical skin regeneration methods, bioprinting offers better automation and standardisation for clinical uses and accuracy in incorporating living cells, growth factors, and other biomolecules [2]. Generally, the main advantage of bioprinting over other techniques is the ability to print not only scaffolds of a specific, personalised shape but also a properly designed internal network in which all processes necessary for regeneration and tissue or organ formation occur.

However, one of its major challenges remains the development of bioink and the application of the appropriate crosslinking technique, which will allow obtaining an object

with specific physicochemical and biological properties. Such a bioink must be printable, i.e., have appropriate rheological parameters, and the obtained scaffolds must be mechanically stable and biocompatible, i.e., provide an appropriate environment in which cells will survive, proliferate, migrate, and differentiate, forming tissues [3–5]. These three parameters determine the quality of the bioink, which, as it turns out, are contradictory because the higher the viscosity of the bioink, the better the printability, and conversely, the worse the biocompatibility. Therefore, already at the stage of designing the bioink and determining its application, it is necessary to focus research and find a compromise between these properties [6].

An example of systems that seem to possess both good physical properties and are biocompatible are hydrogels, which form a three-dimensional network of hydrophilic polymer chains. Additionally, hydrogels can effectively recreate the extracellular matrix and the natural environment of cells. They also have mechanical properties similar to tissues and can provide cells with structural support and hydration. Another desirable property of hydrogels is shear-thinning, which allows the extrusion of bioinks under high shear stress while maintaining the mechanical properties of the system [7].

In tissue engineering and bioprinting, both natural polymers, such as alginate, chitosan (CS), hyaluronic acid, and gelatin, and synthetic ones, which include polyacrylamide, polyvinyl alcohol, polyethylene glycol, and polylactic acid, are used. The main advantages of natural polymers are their biocompatibility and specific enzymatic degradation, as well as the presence of functional groups and domains, which provide better interactions with cells than synthetic ones. These, in turn, are characterised by strong water adsorption and high gel strength. However, despite the introduction of synthetic polymers, which allow researchers' precise control of the gels' structure and properties, special attention should be paid to their biocompatibility. This problem concerns potential residues during the production of such polymers, i.e., unreacted monomers and remnants of initiators [8].

This work is a continuation of a series of studies on the development of a hydrogel polymer bioink based on CS obtained by the carbon dioxide saturation method and agarose (AG). The concept of combining CS in bioink with fibroblast and keratinocyte stem cells emerges from the positive impact of this polymer on the skin tissue regeneration process, confirmed by numerous studies. The primary mechanism of action of CS is based on the activation of key components of the immune system, namely inflammatory cells, macrophages, and fibroblasts. This, in turn, contributes to the shortening of the inflammatory phase and accelerates the transition to the proliferation phase, which is essential in rebuilding damaged tissue. Furthermore, CS promotes the formation of granulation tissue and angiogenic processes, facilitating the effective deposition of collagen fibres, which is crucial for the repair of skin damage [9,10]. Angiogenesis plays a crucial role in regeneration, as vascularisation is needed to supply oxygen, nutrients, and growth factors to the regenerating tissue. Proper angiogenesis can accelerate wound healing and prevent necrosis; however, abnormal angiogenesis contributes to a significant slowdown of this process [11].

The main issue with current bioprinting formulations lies in their limited versatility. Many commercially available and researched systems rely on three primary polymers: alginate, collagen, and gelatin. These systems have gained widespread adoption due to their simplicity in crosslinking using methods like calcium chloride and UV radiation, especially after modification to methacrylated derivatives. However, these formulations predominantly focus on supporting cell viability post-printing, lacking additional biological effects such as promoting angiogenesis or cellular differentiation. To date, only a few solutions for alternative bioink compositions have been reported in the literature. One approach involves carboxymethylchitosan combined with agarose and sodium alginate [6], while another utilises N,O-carboxymethylchitosan with agarose [12]. Modifications to chitosan to enhance solubility aim to eliminate the use of cytotoxic acids but necessitate the use of organic solvents for derivatisation. Nevertheless, chemical modifications of polymers pose risks of residual toxic solvents and involve time-consuming processes, complicating

their practical application and potentially leading to the release of cytotoxic degradation products over time.

This study aims to demonstrate additional physicochemical and biological properties confirming the practical application and meeting the acceptance criteria of a chitosan–agarose bioink, essential for biomaterials in tissue engineering. Our previous research has demonstrated that blending two polymers with diverse physicochemical and biological properties enables the creation of a bioink that fulfils all necessary system requirements: it is printable, is biocompatible, and possesses suitable rheological properties for bioprinting applications [13]. We have identified composites with significant application potential through rheological studies and extrusion tests. These blends underwent rigorous biological testing to assess their suitability for wound healing and broader tissue engineering applications. This approach represents a straightforward solution for producing a bioink, based on just two components, that already meets numerous critical criteria for tissue engineering applications from inception.

2. Results

2.1. Physiochemical Properties of Chitosan–Agarose Composition

2.1.1. Rheological Properties

The rheological properties of CS agarose solutions and their composites were evaluated using the three-interval thixotropy test (3ITT), conducted in the oscillatory–rotational–oscillatory (ORO) variant, which applies high rotational stress immediately after a low-strain oscillatory stage within the LVE region. This approach effectively simulates the unidirectional extrusion of bioink from the printer head and assesses its behaviour post-stress relaxation under conditions similar to the physiological ones optimal for cells in the prepared bioink for printing (37 °C) [14]. Figure 1 shows the change in complex viscosity (oscillatory part) and dynamic viscosity (rotational part) over time for 1% solutions of CS and AG, as well as their mixtures. The viscosity changes over time suggest processes related to the degradation and regeneration of the studied fluids' structure. Complex viscosity describes a material's resistance to deformation under stress, encompassing both viscous (loss) and elastic components, making it particularly useful for analysing thixotropic materials with time-dependent structures. The viscosity levels in the first test cycle indicate that chitosan and agarose as single-component solutions exhibit a more developed structure that is resistant to deformation under dynamic loads. In other words, under oscillatory conditions in the LVE region, the internal molecular connections in these single-component materials are more robust than in their composites. Introducing rapid rotation in the second region caused the destruction of the structure of all tested samples. Viscosity values in this range confirm the trend observed in the first cycle, where a chitosan content of 20% and 40% in the composite shows the most significant susceptibility to deformation induced by stresses mimicking unidirectional shear. The third region of the graph indicates the ability to rebuild the structure of the studied polymer sols, but with different characteristics. Based on this part of the graph, it can be concluded that the reconstruction of the structure of pure agarose takes the longest, but at the same time, the most durable network is created. The values of the complex viscosity of composite materials at the end of the first oscillation and at the beginning of the third are similar, which indicates that the three-dimensional structure of the material will be quickly recovered after unidirectional squeezing from the syringe, which is an advantage of using the composite.

2.1.2. Permeability

The permeability of scaffolds to nutrients, gases, and metabolites is a key feature that provides the scaffold-embedded cells with the correct conditions for proliferation, differentiation, and migration. For this purpose, a series of measurements were carried out to determine how changing the composition of the scaffold, i.e., the ratio of AG to CS, affects the migration of components of the standard glucose and compounds differing in molecular weight.

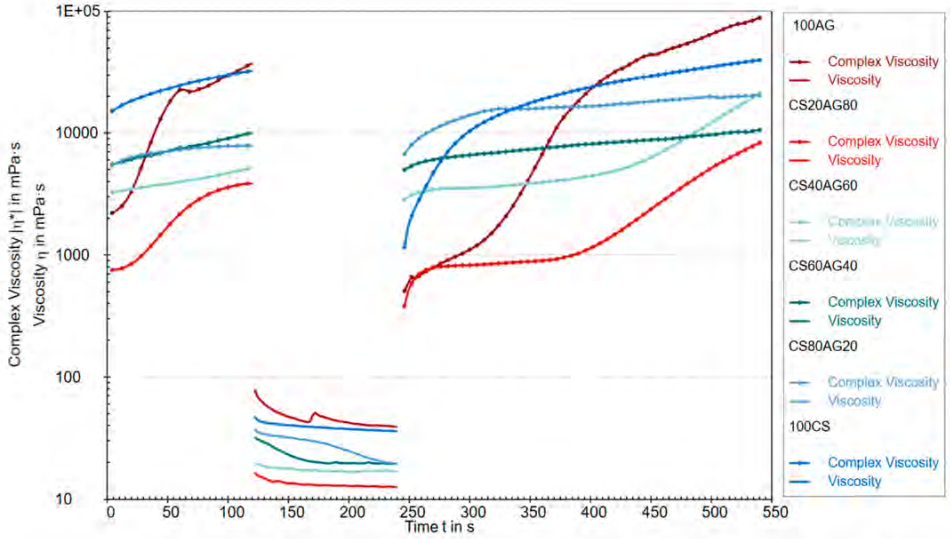

Figure 1. Comparison of complex viscosity and dynamic viscosity during the ORO test.

This study of the effect of the molecular weight of dyes on their permeability through membranes showed that the diffusion rate for the compounds with the lowest molecular masses is the highest (Figure 2). Furthermore, for the dye with the lowest molecular weight, Resazurin (251.17 g/mol), the most prominent spot diameters were observed, indicating its highest permeability through hydrogel membranes, more than double compared to Nigrosin (616.49 g/mol). For example, increasing the molecular weight of a compound from approximately 251 to 482 significantly reduced permeability, which after 24 h of incubation for Resazurin was about 50 mm, and for Brilliant Green, it was below 40 mm in dye spot diameter. Comparing Nigrosin and Resazurin dye diffusion, for the 100% AG system, the average dye stain after 24 h was approximately 1.6 times smaller.

Based on the conducted studies, it can be concluded that the composition of CS/AG composites, i.e., the proportion of each polymer and the molecular weight of diffusing substances, significantly impacts their permeability through hydrogel membranes. It has been shown that 100% AG membranes display a higher permeability than 100% CS membranes. This phenomenon is consistent with the results available in the scientific literature, which explain it by the lower crosslinking density and higher porosity of AG membranes. The looser structure of AG facilitates the diffusion of particles. On the other hand, adding CS to the composite reduces the diffusion of dyes through the membrane, mainly observed as the molecular weight of the tested substance increases. This phenomenon can be attributed to the stronger intermolecular bonds of CS affecting, in turn, its lower permeability. Consequently, mixing CS with AG makes it possible to regulate the porosity and crosslinking density of membranes, allowing for the modification of their permeability.

Also, Reys et al. deduced that pure AG shows better permeability towards methylene blue than a fucoidan–agarose-based hydrogel. As a result of the more robust interactions between the polymers, a more cohesive and compact system is formed, resulting in slower diffusion of the dye. Furthermore, the same study showed that permeability decreases with increasing agarose concentration, resulting in a denser hydrogel matrix [15]. Based on these results, it can be assumed that compounds with a lower molecular weight, such as glucose (180.17 g/mol), will effectively diffuse through hydrogel membranes, regardless of the CS/AG composition. Such membrane properties open up possibilities for their application

in many fields, from biotechnology to regenerative medicine, where controlling substance diffusion through membranes is crucial.

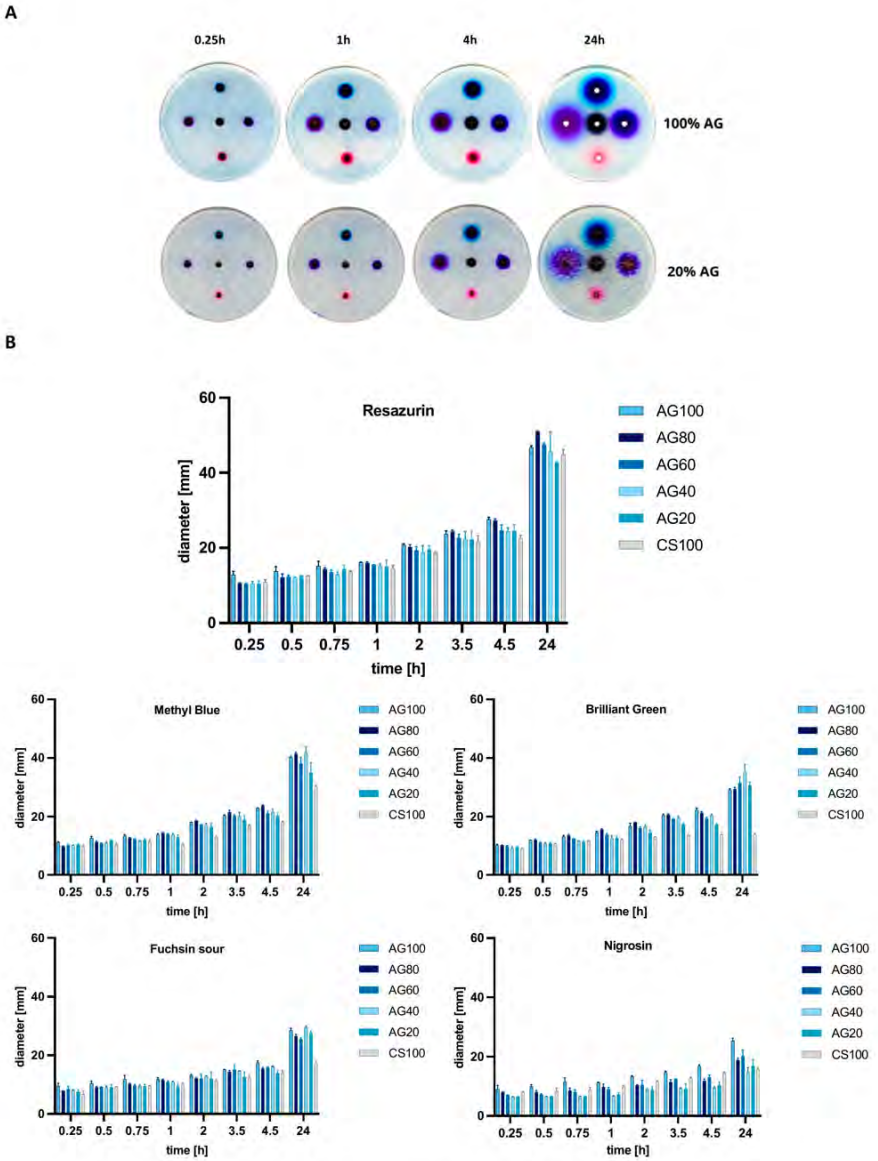

Figure 2. (**A**) Images of dye-applied hydrogel samples over 24 h of incubation. (**B**) Sizes of dye stain diameters from 0.25 to 24 h at specific time points. Data represent mean ± standard deviation; $p < 0.05$.

Therefore, in the study of glucose diffusion through hydrogel membranes (Figure 3) based on CS, CS/AG, and AG, no significant differences were observed in the change in glucose concentration in the acceptor chamber over time. Initially, the CS membrane demonstrated a greater ability to diffuse glucose molecules. However, after 4 h, the glucose concentration diffusing through the hydrogel membranes became similar. After 24 h, the glucose concentrations in both the acceptor and donor chambers equalised, with the glucose concentration after 24 h being 3.97 ± 0.2.

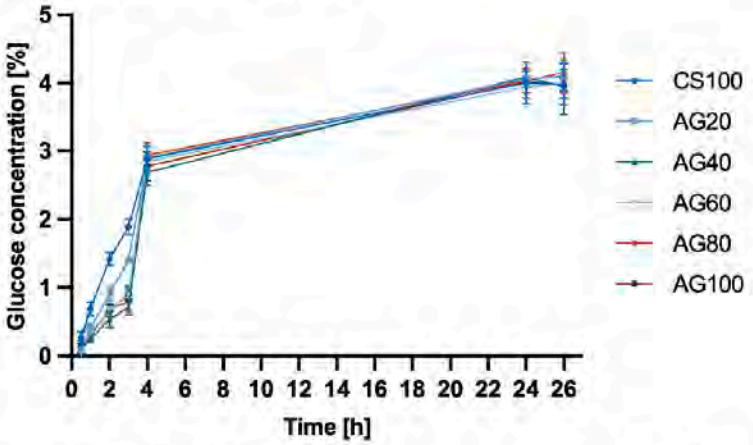

Figure 3. Glucose diffusion into the acceptor chamber through chitosan CS, agarose AG, and chitosan–agarose CS/AG membranes at 25 °C.

2.2. Biological Properties of Chitosan–Agarose Composition

2.2.1. MTT Test

The MTT assay was conducted on skin cell lines, namely fibroblasts 46BR.1N and keratinocytes HaCaT, for which the developed bioinks will be used as carriers in future applications. The results provide further evidence confirming the biological safety of CS, AG, and their composites, and they are consistent with our previous studies, which, according to ISO standard 10993-5, demonstrated that both AG and CS of various degrees of DD and MW are not cytotoxic towards the standardised mouse fibroblast L929 cell line [13]. In the present study, in order to investigate potential cytotoxicity towards skin cells, cell viability was assessed following 24 h contact with the extracts from the tested samples.

According to ISO standard 10993-5, materials for which cell viability exceeds 70% are considered biocompatible. The tested samples showed high cell viability, with values ranging from approximately 85 to 112% (Figure 4A) for the 46BR.1N cell line and from approximately 90 to 137% (Figure 4B) for the HaCaT line, suggesting the favourable biological safety of these materials.

2.2.2. Migration Test

An essential aspect of cellular scaffold design is the selection of biomaterials capable of stimulating cell migration processes. This applies to both cells contained in the bioink and those naturally present at the site of the scaffold application. Currently, two approaches are used in bioprinting: the first involves placing cells in the bioink, within which they are supposed to differentiate and migrate; the second promotes the migration of cells from the body into the scaffold.

The use of extracts in the Ibidi wound healing assay model was due to the need to assess the impact of biomaterials under conditions close to real applications, where, in addition to placing cells inside the scaffolds, which are porous, there is also a necessity

for cell migration into the pores where they proliferate and differentiate. The fact that extracts were used also stemmed from the fact that AG as well as CS/AG systems gel at 37 °C, as do CS solutions along with carbon dioxide release, especially at elevated temperatures. Consequently, examining cell migration using the above set directly in solutions would have been impossible. Furthermore, CS, AG, and CS/AG solutions have different viscosities before and after gelation, significantly disturbing the measurement. Therefore, the effect on cell migration and the absence of cytotoxicity were assessed by determining cell viability using extracts obtained from the tested biomaterials.

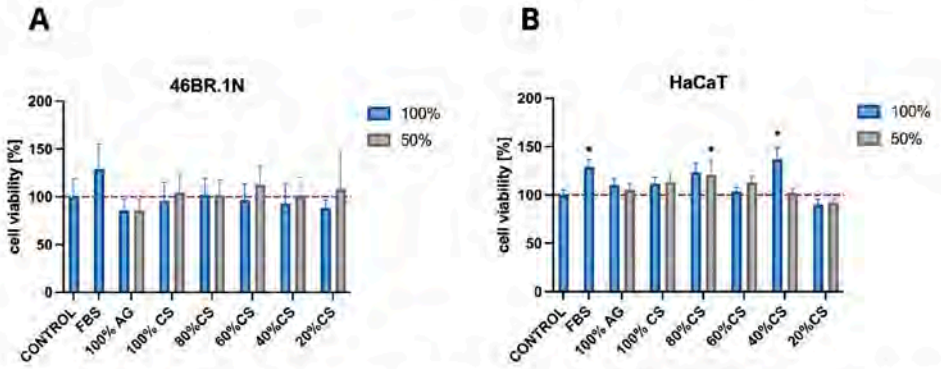

Figure 4. The cytotoxicity of chitosan (CS), agarose (AG), and their composites CS/AG following 24 h incubation in two concentrations against (**A**) fibroblasts 46BR.1N and (**B**) keratinocytes HaCaT. Data are expressed as the mean ± standard deviation of three independent experiments. The results were analysed by one-way ANOVA with comparisons vs. control: $p > 0.05$, * $p < 0.05$.

The analysis of the results showed (Figure 5) that in the case of HaCaT cells, all CS extracts significantly supported cell migration, achieving better results than the negative (cells stimulated with DMEM HG medium) and positive (cells stimulated with DMEM HG medium containing 10% FBS) controls. In the case of AG, no statistically significant differences were observed compared to the control. For the 46BR.1N cells, despite statistically significant differences compared to the control, the pro-migratory effect was moderate, and the lack of stimulation by FBS suggests the specific requirements of these cells. These results indicate that AG extracts do not support cell migration, while CS shows promising pro-migratory properties for HaCaT cells, which is not observed in cultures of 46BR.1N fibroblasts.

2.2.3. Cell Viability

As part of the further analysis of the biological properties of the tested bioinks, the cell viability of the HaCaT line and 46BR.1N fibroblasts in contact with scaffolds containing 1% AG and the CS/AG composite in a 1:1 ratio was examined. The viability assessment was conducted at three time points, 2, 7, and 14 days post-scaffold extrusion, allowing for the observation of the long-term effects of the tested biomaterials on the cells. This selection of time points allowed for the examination of both the biological safety of the system, i.e., its cytotoxic effects, and its influence on cell proliferation and migration.

According to the results presented in Figure 6, after two days of incubation, a similar viability was observed for both cell lines across all tested systems, oscillating around 100%. These results indicate a lack of cytotoxicity, previously demonstrated in the MTT assays for the extracts of the tested biomaterials. Seven days after scaffold extrusion, a slight decrease in the viability of both cell lines and in both types of scaffolds was observed; however, these values remained at an acceptable level, ranging between 70% and 78%. This decrease in

living cells may be attributed to adapting to the new environment. Nevertheless, a positive impact on the survival and proliferation of cells was noted for the CS/AG composite after 14 days for both 46BR.1N and HaCaT cells, where viability reached 117% and 129%, respectively. In systems based solely on AG, cells tended to cluster outside the scaffold area, resulting in a slight decrease in cell viability within the scaffold. Moreover, this observation aligns with the literature data indicating that AG scaffolds do not promote cell adhesion.

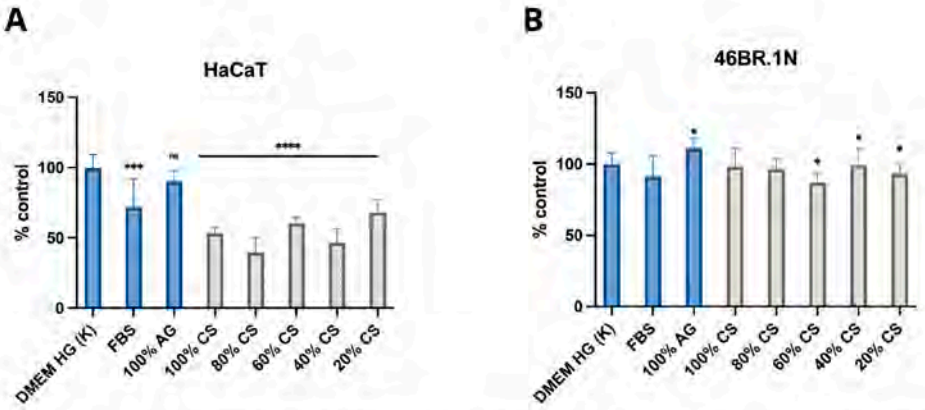

Figure 5. Effects of MMW chitosan (CS), agarose (AG), and their composites on the migration of (**A**) fibroblasts 46BR.1N and (**B**) keratinocytes HaCaT. The graphs show the results (calculated from scratch area) of at least three experiments, which are presented as the mean ± SEM. The results were analysed by one-way ANOVA with comparison to control DMEM HG. ns (not statistically significant, $p > 0.05$), * $p < 0.05$, *** $p < 0.001$, **** $p < 0.0001$).

In summary, both materials tested demonstrated compatibility with HaCaT and 46BR.1N cells, showing no cytotoxic action over up to 14 days of incubation. Furthermore, the data confirm that the CS/AG composite is not only compatible with the cells but also promotes their proliferation, providing favourable rheological parameters while maintaining high cell viability.

The bioprinting process significantly impacts cell survival, especially during extrusion, influenced by factors like bioink viscosity, printing speed, pressure, nozzle geometry, build platform temperature, needle diameter, and construct geometry [16]. Insufficient initial cell density can lead to slower cell and tissue growth rates and inadequate scaffold integration in vivo [17]. The bioink's composition, construct geometry (porosity, permeability, degradability), growth factors, peptide sequences, and culture conditions (temperature, nutrient composition) further affect cell survival [13]. Comparing cell survival rates over different time intervals is challenging due to numerous variables in bioprinting parameters. For instance, human keratinocytes and fibroblast cells in a genipin-crosslinked CS-PEG system showed up to 85% survival after 7 days [18]. In a self-crosslinkable CS–gallic acid system, NIH 3T3 cell survival was 92% after 7 days [19]. Over a more extended period, NIH 3T3 cells in an aldehyde hyaluronic acid-N-carboxymethyl chitosan–gelatin–alginate system maintained approximately 91% viability after 29 days [20]. Fluorescent staining of fibroblast and keratinocyte cells in CS/AG and AG systems revealed nearly 100% survival, indicating that the optimal extrusion temperature did not induce cell death. However, survival declined to 70% by day 7, potentially due to new environmental or mechanical stress from the printing process. Beyond this adaptation phase, survival increased to 110% by day 14, suggesting the cells adapted and began proliferating, potentially facilitated by biocompatible materials like CS supporting tissue regeneration and creating favourable conditions for cell expansion.

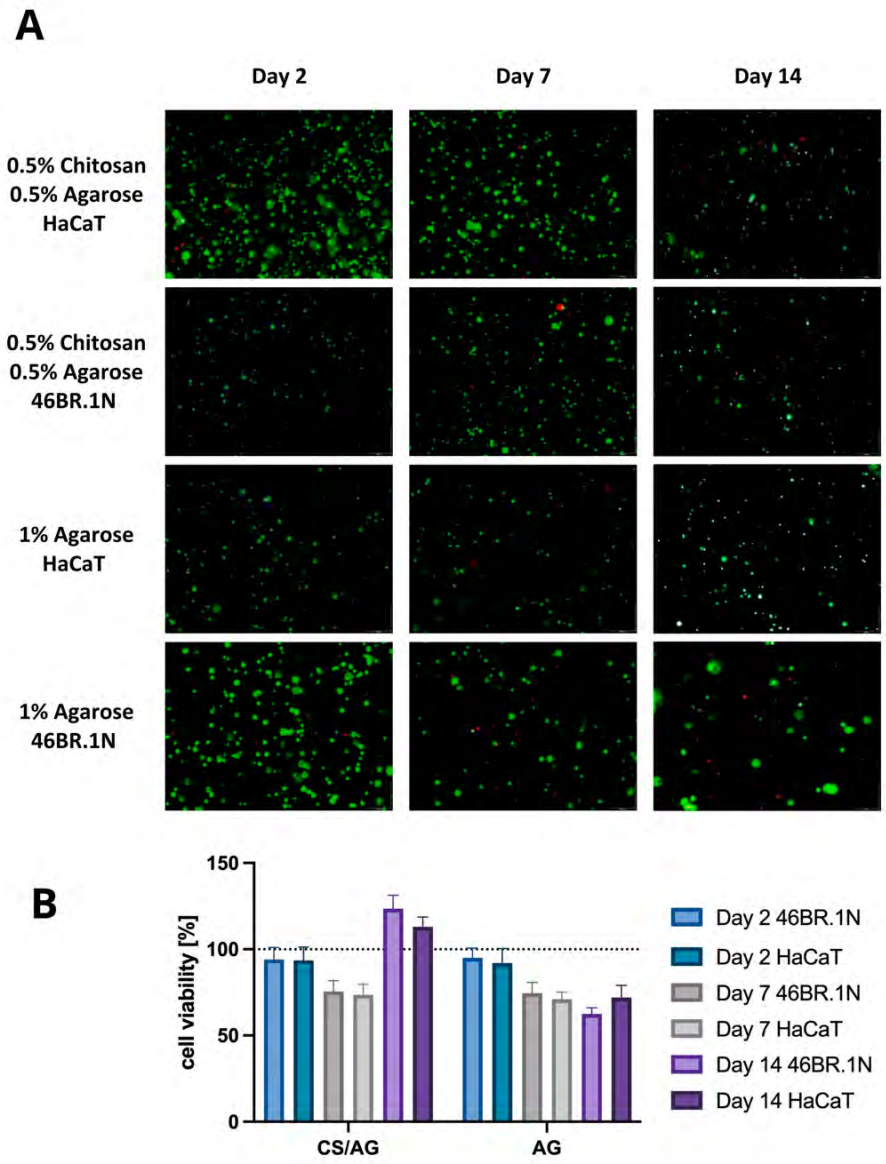

Figure 6. (**A**) Viability of 46BR.1N fibroblasts and HaCaT keratinocytes embedded in chitosan–agarose CS/AG composite and in agarose AG alone. This figure presents fluorescent microscope images showing live–dead staining of cells in the scaffolds on days 2, 7, and 14 of cultivation. Viable cells are stained green with calcein, while dead cells are stained red with propidium iodide; the scale bar is 250 µm. (**B**) Graph of changes in survival rates of both cell lines over time. The results were evaluated using a Leica DMIL LED inverted microscope and Graphpad Prism 5.0.

2.2.4. Angiogenesis

The proangiogenic potential of CS- and AG-based materials was evaluated using a CAM assay on 8-day-old embryos. Materials including CS, AG, and a combination of both were tested against a Whatman filter paper control (Figure 7A,B). The analysis focused on several parameters of the vascular network, including the number of branching points, vessel network length, total vascular area, and mean vessel thickness. Branching points are crucial for evaluating angiogenesis, as new vascular branches arise through mechanisms like sprouting or intussusception from existing vessels. A notable increase in branching points was observed with CS and the CS/AG combination, particularly at 72 h, while AG alone showed a slight increase compared to the control (Figure 7C). Another vital phase in angiogenesis is the extension of blood vessels. At 48 h, the total vessel length was similar across the control, AG, and CS/AG combination treatments. However, CS alone exhibited a consistent increase in vessel length at both 48 and 72 h (Figure 7D). The total vascular area reflecting the surface area of all vessels in an image increased as the vascular network expanded. As shown in Figure 7E, the total vascular area displays a slight increase across all materials over time, and it is more pronounced after 48 h, whereas after the next 24 h, it remains almost constant. The thickness of the blood vessels also influences the total vascular area. Since new vascular sprouts that form during angiogenesis are thin, they may not significantly affect the total vascular area compared to other parameters. Alterations in the average thickness of the vasculature were observed, as newly formed thin sprouts contributed to a reduction in the overall diameter of the vascular network. The mean thickness increased only with the combination of CS/AG and with CS alone at 48 h, whereas at 72 h, the mean vessel thickness remained relatively consistent across all treatments with slight variations (Figure 7F).

Although the CAM model is a recommended test for assessing the biocompatibility of biomaterials, few studies have focused on this aspect. The angiogenesis results for CS- and AG-based materials can be compared with those of the other biomaterials that were analysed in the study by Kohli et al. [21] using the CAM test. In this study, a variety of materials, natural and synthetic, and their combinations were compared. A pronounced proangiogenic effect was observed in fibrin-based materials, which significantly increased vessel density and the number of branching points compared to natural materials, such as collagen and elastin, and synthetic materials, such as PCL (poly-ε-caprolactone), which exhibited much weaker proangiogenic effects. Concerning the results presented by the research team, collagen and elastin demonstrated effects similar to CS and AG in terms of vessel density and total vascular area. Additionally, they also noted that not only the composition of biomaterials but also their porosity influences vessel growth. Biomaterials with greater porosity, such as fibrin, promoted more intense vessel growth, which may result from better access for cells and vessels to the biomaterial. Even though synthetic materials, such as PCL, had high porosity, without the support of natural components, their impact on angiogenesis was limited [21].

In summary, CS and CS/AG combinations generally promoted slight increases in various vascular parameters compared to the control, while AG alone had minimal effects and showed varied results depending on the specific parameter and time point. CS alone demonstrated the most consistent proangiogenic effects, enhancing both vessel length and the number of branching points. These findings suggest the potential application of CS and CS/AG materials in therapeutic angiogenesis, warranting further investigation into their mechanisms and long-term effects on vascular development.

2.2.5. Wound Healing

An animal model is an essential element in biomedical research. Due to their genetic, physiological, and pathological similarities to humans, mice are helpful in preclinical studies. Experiments conducted on small rodents are essential for evaluating developed biologics, as they provide preliminary information about interactions with living organisms, specifically regarding biocompatibility and therapeutic efficacy. Furthermore, studies on

animal models complement earlier biological research on proliferation, cytotoxicity, or cell migration. Moreover, the results from studies conducted on animal models constitute the first step that allows the conduct of clinical trials, which are decisive for confirming the utility of scaffolds in medical applications.

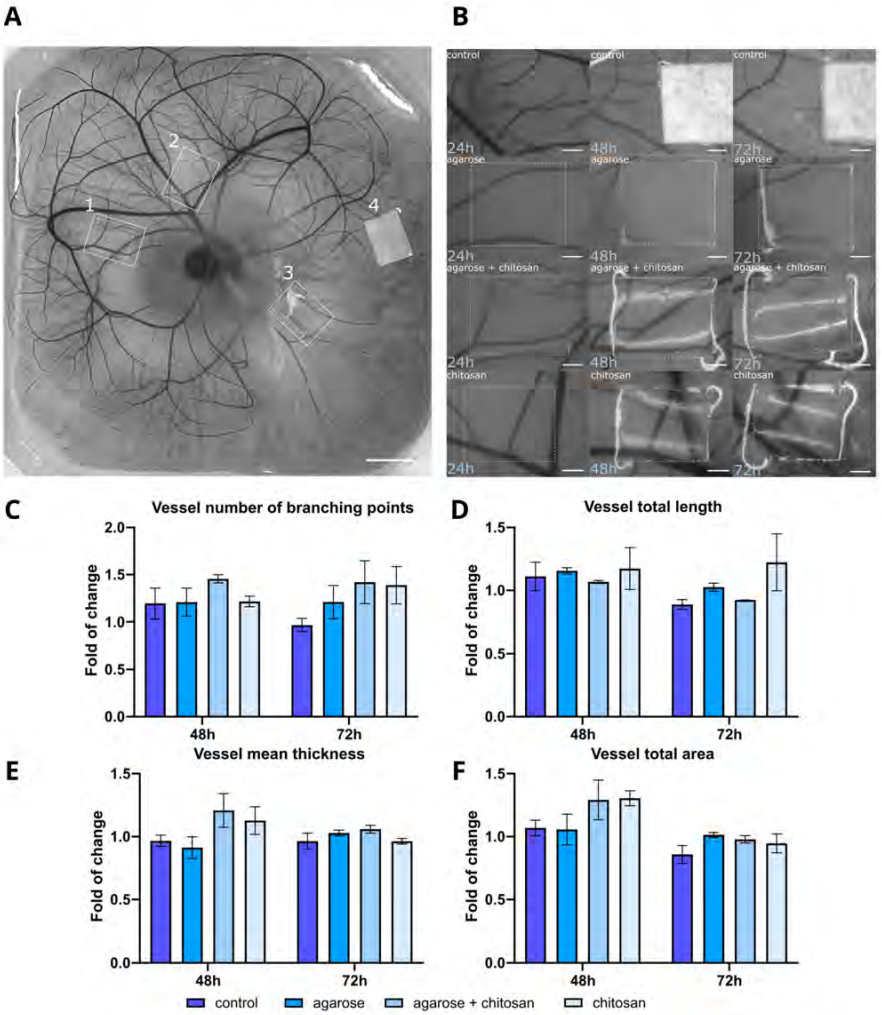

Figure 7. The ex ovo CAM angiogenesis assay. (**A**) Representative image of an ex ovo-cultivated chicken embryo with different tested materials on embryonic development day (EDD) 9. The materials are indicated as follows: 1—agarose + chitosan, 2—chitosan, 3—agarose, 4—Whatman filter paper. Scale bar = 5 mm. (**B**) Representative microscopic images showing material-induced angiogenesis after 24, 48, and 72 h of incubation with the materials. Scale bar = 1 mm. Analysis of changes in the vascular network, including the number of vessel branching points (**C**), total vessel length (**D**), mean vessel thickness (**E**), and total vascular area (**F**), presented as fold changes relative to the 24 h incubation. Data represent mean values ± s.d. from at least two independent experiments.

In this experiment, the effect of the CS/AG composition and its components, namely CS and AG applied alone, on wound healing was evaluated in a model of excisional dorsal skin injury in mice. CO_2-saturated water (Water CO_2) was applied to wounds in control mice. According to the literature, CS accelerates wound healing by stimulating immune cells like macrophages and fibroblasts, which shortens the inflammatory phase and promotes tissue proliferation. Additionally, CS enhances granulation tissue formation and angiogenesis, aiding collagen deposition for skin repair [9,10]. Therefore, this study aimed to determine whether the CS/AG composition accelerates wound healing, and specifically if the addition of agarose affects the efficacy of this process.

CS/AG and CS dressings applied as 6 mm hydrogel discs onto wounds (Figure 8A) significantly accelerated wound closure, resulting in 82.0 and 83.2% closure, respectively, on day 7 post-injury compared to the control (66.9%) (Figure 8B,C). On day 14 post-injury, wound closure in mice treated with each of three types of hydrogel dressings and in the controls reached approximately 90%. In the case of AG, the pace of wound closure was similar to that of the control group (Water CO_2). On day 14 post-injury, wound closure equalled in all tested groups, including the controls, reaching approximately 90%. No complications in the wounds were observed, thus confirming the biocompatibility of the applied dressings. Histological examination (Figure 8D) indicated typical wound healing in all groups (Figure 8D).

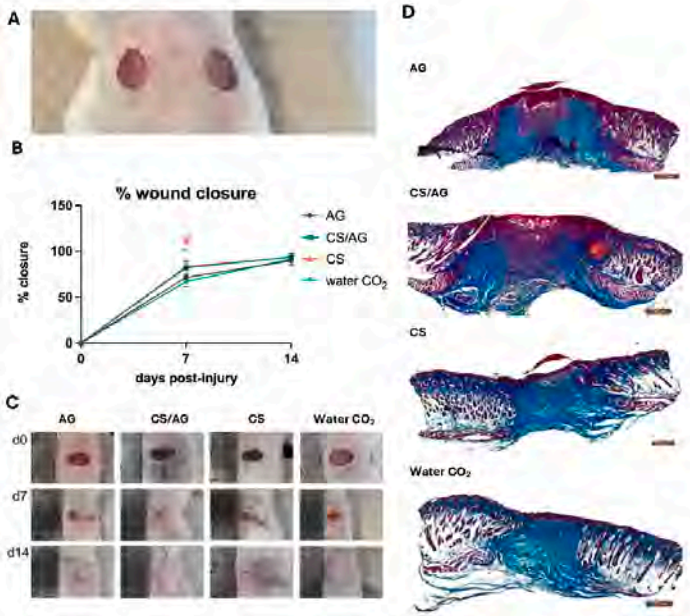

Figure 8. Effects of tested hydrogels on skin wound healing in mice. (**A**) Example photo of hydrogel discs applied on dorsal skin wounds; (**B**) mean percentage of wound closure; error bars represent SD, $n = 12$—a number of wounds representing 6 mice in each group; statistical significance relative to Water CO_2 control was determined using the two-tailed Mann–Whitney test and denoted with an asterisk "*" for CS/AG and a hash "#" for CS alone; (**C**) representative images of wounds at 0, d7, and d14; (**D**) representative skin sections were collected on day 14 post-injury and stained with Masson trichrome to visualise tissue architecture: red—muscles and keratin; blue—collagen; pink—cytoplasm; brown—nuclei. The samples are indicated as follows: CS/AG—chitosan–agarose composition, CS—chitosan alone; AG—agarose alone; Water CO_2—carbon dioxide-saturated water.

It is crucial not only to concentrate on CS but also to apply it to the skin. The CS hydrogel rapidly releases CO_2 and dries quickly. The AG in CS/AG allows the maintenance of a moist environment in contact with the wound, providing adequate moisture and protection against drying. This may be because AG creates a more stable and durable scaffold that better mimics the natural tissue environment. As a result, CS/AG dressings can combine chitosan's biological activities with agarose's physicochemical properties, promoting the maintenance of a moist microenvironment.

3. Materials and Methods

3.1. Materials

Chitosan—CS (MMW, DD > 75%), agarose—AG (low EEO, 34.5–37.5 °C gel point), phosphate-buffer saline (PBS) sodium hydroxide, and glycolic acid were purchased from Merck (Darmstadt, Germany). The carbon dioxide used to saturate the CS precipitate was derived from Linde Gaz Polska Sp. z o. o. (Gdańsk, Poland). Immortalised human keratinocyte HaCaT cells were purchased from the German Cancer Research Center (DKFZ, Heidelberg, Germany). The human skin fibroblast cell line 46BR.1N was obtained from the European Collection of Authenticated Cell Cultures (ECACC, Sigma Aldrich, St. Louis, MO, USA). The 3-(4,5-dimethylthiazol-2-yl)-2,5-diphenyltetrazolium bromide (MTT), DMEM, antibiotics, propidium iodide, calcein, and supplements necessary for cell culture were obtained from Sigma-Aldrich (St. Louis, MO, USA). Wound healing assay kits were obtained from Ibidi GmbH (Darmstadt, Germany). MilliQ water was used to prepare all aqueous solutions. All other reagents were of analytical grade or higher. The experiments on mice were conducted in the Tri-City Academic Laboratory Animal Centre of the Medical University of Gdańsk, where the animals were bred and maintained. 3,5-dinitrosalicylic acid, glucose, Resazurin sodium salt, methylene blue, Brilliant Green, Acid Fuchsin, and Nigrosin were purchased from Merck (Germany).

3.2. Hydrogel Preparation

The composition based on chitosan (CS) and agarose (AG), as well as their individual solutions, was prepared according to the methodology described by Banach-Kopeć et al., 2024 [22] (Figure 9). To summarise, a 1% CS solution with an average molecular weight was prepared using an innovative carbon dioxide saturation method. Meanwhile, a 1% AG solution was prepared in distilled water at 80 °C while stirring at 200 RPM (RA 2020, Heidolph Instruments GmbH & Co. KG, Kelheim, Germany). The CS/AG-based compositions were prepared by cooling the hot AG solution to 45 °C and immediately combining it with the CS solution in various weight ratios using a mechanical stirrer at a speed of 300 revolutions per minute for 2 min (BIOMIXBMX-10, Gdańsk, Poland). To evaluate the rheological properties, the temperature of the mixture was maintained at 40 °C to prevent gelation.

To standardise the water content of the CS/AG hydrogel membranes, it was necessary to initially reduce the water content and then replenish it through conditioning. This process ensured that the samples were consistent for repeatable testing. The membranes were cast onto 90 mm Petri dishes, dried at 25 °C for 48 h, and then incubated in distilled water for 24 h before measurement, resulting in a thickness of 0.4 mm. Samples for angiogenesis assessment were prepared in the same way, with the difference that they were incubated in a 0.9% saline solution. For the evaluation of wound closure, CS/AG and AG samples were cast onto 90 mm Petri dishes, and after gelation, 6 mm diameter discs were cut using a biopsy punch.

To conduct biological safety tests and assess the system's impact on cell migration, samples of CS, AG, and their composites were frozen at −80 °C and then freeze-dried (Christ Alpha 12–4 LD Plus, Osterode am Harz, Germany). According to the standards of the MTT test and the Ibidi wound healing assay methodology, it is necessary to prepare extracts of the tested materials. To ensure the most rigorous conditions and achieve the highest possible concentrations of the tested extracts, the samples were freeze-dried rather

than preparing extracts from their solutions. This approach is critical because, during the bioprinting process, the printed scaffolds are placed in the medium only after the process is complete, which can lead to significant water loss, especially in the first printed layers.

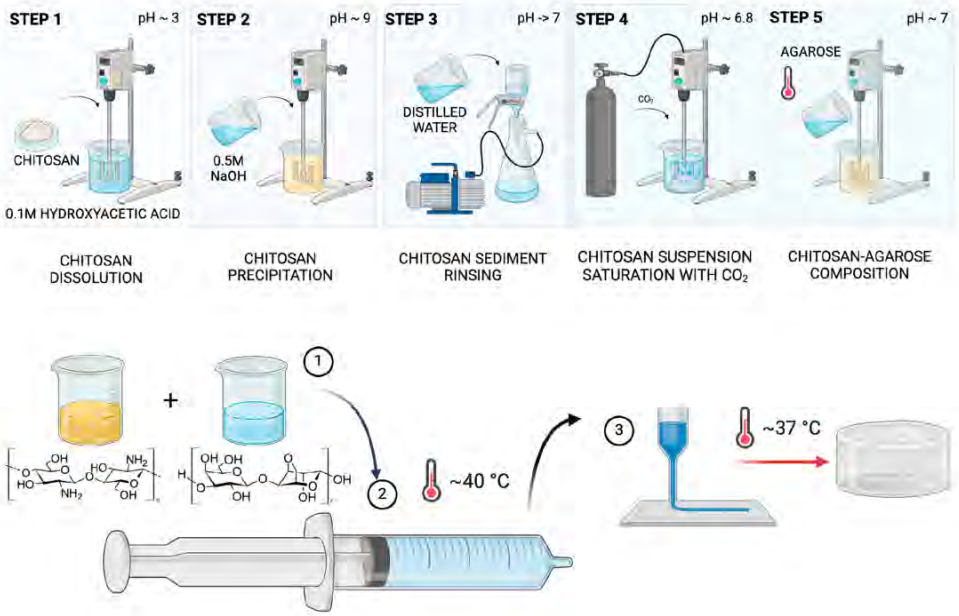

Figure 9. Schematic representation of the preparation of the chitosan–agarose composite using the carbon dioxide saturation method for chitosan processing. Created with Biorender.com.

3.3. Physiochemical Characterisation of Chitosan–Agarose Composition

3.3.1. Rheological Properties Assessment

The rheological properties of the CS and AG solutions and their composites were measured using an oscillating rheometer Anton Paar series MCR 302e (Anton Paar, Warsaw, Poland). A plate–plate system with a 25 mm diameter and 1 mm gap was used for the measurements. The impact of the shear rate on the deformation of the samples was conducted at a temperature of 37 °C and the method of a three-interval thixotropy test was applied (three-interval thixotropy test (3ITT) oscillations–rotations–oscillations). In the middle interval, the sample was deformed at a constant shear rate (1000 1/s). In the initial and final interval, the sample was tested through oscillatory shear at a constant deformation amplitude γ = 1% and angular frequency ω = 5 rad/s in order to establish the properties before and after the rotational deformation process.

3.3.2. Permeability Assessment

A modified Kirby–Bauer method was applied to study permeability in AG and CS hydrogels [23]. This modification involved the use of dyes with varying molecular weights. Initially, 1% AG and CS solutions and their compositions were prepared, then spread on Petri dishes and left to gel. For the CS solutions, this process took 48 h to allow the release of carbon dioxide necessary for gelling. After the completion of the gelling process, 100 mM solutions of dyes with molecular weights ranging from 251 to 616 g/mol were prepared. In the next step, holes with a diameter of 6 mm were cut in the gelled samples using a biopsy punch. A total of 0.150 mL of the respective dye solution was applied to each of these holes.

The samples were incubated at a temperature of 25 °C. The diameters of the dye spots were measured with a calliper at regular time intervals, which allowed for the assessment of the degree of diffusion of the dyes in the hydrogel matrices.

To assess glucose permeability, the method described by Reys and co-workers was used with slight modifications [15]. A laboratory setup was configured in which a round-bottomed three-necked flask was used as an acceptor. To this acceptor, a funnel and a metal filter from a filtration system under vacuum were connected to form the receptor part of the apparatus. The flask was placed in a temperature-controlled, i.e., 37 °C, water bath. Hydrogel membranes based on CS, AG, and their composites with a thickness of 0.4 mm were placed in the receptor part of the apparatus, stabilised with a stainless steel clamp. Before measurement, the samples were incubated for 24 h in distilled water. The round-bottom flask was then filled with distilled water and the donor space with a 10% glucose solution. At fixed time points, 2 mL samples were taken from the acceptor chamber, each time topped up with an equal amount of fresh water. The experiments were carried out with continuous stirring of the contents of the round-bottom flask using a magnetic rod to eliminate boundary layer effects that would interfere with the measurement. A colourimetric method for the determination of reducing sugars by reaction with 3,5-dinitrosalicylic acid (DNS method) was used to analyse the concentration of glucose that permeated the membrane into the round-bottom chamber. The measurement was performed at 540 nm using a Mettler UV5 spectrophotometer.

3.4. Biological Properties of Chitosan–Agarose Composition Assessment

3.4.1. Cell Culture Conditions

Immortalised human HaCaT keratinocytes (DKFZ, Heidelberg, Germany) [24,25] and the human dermal fibroblast cell line 46BR.1N (ECACC, Sigma Aldrich, St. Louis, MO, USA) were used in this study. Cells were routinely grown in culture flasks (growth surface area 25 cm^2) in Dulbecco's modified Eagle medium (DMEM, Sigma Aldrich, St. Louis, MO, USA) with 4500 mg/L of glucose, 584 mg/L of L-glutamine, sodium pyruvate, and sodium bicarbonate, supplemented with 10% FBS, 100 units/mL of penicillin, and 100 µg/mL of streptomycin (Sigma Aldrich, St. Louis, MO, USA) under a humidified atmosphere with 5% CO_2 at 37 °C. The medium was changed every 2–3 days.

3.4.2. MTT

AG, CS, and CS/AG composites were prepared in accordance with the ISO 10993-5:2009 standard. An appropriate amount of medium dedicated to 46BR.1N and HaCaT cells was added to a given composite weight (25 mg per 1 mL culture medium). Then, the prepared composites were placed in a CO_2 incubator for 24 h. After this time, the cells of the 46BR.1N and HaCaT lines seeded in a 96-well plate were replaced with the medium corresponding to a given composite for stimulation in two concentrations: 100%—adding the full volume of undiluted supernatant from previously prepared composites; and 50%—half the volume of the supernatant from a given composite diluted with DMEM HG. The cells were incubated for 24 h. After this time, the MTT test was performed in accordance with the manufacturer's instructions. MTT solution (5 mg/mL) was added to each well. After 3 h, the medium was removed, and isopropanol (6 mM) was added to the cells. Then, the plates with the cells were shaken for 30 min, and a spectrophotometric reading was performed (Synergy LX, Biotek, Winooski, VT, USA) at a wavelength of 575 nm.

3.4.3. Cell Viability Assessment

To investigate the effectiveness of the newly developed bioink in maintaining cellular viability, an experiment was conducted using a mixture of CS (1% *w*/*v*) of medium molecular weight and AG (1% *w*/*v*). These components were combined in equal proportions and incubated at 37 °C to prevent the composition from gelling. Cells, at a concentration of 1×10^6 cells/mL, were integrated with the prepared bioink and then applied to 24-well culture plates using a syringe, forming 3D structures. After the scaffolding gelled below

37 °C, the wells were filled with the appropriate medium and placed in an incubator (37 °C, 5% CO_2).

Selective staining was performed to colour live cells green and dead cells red to assess cellular viability in the produced structures. After removing the medium, the scaffolds were cleansed with phosphate-buffered saline (PBS). Then, 3 mL of PBS solution with the addition of calcein-AM (8 µM) and propidium iodide (2 µg/mL) was applied into each well. The scaffolds were incubated with the dyes in darkness at a constant temperature of 37 °C in a 5% CO_2 environment for 45 min. After the incubation, the staining solution was removed, and fluorescence microscopy observations were made (Nikon Eclipse TE300, Nikon, Tokyo, Japan). The use of CellProfiler 4.2.5 software enabled detailed analysis of the obtained images and quantification of live and dead cells.

3.4.4. Wound Healing Ibidi

The study on the impact of CS in combination with AG on the migratory capacity of cells after 24 h was conducted using Ibidi culture inserts with a predefined cell-free area, crucial for research in wound healing and cell migration. For the experiment, cells were seeded in the inserts at a concentration of 20,000 per well, utilising DMEM enriched with 10% FBS. After 24 h, the medium was replaced with serum-free DMEM, and cellular growth was inhibited by adding mitomycin C (5 µg/mL) for 2 h. Following this procedure, the medium was changed, and the cells were subjected to the extracts of the tested CS, AG, and CS/AG compositions. After another 24 h, the cells were fixed using 3.7% paraformaldehyde and then stained with a 0.05% solution of crystal violet. The results were evaluated using a Leica DMIL LED inverted microscope and GRAPHAX software.

3.4.5. Angiogenesis Assessment

Fertilised chicken eggs were obtained from a local provider (EKO ELITA, Jawory, Poland) and incubated horizontally with intermittent rotation at 37 °C and 65% humidity for 3 days. Subsequently, the eggshells were cracked open, and the embryos were transferred into sterile containers for further incubation at 37 °C with 0.5% CO_2 for 5 days. On day 8, approximately 5 mm square pieces of various materials (CS, AG, CS/AG, or Whatman filter paper) were placed on the chorioallantoic membrane (CAM). Prior to placement, all materials were UV-sterilised and rinsed with 0.9% NaCl solution. The materials were incubated on the CAM for up to 72 h. The integration of the materials with the CAM was photographed every 24 h using a stereomicroscope attached to a digital camera (Olympus Stemi 2000-C). Angiogenesis around the materials was quantified using the AngioTool 0.6 software on the IKOSA platform. On embryonic development day (EDD) 12, the embryos were humanely sacrificed. In the European Union, the CAM assay is not legally classified as an animal experiment and, therefore, does not require ethical approval (EU Directive 2010/63/EU and European Commission 2021/2784 (RSP)).

3.4.6. Wound Healing Model in Mice

A full-thickness excisional skin injury model in mice was used to investigate the effects of hydrogel compositions on wound healing. The mice, 8–10-week-old females of the BALB/c strain, were purchased from the Tri-City Academic Laboratory Animal Centre of the Medical University of Gdańsk, where they were maintained. All animal experiments were performed in compliance with the ARRIVE guidelines. The experiment protocol received approval from the Local Ethical Committee in Bydgoszcz (approval number 51/2020).

Mice were anaesthetised with isoflurane inhalations at 2–5% concentration. Before starting the experiment, the animals' backs were shaved and disinfected with Octanisept. Then, the skin on the back was folded and lifted towards the head and tail along the spinal line and biopsied using 6.0 mm diameter punches to create two symmetrical wounds. Before the application of the tested samples, mice were randomly divided into therapeutic and control groups, each consisting of six animals. Then, 2 mm thick discs of 6 mm diameter

prepared from CS/AG and AG hydrogels were placed onto the wounds. The wounds in the control mice were treated with 10 µL of carbon dioxide-saturated water. The wounds were then covered with transparent Tegaderm™ dressing (25 × 25 mm) and fastened with a self-adhesive bandage wrapped around the animal torso. After 7 days, the dressings and test preparations were replaced to avoid damaging the newly formed skin layer. After 14 days, the dressings were removed. A ruler was placed beside the wound area to measure the wound area, and photographs were taken weekly. Wound sizes were calculated using ImageJ 1.52a/Java 1.8.0_112 [26].

3.4.7. Tissue Isolation for Histological Analyses

After collection, the ears were preserved in 4% formalin buffered with PBS. The tissues were then transferred to a 15% sucrose in PBS for 24 h and then to a 30% sucrose solution in PBS for another 24 h. Then, the tissues were sectioned to 10 µm thickness on the cryostat Leica CM1520 and stained with Masson's trichrome. Image acquisition was performed with a Leica DM IL microscope at 40× magnification.

3.5. Statistical Analysis

All data reported were based on the means of three replicates ($n = 3$), except for Ibidi wound healing tests, which were performed in repetitions for three independent tests ($n = 15$), and wound healing tests in mice, where the results represented means for 12 wounds in 6 mice ($n = 12$). Experimental results were expressed as mean ± standard deviation (SD). Statistical analysis of biocompatibility of cell culture results was performed with one-way ANOVA. The differences were considered to be statistically significant at $p < 0.05$. Prism 10 V10.0.3 (GraphPad software, Boston, MA, USA) was used for the statistical computations.

4. Summary and Conclusions

This research continues the investigation into an innovative thermosensitive bioink composed of a medium-molecular-weight chitosan hydrogel formed by CO_2 saturation and an agarose hydrogel responsible for gelling. After meeting the bioink acceptance criteria, we conducted further characterisation to assess detailed flow characteristics during simulated syringe extrusion in 3D printing. An ORO test revealed that the three-dimensional structure of the CS/AG composite rapidly recovers after extrusion, unlike its components. Studies on the diffusion rates of dyes through CS/AG membranes showed that both polymer proportions and molecular weight significantly affect diffusion. Glucose permeability tests, using glucose as a model compound mimicking nutrient diffusion, confirmed effective diffusion through various CS/AG compositions, highlighting its regenerative potential.

Further studies evaluating biological safety and activity used MTT tests on selected skin cell lines (46BR.1N fibroblasts and HaCaT keratinocytes) intended as key components of the bioink. These tests confirmed the biological safety of CS, AG, and their composites in line with ISO 10993-5. The tested samples showed high cell viability, with values ranging from 85% to 112% for 46BR.1N and 90% to 137% for HaCaT cells, indicating a favourable safety profile. Additionally, it was shown that the CS/AG composition favours HaCaT cell migration, a promising finding for regenerative applications. However, 46BR.1N cells displayed moderate pro-migratory effects, suggesting the need for further optimisation to meet specific cell requirements.

In addition to cytotoxicity tests conducted after a 24 h incubation, the long-term survival of cells within the CS/AG composition was monitored. Cell survival rates for HaCaT and 46BR.1N fibroblasts after 2, 7, and 14 days confirmed that the biomaterials not only support cell proliferation but are also biocompatible. High survival rates, particularly at day 14, demonstrated the crucial role of chitosan in enhancing cell survival over time.

Based on studies using L929, HaCaT, and 46BR.1N cell lines, along with preliminary evaluations of printability and functionality, a detailed analysis of the proangiogenic potential of CS/AG biomaterials was performed. Both CS and CS/AG composites exhibited

superior proangiogenic properties compared to pure AG and the control. The absence of angiogenesis inhibition further emphasises the potential of the CS/AG composition for tissue engineering applications.

The confirmed biological safety and favourable properties of CS/AG enabled the transition to animal model studies, a critical step in assessing the effectiveness of biological therapeutic systems. Studies conducted on mice showed that CS/AG and CS dressings accelerated skin wound closure, demonstrating strong potential for future use in regenerative medicine.

5. Further Action

In our most recent studies, we were able to confirm the positive impact of the CS/AG composition on many critical biological parameters, opening up new possibilities for its use in tissue engineering. The next step will be to investigate the impact of the addition of time-releasing bioactive peptides on migratory effects and the wound healing process, as well as the possibility of creating a vascularised scaffold. Additionally, future research stages will include designing the geometry of the scaffold, optimising the arrangement of layers and cells, and determining the porosity of the scaffold to assess its permeability. Such a comprehensive approach will allow for the further customisation of bioink properties, which is crucial for its future clinical applications.

Author Contributions: A.B.-K.: Writing—review and editing, writing—original draft, visualisation, validation, conceptualisation, software, resources, methodology, investigation, formal analysis, data curation. S.M.: Project administration, methodology, investigation, funding acquisition, formal analysis, data curation, resources, software, supervision, validation, writing—original draft, writing—review and editing. N.M.: Methodology, investigation, data curation, resources, software, validation, visualisation, writing—original draft, writing—review and editing. K.C.: Methodology, investigation, data curation, resources, software, validation, visualisation, writing—original draft, writing—review and editing. P.S. (Paulina Słonimska): Data curation, formal analysis, investigation, methodology, software, validation, visualisation. M.D.: Data curation, investigation, methodology, resources, software, supervision, validation, visualisation, writing—original draft, writing—review and editing. J.B.-K.: Data curation, formal analysis, investigation, methodology, software, visualisation, validation. M.P.: Data curation, investigation, methodology, software, supervision, validation, writing—original draft, writing—review and editing. P.S. (Paweł Sachadyn): Conceptualisation, supervision, resources, data curation, formal analysis, funding acquisition, writing—review and editing. R.T.: Project administration, resources, writing—review and editing, writing—original draft, conceptualisation, validation, supervision, software, methodology, investigation, formal analysis, data curation, funding acquisition. All authors have read and agreed to the published version of the manuscript.

Funding: The financial support of these studies from Gdańsk University of Technology by the DEC-10/2021/IDUB/I.3.3 grant under the Argentum Triggering Research Grants—'Excellence Initiative—Research University' programme is gratefully acknowledged. The financial support for this research by the Gdansk University of Technology under the minigrant 2022 (036073)—'Research University' programme is gratefully acknowledged.

Institutional Review Board Statement: The experiment protocol received approval from the Local Ethical Committee in Bydgoszcz (approval number 51/2020, date 24 January 2020).

Informed Consent Statement: Not applicable.

Data Availability Statement: Data are contained within the article.

Conflicts of Interest: The authors declare no conflict of interest.

References

1. Fornetti, E.; De Paolis, F.; Fuoco, C.; Bernardini, S.; Giannitelli, S.M.; Rainer, A.; Seliktar, D.; Magdinier, F.; Baldi, J.; Biagini, R.; et al. A Novel Extrusion-Based 3D Bioprinting System for Skeletal Muscle Tissue Engineering. *Biofabrication* **2023**, *15*, 025009. [CrossRef] [PubMed]
2. Antezana, P.E.; Municoy, S.; Álvarez-Echazú, M.I.; Santo-Orihuela, P.L.; Catalano, P.N.; Al-Tel, T.H.; Kadumudi, F.B.; Dolatshahi-Pirouz, A.; Orive, G.; Desimone, M.F. The 3D Bioprinted Scaffolds for Wound Healing. *Pharmaceutics* **2022**, *14*, 464. [CrossRef]

3. DeSimone, E.; Schacht, K.; Jungst, T.; Groll, J.; Scheibel, T. Biofabrication of 3D Constructs: Fabrication Technologies and Spider Silk Proteins as Bioinks. *Pure Appl. Chem.* **2015**, *87*, 737–749. [CrossRef]
4. Deptuła, M.; Karpowicz, P.; Wardowska, A.; Sass, P.; Sosnowski, P.; Mieczkowska, A.; Filipowicz, N.; Dzierżyńska, M.; Sawicka, J.; Nowicka, E.; et al. Development of a Peptide Derived from Platelet-Derived Growth Factor (PDGF-BB) into a Potential Drug Candidate for the Treatment of Wounds. *Adv. Wound Care* **2020**, *9*, 657–675. [CrossRef] [PubMed]
5. Banach-Kopeć, A.; Mania, S.; Pilch, J.; Augustin, E.; Gabriel, I.; Tylingo, R. A novel method of endotoxins removal from chitosan hydrogel as a potential bioink component obtained by CO_2 saturation. *Int. J. Mol. Sci.* **2022**, *23*, 5505. [CrossRef]
6. Gu, Z.; Fu, J.; Lin, H.; He, Y. Development of 3D Bioprinting: From Printing Methods to Biomedical Applications. *Asian J. Pharm. Sci.* **2020**, *15*, 529–557. [CrossRef] [PubMed]
7. Dell, A.C.; Wagner, G.; Own, J.; Geibel, J.P. 3D Bioprinting Using Hydrogels: Cell Inks and Tissue Engineering Applications. *Pharmaceutics* **2022**, *14*, 2596. [CrossRef] [PubMed]
8. Nie, L.; Wang, C.; Deng, Y.; Shavandi, A. Bio-Inspired Hydrogels via 3D Bioprinting. In *Biomimetics*; Bio-Inspired Hydrogels via 3D Bioprinting; IntechOpen: London, UK, 2020. [CrossRef]
9. Feng, P.; Luo, Y.; Ke, C.; Qiu, H.; Wang, W.; Zhu, Y.; Hou, R.; Xu, L.; Wu, S. Chitosan-Based Functional Materials for Skin Wound Repair: Mechanisms and Applications. *Front Bioeng. Biotechnol.* **2021**, *9*, 650598. [CrossRef]
10. Matica, M.A.; Aachmann, F.L.; Tøndervik, A.; Sletta, H.; Ostafe, V. Chitosan as a wound dressing starting material: Antimicrobial properties and mode of action. *Int. J. Mol. Sci.* **2019**, *20*, 5889. [CrossRef]
11. Guo, Y.; Huang, J.; Fang, Y.; Huang, H.; Wu, J. 1D, 2D, and 3D scaffolds promoting angiogenesis for enhanced wound healing. *Chem. Eng. J.* **2022**, *437*, 134690. [CrossRef]
12. Butler, H.M.; Naseri, E.; MacDonald, D.S.; Tasker, R.A.; Ahmadi, A. Investigation of rheology, printability, and biocompatibility of N, O-carboxymethyl chitosan and agarose bioinks for 3D bioprinting of neuron cells. *Materialia* **2021**, *18*, 101169. [CrossRef]
13. Banach-Kopeć, A.; Mania, S.; Tylingo, R. Marine polymers in tissue bioprinting: Current achievements and challenges. *Rev. Adv. Mater. Sci.* **2024**, *63*, 20230180. [CrossRef]
14. Reys, L.L.; Silva, S.S.; Soares da Costa, D.; Rodrigues, L.C.; Reis, R.L.; Silva, T.H. Building Fucoidan/Agarose-Based Hydrogels as a Platform for the Development of Therapeutic Approaches against Diabetes. *Molecules* **2023**, *28*, 4523. [CrossRef] [PubMed]
15. Owczarz, P.; Ziółkowski, P.; Modrzejewska, Z.; Kuberski, S.; Dziubiński, M. Rheo-Kinetic Study of Sol-Gel Phase Transition of Chitosan Colloidal Systems. *Polymers* **2018**, *10*, 47. [CrossRef] [PubMed]
16. Xu, H.; Liu, J.C.; Zhang, Z.Y.; Xu, C.X. A review on cell damage, viability, and functionality during 3D bioprinting. *Mil. Med. Res.* **2022**, *9*, 70. [CrossRef] [PubMed]
17. Ozbolat, I.T.; Hospodiuk, M. Current advances and future perspectives in extrusion-based bioprinting. *Biomaterials* **2016**, *76*, 321–343. [CrossRef] [PubMed]
18. Hafezi, F.; Shorter, S.; Tabriz, A.G.; Hurt, A.; Elmes, V.; Boateng, J.; Douroumis, D. Bioprinting and Preliminary Testing of Highly Reproducible Novel Bioink for Potential Skin Regeneration. *Pharmaceutics* **2020**, *12*, 550. [CrossRef] [PubMed]
19. Gwak, M.A.; Lee, S.J.; Lee, D.; Park, S.A.; Park, W.H. Highly gallol-substituted, rapidly self-crosslinkable, and robust chitosan hydrogel for 3D bioprinting. *Int. J. Biol. Macromol.* **2023**, *227*, 493–504. [CrossRef] [PubMed]
20. Chen, H.; Fei, F.; Li, X.; Nie, Z.; Zhou, D.; Liu, L.; Zhang, J.; Zhang, H.; Fei, Z.; Xu, T. A facile, versatile hydrogel bioink for 3D bioprinting benefits long-term subaqueous fidelity, cell viability and proliferation. *Regen Biomater.* **2021**, *8*, rbab026. [CrossRef]
21. Kohli, N.; Sawadkar, P.; Ho, S.; Sharma, V.; Snow, M.; Powell, S.; Woodruff, M.A.; Hook, L.; Garcia-Gareta, E. Pre-screening the intrinsic angiogenic capacity of biomaterials in an optimised ex ovo chorioallantoic membrane model. *J. Tissue Eng.* **2020**, *11*. [CrossRef]
22. Banach-Kopeć, A.; Mania, S.; Tylingo, R.; Wawrzynowicz, A.; Pawłowska, M.; Czerwiec, K.; Pikuła, M. Thermosensitive composite based on agarose and chitosan saturated with carbon dioxide. Preliminary study of requirements for production of new CSAC bioink. *Carbohydr. Polym.* **2024**, *336*, 122120. [CrossRef] [PubMed]
23. Jan, H. Kirby-Bauer Disk Diffusion Susceptibility Test Protocol. *Am. Soc. Microbiol.* **2009**, *15*, 1–23.
24. Boukamp, P.; Popp, S.; Altmeyer, S.; Hülsen, A.; Fasching, C.; Cremer, T.; Fusenig, N.E. Sustained nontumorigenic phenotype correlates with a largely stable chromosome content during long-term culture of the human keratinocyte line HaCaT. *Genes Chromosomes Cancer* **1997**, *19*, 201–214. [CrossRef]
25. Boukamp, P.; Petrussevska, R.T.; Breitkreutz, D.; Hornung, J.; Markham, A.; Fusenig, N.E. Normal keratinisation in a spontaneously immortalised aneuploid human keratinocyte cell line. *J. Cell Biol.* **1988**, *106*, 761–771. [CrossRef] [PubMed]
26. Schneider, C.A.; Rasband, W.S.; Eliceiri, K.W. NIH Image to ImageJ: 25 years of image analysis. *Nat. Methods* **2012**, *9*, 671–675. [CrossRef] [PubMed]

6.5 [A5] Marine polymers in tissue bioprinting: Current achievements and challenges.

6.5.1 Wkład pracy doktoranta

Tytuł: Marine polymers in tissue bioprinting: Current achievements and challenges.
Autorzy: Adrianna Banach-Kopeć, Szymon Mania, Robert Tylingo
Czasopismo: REVIEWS ON ADVANCED MATERIALS SCIENCE
Rok wydania: 2024
Impact factor: 3,6
Liczba punktów wg MNiSW: 100
DOI: 10.1515/rams-2023-0180
Procentowy wkład pracy doktoranta: 60%

Mój wkład w przygotowanie niniejszego artykułu polegał na przeprowadzeniu szczegółowego przeglądu literatury dotyczącego wykorzystania polimerów morskich w biodruku, ze szczególnym uwzględnieniem obecnych osiągnięć i wyzwań w tej dziedzinie. Przegląd literatury przeprowadziłam w oparciu o następujące bazy danych takie jak PubMed, ScienceDirect oraz *Wiley* i *Taylor & Francis*, kładąc nacisk na najnowsze prace opublikowane w ciągu ostatnich 20 lat. Zebrane informacje pozwoliły na stworzenie kompleksowego przeglądu literaturowego, w którym omówiłam kluczowe zastosowania, problemy i potencjał aplikacyjny w tej dziedzinie. Dodatkowo, pełniłam rolę autora korespondencyjnego oraz przygotowywałam odpowiedzi na uwagi recenzentów.

6.5.2 Treść artykułu

DE GRUYTER Reviews on Advanced Materials Science 2024; 63: 20230180

Review Article

Adrianna Banach-Kopeć*, Szymon Mania, and Robert Tylingo

Marine polymers in tissue bioprinting: Current achievements and challenges

https://doi.org/10.1515/rams-2023-0180
received August 30, 2023; accepted January 19, 2024

Abstract: Bioprinting has a critical role in tissue engineering, allowing the creation of sophisticated cellular scaffolds with high resolution, shape fidelity, and cell viability. Achieving these parameters remains a challenge, necessitating bioinks that are biocompatible, printable, and biodegradable. This review highlights the potential of marine-derived polymers and crosslinking techniques including mammalian collagen and gelatin along with their marine equivalents. While denaturation temperatures vary based on origin, warm-water fish collagen and gelatin emerge as promising solutions. Building on the applications of mammalian collagen and gelatin, this study investigates their marine counterparts. Diverse research groups present different perspectives on printability and cell survival. Despite advances, current scaffolds are limited in size and layers, making applications such as extensive skin burn treatment or tissue regeneration difficult. The authors argue for the development of bioprinting, which includes spherical and adaptive printing. In adaptive printing, layers differentiate and propagate sequentially to overcome the challenges of multilayer printing and provide optimal conditions for the growth of deeply embedded cells. Moving the boundaries of bioprinting, future prospects include transformative applications in regenerative medicine.

Keywords: bioprinting, polymers, marine-derived polymers, tissue engineering

* **Corresponding author: Adrianna Banach-Kopeć,** Department of Chemistry, Technology and Biotechnology of Food, Faculty of Chemistry, Gdansk University of Technology, 11/12 G. Narutowicza Street, 80-233 Gdansk, Poland, e-mail: adrianna.banach@pg.edu.pl
Szymon Mania, Robert Tylingo: Department of Chemistry, Technology and Biotechnology of Food, Faculty of Chemistry, Gdansk University of Technology, 11/12 G. Narutowicza Street, 80-233 Gdansk, Poland

1 Introduction

The development of regenerative medicine, and thus new opportunities so far unattained in tissue engineering, has been made possible by combining cell culture-related technologies, materials science, and 3D printing. The primary tissue engineering strategy is to produce functional *in vitro* constructs capable of restoring, preserving, and revitalizing lost tissues and organs using bioprinting [1,2]. The advantage of bioprinting over conventional cell scaffolds fabrication techniques such as solvent casting, gas forming, membrane lamination, salt leaching, and fiber binding makes it possible to mimic the complex microstructure of biological tissues. The bioprinting technique provides the ability and versatility to deliver cells from complex microstructures with excellent spatial distribution by focusing on three approaches: biomimicry, autonomous cell self-organization, and mini-tissue building blocks [3]. The first approach involves understanding the microenvironment of a given tissue. Therefore, when designing cellular scaffolds, the distribution of cells and the composition of the extracellular matrix (ECM), among other things, must be taken into account. On the other hand, autonomous self-assembly is based on the ability of early cellular components to develop into tissues that produce their own ECM, appropriate cellular signals, and organization to achieve the desired structure and function. The last concept, mini-tissue blocks, assumes that organs and tissues are built from smaller building blocks called mini-tissues that can self-assemble [1]. The advantage of bioprinting over typical regenerative medicine methods is the accurate distribution and high-resolution deposition of cells. However, the main disadvantages of this method due to printing techniques, such as printing speed, scalability, and resolution, limit its application in medicine. Therefore, the critical issue of bioprinting is optimizing their mechanical and biological properties, which will be suitable for depositing living cells and enabling the regenerated tissue to function correctly. Additionally, these parameters are essential for achieving specific biological functions without compromising mechanical properties [4]. Another critical problem of bioprinting is

the selection of suitable biomaterials, *i.e.*, those that meet all the criteria for scaffolds: biodegradability, biocompatibility, non-cytotoxicity, and porosity that provides the conditions necessary to form new tissue and promote cell growth throughout the regeneration period. An essential property of cellular scaffolds is that they adhere well to the application site, have good mechanical properties and are permeable to gases and cellular metabolites. Hydrogels, for instance, are a group of biomaterials with the advantage of having a structure similar to ECM, so they can imitate the properties of various tissues. Other properties of hydrogels, particularly relevant to cellular scaffolding, include their high porosity and ability to carry low molecular weight substances and nutrients necessary for cell activity [5]. Moreover, the adaptation of hydrogels in 3D printing is possible due to their sol–gel transformation through appropriately selected conditions.

This publication focuses on the latest literature data on the development of bioprinting in recent years. Crucial issues from the point of view of the requirements of bioinks in terms of their biological and physicochemical properties, as well as the possibilities of the bioprinting techniques used so far, are discussed. Accordingly, the advantages and disadvantages of the various systems were pointed out, and the future direction of research on bioprinting and bioinks was determined. This review highlights innovative applications of marine polymers in bioprinting, emphasizing their unique biological properties and the necessity to develop multi-component systems compatible with tissue engineering requirements. Additionally, this review exemplifies an interdisciplinary approach, integrating scientific fields such as biology, chemistry, and materials engineering, which are crucial in bioink design. Having this focus on marine-derived polymers as basic components of bioinks offers a new perspective on material selection and functionality. In conclusion, this review summarizes and analyzes recent developments and potential future directions in bioprinting, while promoting further research and innovation in the use of marine polymers for bioprinting applications.

2 Bioprinting techniques

Bioprinting is a type of additive manufacturing, or three-dimensional printing, which aims to produce a scaffold with a microarchitecture that ensures its stability and the proliferation of cells within it. Inherent in bioprinting is the bioink, which consists of cells, biomaterials, and biological molecules. Bioprinting aims to provide an alternative to autologous and allogeneic tissue transplants. In addition, using bioprinting, it will be possible to bypass animal testing to study diseases and develop new treatments [6]. Among bioprinting techniques (Table 1), there are four leading technologies, each derived from analogous 3D printing methods: inkjet printing, extrusion, stereolithography and laser-assisted bioprinting. With the continuous progress in the field of bioprinting, parameters such as resolution or cell viability in the mentioned bioprinting methods have become more convergent and similar. The only differences between these methods, other than the printing method used, are mainly the viscosity of the applied composition and the possibility of using particular crosslinking techniques. Comparing these four methods, it is extrusion printing and inkjet that offers the most possibilities. This is a result of the possibility to choose from several crosslinking methods and the natural polymers used, which are characterized by higher viscosity and not always the possibility of their crosslinking, such as under UV without additional modifications or the addition of crosslinking agent. Figure 1 provides a summary of the various bioprinting methods described in detail in Sections 2.1–2.4 below. The graphic shows a comparative analysis of bioprinting techniques – presenting a comprehensive overview of the bioprinting landscape based on the Scopus database.

2.1 Inkjet bioprinting

The first bioprinting technology was inkjet bioprinting, published in 2003, the principle of which is similar to conventional inkjet printing. This method involves generating a droplet composed of cells and biomaterials by the printer head and then placing it on a substrate [7]. The disadvantages of this method are the generation of high thermal and mechanical stresses, which can damage the cells encapsulated in the bioink, and the restriction to low-viscosity solutions, unlike extrusion bioprinting [8]. It is commonly believed that inkjet printing is for solutions with viscosity in the range of 3–30 mPa·s (Table 1), surface tension of 20–70 $mJ \cdot m^{-2}$, and a density of about 1,000 $kg \cdot m^{-3}$. In the case of suspended particles, their diameter is approximately 50 μm due to the diameter of the nozzle. The advantage of inkjet printing is that it provides the best printing resolution, as a result of the ability to control both the size of the droplets and their position and deposition rate. In inkjet bioprinting, there are two droplet formation methods, *i.e.*, continuous inkjet and drop-on-demand type (DOD). The first method relies on the natural ability of the liquid stream to turn into a string of droplets, whose position is determined

Table 1: Comparison of 3D printing methods used in bioprinting [27,36–40]

Parameters	Bioprinting methods			
	Inkjet	Extrusion	Laser assisted	Stereolithography
Printing process	Serial (drop by drop)	Serial (line by line)	Serial (dot by dot)	Parallel and continuous (projection based)
Gelation strategy	Chemical-crosslinking	Chemical-crosslinking (Schiff base or genipin)	Chemical-crosslinking	Chemical-crosslinking
	Photo-crosslinking	Physical-crosslinking (ionic or electrostatic interaction)	Photo-crosslinking	Photo-crosslinking
	Temperature induced	Photo-crosslinking		
		Temperature induced		
		Enzymatic cross-linking (tyrosinase)		
Material viscosity	3–30 mPa·s	up to 6×10^7 mPa·s	1–300 mPa·s	No limitation
Printing speed	Fast	Slow	Medium	Fast
Resolution	High	Dependent on bio-ink and crosslinking method	High	High
	Thermal: 30–80 µm	from low to high	10–100 µm	
	Piezoelectric: 50–100 µm			
Cell viability	Thermal: 90%	80–96%	>95%	Up to 93%
	Piezoelectric: 70–95%			
Bionk composition	Alginate-gelatin [41]	Alginate-carboxymethylated chitosan-agarose [48]	Methacrylated gelatin [59]	Gelma [61–64]
	Methacrylated gelatin [42]	*N,O*-carboxymethyl chitosan-agarose [49]	Human collagen type I [60]	Methacrylated hyaluronic acid (HAMA)-methacrylated gelatin [65,66]
	Collagen-fibrinogen-thrombin proteins [35]	Alginate-agarose-nanocellulose [50]	MatriDerm® collagen matrix [34]	Alginate or agarose [67]
	Alginate [43]	Alginate-agarose-methylcellulose [51]	Alginate [59]	
	Alginate [44,45]	Agarose-gelatin [52]		
	Alginate-fibrinogen [46]	Alginate-κ-carrageenan [53]		
	Alginate-silk fibroin [47]	Alginate-oxidized alginate [54]		
		Gelatin-alginate [55–58]		
Conclusion	High printing resolution, but only for materials with low viscosity	Wide range of viscosity for the compositions used, but better resolution for those with high viscosity	One of the highest cell survival indices, high precision, and resolution, but there is a need to protect cells from high-energy UV radiation by additional layers, for example, of metal, which absorbs the laser and protects the cells	High resolution and cell viability. However, UV radiation may damage the cells, hence the necessity of using specific PIs
	High survivability, but membrane damage may occur as a result of sonication	A wide range of crosslinking methods and polymers used, however, there is a problem with maintaining high printability and cell viability simultaneously		

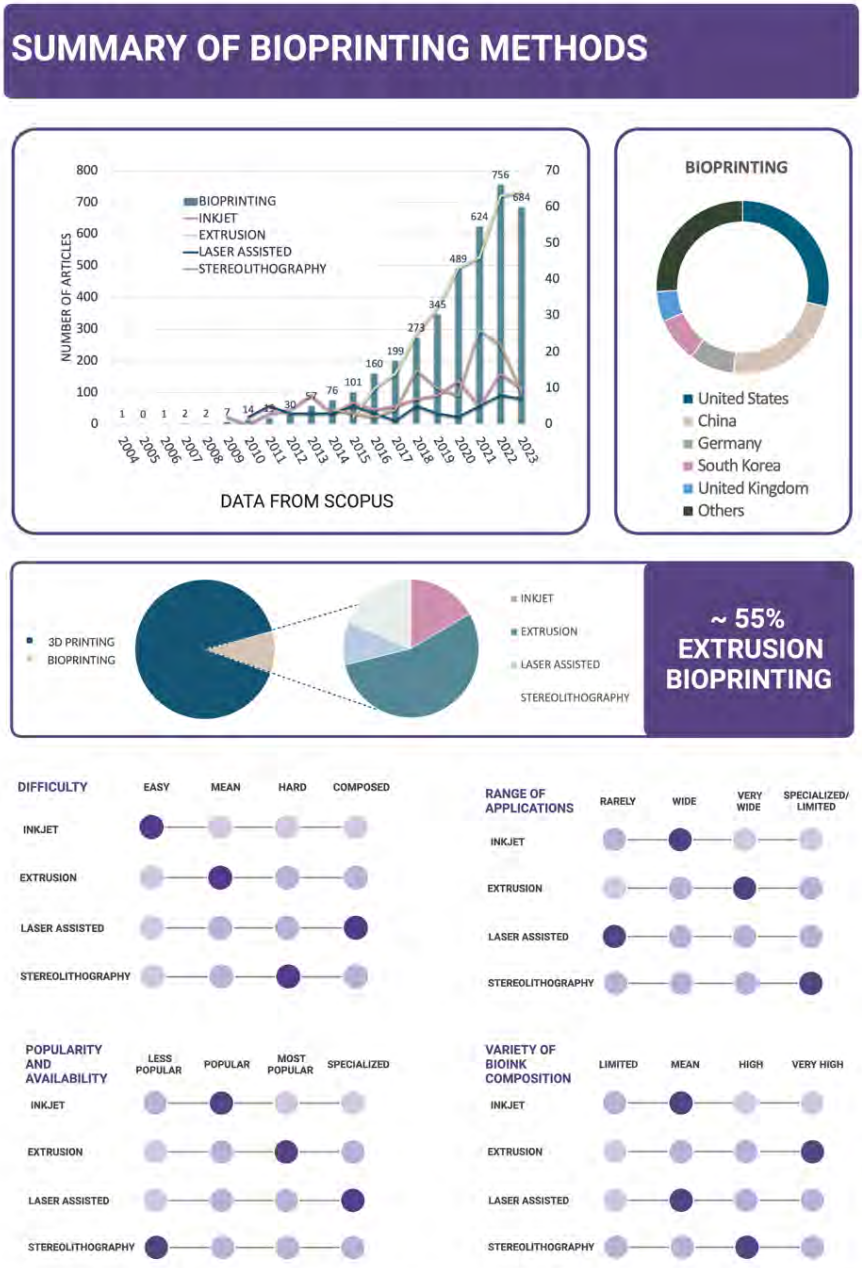

Figure 1: A comparative analysis of bioprinting techniques – a comprehensive overview of the bioprinting landscape, showing the increase in the number of scientific articles from 2004 to 2023, each country's contribution to the field, and the breakdown of articles into 3D printing and bioprinting by method. In addition, it provides a qualitative assessment of different bioprinting methods based on difficulty, range of applications, popularity, and complexity of biomaterials, with extrusion bioprinting highlighted as the most common method, accounting for about 55% of research. The data come from the Scopus database (created with BioRender.com).

by magnetic and electric fields that interact with the charged droplets. However, this method is rarely used in bioprinting due to its poor resolution. The second technique, with better resolution, is DOD, which distinguishes between thermal and piezoelectric control. Thermal control involves quickly heating a small part of the injecting head to 300°C. The temperature rise generates vapor bubbles in the bioink, which combine and expand to generate a pressure pulse. The short temperature rise time does not contribute significantly to cell survival. As a result, the temperature of the bioink increases by 4–10°C, which results in a post-printing cell survival rate of about 90% [9]. However, the main problem with thermal inkjet printing is the nozzle clogging during bioprinting.

Nozzle clogging can occur when the printer's parameters are not properly adjusted to the properties of the bioink. Clogging may happen if the nozzle's diameter is smaller than the particles within the ink. Therefore, it is advisable for the printer nozzle's diameter to be at least 100 times greater than the largest particles in the bioink. Besides particle size, cell concentration also influences the risk of clogging. At concentrations around 5×10^6 cells per milliliter, clogging can result from cell agglomeration within the ink. It is thus recommended to use bioinks with a cell concentration between 1×10^6 and 4×10^6 cells per milliliter. The design of the printer head may also contribute to nozzle clogging. Considerations during bioprinting should include the height of the inner chamber and the various types of coatings within the jet chamber [10]. Li *et al.* have addressed the issue of clogging in piezoelectric inkjet printers using inks that contain dispersed nanoparticles ranging from 28 to 530 nm, which can aggregate and lead to the formation of thick layers on the head's surface. Hydrophobic nanoparticles are particularly problematic as they can cause air entrapment due to the deformation of the ink–air meniscus, leading to air being drawn in and air bubbles adhering to the head's internal surfaces. This can result in blockages, which may be minimized by employing colloidal stable inks and suitably modifying the head surfaces to prevent particle adsorption [11].

The second method, with control by a piezoelectric motor placed in the head, involves applying a voltage and mechanically deforming the shape of the bioink. The resulting acoustic wave creates pressure, which ejects the droplet onto the substrate. Unfortunately, due to sonication in the 15–25 kHz frequency range, damage to cell membranes can occur, leading to cell lysis [12].

A key aspect in DOD bioprinting is shear stress, which affects cell viability and proliferation. This variable depends on both the properties of the bioink, such as viscosity, and the parameters of the bioprinter, such as voltage and nozzle diameter. Shi and colleagues found that the shear stress exhibits significant fluctuations at the nozzle orifice, especially throughout the period of the voltage pulse's increase and its sustained duration in the process. Another phenomenon that negatively affects cell survival is the increase in shear stress on the walls caused by backflow, which pushes the incoming fluid down along the wall [13].

Another factor significantly affecting cell viability and proliferation is the droplet impact velocity and its volume. Ng and colleagues have shown that a lower droplet impact velocity, achievable by increasing the concentration of cells in the bioink, reduces splashing and thus enhances cell survival. They concluded that the optimal droplet volume, which significantly limits evaporation, is about 20 nL. Maintaining the printing time for each layer at approximately 2 min prevents excessive evaporation, and ensuring an optimal concentration of 4×10^6 cells per milliliter is crucial for maintaining cell viability and promoting cell proliferation [10].

Inkjet printing was used, among other things, in a study by Lee *et al.* to print scaffolds for human skin regeneration. The bioscaffold consisted of keratinocyte and fibroblast cells representing components of the epidermis and dermis, as well as collagen as a component of the dermis matrix. The study was a preliminary optimization of printing parameters to achieve maximum cell survival, which was as high as 98% [14]. One of the widely used bioink in inkjet printing is that based on alginate. Jia *et al.* used this technique to investigate the viscosity and density of alginate solutions on their printability and the effect of oxidation level on the proliferation of human adipose tissue stem cells hADSCs. The results were used to create a tunable platform to determine the ideal concentration ranges of oxidized alginate suitable for printing and providing high survival rates as well as modulating hADSC function [15]. Another study by Boland *et al.* investigated a hybrid bioink based on alginate and gelatin, which were cross-linked with a calcium chloride solution. It was shown that the developed bioink with the applied bioprinting method enabled the contraction of a scaffold with the appropriate architecture, enabling the adhesion of endothelial cells [16].

The idea of inkjet bioprinting captures attention due to its precision in depositing droplets, enabling exact placement of individual cells. Yet, this is a sophisticated and intricate method, and its application in tissue engineering is not yet fully realized. The demand for low-viscosity bioinks necessitates almost instantaneous crosslinking; conversely, introducing a crosslinking agent into the bio-ink risks clogging the nozzle. The timing and dimensions of the print job are also crucial considerations. To print a large object with inkjet technology requires a coordinated effort

from multiple print heads, which adds complexity to the process. From our perspective, inkjet bioprinting is poised to remain a tool predominantly used in research settings, where the focus is on small-scale analysis, the development of novel bio-inks, and the meticulous positioning of a variety of cells. However, it is important to acknowledge that similar outcomes may be attainable with extrusion bioprinting. This method benefits from the higher viscosity of bio-inks, which affords a more generous window for crosslinking. We posit that until the inkjet bioprinting technology and its strategic applications are fully refined, alternative methods like extrusion bioprinting may advance the field by enhancing the existing scope of applications.

2.2 Extrusion bioprinting

Another bioprinting method is extrusion, the most widely used continuous printing technology developed as an alternative to inkjet bioprinting, which is limited to low-viscosity solutions.

However, extrusion bioprinting does not apply only to hydrogels. When the material used in the printing is filaments, their printing is done by melting it and depositing it on previously created layers of solidified material. This type of extrusion printing is a fused deposition method (FDM) of thermoplastic polymers. Tylingo *et al.* proposed a new method for producing chitosan-based thermoplastic fibers that can be extruded and used in biomedical engineering [17]. Also, Zenobi *et al.* proposed first printing a bone implant and then seeding a SAOS-2 bone-like cell model onto it [18]. On the other hand, Kalva *et al.* proposed an FDM for printing bone implants based on polylactic acid and magnesium [19]. However, the possibilities of extrusion printing methods are much broader from implants, prostheses, surgical instruments to laboratory models and even other fields such as textiles, armaments, automobiles, and music [20]. The method involves extruding bio-ink through a print head and creating a three-dimensional scaffold using a layer-by-layer method in the form of fibers. Extrusion bioprinters can be driven by piston, screw, or pneumatic mechanisms [21]. Extrusion bioprinting has a wide range of applications due to its ability to print hydrogels with viscosities in the range of 30 mPa·s to more than 6×10^7 mPa·s (Table 1) and print large-sized objects. However, a significant limitation of this printing method is its low resolution compared to other methods, *i.e.*, the minimum size that can be printed. The resolution of extrusion bioprinting is 200–1,000 μm, making it challenging to obtain objects with complex features. In addition, a trade-off between printability and cell survival is necessary using extrusion technology. The only solution to get the best performance of the print itself as well as good cell survival is to find a bio-ink that shears when a deforming force is applied and whose viscosity increases as soon as the force is removed, in order to preserve the shape. Another important parameter is yield stress, which determines what is required to maintain continuous and smooth deposition. An important parameter that must be controlled during bioprinting is also the shear stress created by the downward movement of the piston at the nozzle interface, which can damage cells suspended in the bio-ink. Therefore, it is necessary to select bioprinting parameters, among others, such as low shear forces to achieve a high cell survival rate [22].

Cell survival during extrusion is a complex process influenced by numerous variables, such as bio-ink composition, printing parameters, and the crosslinking method. For instance, a smaller nozzle size necessitates higher extrusion pressure, which, while crucial for high printability, may compromise cell viability. In contrast, larger nozzle sizes may enhance cell survival. Thus, optimizing the bioprinting process settings is crucial [23]. The diversity of crosslinking methods in extrusion printing is also noteworthy, necessitating the careful selection and optimization of the most suitable method. When crosslinking alginate-based bio-inks with calcium ions, the method of ion incorporation and the duration of the polymer solution's exposure to metal ions are critical. Techniques such as bath-assisted printing, spraying a mist of metal ions onto the printing nozzle, or pre-crosslinking must be finely tuned. Overlong exposure to metal ions or too high concentrations can diminish cell viability. Similarly, with chemical crosslinking methods, fine-tuning the concentration and duration of crosslinking is essential to prevent cell damage. In light-induced crosslinking, minimizing the concentration of photoinitiators (PIs) and the intensity of light is paramount. Nonetheless, a lower concentration of PIs necessitates longer exposure times. Crosslinking with visible light may offer a preferable alternative. Generally, UV exposure and the generation of free radicals by PIs can cause cell damage. When selecting a crosslinking method, it is imperative to consider not only cell viability but also the gelation time and the mechanical properties of the constructs. Constructs produced by physical or thermal methods often fracture and lack strength. For thermal crosslinking, maintaining temperatures close to physiological levels is vital to avoid negatively impacting cell survival and proliferation [24].

Extrusion bioprinting technology was used, among others, in a study by Lee *et al.*, where they compared the effect of the type of methacrylated gelatin type A and B on

their printability. The study showed that even a 20% concentration of both gels in the bioprint enabled the survival of about 75% of Huh-7.5 human liver cancer cells [25]. Other studies on extrusion printing include the work of López Marcial *et al.*, which focused on agarose-enhanced alginate bio-ink and compared it with the commercially available hydrogel Pluronic, known for its specific printing properties. Cell survival was assessed using chondrocytes taken from the ankle joints of young cattle. The study showed that cell survival after 28 days was about 70%. After this time, the formation of a spatial structure produced by the embedded cells in the bio-ink was also observed [26]. In Li *et al.*'s study, on the other hand, research was conducted on developing a bio-ink consisting of anionic hydrogel, *e.g.*, alginate, xanthan, and κ-carrageenan, and cationic hydrogel, *e.g.*, chitosan, gelatin, and methacrylated gelatin, to form a polyelectrolyte complex. Using extrusion technology, they developed a bio-ink based on κ-carrageenan and methacrylated gelatin that provided good survival of C2C12 mouse myoblast cells of more than 96% after 2 days of printing. In addition, after 5 days, it was noted that the cells began to form their three-dimensional network [27].

Extrusion bioprinting is the predominant method in bioprinting, prized for its versatility and broad applicability. A significant advantage of extrusion printing is the ability to employ readily available natural polymers, often without the necessity for further modification. This greatly streamlines the bioprinting process. Although the precision of extrusion printing is slightly less than that of other techniques, we believe it is adequate for bioprinting. In this field, the primary goal is to enable cells to proliferate and form tissues or organs, rather than to replicate designs with high precision. Deviations of a few micrometers compared to other printing techniques are tolerable, as cells ultimately dictate the geometry of the final structure. However, despite its simplicity and accessibility, selecting appropriate raw materials and curing techniques to ensure the correct bio-ink viscosity remains a challenge. This viscosity is crucial to ensure both optimal printability and cell survival. Furthermore, we see the adaptability of extrusion printing as a significant benefit. It allows for the modification of standard 3D printers for bioprinting purposes, thereby expanding personalization and innovation opportunities. We are already witnessing advancements in extrusion printing, such as its integration with robotic systems for what is known as spherical printing. In summary, extrusion printing, with its simplicity and efficiency, represents a promising future for bioprinting. It offers rapid, cost-effective solutions in tissue engineering and regenerative medicine and, most importantly, provides wide-ranging application possibilities.

2.3 Stereolithography bioprinting

Another bioprinting technique is stereolithography, or crosslinking by photopolymerization. Stereolithography is a technique whose printing fidelity, architectural complexity, and bioprinting applications have not been fully explored [28].

Unlike other techniques where layers are printed sequentially, stereolithography depends on the spatial control of illumination to achieve a higher resolution of the bioprint. In this technique, the source of the laser is pivotal, providing the energy necessary to initiate the polymerization reaction through light of an appropriate wavelength. Hence, the optimization of the wavelength, intensity, and exposure time is crucial. This includes wavelengths in the UV range (365–385 nm) and visible light (405 nm). The shorter the excitation wavelength, the more potentially harmful it can be to cell survival, as shorter wavelengths carry higher energy, which may cause greater damage to cellular DNA. Another significant factor affecting cell survival is the viscosity of the bioresins, which in this technique range from approximately 0.25–10 Pa·s. A low viscosity of the bioresin facilitates rapid curing. However, excessively low viscosity can cause cell sedimentation, leading to reduced uniformity of the constructs. Therefore, a balance must be struck between the speed of fabrication and the precision of printing. When bioprinting multi-material scaffolds, an additional rinsing step with water or saline is required to diminish the mixing of bio-inks due to the infiltration of excess uncrosslinked solvent, which complicates the bioprinting process. Moreover, due to the harmful effects of UV radiation on cells, the use of PIs that cure under visible light, such as lithium phenyl-2,4,6-trimethylbenzoylphosphinate, camphorquinone, Eosin Y, and their derivatives, is recommended [29]. These PIs are essential for cell survival, as their properties – biocompatibility, water solubility, and efficiency in light absorption – directly influence the cells' ability to adhere, proliferate, and survive. Therefore, selecting the appropriate PI is essential to ensure that cells can endure and function both during and after the printing process. Additionally, PIs are responsible for the generation of free radicals through PI dissociation, as well as any subsequent effects from unreacted double bonds that may have cytotoxic consequences. It is these free radicals that most adversely affect cell viability [30].

Morris *et al.* conducted research on the use of stereolithography in bioprinting. In their work, researchers developed a hybrid resin using chitosan and polyethylene glycol diacrylate (PEGDA) and the corresponding PI Irgacure 819. PEGDA is a frequently used compound for the photopolymerization of cell scaffolds. It is non-cytotoxic and non-immunogenic; however, it does not degrade. With the addition of chitosan, it was possible to increase the

viscosity of the bio-ink while reducing the concentration of PEGDA from 30 to 6.5%, which in turn allowed for better cell survival and adhesion in the scaffold [31].

Stereolithography is one of the most advanced printing methods that allows the creation of extremely precise objects superior to many other bioprinting techniques and, moreover, at high speed. Like inkjet printing, however, it is characterized by a certain complexity. It requires the use of photosensitive resins, and this results in certain material limitations. Due to the need for high cell survival rates, it is optimal to adjust the PIs so that UV radiation is in the visible light range. Further, as with inkjet printing, the ability to print large objects is not possible due to the small size of the printers. Certainly, high precision is an important advantage in bioprinting, but it must be remembered that the variety of materials in stereolithography is limited. As for the printing system itself, there is no room for additional modifications to be controlled here. It is crucial to develop new resins and PIs that are safe for cells and provide the expected functionality of the printed structures.

2.4 Laser-assisted bioprinting (LAB)

LAB is a technique that prevents cell stress by enabling cell survival rates of more than 95% (Table 1). This type of bioprinting provides such high cell survival rates because there is no direct contact between the bio-ink and the dispenser during printing [7]. LAB makes it possible to obtain prints with high precision and resolution. A typical LAB consists of a 193 nm, 248 nm pulsed UV laser source, a near-UV 1,064 nm laser whose deposition energy is 1–20 J per pulse, and a ribbon coated with a bio-ink and a receiving substrate with a medium on which the bio-ink will be deposited [32]. In order to protect the cells contained in the bio-ink from the damaging effects of high-energy UV radiation, an additional layer of metal, *e.g.*, titanium and gold or its oxide, is placed between the ribbon and the bio-ink, which absorbs the laser and, due to rapid thermal expansion, allows a small amount of bio-ink to be spread onto the substrate. Of course, this bioprinting technique has variations involving the use of, for example, low-power pulsed radiation, which eliminates the need for an additional sacrificial layer [33].

The unique properties of LAB, such as the ability to position different cell types in an exact three-dimensional spatial pattern, were exploited in their study by Michael *et al.* To construct a multilayer skin substitute, they placed fibroblast and keratinocyte cells in Matriderm® bio-ink, which was a mixture of collagen and elastin [34]. In a study by Gudapati *et al.*, the effects of alginate concentration, gel time, and laser influence were examined, showing that the survival of NIH 3T3 cells decreased as they increased. An increase in laser energy and polymer concentration negatively affected the morphology of cell-loaded microspheres, limiting the permeability of the scaffolds. A similar effect was exerted by the gelation time, which, the longer it was, contributed to the formation of a thicker and thicker gel membrane, which also caused restrictions in diffusion [35].

Similar to inkjet or stereolithographic printing, laser-assisted bioprinting allows high precision of the printed objects, which is of course important but not the most important. Moreover, with the right parameters, such as laser energy and protection of cells from direct contact with radiation, cell survival rates are high. One reason for this is the non-contact printing system, *i.e.*, no direct contact between the bio-ink and the dispenser. Nevertheless, it is a method that does not show as much application potential as extrusion printing. In summary, compared to other bioprinting methods, the main challenges for laser-assisted printing are material limitations and the scale of the printed objects. These are aspects to which special attention must be paid in the further development of the technology. Not every material that is suitable for the printing process allows for efficient cell differentiation and growth, which is also closely related to the mechanical properties of such scaffolds, crucial for their biomedical applications.

3 Hydrogel-based bio-ink

In addition to selecting a suitable 3D printing technique, crucial for bioprinting is the choice of a specific bio-ink that will provide several biochemical and physical cues for proper cell growth, development, and proliferation [68]. During the development of the bio-ink formulation (Figure 2), it is necessary to consider rheological and biological properties to understand the behavior of the bio-ink both before, during, and after gelation, as each of these steps will affect the resolution of the structure and the preservation of its shape as well as cell survival [69]. In addition to constructs, bioactive molecules such as growth factors that signal cells to migrate, proliferate, and differentiate can also be incorporated into the formulation of the bio-ink [70]. Additionally, the addition of bioactive substances to the scaffold can activate the immune system and facilitate the secretion of repair factors by macrophages which in turn increases implantation success. Growth factors called diffusible signaling proteins are a group of bioactive components. In addition to activating proliferation and

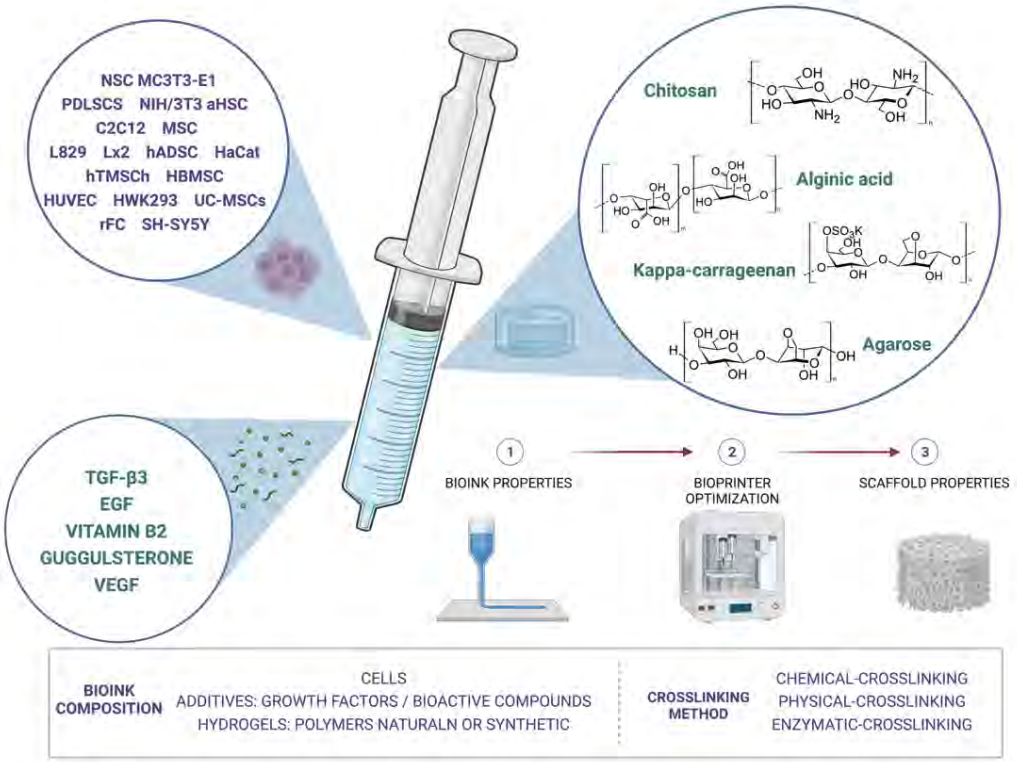

Figure 2: Example of bio-ink formulation containing cells and hydrogel along with its optimization procedure (created with BioRender.com).

differentiation, growth factors also stimulate vascularization and tissue repair through their binding to the surface of target cells [71]. In a study by Shi *et al.*, tyrosinase was used in a bio-ink based on methacrylated gelatin and collagen to bioprint living skin tissues. In this formulation, tyrosinase had a dual function. On the one hand, it was an essential compound in the skin regeneration process responsible for the skin color effect and as an enzyme facilitating the crosslinking of bio-ink components [72]. On the other hand, in order to bioprint cartilage tissue, Wang *et al.* chose to use alginatesulfate with methacrylated gelatin together with growth factor β3 (TGF-β3) providing an environment of strong chondrogenesis in the subcutaneous environment. Also, controlled release of TGF-β3 due to the presence of alginatesulfate promoted significantly higher levels of cartilage-specific ECM deposition [73]. When bioprinting dermal tissue, one of the problems is the regeneration of sweat glands, which have an important thermoregulatory function in the tissue. As the regenerative potential in the results of injury to these glands is low, Huang *et al.* decided to develop a gelatin-alginate hydrogel loaded with epidermal progenitor cells that differentiate into a cell line of sweat glands under the influence of mouse plantar dermis and epidermal growth factors [74]. In order to adjust the mechanical properties of the decellularized ECM bio-ink, one of the additional components was vitamin B2, which gels under the influence of UVA [75]. Another solution is to add drugs to the bio-ink. Such scaffolds for the regeneration of damaged tissues with simultaneous control of drug delivery represent a novel approach. For example, in the work of Sharma *et al.*, a novel bio-ink was presented that, in addition to fibrin and hiPSC pluripotent stem cells in its formulation, contained the drug guggulsterone to promote cell differentiation into dopaminergic neurons [76]. Through the application of specific growth factors, it is possible to target universal bio-inks for a specific task. This approach significantly facilitates the procedure of bio-ink design, in which a base consisting of a mixture of polymers that imparts specific rheological, mechanical, and basic biological properties such

as biosafety and appropriate biodegradation rate of cell scaffolds is established. Then, through the addition of appropriate growth factors, further biological properties are improved or imparted, *i.e.*, improved cell proliferation and differentiation.

ECM is a cross-linked, hydrophilic polymer network composed mainly of water. In fact, water, which naturally occurs in tissues, is the ideal medium, *i.e.*, solvent for all biochemical reactions. Consequently, hydrogels, which in many respects are composed mainly of water, are very similar to it [8,68]. However, in order to be able to use a given hydrogel in 3D printing, an important issue remains its crosslinking, which can be done by both physical and chemical methods. Physical crosslinking, such as thermal condensation, is a thermally driven gelation characteristic of agarose, carrageenan, gelatin, elastin, and collagen. Among physical gelation methods, molecular self-organization is also prominent. This phenomenon occurs mainly in peptide- and protein-based hydrogels and is driven by reversible, non-covalent and weak binding mechanisms, such as hydrogen bonds and hydrophobic and electrostatic interactions. Other physical methods include electrostatic interactions between oppositely charged compounds, such as alginate polyanion and chitosan polycation. Chemical crosslinking, on the other hand, produces more stable hydrogels by forming irreversible covalent bonds. Their disadvantage, however, is limitations in cell proliferation and migration in such a cross-linked scaffold [3]. Among hydrogels, a fascinating group from the point of view of tissue engineering are those based on polymers of natural origin, *e.g.*, gelatin, collagen, chitosan, alginate and agarose, which have great application potential. In addition, they are sensitive to a range of stimuli, such as pH, temperature, ionic strength, electric or magnetic fields, light, and chemical and biological compounds [77]. There are many studies on thermosensitive polymers, among which are lower critical solution temperature (LCST) and higher critical solution temperature (UCST) polymers. LCST and UCST refer to critical temperature points below or above which a polymer can thoroughly mix with a solvent [78]. A common use of thermosensitive polymers in tissue engineering is as substrates for proper cell differentiation and as gels administered *in situ* by injection. In the former case, the mechanism is to regulate the attachment and detachment of cells from the surface by thermosensitive polymers [79], and in the latter case, to encapsulate cells in three-dimensional structures [78]. The advantage of *in situ* methods over the creation of *in vitro* constructs is the less invasive techniques, which use the simple phenomenon of the transformation of a sol into a gel at body temperature, *i.e.*, 37°C, which is the LCST of the polymer.

For a hydrogel to be used in tissue engineering to produce a bio-ink, it must meet several criteria (Figure 3)

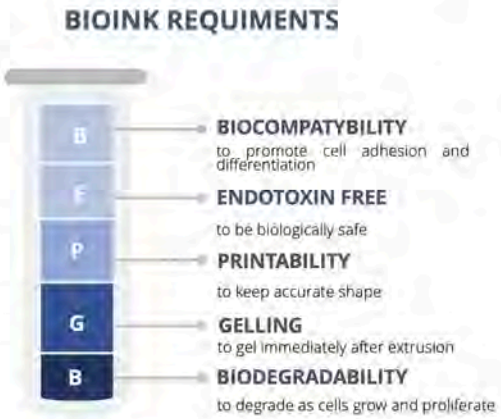

Figure 3: Requirements for bio-inks in tissue engineering (created with BioRender.com).

to reflect the ECM's properties best. A critical factor in determining the applicability of a material is its biocompatibility. The material must not interact with the body by contributing to the activation of harmful immune reactions. Furthermore, Banach-Kopeć *et al.* proposed a method to purify chitosan from endotoxins as an input criterion for creating a bio-ink [80]. Biocompatibility must be maintained at every stage, including degradation of the cellular scaffold. Among other things, toxic groupings and chemicals used to polymerize synthetic hydrogels can have harmful effects. High risk is also associated with unreacted monomers, stabilizers, initiators, organic solvents, and emulsifiers. Therefore, another requirement is the non-cytotoxicity of the bio-ink known as biosafety. Another criterion is porosity and the associated pore size, volume, shape, *etc.*, which are critical parameters determining whether cell penetration, ECM production, and neovascularization will be possible. For bio-ink to be used in bioprinting, it must have characteristics that will ensure that scaffolds are obtained with appropriate tissue-specific mechanical properties, and that can be controlled, for example, by selecting crosslinking density [81]. In addition to compatibility, the bio-ink must ensure proper adhesion, proliferation, migration, and function of both endo and exogenous cells. From the point of view of the bio-ink itself, it must be printable and ensure timely polymerization. Degradation of such a bio-ink must occur through controlled degradation kinetics [82]. Biodegradability of scaffolds is very important, as it has been shown that cell proliferation in non-biodegradable scaffolds decreases after some time. However, this is not an obligatory requirement for all types of scaffolds since it is recommended that scaffolds be semi-permanent or permanent for articular

cartilage or cornea regeneration. The main factors that make natural polymers suitable for raw materials for bio-inks are biocompatibility and degradability [81].

Marine organisms are a source of various polymers, including collagen, gelatin, chitosan, alginate, and agarose. Because of their natural origin, they are raw materials with essential properties required for tissue engineering. Many publications compare marine-derived polymers to mammalian resources, as their key advantage is the lack of risk of transmitting infectious diseases and religious restrictions [83–86]. However, both marine-derived and mammalian polymers have certain advantages and disadvantages. For example, Maher *et al.* compared marine-derived and porcine type I collagen hydrogels for use in bioprinting on the basis of their research. In their conclusion, the authors pointed out the potential of marine-derived collagen with its limitations due to the need to improve its thermal stability [76]. The crucial issue during the initiation of work on biopriniting to design and consider every step from the very beginning, for instance, from the bio-ink, *i.e.*, the composition, the bioprinter, the cross-linking method, the applied bio-ink system as well as the bioprinter, to the target. These three variables, *i.e.*, the parameters of the bio-ink, the bioprinter, and the application, are what determine the final product and the success of the research undertaken. Skipping any of these steps often leads to failure, such as incompatibility between the bio-ink and the printer. An example diagram in the form of a SWOT analysis of how to design a bio-inks composition and what key aspects need to be considered in the first step to begin further design steps is shown in Figure 4.

3.1 Protein-based bio-ink hydrogel of marine origin

3.1.1 Collagen and gelatin polymers

The most abundant protein in the ECM is **collagen**, which acts as a structural element that stabilizes tissues and organs and maintains the integrity of the ECM. A characteristic feature of the 28 genetically distinct collagen types [87] is a tripeptide repeat domain (-Gly-Xaa-Yaa-), where Xaa and Yaa are 28% proline and 38% hydroxyproline, respectively. All collagens form a right-handed triple helix made of three polypeptide chains. In addition to its structural function, collagen has many additional roles due to the presence of additional protein domains, and these vary according to the distribution of collagens in tissues. Type I collagen is found mainly in bones, tendons, skin, ligaments, corneas, and many other interstitial connective tissues. Type II collagen, on the other hand, is the predominant component of vitreous cartilage [88]. Most collagen-based bio-ink are made from type I, which accounts for 90% of the protein mass in mammalian connective tissues [89]. The primary raw material for collagen is bovine and porcine hides. Another less commonly used source is organisms of marine origin, such as fish, which are of increasing interest to tissue engineering. On the one hand, the marine raw material from which collagen is most easily isolated is variegated fish. On the other hand, because of the different rheological properties of the collagens obtained from them, such a procedure requires standardization due to their different rheological properties [90]. The current solution

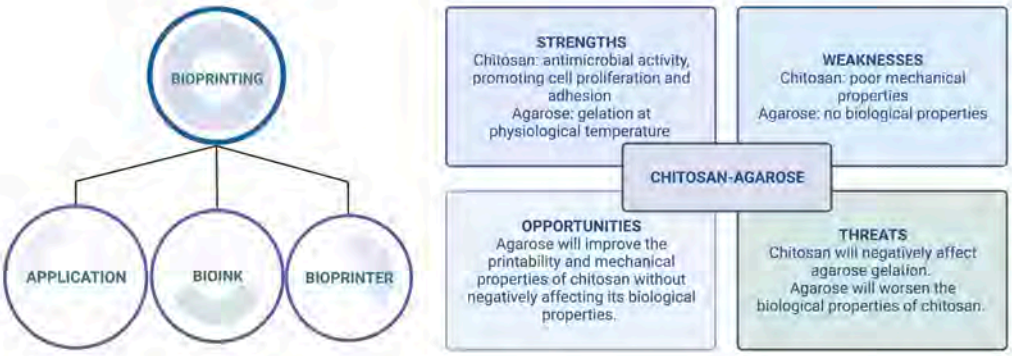

Figure 4: Three variables determining the final product and an example of SWOT analysis for chitosan-agarose composition when selecting bio-ink substrates (created with BioRender.com).

is commercially available Fribrogen®, recombinant human collagen whose composition is consistent regardless of batch and potentially less immunogenic [91].

Collagen is a biodegradable and biocompatible polymer with versatile applications. Collagen's great potential in biodegradation and biomedical engineering is due to its high affinity for cells, thanks to the presence of the sequence, *i.e.*, the Gly-Pro-Hyp motif and the Hly-Phe-Hyp so-called GPO and GFO. Cell receptors recognize this sequence and adhere to this site. In turn, the ability to degrade collagen is demonstrated by matrix metalloproteinases, which unwind the three α chains and then cleave each of them [92]. However, the three main reasons why the use of marine-derived collagen in bioprinting is problematic are the low denaturation temperature, which can vary depending on the organisms' residence, but always less than 35°C, the rate of degradation, and pure mechanical properties.

The degree of hydroxylation, or hydroxylation of proline residues at the Yaa position with the formation of 4-hydroxyproline (Hyp), is high for warm-blooded animals, *i.e.*, mammals, and low for warm-blooded animals, *i.e.*, fish. This relationship is due to the ambient temperature for a given species, *e.g.*, for the stability of collagen at 37°C, about 10% of the residues are Hyp, 8.5% Hyp for the tropical fish Tilapia (*Oreochromis niloticas*) at a melting temperature (Tm) of 34°C, and 4.5% Hyp for the Antarctic fish (*Trematomus eulepidotus*) at a Tm of 6°C [93].

Unfortunately, the rate of enzymatic degradation makes it necessary to regulate this process through crosslinking techniques, among others [94]. Another problem in its application is its poor mechanical properties and the use of low concentrations not exceeding 10 $mg \cdot mL^{-1}$. With this type of solution, the polymerization time is as long as 40–60 min. The solution to this problem, on the other hand, is the addition of other so-called booster hydrogels to the bio-ink [89]. In the study by Hinton *et al.*, one bioprinting technique was FRESH, which is the reversible deposition of suspended hydrogels. Low mechanical resistance was achieved using a gelatin suspension bath at 22°C. After bioprinting was completed, raising the bath temperature to 37°C allowed recovery of the printed object. This technique is recommended for hydrogels with a modulus of elasticity <500 kPa, including alginate, Matrigel, and collagen [95].

Gelatin is a molecular derivative of collagen obtained by its irreversible denaturation mainly from warm-blooded animals. Thus, it is much more common to find gelatin, which is a kind of equivalent to collagen, in compositions. It is a biodegradable and biocompatible polymer that is 85–92% composed of proteins and water. As gelatin has a similar molecular structure to collagen, it can replace it and perform similar functions as a biomaterial for cell growth *in vitro*. Based on the raw material, a distinction is made between bovine, porcine, and fish gelatins. Gelatin is obtained by treatment with acid (type A) or base (type B). Depending on the gelatin type, they differ in amino acid composition, gelation strength (Bloom), isoelectric point (pI) and charge. The pI of gelatin type A is 6–9, and type B is 5. The Bloom index is a parameter that directly reflects the hardness of gelatin and indirectly its molecular weight, and ranges from 30 to 200 (<150 for low, 150–220 medium, and 220–300 high Bloom values). The primary raw materials for gelatin are pork hides 45% and bovine hides 29.4%. In the case of cattle hides, gelatin extraction is mainly by alkaline method, and in the case of pig hides, by acid method [96]. The advantage of acid treatment of collagen, and thus of type A gelatin, is that the electrostatic properties of this protein are slightly affected, making them similar to the parameters of collagen [97]. On the one hand, in contrast to bovine gelatin (type B), porcine gelatin has a lower viscosity but a higher Bloom scale hardness and gelling power [96]. Gelatin's advantages over other proteins found in the ECM are its availability, low cost of obtaining it, and the presence of moieties that allow it to bind cells.

Gelatin is well soluble in water, making its application in tissue engineering simpler than other proteins. In addition, regardless of the raw material from which gelatin is obtained, it is biocompatible, biodegradable, and non-toxic. In contrast, the main disadvantages of gelatin gel are its moderate mechanical properties, thermal instability, and rapid degradation under the influence of proteases. The solution to this problem in terms of applying this protein in tissue engineering is its blending with, *e.g.*, polysaccharides to increase gelatin's stability and the composite's bioactivity [98]. Gel formation between gelatin and polysaccharides occurs through the formation of electrostatic, hydrophobic, and hydrogen bonds.

However, a fundamental limitation of the formation of the above systems is phase separation, which occurs when the gel formation time is longer than the phase separation time [99]. Currently, many studies are being conducted on the possibility of using marine-derived raw materials to produce gelatin as well as its application in tissue engineering. However, what should be emphasized is that there are still many authors who erroneously point to the possibility of using marine waste as a raw material for cell scaffolds as one of the advantages. The key point is that in order for such gelatin, like any other raw material, to be used in tissue engineering and thus in bioprinting it must meet pharmaceutical standards. None of the raw materials used must have a waste category. Another issue relates to intermediates, which having appropriate medical standards can be successfully used in bioprinting, which is

often confused by scientists. In summary, fish gelatin shows many properties similar to pork gelatin, making it a good alternative. However, it has moderate mechanical properties [44], which can be modified by the addition of, for example, other polymers or the use of appropriate crosslinking techniques.

A characteristic feature of all gelatins is the sol–gel transition temperature, about 10–25°C. Gelatin hydrogels melt at physiological temperature, *i.e.*, 37°C, which limits their application in tissue engineering as in the case of collagen. The solution is chemical crosslinking with methacrylate, among others. Adding methacrylate groups to the amine side groups of the polymer makes it possible to obtain stable hydrogels at physiological temperature after their polymerization under UV light. In addition, mechanical properties can be modified by adjusting the degree of methacrylation and the concentration of the polymer. The short UV exposure time does not contribute to a significant decrease in cell survival, which for 5% methacrylated gelatin is about 92% at 8 h after printing. The only factor that contributes to significant cell mortality is the increase in polymer concentration. For example, cell survival for a 15% concentration of polymer in the bio-ink is about 75% [100]. Still, another solution to improve the mechanical properties of the polymer is to use polysaccharides to form complex, hybrid polymer structures. The role of the polysaccharide in this system is to increase the scaffold's stability, while gelatin improves biological properties. Induction of gel formation after mixing a protein with a polysaccharide occurs through chemical and physical interactions such as electrostatic, hydrophobic, and hydrogen interactions [99].

Collagen and gelatin of mammalian origin have long been used in bioprinting to create highly porous scaffolds that support cell growth and differentiation. Like most polymers, they require modifications to achieve satisfactory results. For instance, fibrillated collagen is additionally cross-linked through bonding with genipin to ensure the proper mechanical properties of the printed scaffolds. Changes in the proportions of bioceramics affect pore size and gelation properties, which are crucial for maintaining cell viability during bioprinting [101]. Another example of modification is the development of bio-inks based on methacrylated collagen mixed with thiolated hyaluronic acid, enabling the printing of structures that support cell-matrix interactions while preserving the properties of the natural microenvironment [102]. Similarly, the modification of gelatin to a methacrylated derivative allows for the creation of biomimetic matrices and scaffolds that support cellular differentiation and tissue regeneration. For example, methacrylated gelatin combined with poly(ethylene oxide) (PEO) and polycaprolactone (PCL) enables the creation of microporous environments with adequate mechanical support [103]. The addition of calcium silicate to methacrylated gelatin not only supports odontogenesis but also improves both the mechanical strength and printability of the polymer [104]. Crosslinking in visible light, thereby improving mechanical properties, is possible by adding tyramine to the modified gelatin [105]. Moreover, adding laponite to methacrylated gelatin increases the viscosity of the bio-ink, enabling the printing of precise scaffolds without affecting the stiffness of the hydrogel, which favors osteogenic proliferation and differentiation [106].

A comparison between marine-derived collagen type I and pork-derived collagen that had been methacrylated for UV crosslinking was made by Maher *et al.* The need for additional stabilization of the constructs is due to the denaturation temperatures of collagen, which is 25°C for marine and 37°C for pork. Due to the different amino acid compositions, the viscosity of the marine bio-ink was slightly lower than that of the porcine. Both the amino acid composition and differences in the degree of methacrylation affected the mechanical properties which was significantly higher for the marine bio-ink. However, for both collagens, the Young's modulus can be adjusted over a wide range which is related to the subsequent application, *e.g.*, soft environment for soft tissues and rigid environment for *e.g.*, bone or muscle. Despite the difference in viscosity, no significant difference in extruded fiber diameter was observed. L929 fibroblasts showed a viability survival rate of over 80% [93]. Among others, Cavallo *et al.* undertook the development of a bio-ink based on collagen derived from bass skin, which was combined with partially cross-linked alginate. The publication examined the effect of collagen concentration on individual parameters. A bio-ink with a collagen content of 20 $mg \cdot mL^{-1}$ compared to one with a concentration of 10 $mg \cdot mL^{-1}$ had better printability, the lowest *in vitro* biodegradation and swelling rates, and better antimicrobial properties [84].

The examples described above for the use of collagen and gelatin, which, can be of marine or mammalian origin. Despite the many benefits of using marine-derived raw materials, there are still few publications on their applied use. The main reason may be the low denaturation temperature of these polymers; however, additional crosslinking mechanisms have also been proposed for them An obvious solution seems to be the use of collagen or gelatin derived from warm-blooded fish, where the denaturation temperature of these polymers is close to that of pigs. In addition, the above examples provide ready-made solutions for the use of marine polymers in bioprinting. Figure 5 discusses the use of gelatin and collagen as the main components of bio-ink. It details their advantages

and disadvantages, as well as current strategies to enhance their biological and mechanical properties.

3.2 Polysaccharide-based bio-ink hydrogel of marine origin

3.2.1 Chitosan

Chitosan is a cationic polymer derived from chitin, the second most common polymer. Chitosan is obtained by deacetylation of chitin, the primary source of which are the exoskeletons of marine invertebrates, insects, and the cell walls of fungi. Chitosan is built from β-1,4 glycosidic bonds of D-glucosamine (70–90%) and *N*-acetyl-D-glucosamine (10–30%). The key parameters affecting the solubility of chitosan are its degree of deacetylation, which is defined as the ratio of the number of glucosamine groups to the total number of *N*-acetylglucosamine and glucosamine groups, as well as its molecular weight [80].

Chitosan has many properties that make it suitable in many industries, such as in pharmaceuticals as a drug carrier, for water purification, and in medicine as wound healing materials. It is a biocompatible and biodegradable polymer. In numerous studies, chitosan has been shown to have the ability to inhibit tumor cells. Chitosan penetrates tumor cell membranes through cellular enzymatic, antiangiogenic, immune enhancing, antioxidant defense, and apoptotic pathways . The high potential of chitosan is due to the presence of *N*-acetylglucosamine in chitosan. This essential structural property is also present in glycosaminoglycans, which interact specifically with growth factors, receptors, and adhesion proteins. It is thought that an analogous structure in chitosan may have similar biological activity [107]. Chitosan is characterized by a stable and rigid crystalline structure resulting from strong hydrogen bonds within and between this polymer's molecules. In addition, due to the presence of amino groups in the structure of the polymer, it also has antimicrobial properties [108]. There are several mechanisms of action of chitosan depending on the environment in which it is found. However, in general, chitosan shows activity against both Gram-positive and Gram-negative bacteria, but the electrostatic interactions between them are different due to differences in the structure of their cell walls. In the case of Gram-positive bacteria, the cell wall consists of a thick layer of peptidoglycan, which is covalently linked to teichoic and lipoteichoic acids that give the cell wall a negative charge. In Gram-negative bacteria, on the other hand, this layer is much thinner and additionally surrounded by an outer membrane that includes lipopolysaccharides and teichoic acids. As a result of the interactions between negatively charged components of the bacterial cell wall and positively charged amino groups of chitosan, destabilization and damage

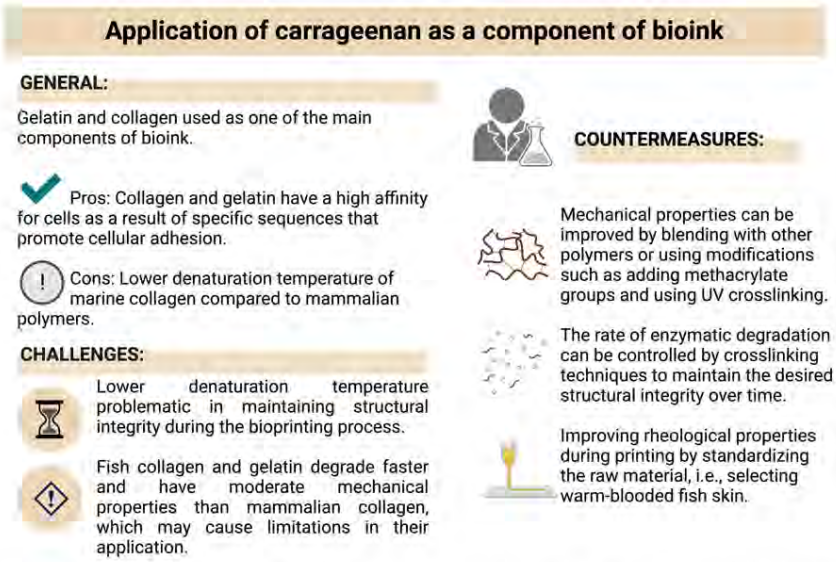

Figure 5: Potential and challenges of using gelatin and collagen as a bio-ink component: scientific solutions (created with BioRender.com).

to the bacterial cell membrane occur, leading to cell death. Damage to the integrity of the cell wall can also occur when metal ions localized on it are chelated by chitosan compounds, more specifically by anionic groups [109]. This is the second mechanism that Mania *et al.* proposed in their study. The antimicrobial activity of chitosan obtained by an innovative carbon dioxide carbonation method, depending on the molecular weight and degree of deacetylation, is different which is most likely due to different interactions. In the case of low-molecular-weight chitosan, there is a disruption of the wall and the polymer enters the cell interior and thus interacts with DNA, while for high-molecular-weight chitosan, the dense film formed on the cell surface impedes the passage of nutrients. In addition, depending on the molecular weight, *i.e.*, high or low, chitosan can correspondingly form a dense polymer film on the cell surface, limiting nutrient exchange [110].

Chitosan, being a deacetylated derivative of chitosan, is soluble only in aqueous, acidic environments where protonation of amino groups occurs [111]. This makes its application in biomedical engineering difficult. However, Gorczyca *et al.* overcame this problem by dissolving chitosan in carbonic acid by carbonation of its water suspension obtained by first dissolving chitosan powder in 0.1M lactic acid and then precipitating with 0.5M sodium hydroxide, and finally obtaining a solution with a pH of about 7 [112]. According to other methods of chitosan dissolving (dilute acid solutions), chitosan's amino groups become protonated, and the molecules became soluble below pH 5. This fact is a severe application limitation of chitosan, especially in tissue engineering, due to the toxic effect of the acid on the cells, which reduces the material's biocompatibility. The disadvantage of chitosan, despite its promising properties, is its poor printability and limited mechanical properties [113]. Therefore, there is a need to find compounds that improve these properties. In numerous studies, chitosan is one of the components of bio-inks. Some point out that one disadvantage of chitosan compared to gelatin is that it lacks cell adhesion sites and thus its properties to promote cell differentiation are limited [114]. On the other hand, chitosan has been shown to support the process of wound healing in individual stages, *i.e.*, promoting platelet adhesion and aggregation, acting as an antibacterial agent, promoting granulation tissue growth, and thus promoting fibroblast proliferation. The latter is particularly evident with chitosan, which has a high degree of deacetylation and low molecular weight [115].

Only about 4% of the publications on bioprinting are on chitosan-based bio-inks, which have so far shown promising results in tissue engineering applications. However, interest in using chitosan for its properties in bioprinting continues to grow. In turn, the disadvantage of chitosan is its limited mechanical properties, so various combinations with other components are proposed in research on its application to improve these properties [116].

Liu *et al.* developed a bio-ink with potential application in central nervous system tissue reconstruction, including spinal cord injury repair. The bio-ink consisted of hydroxypropyl chitosan, thiolated hyaluronic acid, vinyl sulfonated hyaluronic acid and Matrigel loaded with neural stem cells (NSCs). The modification of chitosan enabled its better solubility in water without the need for acid and thermal reactivity, allowing spontaneous hydrogel formation at higher temperatures, *i.e.*, 22–37°C. Despite a good gelation time of 20 seconds at 37°C, the mechanical properties of the scaffold were insufficient. Therefore, hyaluronic acid was used, which underwent additional modifications to improve mechanical properties and structural integrity. The bioprinting process involved an extrusion method. The syringe temperature was maintained at 10°C and the working table at 37°C. In this case, dual crosslinking takes place. One of them is the crosslinking of hydroxypropylchitosan when exposed to temperature, *i.e.*, 37°C. Therefore, in order to keep the viscosity of the bio-ink low enough before extrusion, the temperature of the syringe was kept between 4–10°C. Another mechanism is secondary *in situ* covalent crosslinking *via* Michael addition. The NSCs exhibited high viability of about 95%, and the microenvironment produced allowed for cell-material interaction, neuronal differentiation, and neural network formation [117].

Maturavongsadit *et al.*, in turn, developed a bio-ink for bone tissue regeneration based on nanocellulose and 3% chitosan. The idea behind the bio-ink was to create a temperature- and pH-responsive tunable hydrogel with suspended MC3T3-E1 preosteoblast cells for repairing minor bone fractures. The bio-ink consisted of chitosan dissolved in acetic acid, β-glycerophosphate as a gelling agent, cellulose nanocrystals, and hydroxyethyl cellulose. The mechanism of gel formation relies on the glyoxal groups of hydroxyethylcellulose, which act as crosslinking agents to form Schiff bases between the amino groups of chitosan and the aldehyde groups of hydroxyethyl cellulose. The role of nanocellulose was to improve mechanical properties by forming hydrogen bonds between it and chitosan. In turn, the role of β-glycerophosphate was to maintain the appropriate osmolality of the bio-ink, encapsulate the cells and promote gel formation at 37°C. The printing method involved using extrusion and temperature stimulation, where the temperatures of the extruder nozzle were 25°C and the working table 37° [118].

Ku *et al.* also proposed a thermosensitive bio-ink for bioprinting applications. Their goal was to develop chitosan-based bio-ink, studying the effects of the solvent used to dissolve this polymer and the crosslinking agent on biocompatibility, gel shape, and gel time. The

bioprinting problem was solved by printing a polycaprolactone-based framework. The study used an extrusion printing method with a head temperature of 65°C and incubation of the printed object at 37°C. It was shown that the type of solvent had no effect on the gelation temperature (37°C), but chitosan hydrogels dissolved in acetic acid showed better biocompatibility than those in lactic and hydrochloric acid. It was shown that the use of potassium phosphate for crosslinking chitosan results in the formation of a large precipitate that can clog the nozzle and thus impede printing, in contrast to β-glycerophosphate and sodium bicarbonate where the precipitate was much smaller. Similarly, gel time was shortest for potassium phosphate, which may be related to the nozzle clogging problem, and longest for sodium bicarbonate. In addition, the chitosan-potassium phosphate hydrogels had smaller pores than the other two, promoting cell dispersion and neovascularization much better. Human periodontal ligament stem cells (PDLSCs) encapsulated in chitosan hydrogels were viable and well dispersed, with a circular morphology that promoted cell adhesion (Figure 4) [119].

Hafezi *et al.* developed a genipin-crosslinked chitosan bio-ink with polyethylene glycol as a plasticizer. The goal was to print by extrusion at 37°C a scaffold containing human epidermal keratinocytes and dermal fibroblast cells for skin tissue regeneration. For structural reinforcement, the first layer of the scaffold was printed from calcium chloride-crosslinked alginate, followed by subsequent layers based on chitosan. Adjusting the concentration of genipin was the basis for achieving the proper printing viscosity. Too low a concentration, on the one hand, resulted in insufficient mechanical strength. At the same time, too high a concentration resulted in too high a viscosity of the bio-ink and consequently the need for higher pressure, which could cause cell death. Despite crosslinking, cell survival after printing was 93% [120].

From publications by Tonda-Turo and colleagues, it is known how to produce both photo- and heat-sensitive biocomponents. For this purpose, chitosan was modified to methacrylated chitosan for subsequent crosslinking under temperature and UV light, and then mixed with β-glycerol phosphate salt to maintain thermosensitivity. The crosslinking mechanism was that the first crosslinking, being mediated by temperature, is responsible for maintaining the printed architecture, and the second crosslinking, induced by UV radiation, increases the stability of the hydrogel in physiological environments. The sol–gel phase transition occurred at 37°C. For this purpose, the temperature of the working table was set to physiological temperature and the head was set to 4°C. The bioprinting was carried out using a laser-assisted bioprinting technique. The researchers developed a bio-ink that had high resolution after printing, thanks to a dual crosslinking mechanism. The bio-ink was not cytotoxic to NIH/3T3 fibroblast cells, Saos-2 osteoblasts, and Sh-SY5Y neuroblasts. Moreover, it enabled their subsequent proliferation and organization toward tissue formation [121].

A highly reproducible bio-ink for skin tissue regeneration composed of carbohydrazide crosslinked {polyethylene oxide-*co*-Chitosan-*co*-poly(methylmethacrylic-acid)} (PEO-CS-PMMA) and loaded with nicotinamide I human skin fibroblasts was synthesized by free radical copolymerization. The gelation of the formulation resulted from electrostatic interactions between the cationic chitosan groups and the anionic PMMA side groups. The bio-ink exhibited optimal reproducibility and printability at an extrusion pressure of 20–50 kPa, at 37°C in the viscosity range of 500–550 Pa·s. Compared to pure chitosan, the survival rate for a given system increased from 67 to 92% [122]. Despite using a mixture of natural and synthetic polymers combined with synthesis methods, obtaining constructs with high cell survival rates was possible. Depending on the purpose, *i.e.*, the application of the scaffold in question, printability may play a lesser role as in the case of soft tissues or a greater one, *e.g.*, heart. In this case, there is a lack of any information regarding printability that would indicate the further potential use of such an array.

Another study looked at combining chitosan with gallic acid, which allows such a bio-ink to self-crosslink at physiological pH. This arrangement makes it possible to produce a bio-ink without using any crosslinking agents. At pH 7.4, the gallium group oxidizes to a quinone structure to form a covalent bond *via* Michael addition or Schiff reaction with the amino group of chitosan. The constructs exhibit very good mechanical properties up to 300 kPa after 3 h of self-crosslinking and >337 kPa after 12 h of self-crosslinking, and a cell survival rate of >92% NIH3T3. Based on the fiber diameter and pore size, the printability of the optimized bio-ink was evaluated by obtaining uniform prints at an extrusion rate of 0.5% and a needle diameter of 25G at which no needle clogging occurred, and Pr was 1 ± 0.05 [123].

A bio-ink with a relatively low chitosan concentration, whose rheological and mechanical properties were significantly improved with the addition of nanohydroxyapatite, was proposed by Coşkun *et al.* Thermal and physical crosslinking occurred with the addition of glycerol phosphate and sodium bicarbonate. The addition of gelling agents improved both the gelation time and the storage modulus. The bio-ink together with MC3T3-E1 cells was printable at a relatively low pressure of 50–70 kPa and a speed of 4–11 $mm \cdot s^{-1}$ while providing high cell survival [124].

Another chitosan-based solution involves water-soluble methacrylated glycol chitosan with a riboflavin PI and cured with visible light. This approach was designed to minimize the toxic effects of UV radiation and the use of synthetic PIs.

It was shown that as the curing time increased, there was relatively high stress and low strain. In addition, the increased time influenced the compressive modulus obtaining an optimal mixture whose elastic modulus corresponds to that for osteogenic differential, *i.e.*, about 25 kPa. During printing, an extrusion pressure of 120 kPa and a speed of 6 $mm \cdot s^{-1}$ was used [125]. Figure 6 discusses the use of chitosan as the main components of bio-ink. It details their advantages and disadvantages, as well as current strategies to enhance their biological and mechanical properties.

3.2.2 Alginate

Alginate or alginateinic acid is the most widely used polymer of natural origin in bioprinting, as a result of its straightforward application in extrusion printing, among other applications. One reason for this is the simple and quick method of crosslinking with calcium chloride or sulfate, which does not significantly affect cell viability.

Alginate is extracted from brown alginateae's cell walls and intracellular spaces with a molecular weight of 32–400 $g \cdot mol^{-1}$. It is a polyanionic, linear copolymer built from (1-4)-linked β-D-mannuronic (M) and α-L-guluronic acids (G). The alginate is built from long blocks of M or G, separated by MG areas. Depending on the source from which the alginate is extracted, the content of each block differs. In addition, the ratio of M/G blocks affects the properties of this polymer as well as the polymer sequence, G block length, and molecular weight. While G blocks increase the gelation of the polymer [126], MG blocks and M blocks increase the flexibility of the polymer. However, too high an M block content may contribute to this polymer's immunogenicity. The capillary forces of the alginate matrix, on the one hand, can trap water and other molecules and, on the other hand, are characterized by their ability to diffuse.

Alginate is a biocompatible, biodegradable and non-immunogenic polymer that promotes cell growth. The gelation process of alginate biodegradation involves the generation of ionic inter-chain bridges between the carboxyl group of the polymer and the multivalent cations, *e.g.*, Ca^{2+}, present after their previous addition to the solution [127].

The disadvantages of alginates are uncontrolled and unpredictable degradation kinetics. Their solubility is due to the leaching of cations into the surrounding medium. High- and low-molecular-weight alginate-strands are also released during dissolution. High-molecular-weight alginates are not degraded in mammals, and their removal from the body is prolonged. In addition, metal leaching can adversely affect surrounding tissues, for example, calcium ions can lead to tissue calcification. The solution is the method proposed by Bouhadir *et al.* for oxidizing alginate with sodium peroxide, which can still be cross-linked with calcium ions. Due to a conformational change of the uronate residue to an open-chain adduct, it behaves like an

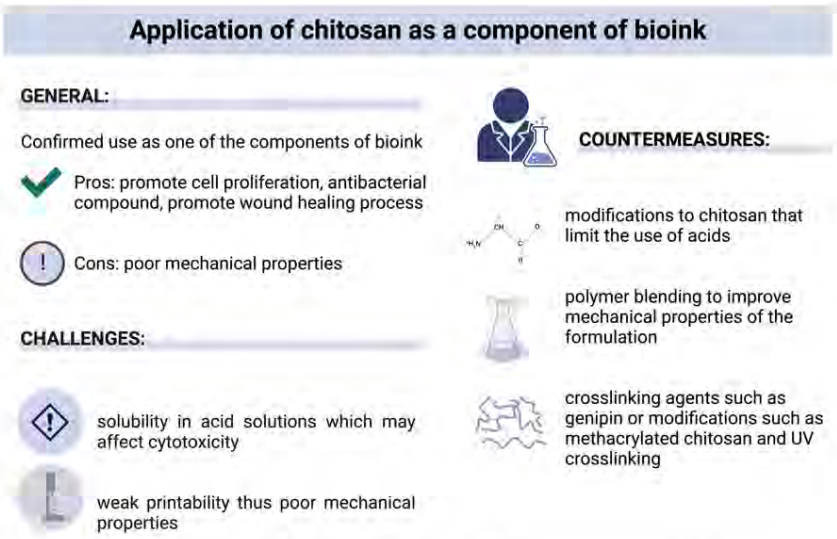

Figure 6: Potential and challenges of using chitosan as a bio-ink component: scientific solutions (created with BioRender.com).

acetal group, so that the alginate is hydrolyzed. In addition, the degradation of alginate is pH and temperature dependent [128], which allows the formation of inteligent bio-inks that respond to the environment.

One of the most commonly used bio-inks are those based on aginate. In addition, this polymer is commonly used as a material for drug delivery or growth factors, among other reasons, because its degradation rate can be adjusted depending on the molecular weight used [129].

The effect of the degree of oxidation of Alginate and its ratio between low and high molecular weight on the degree of biodegradation was studied by Boontheekul *et al.* Partially oxidized Alginate was obtained using 1% sodium periodate. Despite the use of high molecular weight, it was shown that such oxidized hydrogels exhibit a significantly lower elastic modulus which is due to lower chain stiffness as a result of oxidation. Wanting to avoid lower biocompatibility due to crosslinking agents, it was investigated whether partial oxidation and combination of Alginate with different molecular weights would allow accelerated biodegradation at low oxidation. It was shown that the degradation machanism involves hydrolytic chain cleavage on oxidized sugar residues rather than dissociation of calcium cross-links. In addition, the binary partially oxidized system did not result in reduced biocompatibility when examining the proliferation and differentiation and adhesion of C2C12 myoblasts [130].

The effect of the degree of oxidation on the rate of biodegradation was also examined in another study by Jia *et al.* Using human adipose tissue-derived stem cells (hADSCs), they created a library of 30 different alginate solutions in the form of oxidized alginate mixtures with broad applications in tissue engineering. Varying the oxidation of 0–10% as well as the concentration of 2–20% alginate was intended to control the degree of degradation. By varying the oxidation and concentration of alginate in the bio-ink, it was possible to achieve densities close to or greater than the cells which ensured their uniform distribution in the bio-ink throughout the 3-h printing process. Similarly, the viscosity showed an increasing trend with the increase in the concentration and decrease in oxidation. The study focused on maintaining the homogeneity of the bio-ink as well as printability and good resolution. In addition, an optimal/average bio-ink viscosity of 400–300 $mm^2 \cdot s^{-1}$ provided good cell survival >90% than one with high viscosity <90 and 0% after 8 days due to impeded nutrient flow [15].

One common treatment when curing alginate-based bio-inks is the use of a calcium-containing crosslinking agent. In Freeman and Kelly's study, it was shown that using low-molecular-weight alginate, the amount of cross-linking agent needed to be 2.5 times higher than using the high-molecular-weight one at 25:9 and 4:3, respectively. Regardless of the type of crosslinking agent used as well as alginate, cells in all constructs maintained high mesenchymal stem cell (MSC) viability, *i.e.*, at least 70% after 24 h. Likewise, the shear stresses acting on the bio-ink during its printing, which vary depending on the molecular weight, *i.e.*, on the viscosity of the alginate, did not significantly affect the decrease in cell survival which was, among other things, due to the use of a tapered needle, which has much lower wall stresses to which the cells are exposed. As the molecular weight increased, the mechanical properties of the constructs were higher. In addition, these properties were influenced by the choice of crosslinking agent, *i.e.*, higher Young's modulus and equilibrium modulus for $CaSO_4$ than for $CaCO_3$ or $CaCl_2$, which is due to the fact that the faster the solubility of the crosslinking agent, the faster the gelation and thus uneven. Furthermore, with the increase in molecular weight of alginate, a lower degree of degradation was observed, in contrast to the low molecular weight variant, for which a significant degree of degradation was noted after 21 days regardless of the crosslinking agent [129].

As one of the major challenges during bioprinting is obtaining a scaffold with a specific shape, Hazur *et al.* proposed a method to pre-crosslink alginate $CaCO_3$ and then post-crosslink $CaCl_2$. By adding D-glucono-δ-lactone, they were able to achieve slow acidification and thus dissolution of the $CaCO_3$ molecules that caused alginate crosslinking. Pre-crosslinking made it possible to achieve much higher printability without loss of NIH3T3 cell viability [131].

Composite with alginates: (2,2,6,6-tetramethylpiperidine-1-oxyl free radical) (TEMPO)-oxidized cellulose nanofibrils (TOCNFs) and polydopamine nanoparticles (PDANPs) and loaded with MC3T3-E1 osteoblast cells for bone tissue regeneration were developed by Im *et al.* Chemical oxidation of cellulose substrates (TOCNF) by TEMPO are widely used in various biomaterials to impart mechanical strength to composite hydrogels. When mixed with alginate, the compound gave the composite the right viscosity and compressive stresses compared to pure alginate. PDANP, on the other hand, interacts strongly with bio-ink components through cationic and ionic interactions, which affect the mechanical and biological properties of the composite. The addition of both TOCNF and PDANP was shown to significantly improve the mechanical properties and printability of alginate bio-inks. TOCNF affected the rheological properties and mechanical strength of alginate hydrogels, while PDNAP in turn improved printability and biological activity by affecting the proliferation, differentiation, and biomineralization of osteoblasts [132]. Figure 7 discusses the use of alginate as the main components of bio-ink. It details their advantages and disadvantages, as well as current strategies to enhance their biological and mechanical properties.

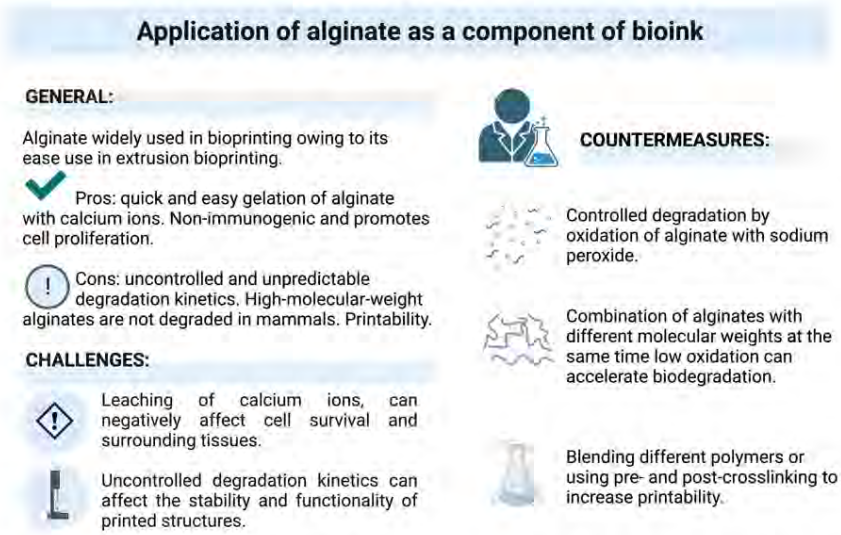

Figure 7: Potential and challenges of using alginate as a bio-ink component: scientific solutions (created with BioRender.com).

3.2.3 Agarose

Agarose is a polysaccharide extracted from seaweed and alginate. It is a linear polymer with a molecular weight of about 12 kDa, consisting of alternating D-galactose and 3,6-anhydro-L-galactopyranose linked by α-(1→3) and β-(1→4) glycosidic bonds [133]. In the process of extracting agaropectin from agar, agarose is obtained. It is a biocompatible polymer whose ability to promote cell adhesion can be improved by, among other things, mixing with other polymers. In research, agarose is combined with other polymers such as collagen, chitosan, and bacterial cellulose to increase cellular affinity. The agarose gelation process is a reaction consisting of three steps: induction, gelation, and pseudo-equilibrium. In the gelation process, the hydrogen bonds formed and electrostatic interactions lead to forming of a helical structure of agarose, after which a gel is formed. The fact that hydrogen bonds are present allows agarose to gel without crosslinking agents [134].

Even though agarose has been used as a chondrocyte matrix for over three decades, its application in tissue engineering is limited. However, agarose is distinguished by a unique gelation hysteresis feature, which means it gels at a lower temperature, while the process of gel–sol transition occurs at a higher temperature. This specific property signifies that agarose exhibits a temperature difference between the gelation process and the dissolving process, which is uncommon in many other gelling materials. Most applications of agarose in bioprinting involve its use as an auxiliary material for other bioprinting components [135].

The main task of agarose in bio-ink compositions is to harden it under temperature. Through our research, we came to the conclusion that the main disadvantage of using this polymer and curing method could be premature gelation of the bio-ink and plugging of the nozzle. This problem occurs when the nozzle temperature is close to the sol–gel transition temperature and the printer has inefficient heating systems at the same time. For example, this type of problem occurs in Cellink Inkredible plus printers. The temperature difference in the syringe at its two extreme ends can be as much as 10°C, which causes agarose gelation at the extrusion nozzle. In turn, an increase in the temperature that allows the extrusion of the bio-ink causes cell death and inadequate viscosity and thus poor printability of the bio-ink.

Numerous studies have shown that agarose addition increases the hardness of printed structures and positively affects printing precision, *i.e.*, resolution. Even though agarose does not have any biological properties to promote cell adhesion, on the other hand, the favorable sol–gel transition temperature for cell survival makes it to be increasingly used in bioprinting to improve the physical and chemical properties of scaffolds [136].

Gu *et al.* proposed a method for obtaining a bio-ink consisting of native and carboxylated agarose. The difference between carboxylated agarose and native agarose is the introduction of β-sheet and β-niche structures into the

polymer backbone and the simultaneous reduction in α-helis, due to which the viscosity is lowered as well as the sol–gel transition temperature, *i.e.*, at or below physiological temperature. After integrating human nasal chondrocyte (NC) cells into the bio-ink formulation and loading it into a printing cartridge, the extrusion printing process was conducted at an optimized temperature of 37°C. Initial assessments of cell viability post-printing indicated a survival rate of approximately 83%. This rate experienced a slight decline to 74% after a period of 7 days, suggesting a relatively stable cellular environment within the bio-ink matrix. Notably, during this period, the presence of diploid cells, specifically cells that had successfully completed the mitotic process, was confirmed, as illustrated in Figure 4, indicating not only survival but also cellular proliferation within the printed structure. Gelation of native agarose results from the physical interaction of double- and single-stranded α-helis *via* hydrogen bonds. For example, the presence of alginate in the bio-ink disrupts this gelation, *i.e.*, the helicate–helical interaction. This study confirmed that a carboxylated agarose derivative interacts with agarose through other acrylate and strand structures. Such gels have interesting mechanical properties, which can be modified by changing the proportion of carboxylated agarose and the gelation temperature [135]. Figure 8 discusses the use of agarose as the main components of bio-ink. It details their advantages and disadvantages, as well as current strategies to enhance their biological and mechanical properties.

3.2.4 Carrageenan

Carrageenans are sulfated polysaccharides derived from red seaweeds, which are classified into different types: κ, ι, α, μ, ν, θ [137]. Classification of the polymer is made according to the presence of a 3,6-anhydro bridge on the galactose residue linked by bond 4 and the position and the number of sulfate groups. Such polymers are built from a repeating disaccharide unit: 3-linked β-D-galactopyranose (G-units) and 4-linked α-D-galactopyranose (D-units) or 4-linked 3,6-anhydro-α-D-galactopyranose (DA-units). Besides the basic building units, carrageens also include other carbohydrate residues such as xylose, glucose, and uronic acid, as well as substituents such as methyl ether or pyruvate groups. Among all carrageens, the ι, κ, and λ polymers are the most commonly used commercially. κ- and ι-carrageens are called gelling polymers, while λ-carrageenan is categorized as a thickening compound [138]. However, the properties of the gels formed by the first two carrageenans are different. The gels of κ-carrageenan are brittle, while those of ι-carrageenan are soft and flexible. This is due to the presence of anhydro bridges in their molecules, which is a key factor in the gelation process. The 1C4 conformation of the 3,6-anhydro-D-galactopyranosyl units in κ- and ι-carrageenan enables the formation of a helical secondary structure. The typical mechanism of gelation involves two stages, *i.e.*, a stage controlled by temperature and calcium and potassium cations, *i.e.*, the transformation of the coil into a helix, with sulfate groups located outside it, followed by the

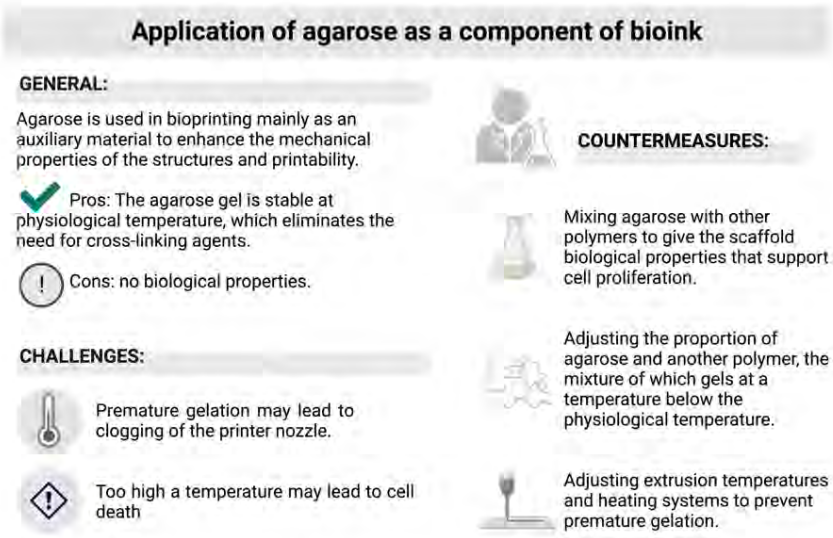

Figure 8: Potential and challenges of using agarose as a bio-ink component: scientific solutions (created with BioRender.com).

parallel joining of the formed helices. Carrageenan gels are thermally reversible, which gel when cooled to about 50°C and melt when heated to 80–90°C. However, in the case of λ-carrageenan, in which there are no units of 3,6-anhydro-D-galactopyranosyl, the formation of gels is impossible due to the presence of a 2-sulfate group that prevents the formation of double helices [139].

The benefits of carrageenan, particularly κ-carrageenan over other alginate-based biomaterials, is the ability to create more stable gels that do not need additional support during 3D printing. Moreover, such solutions do not require additional crosslinking like, *e.g.*, alginate, which gels in the presence of calcium ions which can induce biological responses depending on the type of cells used [140]. κ-Carrageenan has potential properties that enable its use in cartilage regeneration and drug delivery systems. These properties include its ability to regulate viscosity depending on concentration, temperature, and the presence of ions and molecular weight. In addition, the polymer is nontoxic, biocompatible, biodegradable, and features shear thinning.

However, the difficulty in controlling its gelation properties makes it impossible to print pure carrageenan and it is necessary to use chemical modifications, *e.g.*, Lim *et al.*, proposed a method to obtain a bio-ink for printing NIH-3T3 cells based on methacrylated kappa-carrageenan, which can undergo both ionic and ultraviolet double cross-linking. The recession of substitution and thus the possibility of UV cross-linking was aimed at controlling the rheological properties of the gel to reduce shear stress. Additionally, it was possible to obtain high cell viability up to 9 days after printing [141].

Among other things, k-carrageenan was used to prepare a so-called double-crosslinked bio-ink. In order to improve gelation, synthesized methacrylated k-carrageenan was used, which can be both ionically and UV-crosslinked. The k-carrageenan substitution makes it possible to control the rheological properties of the gel to reduce the crosslinking stresses that affect the survival of the NIH-3T3 cells used. It was shown that as the degree of polymer substitution increases, the viscosity of the formulation decreases as a result of the disruption of the doubly entangled structure. The degree of substitution equally affected the mechanical properties with high survival for 5 days and the ability to form self-organization into 3D spheroids [105].

In contrast, an attempt to print k-carrageenan without any modifications was carried out by Marques *et al.* Among several concentrations of 10–25 $g \cdot L^{-1}$, only the polymer at 15 $g \cdot L^{-1}$ was shown to be printable. At the other concentrations, the viscosity of the solution was too low or immediate gelation in the printhead occurred. In addition, the temperature of 29°C corresponded to that at the boundary of the sol–gel transition. L929 mouse fibroblasts seeded on the scaffold after 8 days showed high viability, *i.e.*, more than 84%, exhibiting a morphology typical of fibroblasts. Despite the fact that 15 $g \cdot L^{-1}$ k-carrageenan had optimal printability, due to the need to provide the cells with optimal conditions for survival, *i.e.*, increased ion concentration, which is not present in ultrapure water, there was a change in conditions and thus there was a need to lower the polymer concentration to 9 $g \cdot L^{-1}$ k-carrageenan, so that premature gelation did not occur. After 11 days, the cells had filled a significant

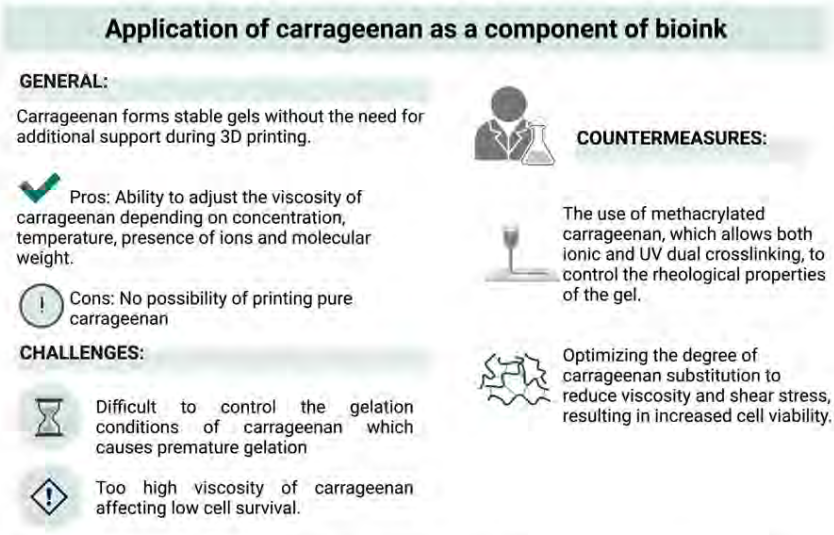

Figure 9: Potential and challenges of using alginate as a bio-ink component: scientific solutions (created with BioRender.com).

portion of the scaffold and presented a more elongated morphology than cells directly embedded on the scaffold (Figure 4) [140]. Figure 9 discusses the use of carrageenan as the main components of bio-ink. It details their advantages and disadvantages, as well as current strategies to enhance their biological and mechanical properties (Figure 10).

3.2.5 Marine-derived polymer blends

All of the polymers described above have unique properties that make them suitable biomaterials as components of biocomponents. However, these properties are insufficient for any of them to be a single component of a bio-ink. Therefore, research is being conducted on compositions such as chitosan-agarose, gelatin-alginate, agarose-gelatin, *N,O*-carboxymethyl chitosan-agarose, alginate-κ-carrageenan composites in which it is one component that promotes cell proliferation and adhesion, while the other component ensures that the appropriate mechanical and printability properties of such a bio-ink are achieved. The following describes bio-inks based on the aforementioned polymers, each of which has a unique role and thanks to which researchers were able to achieve certain scaffolding characteristics.

A bio-ink for 3D printing of functional mini neural tissues was described in a publication by Gu and colleagues. The proposed bio-ink consisted of alginate, carboxymethylated chitosan and agarose, and NSCs. The authors used the individual components because of the excellent alginate gelation under the influence of calcium ions, carboxymethyl chitosan, which gave the scaffold the proper porosity and thus permeability, and agarose to achieve the proper rheology. The bio-ink was printed by extrusion, followed by an additional step of crosslinking the alginate

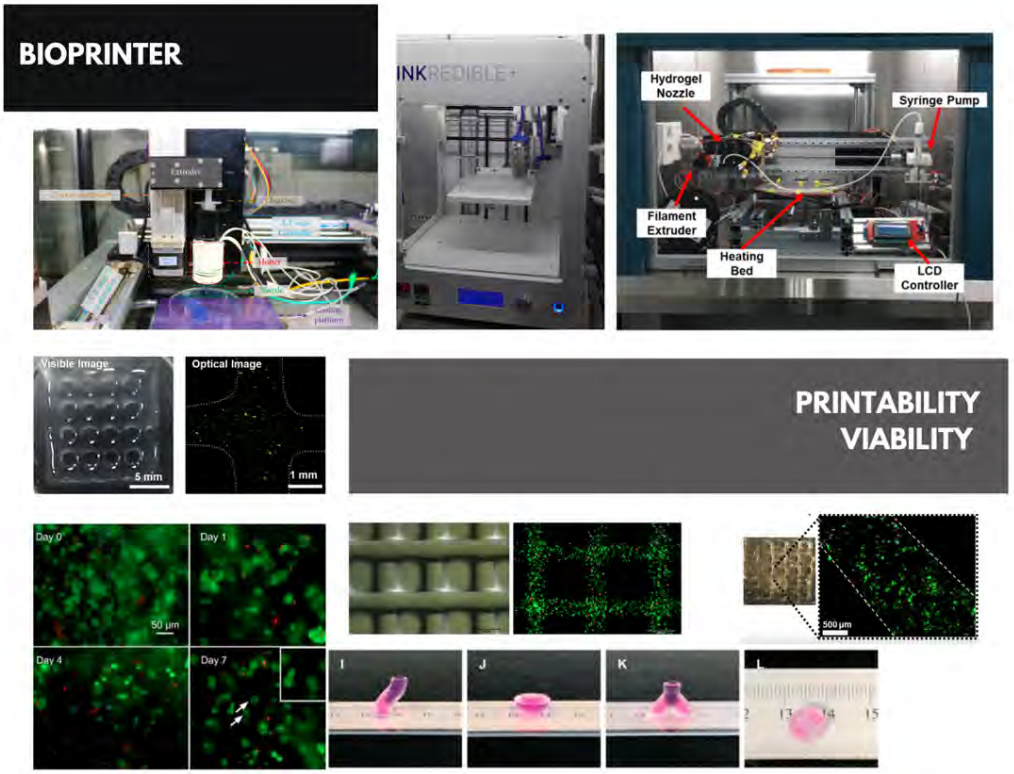

Figure 10: Presentation of commercial and custom-made bioprinters and comparison of printability and viability of bio-ink-embedded cells [57,119,135,140,141], CC-BY license.

with calcium chloride. The cells could proliferate and differentiate into self-assembling cell aggregates [48].

Butler *et al.* also chose to modify chitosan to *N,O*-carboxymethyl chitosan. This polymer derivative is soluble in water at neutral pH. However, due to the rapid degradation of this polymer in the media, it is necessary to use additional compounds to produce the bio-ink. It was decided to add agarose because of its excellent biocompatibility and physicochemical properties. Agarose alone, like chitosan, is not used as a bio-ink due to its limited rheological properties. However, it is the one that provides a longer scaffold degradation time compared to modified chitosan. Regarding rheological, mechanical, and biological properties, it was shown that the best properties were found to be bio-ink containing 40% agarose and 60% modified chitosan, which was a compromise between mechanical and biological properties. Increasing agarose concentration reduces rheological and mechanical properties, while a higher concentration of modified chitosan reduces cell viability. Cell survival studies were conducted on immature neuroblastoma cells from a neuro 2a cell line from mice for which the survival rate after extrusion printing of the bio-ink with 40% agarose was 100% [49].

Other studies on genipin were conducted by Mainardi *et al.* In addition, to achieve printability and structural fidelity, the alumina-chitosan nanocomposite gel was doped with alginate, which helped adjust the gel's rheological parameters and increase its biocompatibility. Escherichia coli was added to the bio-ink to analyze the biocompatibility of the composite. This work was a continuation of previous studies that used genipin and alumina. However, due to the lack of crosslinking of the covalent scaffold and thus its rapid degradation over time, it was necessary to reinforce the composite by using polyelectrolytic interactions with an oppositely charged polymer such as chitosan. Due to the gelation time, genipin did not affect the printability of the bio-ink. The survival test showed that alginate played a key role. Scaffolds without alginate showed about 30 and 135% survival rates. There are several solutions as to why significant differences in cell survival were observed, such as the effect of the antimicrobial properties of chitosan or genipin on cell viability or weaker bacterial accessibility due to the nanocomposite structure. However, further studies showed that cell death was significantly affected by the concentration of genipin in solution, and alginate protects cells from the effects of genipin. These studies support the potential use of chitosan as a bio-ink component [116].

Both chitosan and collagen have excellent properties as biomaterials in tissue engineering, but due to their limited mechanical properties, their use is rare. The researchers solved this problem by adding crosslinking compounds such as 1-ethyl-3-(dimethyl aminopropyl)carbodiimide and *N*-hydroxysuccinimide. The crosslinking mechanism involved the formation of covalent bonds between carboxyl or phosphate groups with primary amines giving covalent amide linkages between collagen-collagen and collagen-chitosan. In addition, due to the pH of the chitosan and collagen solutions, it was decided to nebulize them in 0.8 M $NaHCO_3$ to neutralize the pH immediately after printing. This procedure made it possible to obtain scaffolds that were non-cytotoxic to fibroblasts. The bio-ink was maintained at 4°C and at room temperature by extrusion at the time of printing [142].

Bioprinting facial reconstruction is challenging due to spatial elements' complex shapes and spatial objects' collapse. To print a cellular scaffold of the face, Zou *et al.* used PVA as a sacrificial material and a composite based on sodium alginate, agarose, and nanocellulose with human umbilical vein endothelial cells human fibroblasts. PVA is a well-water-soluble polymer that can be easily removed. It has been shown that with the concentration of agarose, the ability of the hydrogel to retain water and reduce the rate of water loss increases. In addition, the use of agarose increases the crosslinking of the gel network, which prevents loosening of the spatial structure and thus water loss. In such a system, the pores are smaller, corresponding to higher shape fidelity. Increasing the agarose concentration also improved the hydrogels' elasticity, suggesting that its presence in the scaffolds may improve biomechanical properties. However, pure agarose is characterized by the brittleness after gelation. In order to enhance the long-term stability of the bio-ink and improve adhesion and proliferation properties, the bio-ink was enriched with the addition of nanocellulose. Alginate was chosen for its wide range of viscosity at room temperature, good gelling ability in the presence of calcium ions, low toxicity, availability, and price. On the other hand, agarose for rapid coagulation. The cell scaffolds showed excellent properties, ensuring cell survival after printing at about 95% and after incubation at 80%. Cell proliferation, spatial network formation, differentiation, and ECM synthesis also occurred [50].

Seidel *et al.*, in turn, proposed alginate, agarose, and methylcellulose-based bio-ink for the formation of three-dimensional matrices with defined internal pore architecture for plant cells of *Ocimum basilicum* L. var. *purpurascens Benth*, "Cinnamon Basil." Based on previous research on alginate-based bio-ink, methylcellulose, mesenchymal cells, and microalginateae, they decided to partially replace methylcellulose with agarose, which gels at room temperature. The presence of methylcellulose was crucial to achieving the proper viscosity of the bio-ink during printing. In addition, the alginate was cross-linked with calcium chloride after printing. Agarose concentrations above 1% have been shown

to cause inhomogeneous strands, so lower concentrations are recommended [51].

Dravid *et al.*, investigated the potential use of agarose- and gelatin-based bio-ink in extrusion-based bioprinting. The rheological properties of the bio-ink were affected by both the ratio in which the components were mixed and the temperature. All the hydrogels showed a sharp increase in viscosity when the temperature was lowered to around 28°C. In addition, the increase in viscosity occurred at a higher concentration of gelatin in the formulation which resulted in an increase in yield stress, the minimum stress required to extrude the material through the nozzle. Although this yield stress in the agarose-gelatin formulation is low, it is possible to maintain it in the cartridge. In addition, due to the rate of gelation of the thermosensitive bio-ink, the agarose components ensure good printability and shape retention after extrusion. In order for the bio-ink to retain its liquid state of the head, it must be heated to 36°C and the printing platform to 10°C to allow immediate gelation. SH-SY5Y cells after printing retained a high viability of >90% after 23 days in culture [52].

Studies on the development of bio-ink, based on alginate and k-carrageenan, which mainly focused on printability as a key parameter, were carried out by Kim *et al.* The role of k-carrageenan was to increase both viscosity and shear modulus without losing shear thinning properties was proposed by Kim *et al.* As k-carrageenan significantly improved the mechanical properties and trioscopic properties of the alginate hydrogel, the printability and shape retention fidelity of the printed objects were also improved. Likewise, the survival rate of MSCs was higher in the presence of k-carrageenan [53].

The effect of adding agarose or collagen I to alginate was investigated by Yang *et al.* to overcome the rapid degradation rate of pure alginate. Chondrocyte cells were used to print a construct with potential use in regenerating cartilage tissue. Both polymers increased the construct's stiffness and thus mechanical strength with significantly lower swelling and water content as well as higher elastic modulus. The advantage of alginate-collagen bio-ink over alginate-agarose was significantly higher proliferation and survival of chondrocytes which was due to the presence of cell adhesion ligands in the collagen [143].

Another bio-ink, methacrylated gelatin with collagen doped tyrosinase was used to print living skin tissue. Tyrosinase provided a higher retaining modulus due to the additional enzymatic crosslinking. At the same time, the higher enzyme concentration made 3D structure formation more difficult due to the higher G' than viscosity of the sample. The optimal viscosity of the bio-ink was found at 20°C. The degradation rate was not significantly different. In addition to crosslinking, additional promotion of HEM cell viability was found. For HaCat cells, on the other hand, the survival rate after bioprinting was over 90% but no significant difference was observed after 7 days in the presence of tyrosinase, which was 93.7%. HDF cells retained a viability of more than 88 and 95% after 7 days; however, here too they did not affect cell behavior [72].

A similar study on modifying the rate of biodegradation so that it is possible to create functional tissue while maintaining the desired shape was conducted by Barceló *et al.* As before, the study showed that mixing alginate in the right proportion with partially oxidized alginate allows a controlled rate of degradation of the scaffold. However, in order to obtain the proper rheology of such a bio-ink, gellatin was added. In addition, lowering the temperature from 37 to 4°C further tuned the viscosity of the bio-ink which was due to the thermal gelation properties of gelatin. As gelatin type B gels at 16°C, it was chosen as the optimal temperature during printing. As the degree of alginate oxidation increased, the degradation rate also increased. Partial oxidation of alginate to 4% allowed for a scaffold that degraded completely after 4 weeks of culture, however, with the structure collapsing over time. The additional contribution of non-oxidized alginate and gelatin resulted in a scaffold that was structurally supportive of MSC differentiation without significant shape changes [54].

Fish gelatin and alginate were mixed together to form a bio-ink with HaCaT cells. As the proportion of alginate increased, higher printing accuracy was observed. In addition, the concentration of gelatin between 4 and 5% did not significantly change this parameter. The highest accuracy was obtained for the gelatin and alginate ratio of 6:11. After 10 min of crosslinking, the scaffold was shown to have adequate strength, *i.e.*, an elastic modulus of 133.25 kPa and an ultimate strength of 63.96 kPa [55].

A similar composition was used to print a tissue model mimicking the cervix. The bio-ink composed with 10% w/v of alginate and 50% w/v of gelatin had high fidelity shape retention and mechanical properties similar to the *in vivo* system. In order to maximize cell survival, HeLa cells were first encapsulated in Alginate microcapsules and then printed on multilayer scaffolds. The main purpose of adding gelatin to the alginate solution was to improve its printability and enhance the structural stability of the print. Alginate solutions are characterized by low thixotropy, which is why they are often mixed with other polymers to prevent expansion and collapse of printed fibers. Therefore, by optimizing both the concentration of added gelatin to the alginate solution and the polymer gelation time, it was possible to increase the viscosity of the bio-ink, contributing to achieving optimal print quality [144]. Improvements in the properties of the

gelatin- and alginate-based bio-ink were achieved by incorporating boron nitride nanotubes (BNNTs). Comparing with gelatin-alginate bio-ink, better deposition and structural stability were noted after BNNT incorporation. In addition, the cells were successfully encapsulated in the hydrogels which increased the survival rate [56]. Alginate-gelatin bio-ink was also used to test the effect of osteoinductive factors on the differentiation of UMSC-derived umbilical cord MSCs along with endothelial cells. The important role played by this factor and UMSC-EC interactions on osteogenic differentiation was demonstrated [58]. Optimization of the printability of gelatin-alginate bio-ink with the addition of cellulose nanofibers and primary rabbit fibrochondrocytes (rFC) was performed by Luo *et al.* to bio-print the lacuna. The addition of CNF enabled the printing of high-precision constructs while maintaining long-term cell viability. Depending on the concentration of gelatin in the system, the bio-ink was characterized by different printing temperatures. At a concentration of 20%, the best filamentation was observed at 25°C, while for 10% the maximum printing temperature was 20°C with the same other parameters. However, only samples with higher gelatin concentrations showed acceptable fidelity and integrity [57]. The suitability of oxidized alginate-gelatin bio-ink (ADA-Gel) for printing C2C12 cells was investigated by Distler *et al.* It was shown that the use of biodegradable oxidized alginate and gel contributed to the migration of C2C12 cells to the hydrogel surface, where cells differentiate into ordered myotube segments in areas of high cell density [145].

A new bio-ink of carboxymethylchitosan and alginate for bioprinting scaffolds for enamel tissue regeneration was developed by Mohabatpour *et al.* Chitosan has good mucoadhesive and biocompatible properties. However, as this polymer dissolves in acid solutions, it was proposed to be modified to carboxymethylchitosan. This one, in turn, is characterized by a high degree of degradation and poor mechanical properties, so it was proposed to mix it with alginate. On the other hand, alginate has slow degradation kinetics and limited cell interaction properties. In addition,

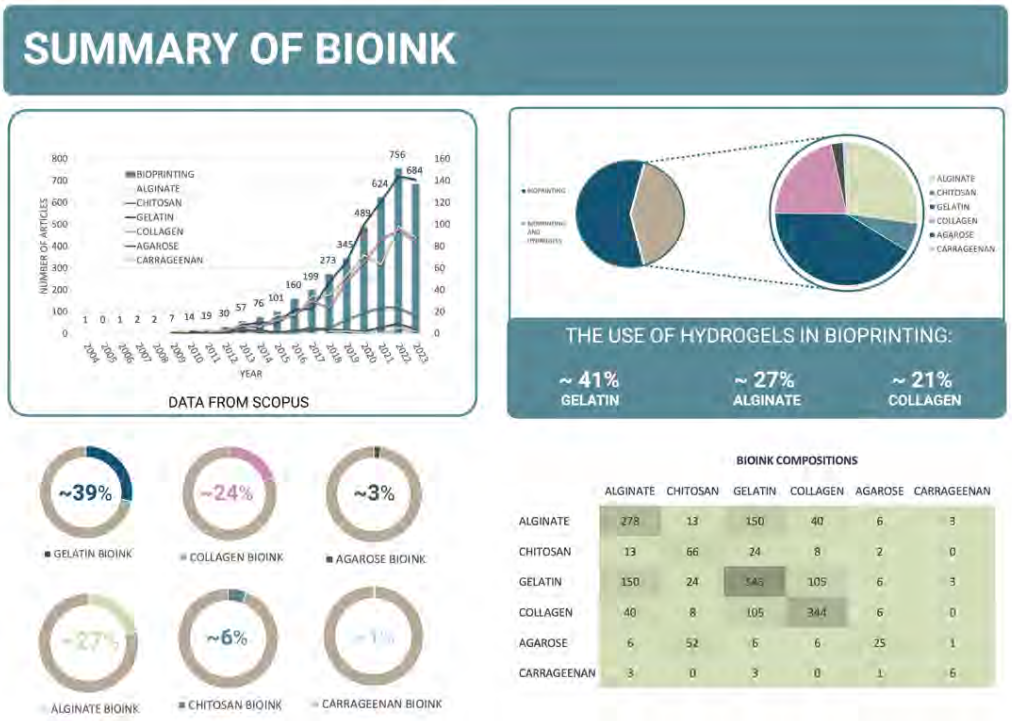

Figure 11: Comparative analysis of bio-inks based on selected polymers used in bioprinting – a comprehensive overview showing the trend of the number of scientific articles from 2004 to 2021, taking into account the contribution of each polymer. The data come from the Scopus database (created with BioRender.com).

dual crosslinking occurs in the scaffold, as both polymers can form hydrogels through physical crosslinking in the presence of calcium ions as well as the amine group of carboxymethylchitosan forms, an ionic bond with the carboxyl group of alginate [146].

A multicomponent bio-ink based on aldehyde hyaluronic acid, carboxymethylchitosan, gelatin, and alginate exhibits weak temperature dependence due to the main crosslinking mechanism relying on Schiff base bonds between carboxymethylchitosan/aldehyde hyaluronic acid and carboxymethylchitosan/alginate electrostatic interactions. In the case of gelatin-alginate compositions, a temperature reduction to 10°C was necessary to maintain good printability. In contrast, carboxymethylchitosan/aldehyde hyaluronic acid itself does not have adequate mechanical properties and cannot be extruded continuously and deposited efficiently [147].

Figure 11 provides a graphical summary of the research trends in the field of bio-ink used for bioprinting. It uses information from the Scopus database to chart the annual distribution of scientific publications that explore the use of various hydrogels such as alginate, chitosan, gelatin, collagen, agarose, and carrageenan in bioprinting. A pronounced rise in publication volume is noted from 2001 onwards, highlighting gelatin, alginate, and collagen as the most frequently investigated materials. Pie charts detail the proportional use of these materials in bio-ink compositions, underscoring the dominance of gelatin, alginate, and collagen in both hydrogel-based bio-inks and the broader spectrum of bio-inks. Furthermore, the data present a cross-comparison of the most prevalent polymer pairings in bio-ink formulations, indicating that gelatin is most commonly combined with alginate (150 articles) and collagen (105 articles).

In conclusion, there is a wide range of application possibilities for the selected marine polymer-based bio-inks in bioprinting, *i.e.*, from the repair of damaged spinal cord to skin regeneration. Table 2 summarizes the bio-inks described above, focusing on two main parameters: the quality of printing, *i.e.*, the ability to print with the bioprinter selected for this purpose, and the viability of the cells used. In addition, depending on the circuits and printing systems used, selected crosslinking methods are presented, *i.e.*, chemical, such as Schiff reactions, or physical, such as temperaature. The application of appropriate crosslinking methods to a given composition, *e.g.*, calcium chloride to alginate or UV crosslinking to methacrylated gelatin, as well as temperature to agarose, makes it possible to achieve control over crosslinking, *i.e.*, hardening of the bio-ink during extrusion and with it the preservation of the best possible cell viability and printability. In addition, these parameters are often subjected to qualitative assessment and are concerned with a selected number of days or layers, which makes it difficult to compare individual systems with one another. However, as for the bioprinters themselves, there is a trend toward customization and prototyping of devices tailored to specific bioprinters which increases their application possibilities.

4 Conclusion and further steps

In recent years, there has been tremendous progress and development in the field of tissue engineering bioprinting. Hydrogels, particularly naturally derived polymers, appear to be optimal and natural tissue-like biomaterials for bioprinting. Indeed, marine-derived polymers specifically have shown enormous potential in this area. After analyzing their properties, as well as the challenges and solutions proposed by researchers in the cited publications (Figures 5–9), it has been noted that there is a trend towards blending several polymers to create multi-component bio-inks. This solution is a known approach in materials engineering, where the search for mutually complementary materials is common. However, it is crucial that these materials are compatible with each other, *i.e.*, they do not negatively influence each other, as shown in the SWOT analysis (Figure 4).

However, despite the enormous potential of bioprinting, finding such systems that enable the printing of mechanically stable scaffolds that enable cell proliferation and differentiation into appropriate tissues remains a major challenge. On the one hand, new methods of combining hydrogels using various chemical modifications, crosslinking compounds, or plasticizers to improve the rheological, mechanical, and biological properties of the resulting scaffolds are still being described. Still the main method of crosslinking bio-inks remains the method of using alginate and calcium chloride, or methacrylated gelatin crosslinked with UV light, each of which has certain disadvantages, including a reduction in cell viability. Beyond the literature data, even today's commercially ready-to-use bio-inks are mainly based on polymers such as alginate, which is cross-linked using the included calcium chloride, or on methacrylated gelatin, which in turn is cross-linked using UV light. Moreover, many bio-inks are a combination of these two crosslinking methods and are based on both alginate, methacrylated alginate, or methacrylated gelatin. However, if these solutions were perfect and free of defects, there would be a huge breakthrough in tissue engineering and regenerative medicine. At the moment, however, these solutions are not perfect, and these bio-inks serve primarily as a tool for further research. Current solutions on the market only allow the evaluation of rheological and biological parameters of bio-inks, which affect cell survival and

Table 2: Comparison of marine polymer-based bio-inks used based on their printability and cell survival rates

Bio-ink composition	Cross-linking method	Bioprinter	Application	Printability	Cell viability	Ref.
Chitosan						
Hydroxypropyl chitosan-thiolated hyaluronic acid-vinyl sulfonated hyaluronic acid-Matrigel	Covalent- crosslinking *in situ via* Michael-addition between thiolated hyaluronic acid-vinyl sulfonated and vinyl sulfonated hyaluronic acid Thermally gellable	Custom microextrusion-based 3D printing system (Bioscaffolder, GeSiM, Germany)	Spinal cord injury repair	Qualitative assessment based on the attached recordings: well-kept shape and resolution 7 mm × 7 mm, thickness = 2 mm, strand distance = 0.8 mm	NSCs up to 95% after 7 days 4 mm × 4 mm × 4 mm	[117]
Chitosan-glycerophosphate-hydroxyethyl cellulose-cellulose nanocrystals	Chemical-crosslinking *via* Schiff-base linkages between chitosan and hydroxyethyl cellulose	Extrusion bioprinter (BioX, Cellink, Gothenburg, Sweden)	Osteogenic differentiation and bone regeneration	Qualitative assessment based on the attached photos: well-kept shape and resolution Images of strands	Pre-osteoblast cell line isolated from mouse calvaria MC3T3-E1 Qualitative assessment based on the attached photos: high viability after 3 and 7 days of bioprinting Cylindrical scaffolds (5 mm diameter × 3 mm thickness)	[118]
Chitosan-gelling agent	Physical-crosslinking by non-covalent interaction	3D bioprinting system consisting of a motorized xyz-stage, a heating bed, and a multi-nozzle printer head was developed	Tissue engineering	Qualitative assessment based on the attached photos: correct Printing into the PCL framework due to not having enough rigidity Problem with nozzle clogging due to gelling time, lattice-type structure was of a thickness of 2 mm with an 8-layer height	Human PDLSCs Qualitative assessment based on the attached photos: good viability up to 7 days after bioprinting No information about different dimensions	[119]
Chitosan-genipin-PEG	Genipin crosslinker	BIO X (Cellink)	Skin regeneration	Unstudied, however, the authors stressed that the rheological properties should be adjusted to improve printability. Qualitative assessment: correct rectangular design 20 mm long × 20 mm wide × 1 mm thick, 3 layers	Keratinocyte and human dermal fibroblast cells Up to 85% after 7 days 6.4 mm width × 3 mm thickness	[120]
Methacrylated Chitosan-β-glycerol phosphate salt	Photo-crosslinking	3D bioprinter (Rokit Invivo 3D Bioprinter, RokitHealthcare)	Tissue engineering	3D structures without defects	Fibroblasts (NIH/3T3), osteoblast-like cells (Saos-2) and neuronal-like cells (SH-SY5Y)	[121]

(Continued)

Table 2: *Continued*

Bio-ink composition	Cross-linking method	Bioprinter	Application	Printability	Cell viability	Ref.
	Thermally gellable			Strain size around 500 µm, 4-layer grid	After 7 days, the whole printed structures were colonized by cells and only few apoptotic cells were observed drops or grid-shaped single-layer structures	
Polyethylene oxide-co-Chitosan-co-poly (methylmethacrylic-acid	Chemical-crosslinking	No information	Skin tissue	Highly flexible and strong architecture Qualitative analysis based on posted photos: very weak, no resolution	Human dermal fibroblast Up to 92% (pure chitosan 67%)	[122]
Self-crosslinkable chitosan-gallic acid	pH responsive crosslinking	INVIVO (Rokit Healthcare)	Tissue engineering	Pr = 1 ± 0.05 Square, grid, zigzag, and honeycomb patterns: 20 mm × 20 mm × 1.25 mm, 5 layers	NIH3T3 Above 92% after 7 days of bioprinting	[123]
Chitosan-nanohydroxyapatite gelled *via* glycerol phosphate and sodium hydrogen carbonate	Physical-crosslinking thermally gellable	3D bioprinter (Cellink BioX, Sweden)	Tissue engineering	Pr = 0.83–0.98 10 layers, height 2 mm Rectilinear multilayers: 18 × 18 mm	MC3T3-E1 Qualitative assessment based on the attached photos: up to 3 days: high	[124]
Methacrylated glycol chitosan	Photo-crosslinking: riboflavin	INVIVO (Rokit Healthcare, Seoul)	Bone tissue engineering	Pr = 1 ± 0.05 Multilayer structure: 8 mm × 8 mm × 0.8 mm, 5 layers	MG-63 cells Above 92% after 7 days	[125]
Alginate						
Alginate partially oxidized-peptide RGD	Ionic-crosslinking: $CaCl_2$	Palmetto Printer, custom-made	Tissue engineering	Qualitative analysis: high resolution and shape accuracy Structures were printed with 7 columns and 7 rows (12 mm × 12 mm)	hADSC Above 90% after 8 days	[15]
Alginate	FRESH technique	3D bioplotter from RegenHU (3D Discovery)	Tissue engineering	Depending on the ratio, the type of agent and the molecular weight of alginate from non-printable to spreading ratio of 5.3 ± 0.28	Above 85.02% after 24 h	[129]
	Ionic-crosslinking: $CaCl_2$			3 mm × 3 mm × 3 mm open single filament boxes	2 mm cylinders of 4 mm in diameters	
			Soft tissue	Pr = 0.898–0.953	Mouse fibroblasts NIH/3T3	[131]

(Continued)

Table 2: *Continued*

Bio-ink composition	Cross-linking method	Bioprinter	Application	Printability	Cell viability	Ref.
Alginate pre- and post-cross-linking	Ionic-crosslinking pre and post: $CaCO_3$	BioScaffolder 2.1 (GeSIM, Radeberg)		Squared structures with a side length of 15 mm	Above 90% up to 7 days then decrease by day 14 because, no adhesion motifs for native alginate	
Alginate-tempo-oxidized cellulose nanofibrils-polydopamine nanoparticles	Ionic-crosslinking: $CaCl_2$	Custom-made, extrusion-based 3D printer	Bone tissue regeneration	Pr = 1 Grid structure (20 mm × 20 mm, 2 layers)	Osteoblast cell lines MC3T3-E1 Above 80% up to 7 days	[132]
Agarose						
CANA carboxylated agarose-native agarose	Physical-crosslinking thermally gellable	Inkredible-2 (Cellink, Sweden)	Tissue engineering	Qualitative assessment based on the attached photos: good hollow cylinders 8–10 mm in height	Human NCs 74% up to 7 days Cylinders (7 mm diameter × 2 mm in height, wall thickness 1.5 mm)	[135]
Carrageenan						
Methacrylated Kappa-Carrageenan	Ionic-crosslinking Photo-crosslinking	Printed using a microfluidic syringe pump	Tissue engineering	Qualitative assessment based on the attached photos: good latticed constructs (15 mm × 15 mm)	Fibroblasts NIH-3T3 up to 9 days: high cylindrical shape (5 mm diameter and 0.3 mm thickness)	[141]
κ-carrageenan	No information	Custom made microextrusion-based 3D printing system	Tissue engineering	Pr = 0.9–1.1 Cylindrical molds with 8 mm diameter and 4–8 mm in height	L929 mouse fibroblasts Up to 90% after 8 days	[140]
Marine-derived polymer blend						
Oxidized alginate-alginate-gelatin	Ionic-crosslinking: $CaCl_2$	3D Discovery bioprinter (RegenHU, Villaz-St-Pierre, Switzerland)	Cartilage tissue	Qualitative assessment based on the attached photos: good cylindrical geometry of 4 mm in diameter by 4 mm height, strand distance of 0.250 mm	Bone marrow derived MSCs Qualitative assessment based on the attached photos: up to 7 days: high	[54]
Collagen-chitosan	Crosslinker: EDC (1-ethyl-3-(3-dimethyl aminopropyl) carbodiimide) and NHS (*N*-hydroxysuccinimide)	Bioprinter (3-DonorRes, trademark LIFE SI, Argentina)	Tissue engineering	Pr = 0.56–0.75 square holes of 4 mm on each side, strand thickness 0.3 mm	None	[142]
Chitosan-alginate-alumina	Genipin crosslinker	Inkredible (Cellink, Gothenburg, Sweden)	Tissue engineering	Pr = 1.07–0.96 lattice cuboid (final size 2 × 2 × 1 cm), 3–8 layers	Bacterial viability decreases up to 50% after a 24-h incubation in pure PBS, but suspensions containing genipin showed a more noticeable reduction in bacteria viability up to 25%	[116]

(Continued)

Table 2: *Continued*

Bio-ink composition	Cross-linking method	Bioprinter	Application	Printability	Cell viability	Ref.
					for 0.25 mM samples and up to 7% for 1 mM samples	
Nanocellulose-agarose-alginate	Ionic-crosslinking: $CaCl_2$	Bioprinter (Creator Pro, Zhejiang Flashforge 3D Technology Co., Ltd)	Autologous full-face reconstruction	Qualitative assessment based on the attached photos: good	Human umbilical vein endothelial cells (HUVECs) and human fibroblasts (hFBs)	[50]
				Face model: 85.11 mm × 50.82 mm × 35.28 mm	Up to 95.69 ± 0.05% after 12 h	
				Disks mode:15 mm in diameter and 5 mm in thickness	Up to 80% after 35 days	
Alginate-agarose-methylcellulose	Ionic-crosslinking: $CaCl_2$	Bioscaffolder 3.1 (GeSiM mbH, Radeberg, Germany)	Immobilization tool for plant cells that enables the development of new bioprocesses for secondary metabolites production	Qualitative assessment based on the attached photos: good, 4 layers-1.5 mm strand distance	Basil (*Ocimum basilicum* L. var. *purpurascens Benth*, "Cinnamon Basil")	[51]
	Thermally gellable			14 layers-strand distance 2 mm	Qualitative assessment based, up to 20 days: high	
				20 layers-strand distance 2.5 mm		
Alginate-carrageenan	Ionic-crosslinking: $CaSO_4$	Self-developed 3D bioprinting system	Bio-ink for tissue engineering applications	Qualitative assessment and measurement of fiber diameter: from poor to good	The rabbit adipose-derived MSCs	[53]
				13.2 mm × 13.2 mm square-shaped	After 24 h: high	
					25 mm × 25 mm, line space: 1.3 mm, 4 layers	
Collagen type I-agarose-alginate	Ionic-crosslinking: $CaCl_2$ Thermally gellable	D-Bioplotter system (Regenovo, Zhejiang, China)	Cartilage tissue engineering	Qualitative assessment based on the attached photos: good	Primary chondrocytes	[143]
				Gird 20 mm × 20 mm, 6 layers	From around 80 to 40% after 14 days	
Agarose-gelatin	Thermally gellable	BIO X 3D bioprinter (Cellink, Gothenburg, Sweden)	Bio-ink	Extrude as continuous filaments	SH-SY5Y cells	[52]
					Above 90% after 23 days	
					Droplets	
Alginate-gelatin	Ionic-crosslinking: $CaCl_2$	Commercial 3D printer (Prusa i3, Czech Republic)	Tissue model mimicking the cervix	Qualitative assessment based on the attached photos: for 3 layers: good. For 2, 4, 8, 10 layers: poor hexagonal scaffold	Human cervical adenocarcinoma (CCL-2, HeLa)	[144]
					Up to 95.25 ± 1.79% after 15 days	
					Hexagonal with 3 layers	
Alginate-gelatin	Ionic-crosslinking: $CaCl_2$	INKREDIBLE+ (Cellink, Sweden)	Tissue engineering	75–96% printing accuracy	HEK293T	[56]
				Gird: 10 mm × 10 mm × 1 mm	Above 80% after 72 h	
Alginate-gelatin	Ionic-crosslinking: $CaCl_2$	BioBot 3D Printer (Biobot Analytics, Inc., MA, USA)	Osteodifferentiation	Qualitative assessment based on the attached photos: good. Three layers (each layer 0.45 mm high	UMSC isolated from an umbilical cord	[58]
					Qualitative assessment based on the attached photos: high	

(Continued)

Table 2: *Continued*

Bio-ink composition	Cross-linking method	Bioprinter	Application	Printability	Cell viability	Ref.
Alginate-gelatin-cellulose nanofiber	Ionic-crosslinking: CaC_2	BioPrinter-1, BP-1 developed by researchers	Meniscus biofabrication.	Qualitative assessment based on the attached photos: good 19 layers	Primary rFCs Up to 96% after 14 days	[57]
Oxidized alginate-gelatin	Ionic-crosslinking: CaC_2	Extrusion-bioprinter Bioscaffolder 2.1 (Gesim, Germany)	Muscle engineering	No information	Qualitative assessment based on the attached photos: high	[145]
Carboxymethyl chitosan-alginate	Ionic-crosslinking: CaC_2	Pneumatic 3D Bioplotter (EnvisionTEC GmbH, Gladbeck, Germany)	Enamel tissue engineering	Pr = 0.9–1.1 latticed structure (10 mm × 10 mm × 5 mm), even 31 layers	after 13 days HAT-7 Above 80% after 14 days 2–3 layers	[146]
Aldehyde hyaluronic acid-N-carboxymethyl chitosan-gelatin-alginate	Chemical-crosslinking *via* Schiff-base linkages between carboxymethyl chitosan and aldehyde hyaluronic acid Ionic crosslinking: $CaCl_2$	Bioprinter (LivPrint Norm, Medprin, China)	Soft tissue	Qualitative assessment based on the attached photos: good grid-12 mm × 12 mm, 6 layers	NIH/3T3 fibroblasts Up to 91.38 ± 1.55% after 29 days	[147]
Fish gelatin type B-alginate	Ionic-crosslinking: CaC_2	INKREDIBLE (Cellink)	Surrounded skin graft for healing chronic wounds as a dressing substitute	Printing accuracy = 97%. Multilayer grid: line diameter is 0.41 mm, and the porosity size is at 1.1 mm for single layer	HaCaT Investigated cell viability	[55]
Methacrylated collagen type I from the skin of blue grenadier fish or methacrylated porcine-derived collagen Type I	Photo-crosslinking	GeSIM Bioscaffolder 3.2 (GeSIM, Radeberg, Germany)	Regenerative medicine applications	Qualitative assessment based on the attached photos: good. 1–2 layers	L929 fibroblasts Above 80% after 7 days	[93]

Table 3: Commercially available ready-to-use bio-ink kits from two leading manufacturers along with a description of crosslinking methods [148,149]

Cellink			Sigma-Aldrich		
Name of product	**Polymers**	**Crosslinking method**	**Name of product**	**Polymers**	**Crosslinking method**
Lifeink 200, 220, 240, 260	Bovine collagen	Temperature	TissueFab GelMA	Gelatin methacrylate	Photo-crosslinking
Cellink A-RGD	Alginate	Ionic ($CaCl_2$)	TissueFab GelAlg	Gelatin Alginate	Photo-crosslinking
Chitolnk	Chitosan Glucomannan Glycerol phosphate salt	Ionic (TPP)	TissueFab (GelAlgHA)MA	Gelatin methacrylate Alginate Methacrylate Hyaluronic acid methacrylate	Photo-crosslinking
GelMA	Gelatin methacrylate	Photo-crosslinking	TissueFab Alg (Gel)MA	Alginate Gelatin methacrylate	Photo-crosslinking Ionic crosslinking
GelMA A	Gelatin methacrylate Alginate	Photo-crosslinking or ionic crosslinking solution ($CaCl_2$)	TissueFab bio-ink Bone	Gelatin methacrylate Hydroxyapatite	Photo-crosslinking and support gel
GelMA C	Gelatin Methacrylate Nanofibrillated cellulose	Photo-crosslinking	TissueFab bio-ink Conductive	Gelatin methacrylate Carbon nanotubes	Photo-crosslinking
Gel XA	Gelatin methacrylate Xanthan gum Alginate	Photo-crosslinking -assisted crosslinking Ionic crosslinking			
Gel XG	Gelatin methacrylate Xanthan gum	Photo-crosslinking			
GelXA laminink+	Gelatin methacrylate Alginate	Photo-crosslinking Ionic crosslinking			
PhotoAlginate	Methacrylated alginate	Photo-crosslinking Ionic crosslinking			
PhotoGel-INK 95% DS PhotoGel-INK 50% DS	Porcine gelatin methacrylate	Photo-crosslinking			
TeloCOL-3 TeleCOL-6 TeleCOL-10	Type I bovine telocollagen				
PureCol	Type I bovine/human atelocollagen				

differentiation. Table 3 summarizes commercially available bio-inks from two leading producers, presenting the main components and crosslinking methods.

From our point of view, crosslinking methods that allow the system to gel as soon as it is excised, *e.g.*, under temperature, have greater potential. Despite promising results in many medical applications, implementation of the systems that have been described above is still minimal. One of the reasons for this is the complex or multi-step chemical modifications of the main components of the scaffolds, which hinder their application and also affect the price of the scaffolds. Therefore, it is necessary to direct further research to develop simple composites consisting of natural polymers alone, without the need for crosslinking compounds and additional chemical modifications that increase cytotoxicity and affect cell behavior by inducing oxidative stress [150]. In addition, due to the different needs and applications of such scaffolds, bio-ink must enable stable scaffolds in both hydrogel and xerogel forms, which is often impossible in the former case due to the poor mechanical properties of other polymers, among other factors. Another major challenge in many studies is finding a bioprinter compatible with a given biocomponent. Developing an optimal bio-ink is much more difficult than technically perfecting a printer. In addition, a drawback of most commercially available bioprinters is

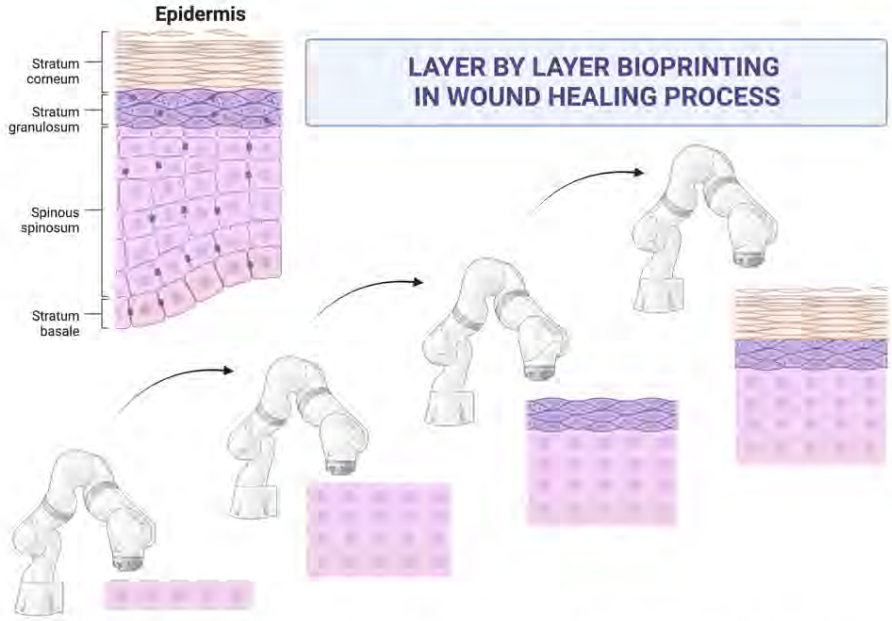

Figure 12: Simplified diagram of the printing methodology layer by layer with integrated robots (created with BioRender.com).

their technology, which allows printing objects limited to only a few layers. Table 2 describes several bio-inks for which the authors have developed their own bioprinters. In addition, for some, it was necessary to modify them to improve the heating properties of the printer. Another challenge remains the issue of assessing printability and cell survival. In the cited publications, these parameters were evaluated for both single and multilayer prints. In practice, all the constructs involve multilayer scaffolds, which, when placed in a living organism, will be subject to natural processes such as the flow of nutrients and metabolites. However, there is still no standardized model to assess the permeability of such a scaffold and the associated survival and biodegradability of such a scaffold. It is difficult to compare results in which the authors, despite specifying the same parameter, used multi- and single- or double-layer scaffolds. Therefore, there is a need to add other natural polymers and adjust printer components to obtain prints with good resolution and controlled 3D architecture. Conducting further research to develop the bio-ink and printing technology to a level that is acceptable from a tissue engineering perspective is crucial for bioprinting. This approach will allow mass production and implementation of new bioprinting technology.

A breakthrough technology with significant potential for advancing bioprinting is the application of machine learning algorithms, particularly in the field of regenerative medicine and tissue engineering. Utilizing the appropriate algorithms enables the printing of scaffolds that replicate natural organs and create complex, functional tissue structures. This tool facilitates the acceleration of the printing process, enhances precision, and minimizes the likelihood of potential errors [151]. The incorporation of deep learning into the quality control loop also permits the automatic optimization of the printing process and the reduction in material waste. This method relies on a dataset derived from high-resolution recordings, which trains a convolutional neural network to adjust the printing parameters, ensuring the complete automation of the printing process [152]. An interesting solution seems to be the use of robots that enable so-called spherical printing in the *xyz* plane. Another solution involves the concept of time-phased printing, that is, printing in which layers are added gradually and differentiated over time, to ensure a constant supply of nutrients to each layer (see Figure 12). The literature also describes the use of electrospinning, which has so far been a stand-alone technique used in the manufacture of cellular scaffolding. Electrospinning is a technology for creating micro- and nanoscale fibers, which makes it highly relevant to tissue engineering. However, the combination of this technology along with bioprinting

offers much greater possibilities, i.e., producing materials with innovative structural and functional properties for potential biomedical applications. Methods such as these can involve cutting electrospun scaffolds into pieces and formulating ink/bio-ink for 3D printing processes [153].

In conclusion, despite the significant development of 3D printing in tissue engineering, it is still necessary to clarify the measurement of key parameters and find such systems that will allow the highest possible cell survival with high printability, i.e., a state in which the biofabrication window will be overcome, when it is crucial for the regeneration of individual tissues.

Funding information: The authors state no funding involved.

Author contributions: All authors have accepted responsibility for the entire content of this manuscript and approved its submission.

Conflict of interest: The authors state no conflict of interest.

References

[1] Murphy, S. V. and A. Atala. 3D bioprinting of tissues and organs. *Nature Biotechnology*, Vol. 32, No. 8, 2014, pp. 773–785.

[2] Ng, W. L., C. K. Chua, and Y. F. Shen. Print Me An Organ! Why We Are Not There Yet. *Progress in Polymer Science*, Vol. 97, 2019, id. 101145.

[3] Unagolla, J. M. and A. C. Jayasuriya. Hydrogel-based 3D bioprinting: A comprehensive review on cell-laden hydrogels, bioink formulations, and future perspectives. *Applied Materials Today*, Vol. 18, 2020, id. 100479.

[4] Xie, Z., M. Gao, A. O. Lobo, and T. J. Webster. 3D bioprinting in tissue engineering for medical applications: The classic and the hybrid. *Polymers (Basel)*, Vol. 12, No. 8, 2020, id. 1717.

[5] Laurenti, M. and V. Cauda. ZnO nanostructures for tissue engineering applications. *Nanomaterials (Basel)*, Vol. 7, No. 11, 2017, id. 374.

[6] Kačarević, Ž. P., P. M. Rider, S. Alkildani, S. Retnasingh, R. Smeets, O. Jung, et al. An introduction to 3D bioprinting: Possibilities, challenges and future aspects. *Materials (Basel)*, Vol. 11, No. 11, 2018, id. 2199.

[7] Zhang, L., S. Chen, X. Wang, D. Wang, Y. Li, Q. Ai, et al. Ambient inkjet-printed high-efficiency perovskite solar cells: manipulating the spreading and crystallization behaviors of picoliter perovskite droplets. *Solar RRL*, Vol. 5, No. 5, 2021, id. 2100106.

[8] Foyt, D. A., M. D. A. Norman, T. T. L. Yu, and E. Gentleman. Exploiting advanced hydrogel technologies to address key challenges in regenerative medicine. *Advanced Healthcare Materials*, Vol. 7, No. 1, 2018, id. e1700939.

[9] Li, X., B. Liu, B. Pei, J. Chen, D. Zhou, J. Peng, et al. Inkjet bioprinting of biomaterials. *Chemical Reviews*, Vol. 120, No. 19, 2020, pp. 10793–10833.

[10] Ng, W. L., X. Huang, V. Shkolnikov, G. L. Goh, R. Suntornnond, and W. Y. Yeong. Controlling droplet impact velocity and droplet volume: key factors to achieving high cell viability in sub-nanoliter droplet-based bioprinting. *International Journal of Bioprinting*, Vol. 8, 2021, id. 424.

[11] Li, Y., O. Dahhan, C. D. M. Filipe, J. D. Brennan, and R. H. Pelton. Deposited nanoparticles can promote air clogging of piezoelectric inkjet printhead nozzles. *Langmuir*, Vol. 35, No. 15, 2019, pp. 5517–5524.

[12] Semba, J. A., A. A. Mieloch, and J. D. Rybka. Introduction to the state-of-the-art 3D bioprinting methods, design, and applications in orthopedics. *Bioprinting*, Vol. 18, 2020, id. e00070.

[13] Shi, J., B. Wu, S. Li, J. Song, B. Song, and W. F. Lu. Shear stress analysis and its effects on cell viability and cell proliferation in drop-on-demand bioprinting. *Biomedical Physics & Engineering Express*, Vol. 4, 2018, id. 045028.

[14] Lee, V., G. Singh, J. P. Trasatti, C. Bjornsson, X. Xu, T. N. Tran, et al. Design and fabrication of human skin by three-dimensional bioprinting. *Tissue Engineering Part C, Methods*, Vol. 20, No. 6, 2014, pp. 473–484.

[15] Jia, J., D. J. Richards, S. Pollard, Y. Tan, J. Rodriguez, R. P. Visconti, et al. Engineering alginate as bioink for bioprinting. *Acta Biomaterialia*, Vol. 10, No. 10, 2014, pp. 4323–4331.

[16] Boland, T., X. Tao, B. J. Damon, B. Manley, P. Kesari, S. Jalota, et al. Drop-on-demand printing of cells and materials for designer tissue constructs. *Materials Science & Engineering, C: Materials for Biological Applications*, Vol. 27, No. 3, 2007, pp. 372–376.

[17] Tylingo, R., P. Kempa, A. Banach-Kopeć, and S. Mania. A novel method of creating thermoplastic chitosan blends to produce cell scaffolds by FDM additive manufacturing. *Carbohydrate Polymers*, Vol. 280, 2022, id. 119028.

[18] Zenobi, E., M. Merco, F. Mochi, J. Ruspi, R. Pecci, R. Marchese, et al. Tailoring the microarchitectures of 3D printed bone-like scaffolds for tissue engineering applications. *Bioengineering (Basel)*, Vol. 10, No. 2, 2023, id. 567.

[19] Kalva, S. N., F. Ali, C. A. Velasquez, and M. Koç. 3D-printable PLA/Mg composite filaments for potential bone tissue engineering applications. *Polymers (Basel)*, Vol. 15, No. 3, 2023, id. 2572.

[20] Cano-Vicent, A., M. M. Tambuwala, S. Hassan Sk, D. Barh, A. A. A. Aljabali, M. Birkett, et al. Fused deposition modelling: Current status, methodology, applications and future prospects. *Addit Manuf*, Vol. 47, 2021, id. 102378.

[21] Rider, P., Ž.P. Kačarević, S. Alkildani, S. Retnasingh, and M. Barbeck. Bioprinting of tissue engineering scaffolds. *Journal of Tissue Engineering*, Vol. 9, 2018, id. 2041731418802090.

[22] Ramesh, S., O. L. A. Harrysson, P. K. Rao, A. Tamayol, D. R. Cormier, Y. Zhang, et al. Extrusion bioprinting: Recent progress, challenges, and future opportunities. *Bioprinting*, Vol. 21, 2021, id. e00116.

[23] Thakare, K., L. Jerpseth, Z. Pei, and H. Qin. Green bioprinting with layer-by-layer photo-crosslinking: A designed experimental investigation on shape fidelity and cell viability of printed constructs. *Journal of Manufacturing and Materials Processing*, Vol. 6, No. 2, 2022, id. 45.

[24] Ghavami Nejad, A., N. Ashammakhi, X. Y. Wu, and A. Khademhosseini. Crosslinking strategies for three-dimensional bioprinting of polymeric hydrogels. *Small*, Vol. 16, No. 31, 2020, id. e2002931.

[25] Lee, B. H., N. Lum, L. Y. Seow, P. Q. Lim, and L. P. Tan. Synthesis and characterization of types A and B gelatin methacryloyl for bioink applications. *Materials (Basel)*, Vol. 9, No. 9, 2016, id. 797.

[26] López-Marcial, G. R., A. Y. Zeng, C. Osuna, J. Dennis, J. M. García, and G. D. O'Connell. Agarose-based hydrogels as suitable bioprinting materials for tissue engineering. *ACS Biomaterials Science & Engineering*, Vol. 4, No. 11, 2018, pp. 3610–3616.
[27] Li, H., Y. J. Tan, S. Liu, and L. Li. Three-dimensional bioprinting of oppositely charged hydrogels with super strong interface bonding. *ACS Applied Materials & Interfaces*, Vol. 10, No. 14, 2018, pp. 11164–11174.
[28] Grigoryan, B., D. W. Sazer, A. Avila, J. L. Albritton, A. Padhye, A. H. Ta, et al. Development, characterization, and applications of multi-material stereolithography bioprinting. *Scientific Reports*, Vol. 11, No. 1, 2021, id. 3171.
[29] Yang, X., M. Mohseni, O. Bas, C. Meinert, E. J. New, and N. J. Castro. Type II photoinitiator and tuneable poly(Ethylene Glycol)-based materials library for visible light photolithography. *Tissue Engineering Part A*, Vol. 26, No. 5–6, 2020, pp. 292–304.
[30] Ng, W. L., J. M. Lee, M. Zhou, Y. W. Chen, K. X. A. Lee, W. Y. Yeong, et al. Vat polymerization-based bioprinting – process, materials, applications and regulatory challenges. *Biofabrication*, Vol. 12, No. 2, 2020, id. 022001.
[31] Morris, V. B., S. Nimbalkar, M. Younesi, P. McClellan, and O. Akkus. Mechanical properties, cytocompatibility and manufacturability of chitosan: PEGDA hybrid-gel scaffolds by stereolithography. *Annals of Biomedical Engineering*, Vol. 45, No. 1, 2017, pp. 286–296.
[32] Venturella, G., V. Ferraro, F. Cirlincione, and M. L. Gargano. Medicinal mushrooms: bioactive compounds, use, and clinical trials. *International Journal of Molecular Sciences*, Vol. 22, No. 2, 2021, id. 634.
[33] Agarwal, K., V. Srinivasan, V. Lather, D. Pandita, and K. S. Vasanthan. Insights of 3D bioprinting and focusing the paradigm shift towards 4D printing for biomedical applications. *Journal of Materials Research*, Vol. 38, No. 1, 2023, pp. 112–141.
[34] Michael, S., H. Sorg, C. T. Peck, L. Koch, A. Deiwick, B. Chichkov, et al. Tissue engineered skin substitutes created by laser-assisted bioprinting form skin-like structures in the dorsal skin fold chamber in mice. *PLoS One*, Vol. 8, No. 7, 2013, id. e57741.
[35] Gudapati, H., J. Yan, Y. Huang, and D. B. Chrisey. Alginate gelation-induced cell death during laser-assisted cell printing. *Biofabrication*, Vol. 6, No. 3, 2014, id. 035022.
[36] Das, S., F. Pati, Y. J. Choi, G. Rijal, J. H. Shim, S. W. Kim, et al. Bioprintable, cell-laden silk fibroin-gelatin hydrogel supporting multilineage differentiation of stem cells for fabrication of three-dimensional tissue constructs. *Acta Biomaterialia*, Vol. 11, 2015, pp. 233–246.
[37] Donderwinkel, I., J. C. M. van Hest, and N. R. Cameron. Bio-inks for 3D bioprinting: recent advances and future prospects. *Polymer Chemistry*, Vol. 8, No. 31, 2017, pp. 4451–4471.
[38] Guillotin, B. and F. Guillemot. Cell patterning technologies for organotypic tissue fabrication. *Trends in Biotechnology*, Vol. 29, No. 4, 2011, pp. 183–190.
[39] Hölzl, K., S. Lin, L. Tytgat, S. Van Vlierberghe, L. Gu, and A. Ovsianikov. Bioink properties before, during and after 3D bioprinting. *Biofabrication*, Vol. 8, No. 3, 2016, id. 032002.
[40] Midha, S., M. Dalela, D. Sybil, P. Patra, and S. Mohanty. Advances in three-dimensional bioprinting of bone: Progress and challenges. *Journal of Tissue Engineering and Regenerative Medicine*, Vol. 13, No. 9, 2019, pp. 925–945.
[41] Iwanaga, S., Y. Hamada, Y. Tsukamoto, K. Arai, T. Kurooka, S. Sakai, et al. Design and fabrication of mature engineered pre-cardiac tissue utilizing 3D bioprinting technology and enzymatically crosslinking hydrogel. *Materials (Basel)*, Vol. 15, No. 3, 2022, id. 7928.
[42] Suntornnond, R., W. L. Ng, X. Huang, C. H. E. Yeow, and W. Y. Yeong. Improving printability of hydrogel-based bio-inks for thermal inkjet bioprinting applications via saponification and heat treatment processes. *Journal of Materials Chemistry B: Materials for Biology and Medicine*, Vol. 10, No. 32, 2022, pp. 5989–6000.
[43] Sakurada, S., M. Sole-Gras, K. Christensen, D. Wallace, and Y. Huang. Liquid-absorbing system-assisted intersecting jets printing of soft structures from reactive biomaterials. *Additive Manufacturing*, Vol. 31, 2019, id. 100934.
[44] Mobed-Miremadi, M., B. Asi, J. Parasseril, E. Wong, M. Tat, and Y. Shan. Comparative diffusivity measurements for alginate-based atomized and inkjet-bioprinted artificial cells using fluorescence microscopy. *Artif Cells Nanomed Biotechnol*, Vol. 41, No. 3, 2013, pp. 196–201.
[45] Xu, H., J. Casillas, and C. Xu. Effects of printing conditions on cell distribution within microspheres during inkjet-based bioprinting. *AIP Advances*, Vol. 9, No. 9, 2019, id. 095055.
[46] Hewes, S., A. D. Wong, and P. C. Searson. Bioprinting microvessels using an inkjet printer. *Bioprinting*, Vol. 7, 2017, pp. 14–18.
[47] Compaan, A. M., K. Christensen, and Y. Huang. Inkjet bioprinting of 3D silk fibroin cellular constructs using sacrificial alginate. *ACS Biomaterials Science & Engineering*, Vol. 3, No. 8, 2017, pp. 1519–1526.
[48] Gu, Q., E. Tomaskovic-Crook, G. G. Wallace, and J. M. Crook. 3D bioprinting human induced pluripotent stem cell constructs for in situ cell proliferation and successive multilineage differentiation. *Advanced Healthcare Materials*, Vol. 6, No. 17, 2017, id. 1700365.
[49] Butler, H. M., E. Naseri, D. S. MacDonald, R. A. Tasker, and A. Ahmadi. Investigation of rheology, printability, and biocompatibility of *N,O*-carboxymethyl chitosan and agarose bioinks for 3D bioprinting of neuron cells. *Materialia*, Vol. 18, 2021, id. 101053.
[50] Zou, Q., X. Tian, S. Luo, D. Yuan, S. Xu, L. Yang, et al. Agarose composite hydrogel and PVA sacrificial materials for bioprinting large-scale, personalized face-like with nutrient networks. *Carbohydrate Polymers*, Vol. 269, 2021, id. 118222.
[51] Seidel, J., T. Ahlfeld, M. Adolph, S. Kümmritz, J. Steingroewer, F. Krujatz, et al. Green bioprinting: extrusion-based fabrication of plant cell-laden biopolymer hydrogel scaffolds. *Biofabrication*, Vol. 9, No. 4, 2017, id. 045011.
[52] Dravid, A., A. McCaughey-Chapman, B. Raos, S. J. O'Carroll, B. Connor, and D. Svirskis. Development of agarose-gelatin bioinks for extrusion-based bioprinting and cell encapsulation. *Biomedical Materials*, Vol. 17, No. 1, 2022, id. 015007.
[53] Kim, M. H., Y. W. Lee, W. K. Jung, J. Oh, and S. Y. Nam. Enhanced rheological behaviors of alginate hydrogels with carrageenan for extrusion-based bioprinting. *Journal of the Mechanical Behavior of Biomedical Materials*, Vol. 98, 2019, pp. 187–194.
[54] Barceló, X., K. F. Eichholz, O. Garcia, and D. J. Kelly. Tuning the degradation rate of alginate-based bioinks for bioprinting functional cartilage tissue. *Biomedicines*, Vol. 10, No. 7, 2022, id. 1621.
[55] Boonyagul, S., D. Pukasamsombut, S. Pengpanich, T. Toobunterng, K. Pasanaphong, N. Sathirapongsasuti, et al. Bioink hydrogel from fish scale gelatin blended with alginate for 3D-bioprinting application. *Journal of Food Processing and Preservation*, Vol. 46, 2022, id. e16563.

[56] Kakarla, A. B., I. Kong, I. Turek, C. Kong, and H. Irving. Printable gelatin, alginate and boron nitride nanotubes hydrogel-based ink for 3D bioprinting and tissue engineering applications. *Materials & Design*, Vol. 213, 2022, id. 110362.

[57] Luo, W., Z. Song, Z. Wang, Z. Wang, Z. Li, C. Wang, et al. Printability optimization of gelatin-alginate bioinks by cellulose nanofiber modification for potential meniscus bioprinting. *Journal of Nanomaterials*, Vol. 2020, 2020, id. 3863428.

[58] Eswaramoorthy, S. D., N. Dhiman, A. Joshi, and S. N. Rath. 3D bioprinting of mesenchymal stem cells and endothelial cells in an alginate-gelatin-based bioink. *Journal of 3D Printing in Medicine*, Vol. 5, No. 1, 2021, pp. 23–36.

[59] Gruene, M., C. Unger, L. Koch, A. Deiwick, and B. Chichkov. Dispensing pico to nanolitre of a natural hydrogel by laser-assisted bioprinting. *Biomedical Engineering Online*, Vol. 10, 2011, id. 19.

[60] Sorkio, A., L. Koch, L. Koivusalo, A. Deiwick, S. Miettinen, B. Chichkov, et al. Human stem cell based corneal tissue mimicking structures using laser-assisted 3D bioprinting and functional bioinks. *Biomaterials*, Vol. 171, 2018, pp. 57–71.

[61] Han, X., M. Sun, B. Chen, Q. Saiding, J. Zhang, H. Song, et al. Lotus seedpod-inspired internal vascularized 3D printed scaffold for bone tissue repair. *Bioact Mater*, Vol. 6, No. 4, 2021, pp. 1639–1652.

[62] Pérez-Cortez, J. E., V. H. Sánchez-Rodríguez, S. Gallegos-Martínez, C. Chuck-Hernández, C. A. Rodríguez, M. M. Álvarez, et al. Low-cost light-based GelMA 3D bioprinting via retrofitting: manufacturability test and cell culture assessment. *Micromachines (Basel)*, Vol. 14, No. 1, 2022, id. 55.

[63] Amler, A. K., P. H. Dinkelborg, D. Schlauch, J. Spinnen, S. Stich, R. Lauster, et al. Comparison of the translational potential of human mesenchymal progenitor cells from different bone entities for autologous 3D bioprinted bone grafts. *International Journal of Molecular Sciences*, Vol. 22, No. 3, 2021, id. 796.

[64] Magalhães, L. S., F. E. Santos, C. D. Elias, S. Afewerki, G. F. Sousa, A. S. Furtado, et al. Printing 3D hydrogel structures employing low-cost stereolithography technology. *Journal of Functional Biomaterials*, Vol. 11, No. 1, 2020, id. 12.

[65] Lam, T., T. Dehne, J. P. Krüger, S. Hondke, M. Endres, A. Thomas, et al. Photopolymerizable gelatin and hyaluronic acid for stereolithographic 3D bioprinting of tissue-engineered cartilage. *Journal of Biomedical Materials Research Part B, Applied Biomaterials*, Vol. 107, No. 8, 2019, pp. 2649–2657.

[66] Shopperly, L. K., J. Spinnen, J. P. Krüger, M. Endres, M. Sittinger, T. Lam, et al. Blends of gelatin and hyaluronic acid stratified by stereolithographic bioprinting approximate cartilaginous matrix gradients. *Journal of Biomedical Materials Research Part B, Applied Biomaterials*, Vol. 110, No. 11, 2022, pp. 2310–2322.

[67] Emerson, A. E., A. B. McCall, S. R. Brady, E. M. Slaby, and J. D. Weaver. Hydrogel injection molding to generate complex cell encapsulation geometries. *ACS Biomaterials Science & Engineering*, Vol. 8, No. 9, 2022, pp. 4002–4013.

[68] Pekař, M.. Editorial: Biopolymer-based hydrogels – Ubiquitous and prospective materials. *Front Mater*, Vol. 7, 2020, id. 570.

[69] Yu, K. F., T. Y. Lu, Y. C. Li, K. C. Teng, Y. C. Chen, Y. Wei, et al. Design and synthesis of stem cell-laden keratin/glycol chitosan methacrylate bioinks for 3D bioprinting. *Biomacromolecules*, Vol. 23, No. 7, 2022, pp. 2814–2826.

[70] Koons, G. L. and A. G. Mikos. Progress in three-dimensional printing with growth factors. *Journal of Controlled Release*, Vol. 295, 2019, pp. 50–59.

[71] Bakhtiari, M., J. Park, Y. C. Ding, S. Shleizer-Burko, S. L. Neuhausen, B. V. Halldórsson, et al. Variable number tandem repeats mediate the expression of proximal genes. *Nature Communications*, Vol. 12, No. 1, 2021, id. 2075.

[72] Shi, Y., T. L. Xing, H. B. Zhang, R. X. Yin, S. M. Yang, J. Wei, et al. Tyrosinase-doped bioink for 3D bioprinting of living skin constructs. *Biomedical Materials*, Vol. 13, No. 3, 2018, id. 035008.

[73] Wang, J. H., C. W. Tsai, N. Y. Tsai, C. Y. Chiang, R. S. Lin, R. F. Pereira, et al. An injectable, dual crosslinkable hybrid pectin methacrylate (PECMA)/gelatin methacryloyl (GelMA) hydrogel for skin hemostasis applications. *International Journal of Biological Macromolecules*, Vol. 185, 2021, pp. 441–450.

[74] Huang, S., B. Yao, J. Xie, and X. Fu. 3D bioprinted extracellular matrix mimics facilitate directed differentiation of epithelial progenitors for sweat gland regeneration. *Acta Biomaterialia*, Vol. 32, 2016, pp. 170–177.

[75] Jang, J., T. G. Kim, B. S. Kim, S. W. Kim, S. M. Kwon, and D. W. Cho. Tailoring mechanical properties of decellularized extracellular matrix bioink by vitamin B2-induced photo-crosslinking. *Acta Biomaterialia*, Vol. 33, 2016, pp. 88–95.

[76] Sharma, A., G. Garcia, Y. Wang, J. T. Plummer, K. Morizono, V. Arumugaswami, et al. Human iPSC-derived cardiomyocytes are susceptible to SARS-CoV-2 infection. *Cell Reports Medicine*, Vol. 1, No. 6, 2020, id. 100052.

[77] Hoffman, A. S.. Hydrogels for biomedical applications. *Advanced Drug Delivery Reviews*, Vol. 54, No. 1, 2002, pp. 3–12.

[78] Ward, M. A. and T. K. Georgiou. Thermoresponsive polymers for biomedical applications. *Polymers (Basel)*, Vol. 3, No. 3, 2011, pp. 1215–1242.

[79] Kumashiro, Y., M. Yamato, and T. Okano. Cell attachment-detachment control on temperature-responsive thin surfaces for novel tissue engineering. *Annals of Biomedical Engineering*, Vol. 38, No. 6, 2010, pp. 1977–1988.

[80] Banach-Kopeć, A., S. Mania, J. Pilch, E. Augustin, I. Gabriel, and R. Tylingo. A novel method of endotoxins removal from chitosan hydrogel as a potential bioink component obtained by CO2 saturation. *International Journal of Molecular Sciences*, Vol. 23, No. 10, 2022, id. 5505.

[81] El-Sherbiny, I. M. and M. H. Yacoub. Hydrogel scaffolds for tissue engineering: Progress and challenges. *Global Cardiology Science & Practice*, Vol. 2013, No. 3, 2013, pp. 316–342.

[82] Isaeva, E. V., E. E. Beketov, V. V. Yuzhakov, N. V. Arguchinskaya, A. A. Kisel, E. P. Malaknov, et al. The use of collagen with high concentration in cartilage tissue engineering by means of 3D-bioprinting. *Cell and Tissue Biology*, Vol. 15, No. 6, 2021, pp. 493–502.

[83] Zhang, Y., D. Zhou, J. Chen, X. Zhang, X. Li, W. Zhao, et al. Biomaterials based on marine resources for 3D bioprinting applications. *Marine Drugs*, Vol. 17, No. 9, 2019, id. 555.

[84] Cavallo, A., T. Al Kayal, A. Mero, A. Mezzetta, A. Pisani, I. Foffa, et al. Marine collagen-based bioink for 3D bioprinting of a bilayered skin model. *Pharmaceutics*, Vol. 15, No. 5, 2023, id. 1331.

[85] Szychlinska, M. A., F. Bucchieri, A. Fucarino, A. Ronca, and U. D'Amora. Three-dimensional bioprinting for cartilage tissue engineering: insights into naturally-derived bioinks from land and marine sources. *Journal of Functional Biomaterials*, Vol. 13, No. 2, 2022, id. 118.

[86] Liu, S., C. S. Lau, K. Liang, F. Wen, and S. H. Teoh. Marine collagen scaffolds in tissue engineering. *Current Opinion in Biotechnology*, Vol. 74, 2022, pp. 92–103.

[87] Fuller, A. M. and T. S. Eisinger-Mathason. Context matters: response heterogeneity to collagen-targeting approaches in desmoplastic cancers. *Cancers (Basel)*, Vol. 14, No. 12, 2022, id. 3132.
[88] Gelse, K., E. Pöschl, and T. Aigner. Collagens–structure, function, and biosynthesis. *Advanced Drug Delivery Reviews*, Vol. 55, No. 12, 2003, pp. 1531–1546.
[89] Osidak, E. O., V. I. Kozhukhov, M. S. Osidak, and S. P. Domogatsky. Collagen as bioink for bioprinting: a comprehensive review. *International Journal of Bioprinting*, Vol. 6, No. 4, 2020, id. 270.
[90] Tylingo, R., S. Mania, P. Anna, R. Piątek, and R. Pawlowicz. Isolation and characterization of acid soluble collagen from the Skin of African Catfish (Clarias gariepinus), Salmon (Salmo salar) and Baltic cod (Gadus morhua). *Journal of Biotechnology Biomaterials*, Vol. 6, No. 1, 2016, pp. 1–6.
[91] Liu, W., K. Merrett, M. Griffith, P. Fagerholm, S. Dravida, B. Heyne, et al. Recombinant human collagen for tissue engineered corneal substitutes. *Biomaterials*, Vol. 29, No. 10, 2008, pp. 1147–1158.
[92] Lee, J. M., S. K. Q. Suen, W. L. Ng, W. C. Ma, and W. Y. Yeong. Bioprinting of collagen: considerations, potentials, and applications. *Macromolecular Bioscience*, Vol. 21, No. 1, 2021, id. 2000280.
[93] Maher, M., V. Glattauer, C. Onofrillo, S. Duchi, Z. Yue, T. C. Hughes, et al. Suitability of marine- and porcine-derived collagen type I hydrogels for bioprinting and tissue engineering scaffolds. *Marine Drugs*, Vol. 20, No. 6, 2022, id. 366.
[94] Parenteau-Bareil, R., R. Gauvin, and F. Berthod. Collagen-based biomaterials for tissue engineering applications. *Materials (Basel)*, Vol. 3, No. 3, 2010, pp. 1863–1887.
[95] Hinton, T. J., Q. Jallerat, R. N. Palchesko, J. H. Park, M. S. Grodzicki, H. J. Shue, et al. Three-dimensional printing of complex biological structures by freeform reversible embedding of suspended hydrogels. *Science Advances*, Vol. 1, No. 9, 2015, id. e1500758.
[96] Said, N. S. and N. M. Sarbon. Physical and mechanical characteristics of gelatin-based films as a potential food packaging material: A review. *Membranes (Basel)*, Vol. 12, No. 5, 2022, id. 442.
[97] Gómez-Guillén, M. C., B. Giménez, M. E. López-Caballero, and M. P. Montero. Functional and bioactive properties of collagen and gelatin from alternative sources: A review. *Food Hydrocolloids*, Vol. 25, No. 8, 2011, pp. 1813–1827.
[98] Bello, A. B., D. Kim, D. Kim, H. Park, and S. H. Lee. Engineering and functionalization of gelatin biomaterials: from cell culture to medical applications. *Tissue Engineering Part B, Reviews*, Vol. 26, No. 2, 2020, pp. 164–180.
[99] Afewerki, S., A. Sheikhi, S. Kannan, S. Ahadian, and A. Khademhosseini. Gelatin-polysaccharide composite scaffolds for 3D cell culture and tissue engineering: Towards natural therapeutics. *Bioengineering & Translational Medicine*, Vol. 4, No. 1, 2019, pp. 96–115.
[100] Nichol, J. W., S. Koshy, H. Bae, C. M. Hwang, S. Yamanlar, and A. Khademhosseini. Cell-laden microengineered gelatin methacrylate hydrogels. *Biomaterials*, Vol. 31, No. 21, 2010, pp. 5536–5544.
[101] Kim, W. and G. Kim. Collagen/bioceramic-based composite bioink to fabricate a porous 3D hASCs-laden structure for bone tissue regeneration. *Biofabrication*, Vol. 12, No. 1, 2019, id. 015007.
[102] Mazzocchi, A., M. Devarasetty, R. Huntwork, S. Soker, and A. Skardal. Optimization of collagen type I-hyaluronan hybrid bioink for 3D bioprinted liver microenvironments. *Biofabrication*, Vol. 11, No. 1, 2018, id. 015003.
[103] Jiao, T., Q. Lian, W. Lian, Y. Wang, D. Li, R. L. Reis, et al. Properties of collagen/sodium alginate hydrogels for bioprinting of skin models. *Journal of Bionic Engineering*, Vol. 20, No. 1, 2023, pp. 105–118.
[104] Lin, Y. T., T. T. Hsu, Y. W. Liu, C. T. Kao, and T. H. Huang. Bidirectional differentiation of human-derived stem cells induced by biomimetic calcium silicate-reinforced gelatin methacryiate bioink for odontogenic regeneration. *Biomedicines*, Vol. 9, No. 8, 2021, id. 929.
[105] Lim, K. S., F. Abinzano, P. N. Bernal, A. Albillos Sanchez, P. Atienza-Roca, I. A. Otto, et al. One-step photoactivation of a dual-functionalized bioink as cell carrier and cartilage-binding glue for chondral regeneration. *Advanced Healthcare Materials*, Vol. 9, No. 17, 2020, id. e1901792.
[106] Cidonio, G., C. R. Alcala-Orozco, K. S. Lim, M. Glinka, I. Mutreja, Y. H. Kim, et al. Osteogenic and angiogenic tissue formation in high fidelity nanocomposite Laponite-gelatin bioinks. *Biofabrication*, Vol. 11, No. 3, 2019, id. 035027.
[107] Suh, J. K. and H. W. Matthew. Application of chitosan-based polysaccharide biomaterials in cartilage tissue engineering: A review. *Biomaterials*, Vol. 21, No. 24, 2000, pp. 2589–2598.
[108] Cheung, R. C. F., T. B. Ng, J. H. Wong, and W. Y. Chan. Chitosan: An update on potential biomedical and pharmaceutical applications. *Marine Drugs*, Vol. 13, No. 8, 2015, pp. 5156–5186.
[109] Yan, D., Y. Li, Y. Liu, N. Li, X. Zhang, and C. Yan. Antimicrobial properties of chitosan and chitosan derivatives in the treatment of enteric infections. *Molecules*, Vol. 26, No. 23, 2021, id. 7136.
[110] Mania, S., A. Banach-Kopeć, K. Staszczyk, J. Kulesza, E. Augustin, and R. Tylingo. An influence of molecular weight, deacetylation degree and method of obtaining chitosan xerogels on their antimicrobial activity and cytotoxicity. *Molecules*, Vol. 28, No. 1, 2023, id. 550.
[111] Aranaz, I., A. R. Alcántara, M. C. Civera, C. Arias, B. Elorza, A. Heras Caballero, et al. Chitosan: An overview of its properties and applications. *Polymers (Basel)*, Vol. 13, No. 16, 2021, id. 3256.
[112] Gorczyca, G., R. Tylingo, P. Szweda, E. Augustin, M. Sadowska, and S. Milewski. Preparation and characterization of genipin cross-linked porous chitosan–collagen–gelatin scaffolds using chitosan–CO_2 solution. *Carbohydrate Polymers*, Vol. 102, 2014, pp. 901–911.
[113] Sadeghianmaryan, A., S. Naghieh, H. Alizadeh Sardroud, Z. Yazdanpanah, Y. Afzal Soltani, J. Sernaglia, et al. Extrusion-based printing of chitosan scaffolds and their in vitro characterization for cartilage tissue engineering. *International Journal of Biological Macromolecules*, Vol. 164, 2020, pp. 3179–3192.
[114] Roehm, K. D. and S. V. Madihally. Bioprinted chitosan-gelatin thermosensitive hydrogels using an inexpensive 3D printer. *Biofabrication*, Vol. 10, No. 1, 2017, id. 015002.
[115] Feng, P., Y. Luo, C. Ke, H. Qiu, W. Wang, Y. Zhu, et al. Chitosan-based functional materials for skin wound repair: mechanisms and applications. *Frontiers in Bioengineering and Biotechnology*, Vol. 9, 2021, id. 617842.
[116] Mainardi, J. C., K. Rezwan, and M. Maas. Genipin-crosslinked chitosan/alginate/alumina nanocomposite gels for 3D bioprinting. *Bioprocess and Biosystems Engineering*, Vol. 45, No. 1, 2022, pp. 171–185.
[117] Liu, X., M. Hao, Z. Chen, T. Zhang, J. Huang, J. Dai, et al. 3D bioprinted neural tissue constructs for spinal cord injury repair. *Biomaterials*, Vol. 272, 2021, id. 120771.
[118] Maturavongsadit, P., L. K. Narayanan, P. Chansoria, R. Shirwaiker, and S. R. Benhabbour. Cell-laden nanocellulose/chitosan-based bioinks for 3D bioprinting and enhanced osteogenic cell

differentiation. *ACS Applied Bio Materials*, Vol. 4, No. 4, 2021, pp. 2342–2353.
[119] Ku, J., H. Seonwoo, S. Park, K. J. Jang, J. Lee, M. Lee, et al. Cell-laden thermosensitive chitosan hydrogel bioinks for 3D bioprinting applications. *Applied Sciences*, Vol. 10, No. 7, 2020, id. 2455.
[120] Hafezi, F., S. Shorter, A. G. Tabriz, A. Hurt, V. Elmes, J. Boateng, et al. Bioprinting and preliminary testing of highly reproducible novel bioink for potential skin regeneration. *Pharmaceutics*, Vol. 12, No. 6, 2020, id. 550.
[121] Tonda-Turo, C., I. Carmagnola, A. Chiappone, Z. Feng, G. Ciardelli, M. Hakkarainen, et al. Photocurable chitosan as bioink for cellularized therapies towards personalized scaffold architecture. *Bioprinting*, Vol. 18, 2020, id. e00082.
[122] Ullah, F., F. Javed, I. Mushtaq, L. U. Rahman, N. Ahmed, I. U. Din, et al. Development of highly-reproducible hydrogel based bioink for regeneration of skin-tissues via 3-D bioprinting technology. *International Journal of Biological Macromolecules*, Vol. 230, 2023, id. 123131.
[123] Gwak, M. A., S. J. Lee, D. Lee, S. A. Park, and W. H. Park. Highly gallol-substituted, rapidly self-crosslinkable, and robust chitosan hydrogel for 3D bioprinting. *International Journal of Biological Macromolecules*, Vol. 227, 2023, pp. 493–504.
[124] Coşkun, S., S. O. Akbulut, B. Sarikaya, S. Çakmak, and M. Gümüşderelioğlu. Formulation of chitosan and chitosan-nanoHAp bioinks and investigation of printability with optimized bioprinting parameters. *International Journal of Biological Macromolecules*, Vol. 222, 2022, pp. 1453–1464.
[125] Chang, H. K., D. H. Yang, M. Y. Ha, H. J. Kim, C. H. Kim, S. H. Kim, et al. 3D printing of cell-laden visible light curable glycol chitosan bioink for bone tissue engineering. *Carbohydrate Polymers*, Vol. 287, 2022, id. 119328.
[126] Lee, K. Y. and D. J. Mooney. Alginate: properties and biomedical applications. *Progress in Polymer Science*, Vol. 37, No. 1, 2012, pp. 106–126.
[127] Axpe, E. and M. L. Oyen. Applications of alginate-based bioinks in 3D bioprinting. *International Journal of Molecular Sciences*, Vol. 17, No. 12, 2016, id. 1976.
[128] Bouhadir, K. H., K. Y. Lee, E. Alsberg, K. L. Damm, K. W. Anderson, and D. J. Mooney. Degradation of partially oxidized alginate and its potential application for tissue engineering. *Biotechnology Progress*, Vol. 17, No. 5, 2001, pp. 945–950.
[129] Freeman, F. E. and D. J. Kelly. Tuning alginate bioink stiffness and composition for controlled growth factor delivery and to spatially direct MSC fate within bioprinted tissues. *Scientific Reports*, Vol. 7, No. 1, 2017, id. 17042.
[130] Boontheekul, T., H. J. Kong, and D. J. Mooney. Controlling alginate gel degradation utilizing partial oxidation and bimodal molecular weight distribution. *Biomaterials*, Vol. 26, No. 15, 2005, pp. 2455–2465.
[131] Hazur, J., R. Detsch, E. Karakaya, J. Kaschta, J. Teßmar, D. Schneidereit, et al. Improving alginate printability for biofabrication: establishment of a universal and homogeneous pre-crosslinking technique. *Biofabrication*, Vol. 12, No. 4, 2020, id. 045004.
[132] Im, S., G. Choe, J. M. Seok, S. J. Yeo, J. H. Lee, W. D. Kim, et al. An osteogenic bioink composed of alginate, cellulose nanofibrils, and polydopamine nanoparticles for 3D bioprinting and bone tissue engineering. *International Journal of Biological Macromolecules*, Vol. 205, 2022, pp. 520–529.
[133] Salati, M. A., J. Khazai, A. M. Tahmuri, A. Samadi, A. Taghizaden, M. Taghizadeh, et al. Agarose-based biomaterials: opportunities and challenges in cartilage tissue engineering. *Polymers (Basel)*, Vol. 12, No. 5, 2020, id. 1150.
[134] Zarrintaj, P., S. Manouchehri, Z. Ahmadi, M. R. Saeb, A. M. Urbanska, D. L. Kaplan, et al. Agarose-based biomaterials for tissue engineering. *Carbohydrate Polymers*, Vol. 187, 2018, pp. 66–84.
[135] Gu, Y., B. Schwarz, A. Forget, A. Barbero, I. Martin, and V. P. Shastri. Advanced bioink for 3D bioprinting of complex free-standing structures with high stiffness. *Bioengineering (Basel)*, Vol. 7, No. 2, 2020, id. 141.
[136] Gong, C., Z. Kong, and X. Wang. The effect of agarose on 3D bioprinting. *Polymers (Basel)*, Vol. 13, No. 3, 2021, id. 4028.
[137] Bui, V. T. N., B. T. Nguyen, F. Renou, and T. Nicolai. Structure and rheological properties of carrageenans extracted from different red algae species cultivated in Cam Ranh Bay, Vietnam. *Journal of Applied Phycology*, Vol. 31, No. 3, 2019, pp. 1947–1953.
[138] Velde, F., S. H. Knutsen, A. I. Usov, H. S. Rollema, and A. S. Cerezo. 1H and 13C high resolution NMR spectroscopy of carrageenans: application in research and industry. *Trends in Food Science and Technology*, Vol. 13, No. 2, 2002, pp. 73–92.
[139] Liu, J., X. Zhan, J. Wan, Y. Wang, and C. Wang. Review for carrageenan-based pharmaceutical biomaterials: favourable physical features versus adverse biological effects. *Carbohydrate Polymers*, Vol. 121, 2015, pp. 27–36.
[140] Marques, D. M. C., J. C. Silva, A. P. Serro, J. M. S. Cabral, P. Sanjuan-Alberte, and F. C. Ferreira. 3D bioprinting of novel κ-carrageenan bioinks: an algae-derived polysaccharide. *Bioengineering (Basel)*, Vol. 9, No. 3, 2022, id. 109.
[141] Lim, W., G. J. Kim, H. W. Kim, J. Lee, X. Zhang, M. G. Kang, et al. Kappa-carrageenan-based dual crosslinkable bioink for extrusion type bioprinting. *Polymers (Basel)*, Vol. 12, No. 10, 2020, id. 2377.
[142] Heidenreich, A. C., M. Pérez-Recalde, A. González Wusener, and É. B. Hermida. Collagen and chitosan blends for 3D bioprinting: A rheological and printability approach. *Polymer Testing*, Vol. 82, 2020, id. 106297.
[143] Yang, X., Z. Lu, H. Wu, W. Li, L. Zheng, and J. Zhao. Collagen-alginate as bioink for three-dimensional (3D) cell printing based cartilage tissue engineering. *Materials Science and Engineering: C*, Vol. 83, 2018, pp. 195–201.
[144] Othman, S. A., C. F. Soon, N. L. Ma, K. S. Tee, G. P. Lim, M. Morsin, et al. Alginate-gelatin bioink for bioprinting of hela spheroids in alginate-gelatin hexagon shaped scaffolds. *Polymer Bulletin (Berlin, Germany)*, Vol. 78, No. 11, 2021, pp. 6115–6135.
[145] Distler, T., A. A. Solisito, D. Schneidereit, O. Friedrich, R. Detsch, and A. R. Boccaccini. 3D printed oxidized alginate-gelatin bioink provides guidance for C2C12 muscle precursor cell orientation and differentiation via shear stress during bioprinting. *Biofabrication*, Vol. 12, No. 4, 2020, id. 045005.
[146] Monabatpour, F., X. Duan, Z. Yazdanpanan, X. L. Tabil, L. Lobanova, N. Zhu, et al. Bioprinting of alginate-carboxymethyl chitosan scaffolds for enamel tissue engineering in vitro. *Biofabrication*, Vol. 15, No. 1, 2022, id. 015017.
[147] Chen, H., F. Fei, X. Li, Z. Nie, D. Zhou, L. Liu, et al. A facile, versatile hydrogel bioink for 3D bioprinting benefits long-term subaqueous fidelity, cell viability and proliferation. *Regenerative Biomaterials*, Vol. 8, No. 2, 2021, id. rbab026.
[148] CELLINK. Ready-to-use bioinks [Internet]. Cited 15.11.2023. https://www.cellink.com/bioinks/ready-to-use-bioinks/
[149] Sigma-Aldrich. 3D Bioprinting Bioinks [Internet]. Cited 15.11.2023. https://www.sigmaaldrich.com/PL/pl/technical-documents/

technical-article/cell-culture-and-cell-culture-analysis/3d-cell-culture/3d-bioprinting-bioinks.
[150] Knowlton, S., B. Yenilmez, S. Anand, and S. Tasoglu. Photocrosslinking-based bioprinting: Examining crosslinking schemes. *Bioprinting*, Vol. 5, 2017, pp. 10–18.
[151] Freeman, S., S. Calabro, R. Williams, S. Jin, and K. Ye. Bioink formulation and machine learning-empowered bioprinting optimization. *Frontiers in Bioengineering and Biotechnology*, Vol. 10, 2022, id. 913579.
[152] Bonatti, A. F., G. Vozzi, C. K. Chua, and C. D. Maria. A deep learning quality control loop of the extrusion-based bioprinting process. *International Journal of Bioprinting*, Vol. 8, No. 4, 2022, id. 620.
[153] Mohamed Ameer J., R. Pai, R. Komeri, V. Damodaran, P. R. Anil Kumar, and N.Kasoju. Combinatorial approaches in electrospinning, electrospraying, and 3D printing for biomedical applications. In: Kasoju N., Ye H., (Eds.) *Biomedical Applications of Electrospinning and Electrospraying*. Woodhead Publishing Series in Biomaterials. Woodhead Publishing, 2021, pp. 355–373.

7 OŚWIADCZENIA

7.1 A Novel Method of Endotoxins Removal from Chitosan Hydrogel as a Potential Bioink Component Obtained by CO_2 Saturation.

POLITECHNIKA GDAŃSKA | WYDZIAŁ CHEMICZNY

Gdańsk, 08.10.2024 r.

dr inż. Szymon Mania
Katedra Chemii, Technologii i Biotechnologii Żywności
Wydział Chemiczny
Politechnika Gdańska
szymon.mania@pg.edu.pl

Oświadczenie współautora publikacji

Oświadczam, że w pracy:
Banach-Kopeć A., Mania S., Pilch J., Augustin E., Gabriel I., & Tylingo R. (2022). A novel method of endotoxins removal from chitosan hydrogel as a potential bioink component obtained by CO_2 saturation. International Journal of Molecular Sciences, 23, 5505. Doi.org/10.3390/ijms23105505.
(IF: 5,6; MNiSW: 140)

mój udział polegał na współopracowaniu koncepcji badań oraz koordynacji ich przebiegu. Byłem zaangażowany w planowanie i realizację badań fizykochemicznych. Brałem również udział w pisaniu wstępnych wersji manuskryptu oraz jego redagowaniu. Pełniłem rolę autora korespondencyjnego.

Niniejszym oświadczam, że mój procentowy wkład wynosi 28 %.

Szymon Mania

podpis współautora publikacji

POLITECHNIKA GDAŃSKA | WYDZIAŁ CHEMICZNY

Gdańsk, 14.10.2024 r.

dr inż. Joanna Franckowska
(dawniej Joanna Pilch)
e-mail: joanna.pilch92@gmail.com

Oświadczenie współautora publikacji

Oświadczam, że w pracy:
Banach-Kopeć A., Mania S., Pilch J., Augustin E., Gabriel I., & Tylingo R. (2022). A novel method of endotoxins removal from chitosan hydrogel as a potential bioink component obtained by CO_2 saturation. International Journal of Molecular Sciences, 23, 5505. Doi.org/10.3390/ijms23105505.
(IF: 5,6; MNiSW: 140)

mój udział polegał na planowaniu i realizacji eksperymentów mających na celu ocenę cytotoksyczności za pomocą testu MTT. Byłam również zaangażowana w proces pisania wstępnej wersji manuskryptu oraz uczestniczyłam w jego redagowaniu.

Niniejszym oświadczam, że mój procentowy wkład wynosi 5%.

Franckowska 14.10.2024
.....
podpis współautora publikacji

POLITECHNIKA GDAŃSKA | WYDZIAŁ CHEMICZNY

Gdańsk, 10.10.2024 r.

dr hab. Ewa Augustin, profesor uczelni
Katedra Technologii Leków i Biochemii
Wydział Chemiczny
Politechnika Gdańska
ewaaugus@pg.edu.pl

Oświadczenie współautora publikacji

Oświadczam, że w pracy:
Banach-Kopeć A., Mania S., Pilch J., Augustin E., Gabriel I., & Tylingo R. (2022). A novel method of endotoxins removal from chitosan hydrogel as a potential bioink component obtained by CO_2 saturation. International Journal of Molecular Sciences, 23, 5505. Doi.org/10.3390/ijms23105505.
(IF: 5,6; MNiSW: 140)

mój udział polegał na planowaniu i realizacji eksperymentów mających na celu ocenę cytotoksyczności badanych materiałów za pomocą testu MTT. Byłam również zaangażowana w proces pisania wstępnej wersji manuskryptu oraz uczestniczyłam w jego redagowaniu.

Niniejszym oświadczam, że mój procentowy wkład wynosi 5 %.

Ewa Augustin

podpis współautora publikacji

POLITECHNIKA GDAŃSKA | WYDZIAŁ CHEMICZNY

Gdańsk, 11.10.2024 r.

dr hab. inż. Iwona Gabriel, profesor uczelni
Katedra Technologii Leków i Biochemii
Wydział Chemiczny
Politechnika Gdańska
iwona.gabriel@pg.edu.pl

Oświadczenie współautora publikacji

Oświadczam, że w pracy:
Banach-Kopeć A., Mania S., Pilch J., Augustin E., Gabriel I., & Tylingo R. (2022). A novel method of endotoxins removal from chitosan hydrogel as a potential bioink component obtained by CO_2 saturation. International Journal of Molecular Sciences, 23, 5505. Doi.org/10.3390/ijms23105505.
(IF: 5,6; MNiSW: 140)

mój udział polegał na uczestnictwie w pracach eksperymentalnych związanych z pomiarami fluorescencyjnymi, oferując wsparcie merytoryczne i metodologiczne.

Niniejszym oświadczam, że mój procentowy wkład wynosi 5 %.

podpis współautora publikacji

POLITECHNIKA GDAŃSKA | WYDZIAŁ CHEMICZNY

Gdańsk, 08.10.2024 r.

dr hab. inż. Robert Tylingo, profesor uczelni
Katedra Chemii, Technologii i Biotechnologii Żywności
Wydział Chemiczny
Politechnika Gdańska
robertt@pg.edu.pl

Oświadczenie współautora publikacji

Oświadczam, że w pracy:
Banach-Kopeć A., Mania S., Pilch J., Augustin E., Gabriel I., & Tylingo R. (2022). A novel method of endotoxins removal from chitosan hydrogel as a potential bioink component obtained by CO_2 saturation. International Journal of Molecular Sciences, 23, 5505. Doi.org/10.3390/ijms23105505.
(IF: 5,6; MNiSW: 140)

mój udział polegał na współopracowaniu koncepcji badań, projektowaniu eksperymentów oraz analizowaniu uzyskanych wyników. Byłem również odpowiedzialny za nadzór nad całym projektem. Uczestniczyłem w pisaniu wstępnych wersji manuskryptu oraz jego późniejszym redagowaniu.

Niniejszym oświadczam, że mój procentowy wkład wynosi 29 %.

.....

podpis współautora publikacji

7.2 An influence of molecular weight, deacetylation degree of chitosan xerogels on their antimicrobial activity and cytotoxicity. Comparison of chitosan materials obtained using lactic acid and CO_2 saturation.

POLITECHNIKA GDAŃSKA | WYDZIAŁ CHEMICZNY

Gdańsk, 08.10.2024 r.

dr inż. Szymon Mania
Katedra Chemii, Technologii i Biotechnologii Żywności
Wydział Chemiczny
Politechnika Gdańska
szymon.mania@pg.edu.pl

Oświadczenie współautora publikacji

Oświadczam, że w pracy:
Mania, S., Banach-Kopeć, A., Staszczyk, K., Kulesza, J., Augustin, E., & Tylingo, R. (2023). An influence of molecular weight, deacetylation degree of chitosan xerogels on their antimicrobial activity and cytotoxicity. Comparison of chitosan materials obtained using lactic acid and CO2 saturation. Carbohydrate Research, 534, 108973. Doi.org/10.1016/j.carres.2023.108973
(IF: 2,4; MNiSW: 100)

mój udział polegał na opracowywaniu koncepcji, metodologii i przeprowadzaniu badań fizykochemicznych, w tym projektowaniu protokołów eksperymentalnych. Zajmowałem się analizą formalną, zarządzaniem oprogramowaniem i zasobami niezbędnymi do przetwarzania danych. Byłem również odpowiedzialna za pozyskiwanie funduszy, administrację projektu oraz nadzór nad bieżącymi pracami badawczymi. Odpowiadałem za wizualizację wyników oraz pisanie i redagowanie manuskryptu. Pełniłem również rolę autora korespondencyjnego.

Niniejszym oświadczam, że mój procentowy wkład wynosi 30 %.

Szymon Mania

.....
podpis współautora publikacji

POLITECHNIKA GDAŃSKA | WYDZIAŁ CHEMICZNY

Gdańsk, 08.10.2024 r.

mgr inż. Karol Staszczyk
Katedra Chemii, Technologii i Biotechnologii Żywności
Wydział Chemiczny
Politechnika Gdańska
karol.staszczyk@pg.edu.pl

Oświadczenie współautora publikacji

Oświadczam, że w pracy:
Mania, S., Banach-Kopeć, A., Staszczyk, K., Kulesza, J., Augustin, E., & Tylingo, R. (2023). An influence of molecular weight, deacetylation degree of chitosan xerogels on their antimicrobial activity and cytotoxicity. Comparison of chitosan materials obtained using lactic acid and CO2 saturation. Carbohydrate Research, 534, 108973. Doi.org/10.1016/j.carres.2023.108973
(IF: 2,4; MNiSW: 100)

mój udział polegał na opracowywaniu metodologii i przeprowadzaniu badań fizykochemicznych i biologicznych. Zajmowałem się zarządzałam oprogramowaniem i zasobami niezbędnymi do przetwarzania danych. Odpowiadałem również za wizualizację wyników oraz pisanie i redagowanie manuskryptu.

Niniejszym oświadczam, że mój procentowy wkład wynosi 10 %.

Karol Staszczyk
.....
podpis współautora publikacji

POLITECHNIKA GDAŃSKA | WYDZIAŁ CHEMICZNY

Gdańsk, 11.10.2024 r.

dr inż. Jolanta Kulesza-Nejman
jolanta.kulesza.pg@gmail.com

Oświadczenie współautora publikacji

Oświadczam, że w pracy:
Mania, S., Banach-Kopeć, A., Staszczyk, K., Kulesza, J., Augustin, E., & Tylingo, R. (2023). An influence of molecular weight, deacetylation degree of chitosan xerogels on their antimicrobial activity and cytotoxicity. Comparison of chitosan materials obtained using lactic acid and CO_2 saturation. Carbohydrate Research, 534, 108973. Doi.org/10.1016/j.carres.2023.108973
(IF: 2,4; MNiSW: 100)

mój udział polegał na zbieraniu danych niezbędnych do analizy i interpretacji wyników badań. Byłam również zaangażowana w formalną analizę tych danych, co obejmowało statystyczną ocenę wyników. Brałam udział w przeprowadzaniu badań i opracowywaniu metodologii wspólnie z innymi członkami zespołu. Byłam odpowiedzialna za administrację projektu, zarządzanie zasobami niezbędnymi do realizacji badań, a także za wizualizację wyników. Dodatkowo, uczestniczyłam w pisaniu wstępnych wersji manuskryptu oraz w procesie jego redagowania i recenzji.

Niniejszym oświadczam, że mój procentowy wkład wynosi 5 %.

Kulesza - Nejman
.....
podpis współautora publikacji

POLITECHNIKA GDAŃSKA | WYDZIAŁ CHEMICZNY

Gdańsk, 10.10.2024 r.

dr hab. Ewa Augustin, profesor uczelni
Katedra Technologii Leków i Biochemii
Wydział Chemiczny
Politechnika Gdańska
ewaaugus@pg.edu.pl

Oświadczenie współautora publikacji

Oświadczam, że w pracy:
Mania, S., Banach-Kopeć, A., Staszczyk, K., Kulesza, J., Augustin, E., & Tylingo, R. (2023). An influence of molecular weight, deacetylation degree of chitosan xerogels on their antimicrobial activity and cytotoxicity. Comparison of chitosan materials obtained using lactic acid and CO2 saturation. Carbohydrate Research, 534, 108973. Doi.org/10.1016/j.carres.2023.108973
(IF: 2,4; MNiSW: 100)

mój udział polegał na opracowywaniu metodologii dla badań cytotoksyczności przy użyciu testu MTT, w tym projektowaniu protokołów eksperymentalnych. Nadzorowałam proces badawczy, zarządzałam zasobami i odpowiadałam za walidację wyników. Byłam również zaangażowana w pisanie oraz redakcję manuskryptu.

Niniejszym oświadczam, że mój procentowy wkład wynosi 5 %.

Ewa Augustin

.....

podpis współautora publikacji

POLITECHNIKA GDAŃSKA | WYDZIAŁ CHEMICZNY

Gdańsk, 08.10.2024 r.

dr inż. Rober Tylingo, profesor uczelni
Katedra Chemii, Technologii i Biotechnologii Żywności
Wydział Chemiczny
Politechnika Gdańska
robertt@pg.edu.pl

Oświadczenie współautora publikacji

Oświadczam, że w pracy:
Mania, S., Banach-Kopeć, A., Staszczyk, K., Kulesza, J., Augustin, E., & Tylingo, R. (2023). An influence of molecular weight, deacetylation degree of chitosan xerogels on their antimicrobial activity and cytotoxicity. Comparison of chitosan materials obtained using lactic acid and CO2 saturation. Carbohydrate Research, 534, 108973. Doi.org/10.1016/j.carres.2023.108973
(IF: 2,4; MNiSW: 100)

mój udział polegał na opracowywaniu metodologii badań, analizie wyników oraz projektowaniu protokołów eksperymentalnych z badań fizykochemicznych i mikrobiologicznych. Zarządzałem zasobami niezbędnymi do przetwarzania danych oraz nadzorowałam bieżące prace badawcze. Byłem odpowiedzialna za pisanie i redagowanie manuskryptu.

Niniejszym oświadczam, że mój procentowy wkład wynosi 20 %.

.....
podpis współautora publikacji

7.3 Thermosensitive composite based on agarose and chitosan saturated with carbon dioxide. Preliminary study of requirements for production of new CSAG bioink.

POLITECHNIKA GDAŃSKA | WYDZIAŁ CHEMICZNY

Gdańsk, 08.10.2024 r.

dr inż. Szymon Mania
Katedra Chemii, Technologii i Biotechnologii Żywności
Wydział Chemiczny
Politechnika Gdańska
szymon.mania@pg.edu.pl

Oświadczenie współautora publikacji

Oświadczam, że w pracy:
Banach-Kopeć A., Mania S., Tylingo R., Wawrzynowicz A., Pawłowska M., Czerwiec K., Deptuła M., Pikuła M. (2024). Thermosensitive composite based on agarose and chitosan saturated with carbon dioxide. Preliminary study of requirements for production of new CSAG bioink. Carbohydrate Polymers, 336, 122120. Doi.org/10.1016/j.carbpol.2024.122120
(IF: 10,7; MNiSW: 140)

mój udział polegał na opracowywaniu koncepcji projektu, metodologii badań oraz zarządzaniu projektem. Prowadziłem badania, analizy formalne i zarządzałem danymi. Byłem odpowiedzialny za pozyskiwanie funduszy, zarządzanie zasobami i oprogramowaniem używanym w badaniach. Nadzorowałem cały projekt, weryfikowałem wyniki oraz odpowiadałem za wizualizację danych. Moje obowiązki obejmowały także pisanie wstępnych wersji manuskryptu oraz jego recenzję i edycję. Pełniłem rolę autora korespondencyjnego.

Niniejszym oświadczam, że mój procentowy wkład wynosi 27 %.

Szymon Mania

.....

podpis współautora publikacji

POLITECHNIKA GDAŃSKA | WYDZIAŁ CHEMICZNY

Gdańsk, 08.10.2024 r.

dr hab. inż. Rober Tylingo, profesor uczelni
Katedra Chemii, Technologii i Biotechnologii Żywności
Wydział Chemiczny
Politechnika Gdańska
robertt@pg.edu.pl

Oświadczenie współautora publikacji

Oświadczam, że w pracy:
Banach-Kopeć A., Mania S., Tylingo R., Wawrzynowicz A., Pawłowska M., Czerwiec K., Deptuła M., Pikuła M. (2024). Thermosensitive composite based on agarose and chitosan saturated with carbon dioxide. Preliminary study of requirements for production of new CSAG bioink. Carbohydrate Polymers, 336, 122120. Doi.org/10.1016/j.carbpol.2024.122120
(IF: 10,7; MNiSW: 140)

mój udział polegał na prowadzeniu formalnej analizy danych, zarządzaniu danymi, opracowywaniu metodologii oraz przeprowadzaniu badań fizykochemicznych. Nadzorowałem prace badawcze, zarządzałem oprogramowaniem używanym w projekcie oraz weryfikowałem wyniki. Byłem również odpowiedzialny za pisanie wstępnych wersji manuskryptu oraz jego recenzję i edycję.

Niniejszym oświadczam, że mój procentowy wkład wynosi 19 %.

.....
podpis współautora publikacji

POLITECHNIKA GDAŃSKA | WYDZIAŁ CHEMICZNY

Gdańsk, 09.10.2024 r.

mgr inż. Agata Wawrzynowicz
wawrzynowicz.aga@gmail.com

Oświadczenie współautora publikacji

Oświadczam, że w pracy:
Banach-Kopeć A., Mania S., Tylingo R., Wawrzynowicz A., Pawłowska M., Czerwiec K., Deptuła M., Pikuła M. (2024). Thermosensitive composite based on agarose and chitosan saturated with carbon dioxide. Preliminary study of requirements for production of new CSAG bioink. Carbohydrate Polymers, 336, 122120. Doi.org/10.1016/j.carbpol.2024.122120
(IF: 10,7; MNiSW: 140)

mój udział polegał na przeprowadzaniu badań mikrobiologicznych i reologicznych oraz zarządzaniu danymi niezbędnymi do analizy i prezentacji wyników. Odpowiadałam za gromadzenie, organizację oraz przygotowanie danych do dalszej analizy i dyskusji w ramach projektu badawczego.

Niniejszym oświadczam, że mój procentowy wkład wynosi 2 %.

Agata Wawrzynowicz
podpis współautora publikacji

POLITECHNIKA GDAŃSKA | WYDZIAŁ CHEMICZNY

Gdańsk, 10.10.2024 r.

dr inż. Monika Pawłowska
Katedra Technologii Leków i Biochemii
Wydział Chemiczny
Politechnika Gdańska
monika.pawlowska@pg.edu.pl

Oświadczenie współautora publikacji

Oświadczam, że w pracy:
Banach-Kopeć A., Mania S., Tylingo R., Wawrzynowicz A., Pawłowska M., Czerwiec K., Deptuła M., Pikuła M. (2024). Thermosensitive composite based on agarose and chitosan saturated with carbon dioxide. Preliminary study of requirements for production of new CSAG bioink. Carbohydrate Polymers, 336, 122120. Doi.org/10.1016/j.carbpol.2024.122120
(IF: 10,7; MNiSW: 140)

mój udział polegał na prowadzeniu badań, zarządzaniu danymi, opracowywaniu metodologii oraz zarządzaniu zasobami niezbędnymi do przeprowadzenia badań nad oceną cytotoksyczności. Byłam odpowiedzialna za weryfikację wyników oraz za wizualizację danych. Odpowiadałam również za pisanie wstępnych wersji manuskryptu, jego recenzję i edycję, a także zarządzanie oprogramowaniem wykorzystywanym w badaniach.

Niniejszym oświadczam, że mój procentowy wkład wynosi 5 %.

Monika Pawłowska
.....
podpis współautora publikacji

GDAŃSKI
UNIWERSYTET
MEDYCZNY

www.gumed.edu.pl
58 349 11 11
info@gumed.edu.pl
ul. M. Skłodowskiej-Curie 3a,
80-210 Gdańsk

Gdańsk, 10.10.2024 r.

dr Katarzyna Czerwiec
Zakład Anatomii Klinicznej, Wydział Lekarski
Gdański Uniwersytet Medyczny
katarzyna.czerwiec@gumed.edu.pl

Oświadczenie współautora publikacji

Oświadczam, że w pracy:
Banach-Kopeć A., Mania S., Tylingo R., Wawrzynowicz A., Pawłowska M., Czerwiec K., Deptuła M., Pikuła M. (2024). Thermosensitive composite based on agarose and chitosan saturated with carbon dioxide. Preliminary study of requirements for production of new CSAG bioink. Carbohydrate Polymers, 336, 122120. Doi.org/10.1016/j.carbpol.2024.122120
(IF: 10,7; MNiSW: 140)

mój udział polegał na opracowywaniu metodologii i prowadzeniu badań dotyczących biokompatybilności badanych materiałów. Zarządzałam danymi, zasobami i oprogramowaniem niezbędnym do realizacji projektu. Byłam odpowiedzialna za weryfikację wyników oraz za ich wizualizację. Brałam również udział w pisaniu wstępnych wersji manuskryptu oraz w jego recenzji i edycji.

Niniejszym oświadczam, że mój procentowy wkład wynosi 10 %.

Katarzyna Czerwiec
.....
podpis współautora publikacji

GDAŃSKI
UNIWERSYTET
MEDYCZNY

www.gumed.edu.pl
58 349 11 11
info@gumed.edu.pl
ul. M. Skłodowskiej-Curie 3a,
80-210 Gdańsk

Gdańsk, 10.10.2024 r.

dr inż. Milena Deptuła
Pracownia Inżynierii Tkankowej i Medycyny Regeneracyjnej
Zakład Embriologii, Katedra Anatomii, Wydział Lekarski
Gdański Uniwersytet Medyczny
milena.deptula@gumed.edu.pl

Oświadczenie współautora publikacji

Oświadczam, że w pracy:
Banach-Kopeć A., Mania S., Tylingo R., Wawrzynowicz A., Pawłowska M., Czerwiec K., Deptuła M., Pikuła M. (2024). Thermosensitive composite based on agarose and chitosan saturated with carbon dioxide. Preliminary study of requirements for production of new CSAG bioink. Carbohydrate Polymers, 336, 122120. Doi.org/10.1016/j.carbpol.2024.122120
(IF: 10,7; MNiSW: 140)

mój udział polegał na opracowywaniu metodologii analizy biokompatybilności badanych materiałów przy użyciu różnych testów. Zarządzałam danymi oraz zasobami niezbędnymi do realizacji projektu i odpowiadałam za obsługę oprogramowania. Nadzorowałam proces badawczy, weryfikowałam wyniki oraz zajmowałam się wizualizacją danych. Brałam również aktywny udział w pisaniu wstępnych wersji manuskryptu, jego recenzji i edycji.

Niniejszym oświadczam, że mój procentowy wkład wynosi 7 %.

Milena Deptuła
.....
podpis współautora publikacji

GDAŃSKI
UNIWERSYTET
MEDYCZNY

www.gumed.edu.pl
58 349 11 11
info@gumed.edu.pl
ul. M. Skłodowskiej-Curie 3a,
80-210 Gdańsk

Gdańsk, 10.10.2024 r.

Prof. dr hab. Michał Pikuła
Pracownia Inżynierii Tkankowej i Medycyny Regeneracyjnej
Zakład Embriologii, Katedra Anatomii, Wydział Lekarski
Gdański Uniwersytet Medyczny
pikula@gume.edu.pl

Oświadczenie współautora publikacji

Oświadczam, że w pracy:
Banach-Kopeć A., Mania S., Tylingo R., Wawrzynowicz A., Pawłowska M., Czerwiec K., Deptuła M., Pikuła M. (2024). Thermosensitive composite based on agarose and chitosan saturated with carbon dioxide. Preliminary study of requirements for production of new CSAG bioink. Carbohydrate Polymers, 336, 122120. Doi.org/10.1016/j.carbpol.2024.122120
(IF: 10,7; MNiSW: 140)

mój udział polegał na opracowywaniu metodologii analizy biokompatybilności badanych materiałów. Zarządzałem danymi i odpowiadałem za oprogramowania używane w projekcie. Nadzorowałem proces badawczy, weryfikowałem wyniki testów, a także brałem aktywny udział w pisaniu wstępnych wersji manuskryptu oraz jego dalszej recenzji i edycji.

Niniejszym oświadczam, że mój procentowy wkład wynosi 3 %.

Zakład Embriologii
Pracownia Inżynierii Tkankowej
i Medycyny Regeneracyjnej

prof. dr hab. Michał Pikuła
Profesor

.....

podpis współautora publikacji

7.4 From Bioink to Tissue: Exploring Chitosan-Agarose Composition in the Context of Printability and Cellular Behaviour.

POLITECHNIKA GDAŃSKA | WYDZIAŁ CHEMICZNY

Gdańsk, 08.10.2024 r.

dr inż. Szymon Mania
Katedra Chemii, Technologii i Biotechnologii Żywności
Wydział Chemiczny
Politechnika Gdańska
szymon.mania@pg.edu.pl

Oświadczenie współautora publikacji

Oświadczam, że w pracy:
Mania S., Banach-Kopeć A., Maciejewska N., Deptuła K., Słonimska P., Deptuła M., Baczyński-Keller J., Pikuła M., Sachadyn P., Tylingo R. (2024). From Bioink to Tissue: Exploring Chitosan-Agarose Composite in the Context of Printability and Cellular Behaviour. *Molecules*, *29*(19), 4648. Doi.org/10.3390/molecules29194648
(IF: 4,2 ; MNiSW: 140)

Mój udział w przygotowaniu tego artykułu obejmował pełnienie roli jednej z głównych osób odpowiedzialnych za opracowanie planu badawczego, pozyskiwaniu funduszy niezbędnych do realizacji projektu badawczego. Opracowywałem metodologię i prowadziłem badania reologiczne materiałów, zarządzałem danymi, zasobami oraz oprogramowaniem. Nadzorowałem proces badawczy, prowadziłem formalną analizę wyników i byłem odpowiedzialny za ich walidację. Brałem również aktywny udział w pisaniu pierwszych wersji manuskryptu oraz w jego recenzji i edycji.

Niniejszym oświadczam, że mój procentowy wkład wynosi 25 %.

Szymon Mania

.....

podpis współautora publikacji

POLITECHNIKA GDAŃSKA | WYDZIAŁ CHEMICZNY

Gdańsk, 10.10.2024 r.

dr inż. Natalia Maciejewska
Katedra Technologii Leków i Biochemii
Wydział Chemiczny
Politechnika Gdańska
natalia.maciejewska@pg.edu.pl

Oświadczenie współautora publikacji

Oświadczam, że w pracy:
Mania S., Banach-Kopeć A., Maciejewska N., Deptuła K., Słonimska P., Deptuła M., Baczyński-Keller J., Pikuła M., Sachadyn P., Tylingo R. (2024). From Bioink to Tissue: Exploring Chitosan-Agarose Composite in the Context of Printability and Cellular Behaviour. *Molecules*, *29*(19), 4648. Doi.org/10.3390/molecules29194648
(IF: 4,2; MNiSW: 140)

mój udział polegał na opracowywaniu metodologii oraz przeprowadzaniu badań z wykorzystaniem modelu błony kosmówkowo-omoczniowej (CAM). Zajmowałam się zarządzaniem danymi oraz zasobami niezbędnymi do realizacji projektu, a także obsługą oprogramowania używanego w badaniach. Odpowiadałam za walidację wyników i ich wizualizację. Brałam również aktywny udział w pisaniu wstępnych wersji manuskryptu oraz jego recenzji i edycji.

Niniejszym oświadczam, że mój procentowy wkład wynosi 5 %.

Natalia Maciejewska
.....
podpis współautora publikacji

GDAŃSKI
UNIWERSYTET
MEDYCZNY

www.gumed.edu.pl
58 349 11 11
info@gumed.edu.pl
ul. M. Skłodowskiej-Curie 3a,
80-210 Gdańsk

Gdańsk, 10.10.2024 r.

dr Katarzyna Czerwiec
Zakład Anatomii Klinicznej, Wydział Lekarski
Gdański Uniwersytet Medyczny
katarzyna.czerwiec@gumed.edu.pl

Oświadczenie współautora publikacji

Oświadczam, że w pracy:
Mania S., Banach-Kopeć A., Maciejewska N., Czeriwec K., Słonimska P., Deptuła M., Baczyński-Keller J., Pikuła M., Sachadyn P., Tylingo R. (2024). From Bioink to Tissue: Exploring Chitosan-Agarose Composite in the Context of Printability and Cellular Behaviour. *Molecules*, *29*(19), 4648. Doi.org/10.3390/molecules29194648
(IF: 4,2; MNiSW: 140)

mój udział polegał na opracowywaniu metodologii i przeprowadzaniu badań dotyczących biokompatybilności badanych materiałów. Zarządzałam danymi, zasobami oraz oprogramowaniem niezbędnym do realizacji projektu. Byłam odpowiedzialna za walidację wyników i ich wizualizację. Brałam również udział w pisaniu pierwszych wersji manuskryptu oraz w jego recenzji i edycji.

Niniejszym oświadczam, że mój procentowy wkład wynosi 8 %.

Katarzyna Czerwiec
.....
podpis współautora publikacji

POLITECHNIKA GDAŃSKA | WYDZIAŁ CHEMICZNY

Gdańsk, 10.10.2024 r.

mgr inż. Paulina Słonimska
Katedra Biotechnologii i Mikrobiologii
Wydział Chemiczny
Politechnika Gdańska
paulina.slonimska@pg.edu.pl

Oświadczenie współautora publikacji

Oświadczam, że w pracy:
Mania S., Banach-Kopeć A., Maciejewska N., Deptuła K., Słonimska P., Deptuła M., Baczyński-Keller J., Pikuła M., Sachadyn P., Tylingo R. (2024). From Bioink to Tissue: Exploring Chitosan-Agarose Composite in the Context of Printability and Cellular Behaviour. *Molecules*, *29*(19), 4648. Doi.org/10.3390/molecules29194648
(IF: 4,2; MNiSW: 140)

mój udział polegał na opracowywaniu metodologii oraz przeprowadzaniu badań na zwierzętach. Zajmowałam się formalną analizą wyników i ich wizualizacją. Odpowiadałam za obsługę oprogramowania używanego w projekcie oraz weryfikację uzyskanych danych.

Niniejszym oświadczam, że mój procentowy wkład wynosi 3 %.

Paulina Słonimska
podpis współautora publikacji

GDAŃSKI
UNIWERSYTET
MEDYCZNY

www.gumed.edu.pl
58 349 11 11
info@gumed.edu.pl
ul. M. Skłodowskiej-Curie 3a,
80-210 Gdańsk

Gdańsk, 10.10.2024 r.

dr inż. Milena Deptuła
Pracownia Inżynierii Tkankowej i Medycyny Regeneracyjnej
Zakład Embriologii, Katedra Anatomii, Wydział Lekarski
Gdański Uniwersytet Medyczny
milena.deptula@gumed.edu.pl

Oświadczenie współautora publikacji

Oświadczam, że w pracy:
Mania S., Banach-Kopeć A., Maciejewska N., Czerwiec K., Słonimska P., Deptuła M., Baczyński-Keller J., Pikuła M., Sachadyn P., Tylingo R. (2024). From Bioink to Tissue: Exploring Chitosan-Agarose Composite in the Context of Printability and Cellular Behaviour. *Molecules*, *29*(19), 4648. Doi.org/10.3390/molecules29194648
(IF: 4,2; MNiSW: 140)

mój udział polegał na opracowywaniu metodologii i przeprowadzaniu badań dotyczących biokompatybilności badanych materiałów. Zarządzałam danymi, zasobami oraz oprogramowaniem niezbędnym do realizacji projektu. Nadzorowałam proces badawczy, byłam odpowiedzialna za walidację wyników i ich wizualizację. Brałam również udział w pisaniu pierwszych wersji manuskryptu oraz w jego recenzji i edycji.

Niniejszym oświadczam, że mój procentowy wkład wynosi 5 %.

Milena Deptuła
.....
podpis współautora publikacji

POLITECHNIKA GDAŃSKA | WYDZIAŁ CHEMICZNY

Gdańsk, 10.10.2024 r.

mgr inż. Jakub Baczyński-Keller
Katedra Biotechnologii i Mikrobiologii
Wydział Chemiczny
Politechnika Gdańska
jakub.keller@pg.edu.pl

Oświadczenie współautora publikacji

Oświadczam, że w pracy:
Mania S., Banach-Kopeć A., Maciejewska N., Deptuła K., Słonimska P., Deptuła M., Baczyński-Keller J., Pikuła M., Sachadyn P., Tylingo R. (2024). From Bioink to Tissue: Exploring Chitosan-Agarose Composite in the Context of Printability and Cellular Behaviour. *Molecules*, *29*(19), 4648. Doi.org/10.3390/molecules29194648
(IF: 4,2; MNiSW: 140)

mój udział polegał na opracowywaniu metodologii oraz przeprowadzaniu badań na zwierzętach. Zajmowałem się formalną analizą wyników i ich wizualizacją. Odpowiadałem za obsługę oprogramowania używanego w projekcie oraz weryfikację uzyskanych danych.

Niniejszym oświadczam, że mój procentowy wkład wynosi 3 %.

Baczyński-Keller

podpis współautora publikacji

GDAŃSKI
UNIWERSYTET
MEDYCZNY

www.gumed.edu.pl
58 349 11 11
info@gumed.edu.pl
ul. M. Skłodowskiej-Curie 3a,
80-210 Gdańsk

Gdańsk, 10.10.2024 r.

Prof. dr hab. Michał Pikuła
Pracownia Inżynierii Tkankowej i Medycyny Regeneracyjnej
Zakład Embriologii, Katedra Anatomii, Wydział Lekarski
Gdański Uniwersytet Medyczny
pikula@gume.edu.pl

Oświadczenie współautora publikacji

Oświadczam, że w pracy:
Mania S., Banach-Kopeć A., Maciejewska N., Czerwiec K., Słonimska P., Deptuła M., Baczyński-Keller J., Pikuła M., Sachadyn P., Tylingo R. (2024). From Bioink to Tissue: Exploring Chitosan-Agarose Composite in the Context of Printability and Cellular Behaviour. *Molecules*, *29*(19), 4648. Doi.org/10.3390/molecules29194648
(IF: 4,2; MNiSW: 140)

mój udział polegał na opracowywaniu metodologii analizy biokompatybilności badanych materiałów. Zarządzałem danymi i odpowiadałem za oprogramowania używane w projekcie. Nadzorowałem proces badawczy, weryfikowałem wyniki testów, a także brałem aktywny udział w pisaniu wstępnych wersji manuskryptu oraz jego dalszej recenzji i edycji.

Niniejszym oświadczam, że mój procentowy wkład wynosi 3 %.

Zakład Embriologii
Pracownia Inżynierii Tkankowej
i Medycyny Regeneracyjnej
prof. dr hab. Michał Pikuła
Profesor

.....
podpis współautora publikacji

POLITECHNIKA GDAŃSKA | WYDZIAŁ CHEMICZNY

Gdańsk, 10.10.2024 r.

Prof. dr hab. inż. Paweł Sachadyn
Katedra Biotechnologii i Mikrobiologii
Wydział Chemiczny
Politechnika Gdańska
pawel.sachadyn@pg.edu.pl

Oświadczenie współautora publikacji

Oświadczam, że w pracy:
Mania S., Banach-Kopeć A., Maciejewska N., Deptuła K., Słonimska P., Deptuła M., Baczyński-Keller J., Pikuła M., Sachadyn P., Tylingo R. (2024). From Bioink to Tissue: Exploring Chitosan-Agarose Composite in the Context of Printability and Cellular Behaviour. *Molecules*, *29*(19), 4648. Doi.org/10.3390/molecules29194648
(IF: 4,2; MNiSW: 140)

mój udział polegał na opracowywaniu koncepcji projektu oraz nadzorowaniu jego realizacji w zakresie badań na zwierzętach. Zarządzałem zasobami, a także prowadziłem formalną analizę wyników. Byłem odpowiedzialny za pozyskiwanie funduszy niezbędnych do przeprowadzenia badań. Ponadto aktywnie uczestniczyłem w pisaniu recenzji oraz edytowaniu manuskryptu.

Niniejszym oświadczam, że mój procentowy wkład wynosi 3 %.

Paweł Sachadyn

.....

podpis współautora publikacji

POLITECHNIKA GDAŃSKA | WYDZIAŁ CHEMICZNY

Gdańsk, 08.10.2024 r.

dr hab. inż. Robert Tylingo
Katedra Chemii, Technologii i Biotechnologii Żywności
Wydział Chemiczny
Politechnika Gdańska
robertt@pg.edu.pl

Oświadczenie współautora publikacji

Oświadczam, że w pracy:
Mania S., Banach-Kopeć A., Maciejewska N., Deptuła K., Słonimska P., Deptuła M., Baczyński-Keller J., Pikuła M., Sachadyn P., Tylingo R. (2024). From Bioink to Tissue: Exploring Chitosan-Agarose Composite in the Context of Printability and Cellular Behaviour. *Molecules*, *29*(19), 4648. Doi.org/10.3390/molecules29194648
(IF: 4,2; MNiSW: 140)

mój udział polegał na opracowywaniu koncepcji projektu oraz administracji nim, a także na pozyskiwaniu funduszy niezbędnych do realizacji badań. Opracowywałem metodologię oraz zajmowałem się formalną analizą danych i weryfikacją wyników. Nadzorowałem cały proces badawczy, zarządzałem zasobami oraz oprogramowaniem wykorzystywanym w projekcie. Brałem aktywny udział w pisaniu wstępnych wersji manuskryptu oraz jego recenzji i edycji.

Niniejszym oświadczam, że mój procentowy wkład wynosi 20 %.

.....
podpis współautora publikacji

7.5 Marine polymers in tissue bioprinting: Current achievements and challenges.

POLITECHNIKA GDAŃSKA | WYDZIAŁ CHEMICZNY

Gdańsk, 08.10.2024 r.

dr inż. Szymon Mania
Katedra Chemii, Technologii i Biotechnologii Żywności
Wydział Chemiczny
Politechnika Gdańska
szymon.mania@pg.edu.pl

Oświadczenie współautora publikacji

Oświadczam, że w pracy:
Banach-Kopeć A., Mania S., & Tylingo R. (2024). Marine polymers in tissue bioprinting: Current achievements and challenges. *Reviews on Advanced Materials Science*, *63*(1), 20230180. Doi.org/10.1515/rams-2023-0180.
(IF: 3,6; MNiSW: 100)

mój udział polegał na nadzorowaniu prac oraz edytowaniu draftu manuskryptu.

Niniejszym oświadczam, że mój procentowy wkład wynosi 20 %.

Szymon Mania

podpis współautora publikacji

POLITECHNIKA GDAŃSKA | WYDZIAŁ CHEMICZNY

Gdańsk, 08.10.2024 r.

dr hab. inż. Robert Tylingo, profesor uczelni
Katedra Chemii, Technologii i Biotechnologii Żywności
Wydział Chemiczny
Politechnika Gdańska
robertt@pg.edu.pl

Oświadczenie współautora publikacji

Oświadczam, że w pracy:
Banach-Kopeć A., Mania S., & Tylingo R. (2024). Marine polymers in tissue bioprinting: Current achievements and challenges. *Reviews on Advanced Materials Science*, *63*(1), 20230180. Doi.org/10.1515/rams-2023-0180.
(IF: 3,6; MNiSW: 100)

mój udział polegał na nadzorowaniu prac oraz edytowanie draftu manuskryptu.

Niniejszym oświadczam, że mój procentowy wkład wynosi 20 %.

.....
podpis współautora publikacji

8 DOROBEK NAUKOWY I ORGANIZACYJNY DOKTORANTA

8.1 Wskaźnik biliometryczny

Dane z bazy Scopus z dnia 08.11.2024:

- H-indeks: 6
- Liczba cytowań: 78
- Liczba cytowani bez autocytowań: 69

8.2 Publikacje

- Mania S., Banach-Kopeć A., Maciejewska N., Deptuła K., Słonimska P., Deptuła M., Baczyński-Keller J., Pikuła M., Sachadyn P., Tylingo R. (2024). From Bioink to Tissue: Exploring Chitosan-Agarose Composite in the Context of Printability and Cellular Behaviour. Molecules, 29(19), 4648. Doi.org/10.3390/molecules29194648

- Bartmański M., Pawłowski Ł., Knabe A., Mania S., Banach-Kopeć A., Sakowicz-Burkiewicz M., Ronowska A. (2024). The Effect of Marginal Zn2+ Excess Released from Titanium Coating on Differentiation of Human Osteoblastic Cells. ACS Applied Materials & Interfaces. DOI:10.1021/acsami.4c13529

- Banach-Kopeć A., Mania S., Tylingo R., Wawrzynowicz A., Pawłowska M., Czerwiec K., Deptuła M., Pikuła M. (2024). Thermosensitive composite based on agarose and chitosan saturated with carbon dioxide. Preliminary study of requirements for production of new CSAG bioink. Carbohydrate Polymers, 336, 122120. DOI:10.1016/j.carbpol.2024.122120

- Banach-Kopeć A., Mania S., Tylingo R. (2024). Marine polymers in tissue bioprinting: Current achievements and challenges. Reviews on Advanced Materials Science, 63(1), 20230180. DOI:10.1515/rams-2023-0180

- Bartmański M., Ronowska A., Mania S., Banach-Kopeć A., Kozłowska J. (2024). Biological and antibacterial properties of chitosan-based coatings with AgNPs and CuNPs obtained on oxidized Ti13Zr13Nb titanium alloy. Materials Letters, 360, 135997. DOI:10.1016/j.matlet.2024.135997

- Pawłowski Ł., Bartmański M., Ronowska A., Banach-Kopeć A., Mania S., Cieślik B., Mielewczyk-Gryń A., Karczewski J., Zieliński A. (2024). Cytocompatibility, antibacterial, and corrosion properties of chitosan/polymethacrylates and chitosan/poly(4-vinylpyridine) smart coatings, electrophoretically deposited on nanosilver-decorated titania nanotubes. Journal of Biomedical Materials Research Part B-Applied Biomaterials, 112, e35332. DOI:10.1002/jbm.b.35332

- Mania S., Banach-Kopeć A., Staszczyk K., Kulesza J., Augustin E., Tylingo R. (2023). An influence of molecular weight, deacetylation degree of chitosan xerogels on their antimicrobial activity and cytotoxicity. Comparison of chitosan materials obtained using lactic acid and CO_2 saturation. Carbohydrate Research, 534, 108973. DOI:10.1016/j.carres.2023.108973

- Deptuła M., Zawrzykraj M., Sawicka J., Banach-Kopeć A., Tylingo R., Pikuła M. (2023). Application of 3D-printed hydrogels in wound healing and regenerative medicine. Biomedicine & Pharmacotherapy, 167, 115416. DOI:10.1016/j.biopha.2023.115416

- Pawłowski Ł., Mania S., Banach-Kopeć A., Bartmański M., Ronowska A., Jurak K., Mielewczyk-Gryń A., Karska N., Rodziewicz-Motowidło S., Zieliński A. (2023). Osteoblast and bacterial cell response on RGD peptide-functionalized chitosan coatings electrophoretically deposited from different suspensions on Ti13Nb13Zr alloy. Journal of Biomedical Materials Research Part B-Applied Biomaterials, 111, 1800-1812. DOI:10.1002/jbm.b.35286

- Tylingo R., Kempa P., Banach-Kopeć A., Mania S. (2022). A novel method of creating thermoplastic chitosan blends to produce cell scaffolds by FDM additive manufacturing. Carbohydrate Polymers, 280, 119028. DOI:10.1016/j.carbpol.2021.119028
- Banach-Kopeć A., Mania S., Pilch J., Augustin E., Gabriel I., Tylingo R. (2022). A Novel Method of Endotoxins Removal from Chitosan Hydrogel as a Potential Bioink Component Obtained by CO_2 Saturation. International Journal of Molecular Sciences, 23, 5505. DOI:10.3390/ijms23105505

- Pawłowski Ł., Wawrzyniak J., Banach-Kopeć A., Cieślik B., Jurak K., Karczewski J., Tylingo R., Siuzdak K., Zieliński A. (2022). Antibacterial properties of laser-encapsulated titanium oxide nanotubes decorated with nanosilver and covered with chitosan/Eudragit polymers. Materials Science & Engineering C-Materials for Biological Applications, 138, 212950. DOI:10.1016/j.bioadv.2022.212950

- Mania S., Cieślik M., Konzorski M., Święcikowski P., Nelson A., Banach A., Tylingo R. (2020). The Synergistic Microbiological Effects of Industrial Produced Packaging Polyethylene Films Incorporated with Zinc Nanoparticles. Polymers, 12, 1198. DOI:10.3390/polym12051198

8.3 Zgłoszenia patentowe

- Mania S. (30%), **Banach-Kopeć A.** (30%), Tylingo R. (30%), Pikuła M. (3%), Deptuła M. (3%), Wawrzynowicz A. (2%), Czerwiec K. (2%), **P.443403** i **EP.2346004**. „Sposób wytwarzania hydrożelowej kompozycji biotuszu".

8.4 Patent

- Mania Szymon (45%), Tylingo Robert (45%), Banach Adrianna (10%). P.435877. „Sposób wytwarzania materiału termoplastycznego".

8.5 Wystąpienia konferencyjne

- 4th International Conferences on Advances Functional Materials & Biomaterials & Biodevices, Rzym, Włochy, 16-17.11.2024, "Biological properties of chitosan-agarose composite as a potential bioink component for 3D printing" **Banach-Kopeć A.**, Mania S., Słonimska P., Czerwiec K., Baczyński-Keller J., Deptuła M., Sachadyn P., Pikuła M., Tylingo R.

- V Ogólnopolska Konferencja Naukowa Implanty 2023, Politechnika Gdańska, 18-20.05.2023, „Właściwości biologiczne materiałów chitozanowych jako głównego surowca w technologii druku 3D" **Banach-Kopeć A.**, Mania S., Staszczyk K., Kulesza J., Augustin E., Tylingo R.

- IV Ogólnopolska Konferencja Naukowa Implanty 2023, Politechnika Gdańska, 27-28.05.2023 „Badanie kompozycji chitozan-agaroza jako potencjalnego składnika biotuszu do druku 3D" **Banach-Kopeć A.**, Mania S., Tylingo R.

8.6 Projekty naukowe

- 2022-2024, Argentum, wykonawca w projekcie „Design a multihead 3D printung system for production of biocompatible scaffolds based on the unstable form of chitosan hydrogen doped with agarose" Kierownik projektu: dr inż. Szymon Mania.

8.7 Projekty B+R

- Tylingo R., **Banach-Kopeć A.** „Opracowanie demonstracyjnej linii technologicznej do produkcji pieczywa z udziałem mąki z samopszy przy wykorzystaniu autorskich szczepionek oraz procesów saturacji ciasta CO_2", Fundusze Europejskie dla Nowoczesnej Gospodarki, 2024-obecnie.

- Tylingo R., Mania S., **Banach-Kopeć A.** „Opracowanie innowacyjnej technologii produkcji liofilizatów z wykorzystaniem emiterów fal dla optymalizacji procesu i poprawy jakości produktu". Europejski Fundusz Rolny na rzecz Rozwoju Obszarów Wiejskich: Europa inwestująca w obszary wiejski, 02.2024-12.2024.

- Tylingo R., Mania S., **Banach-Kopeć A.** „Opracowanie i wdrożenie innowacyjnych technologii suchego frakcjonowania wraz z mikronizacją suszonych ziaren kukurydzy". Europejski Fundusz Rolny na rzecz Rozwoju Obszarów Wiejskich: Europa inwestująca w obszary wiejski, 04.2023-11.2024.

- Tylingo R., Mania S., **Banach-Kopeć A.** "Wprowadzenie mąk grysikowych jako kluczowego składnika prowadzącego do obniżenia zawartości tłuszczów w produktach cukierniczych smażonych w głębokim tłuszczu". Vital Sp. z o.o., 31.08.2024.

- Tylingo R., Mania S., **Banach-Kopeć A.**, Staszczyk K. „Innowacyjna receptura piekarnicza z autorską szczepionką, dodatkiem prebiotycznym i substancjami wiążącymi wodę dla zwiększenia świeżości, powtarzalności i wydajności produkcji pieczywa o optymalnych". Piekarnia Jul-Ka Sp. z o. o., 30.09,2024.

- Tylingo R., Mania S., **Banach-Kopeć A.**, Staszczyk K. „Badania w kierunku opracowania suchego papieru myjącego wytwarzanego w technologii natryskiwania bazy myjącej". MISTRAL Bartosz Chmiel, 31.08.2023.

- Tylingo R., Mania S., **Banach-Kopeć A.** "Dobór konserwantów do produktu oraz mikrobiologiczna ocena jego stabilności". Gdańskie Młyny Sp. z o. o, 31.08.2023.

- Tylingo R., **Banach-Kopeć A.**, Mania S., Opracowanie receptur i prototypów baz w produkcji liofilizowanych przekąsek owocowych". MLB Biotrade Sp. z o.o., 10.07.2023.

- Tylingo R., Mania S., **Banach-Kopeć A.**, Staszczyk K. "Badania wytrzymałościowe oraz analiza sprawozdania z oceny właściwości cieplnych desek kompozytowych". Deska Marzeń Sp. z o.o., 31.05.2023.

- Mania S., **Banach-Kopeć A.** "Przeprowadzenie prac badawczych umożliwiających wdrożenie linii produktów dań gotowych na bazie pierogów z dodatkami funkcjonalnymi dedykowanych osobom starszym". IGLOTEX S.A., 31.03.2023.

- Tylingo R., Mania S., **Banach-Kopeć A.** “Sprawdzenie innowacyjnych cech produktu w ramach projektu POIR.03.02.01.-06-0020/17 w nawiązaniu do umowy ramowej o współpracy z dn. 05.01.2017 r.”, UNI-MASZ. H.M. Juszczuk Sp. J., 30.09.2022.

- Tylingo R., Mania S., **Banach-Kopeć A.** “Przeprowadzenie hermetyzacji szczepów probiotycznych. Zbadanie stabilności i żywotności kapsułkowanych drobnoustrojów w opracowanej bazie kosmetycznej”. BabyBiom Sp. z o.o., 31.07.2022.

- Tylingo R., Mania S., **Banach-Kopeć A.**, Staszczyk K. “Gitary o zmniejszonej masie”. Gitary MAYONES S.C., 31.03.2023.

- Tylingo R., Mania S., **Banach-Kopeć A.** “Opracowanie technologii produkcji kiełków”. NORT Sp. z o.o., 31.05.2022.

- Tylingo R., Mania S., **Banach-Kopeć A.** “Opracowanie pochłaniaczy formaldehydu w produkcji sklejek”. Paged LabTech Sp. z o.o., 30.05.2022.

- Tylingo R., Mania S., **Banach-Kopeć A.** “Analiza porównawcza piwa wysokoprocentowego w odniesieniu do wybranego produktu rynkowego”. Browar Kościerzyna S.A., 17.01.2022.

- Tylingo R., Mania S., **Banach-Kopeć A.** “Opracowanie technologii racjonalnego zagospodarowania strużyn z przetwórstwa skór (MIZDRA 2.0)”, 17.09.2021.

- Tylingo R., Mania S., **Banach-Kopeć A.** “Ocena wpływu dodatku mielonego siemienia lnianego na parametry wypiekowe oraz właściwości fizykochemiczne i sensoryczne pieczywa tostowego”. Vital Sp. z o.o., 25.05.2021.

- Tylingo R., Mania S., **Banach-Kopeć A.**, Kozłowska-Tylingo K. “Ocena wpływu dodatku topinamburu na parametry wypiekowe oraz właściwości fizykochemiczne i sensoryczne pieczywa pszennego i żytniego”. Piekarnia Cukiernia Piotr Kropidłowski - "KROPEK”, 15.01.2021.

- Tylingo R., Mania S., **Banach-Kopeć A.** “Opracowanie innowacyjnego suplementu diety w postaci gryzaka o zwiększonej zawartości kolagenu”. Petmex Company Krzysztof Napora Sp.J., 15.02.2021.

- Tylingo R., Mania S., **Banach-Kopeć A.** “Opracowanie naturalnego sorbentu zbrylającego dla zwierząt o poprawionej chłonności i zmniejszonej adhezyjności”. Pelletsfarm S., 31.12.2020.

- Tylingo R., Mania S., **Banach-Kopeć A.** “Przeprowadzenie analizy produktów jarskich wytworzonych na bazie analogów mięsa otrzymanych metodą HMEC”. G-W Sp. z o.o., 15.02.2021.

8.8 Staże naukowo-badawcze

- Staż naukowy w Pracowni Inżynierii Tkankowej i Medycyny Regeneracyjnej Zakładu Embriologii, w Katedrze Anatomii, Gdański Uniwersytet Medyczny, Polska, opiekun: prof. dr hab. Michał Pikuła, 10.01-29.06 2023.

8.9 Działalność organizacyjna

- Członek Komitetu Organizacyjnego, VI Ogólnopolska Konferencja Naukowa Implanty 2023, Politechnika Gdańska, 22-24.05.2023.

- Członek Komitetu Organizacyjnego, XXVIII Sesja Naukowa Sekcji Młodej Kadry Naukowej, Politechnika Gdańska, 16-17.05.2024.

- Członek Komitetu Organizacyjnego, V Ogólnopolska Konferencja Naukowa Implanty 2023, Politechnika Gdańska, 18-20.05.2023.

- Członek Komitetu Organizacyjnego, XLV Sesja Naukowa Komitetu Nauk o Żywności i Żywieniu PAN, Politechnika Gdańska, 1-2.06.2021.